NASA CR-132560

# SCOUT FOURTH STAGE ATTITUDE AND VELOCITY CONTROL (AVC) SYSTEM FEASIBILITY STUDY

By L. B. Byars



FEBRUARY 1975

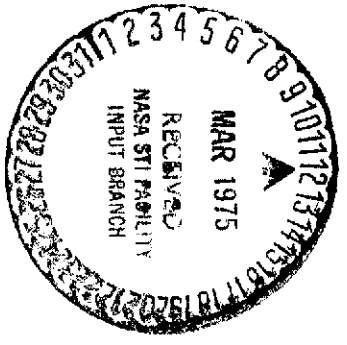


Prepared under Contract No. NAS1-10000 R-78 by

VOUGHT SYSTEMS DIVISION
LTV AEROSPACE CORPORATION
Dallas, Texas 75222

for

NATIONAL AERONAUTICS AND SPACE ADMINISTRATION

NASA CR-132560

# SCOUT FOURTH STAGE ATTITUDE AND VELOCITY CONTROL (AVC) SYSTEM FEASIBILITY STUDY

By L. B. Byars

Prepared under Contract No. NAS1-10000 R-78 by

VOUGHT SYSTEMS DIVISION
LTV AEROSPACE CORPORATION
Dallas, Texas 75222

for

NATIONAL AERONAUTICS AND SPACE ADMINISTRATION

Final Report

# SCOUT FOURTH STAGE ATTITUDE AND VELOCITY CONTROL (AVC) SYSTEM FEASIBILITY STUDY

By L. B. Byars

## FOREWARD

This final report presents the results of a conceptual design study performed by Vought Systems Division (VSD) of LTV Aerospace Corporation to determine the feasibility of incorporating an optional guidance and control system in the fourth stage of the Scout Launch Vehicle. The add-on system will operate in conjunction with the existing Scout guidance system and in the nominal spin-stabilized fourth stage environment to provide an increased payload orbital accuracy capability. This report contains the evaluation of possible utilization methods and the selection of the most desirable system configuration. The study was conducted under NASA Contract NAS1-10000, Task R-78. VSD wishes to express its appreciation to the following companies for their contributions to this study in providing guidance systems data: Ball Brothers Research Corporation; Electronic Systems Division, Ordnance Systems, General Electric Company; Hamilton Standard Division of United Aircraft Corporation; Aerospace Division, Honeywell Incorporated; Kearfott Division, The Singer Company, Aerospace & Marine Systems; Electronics Division, Northrop Corporation; Sperry Gyroscope Division, Sperry Rand Corporation; and Teledyne Systems Company.

TABLE OF CONTENTS

LIST OF FIGURES

LIST OF TABLES

# SCOUT FOURTH STAGE ATTITUDE AND VELOCITY CONTROL (AVC) SYSTEM FEASIBILITY STUDY

By B. L. Byars
LTV Aerospace Corporation

## 1.0 SUMMARY

The Scout Fourth Stage Attitude and Velocity Control (AVC) Study was initiated in September 1973. The study was authorized under Contract NAS1-10000, Task R-78. The study was directed toward the evaluation of the feasibility of incorporating a system in the fourth stage, operating in the normal spin-stabilization environment, to control the attitude during fourth stage burn and accomplish a velocity correction after burnout. Data were obtained from inertial guidance vendors from which equipment error budgets representing the extremities of the performance spectrum were established. Reference orbital trajectories for high and low circular orbits with the Scout F-1 configuration were generated. These trajectories were utilized to evaluate various concepts for utilization of the AVC system and to determine the effect of the guidance equipment error budgets.

The first AVC concept evaluated consisted of controlling the fourth stage attitude to a nominal orientation established in the prelaunch phase and making a velocity correction based upon the integral of the measured vehicle longitudinal load factor (integral of $N_X$). This approach resulted in insufficient reduction of apogee-perigee deviations to warrant development of the system.

Additional AVC utilization concepts were explored to achieve greater accuracy improvements; these concepts involve adjustments in fourth stage pitch and yaw attitude to compensate for measured errors in inertial velocity through the first three stages and a vernier velocity ($\Delta V$) correction after burnout as computed from the inertial velocity measurements. All options studied employ simple correction techniques with closed loop type control laws requiring minimal in-flight computations. Pitch attitude maneuvers after burnout are required to achieve the proper orientation for the vernier velocity correction. Two options were identified which result in drastic reduction in the apogee-perigee deviations. The analysis indicated a low sensitivity to the guidance equipment error budgets.

AVC systems, consisting of guidance and Reaction Control System (RCS) equipments, together with the vehicle transition sections were synthesized to determine the resulting payload weight penalties. With an RCS sized to correct a mean plus two sigma inertial velocity error and a reference set of guidance components the net payload weight penalty is 105.08 pounds (47.66 kg). A payload weight reduction of this magnitude is excessive and probably unacceptable. However, additional system studies identified means by which the payload penalty can be significantly reduced. The sensitivity of orbital deviations to the magnitude of the $\Delta V$ correction was established to determine the feasibility of reducing the RCS weight. Surprisingly, the degradation in apogee-perigee deviations resulting from limiting the $\Delta V$ to approximately the mean value of the inertial velocity error is very minor. Reducing the $\Delta V$ capability of the RCS from 196 ft/s (59.74 m/s) to 90 ft/s (27.43 m/s) decreases the RCS weight by 20 pounds (9.07 kg). Use of a typical alternate guidance system saves another 12 pounds (5.44 kg).

A fourth stage AVC system with the reduced ΔV capability and the alternate guidance system results in a net payload weight penalty of about 73.23 pounds (33.22 kg). A weight penalty of this magnitude is thought to be more compatible with payload requirements. The development of such an AVC system can be accomplished using subsystems (modified as needed) which are currently in or near production status.

Based upon the results of this study, VSD recommends that the design and development phase of the AVC system be initiated. Design studies directed toward further weight reductions in the AVC system and payload transition section are identified. AVC development should be accompanied, in a timely manner, by a continuation of the current efforts to achieve a substantial improvement in Scout payload carrying capability.

## 2.0 INTRODUCTION

The NASA/DOD Scout launch vehicle has been operating since 1960. It has launched a wide variety of small scientific and military applications satellites on orbital, reentry and probe missions. During this period of operation a number of programs have been undertaken to improve the Scout vehicle by taking advantage of new concepts and state-of-the-art developments. These planned improvements have increased both the payload carrying capability and flight reliability. Payload weight capability has increased by a factor of three. The high degree of flight reliability has been maintained throughout all improvement programs. Operational reliability has been demonstrated by the Scout record of consecutive successful missions.

The payload delivery accuracy of the Scout launch vehicle is satisfactory for most missions; however, to insure that Scout continues to meet the accuracy goals of the wide spectrum of users, it is desirable to provide a means of improving the payload delivery accuracy. The improvement goal is to provide a means of controlling the attitude of the fourth stage and correcting the velocity errors subsequent to fourth stage burnout. In keeping with the history of planned improvements, the NASA/LRC contracted with Vought Systems Division (VSD), LTV Aerospace Corporation to study the feasibility of incorporating an Attitude and Velocity Control (AVC) System in the fourth stage. The Statement of Work (SOW) governing this study was released in August 1973.

### 2.1 Scope And Objective

The objective of the study was to establish the feasibility of incorporating a guidance system in the Scout fourth stage to achieve a significant improvement in expected payload delivery accuracy (reduction in deviations). The study was to be conducted in sufficient detail to define the functional operation and usage of the AVC system. The scope of the technical investigations was to include the determination of the AVC equipment performance requirements, establishment of qualification and acceptance test levels, generation of layouts illustrating design approaches for the upper D and payload transition sections to incorporate the hardware and the preparation of a vendor bid package.

## 2.2 Study Guidelines

The following technical guidelines were established to govern the study and the AVC system equipments considered:

(1) The fourth stage AVC system shall operate in conjunction with the existing Scout guidance system located in the third stage lower D transition section.

(2) No changes or modifications to the existing guidance system shall be required except to provide the AVC system with necessary timing functions.

(3) The AVC system must possess the capability of operating in the spinning environment as currently employed with the fourth stage (nominally 3 revolutions per second).

(4) The AVC system will be designed, packaged and integrated such that it can be incorporated in the Scout 4th stage as an optional "add-on" system.

(5) The AVC guidance equipment must make maximum use of developed and qualified hardware -- no sensor (gyro and accelerometer) development will be considered.

(6) The Scout F-1 vehicle configuration will be used as the reference for the accomplishment of the study.

(7) The AVC system design must be compatible with all three Scout heatshields, two of which are 34 in. (.864 m) diameter and one 42 in. (1.067 m) diameter.

## 2.3 Study Approach

2.3.1 Definition of Equipments. – the AVC system is defined to consist of the following major equipment items:

(1) Inertial Measurement Unit (IMU)

(2) Velocity measurements system which may be integrated in the IMU

(3) Control Electronics Unit (CEU) which includes the necessary digital processing or computational equipment

(4) Reaction Control System (RCS) to provide the control force for both the fourth stage attitude control and the velocity correction after fourth stage burnout.

2.3.2 Study Execution. – VSD's approach to performing the study tasks was to accomplish the following steps:

(1) Establish the spectrum of expected guidance equipment error sources. Guidance vendor data were used to define maximum and minimum error budgets.

(2) Develop two reference trajectories (one high and one low circular orbit mission) for use in evaluation of the AVC systems.

(3) Compute the orbital deviations for each reference trajectory and for each error budget.

(4) Define equipment environmental qualification levels.

(5) Define AVC system test sequence and checkout requirements.

(6) Accomplish Reaction Control System (RCS) and telemetry subsystem trades.

(7) Make Advanced Vehicle Design Layouts (AVDL's) for a typical set of AVC hardware.

(8) Prepare vendor bid package including the AVC guidance equipment procurement specifications.

The initial SOW required the investigation of a velocity correction based upon the integral of the measured value of the applied vehicle longitudinal acceleration or load factor, $\int N_X$. However the scope was expanded to consider the measurement of inertial velocity components from which to accomplish the velocity correction.

## 3.0 FOURTH STAGE AVC OPERATION

### 3.1 Scout Vehicle

The standard Scout launch vehicle is a solid propellant four-stage booster system capable of boosting orbital, probe and re-entry payloads. The vehicle is about 73 ft (22.25 m) in length with a lift-off weight of 47 500 lbm (21 546 kg). It is launched from the vertical position.

Scout is equipped with a guidance system located in the third stage, lower D transition section. The guidance system provides attitude and stabilization control signals for a first stage hydraulic servo control system and second and third stage reaction control systems. The signals provide correction of attitude and stabilization to maintain the vehicle in a zero-G flight path by changes in pitch attitude as dictated by pitch programming. The guidance system also provides sequenced ignition signals to second, third, and fourth stage rocket igniters and initiates separation of the fourth stage and spin rocket ignition. The ignition signals are preset in an intervalometer (timer) which initiates the functions according to required sequence and time intervals. Signals for correcting yaw, roll and pitch deviations originate from yaw, roll and pitch displacement gyros in a strapdown type Inertial Reference Package (IRP). The gyros detect errors or deviations from reference attitude and generate correction signals. The generated signals are combined with rate gyro signals to produce a signal which is amplified and applied to provide corrective control functions. Reference for the yaw and roll gyros is launch position and reference for the pitch gyro is the torqued position of the gyro which changes with each programmed pitch rate step starting from the launch position.

Programmed changes in vehicle pitch attitude to maintain a zero-G flight path are accomplished by torquing the IRP pitch gyro at predetermined rates and for predetermined intervals. Signals generated by the torqued gyro are applied to pitch controls which change the vehicle pitch attitude. The points in flight at which gyro torquing occurs to change pitch attitude are determined by the desired mission profile and are preset into the intervalometer and programmer. Programmed changes in vehicle yaw attitude are also possible, with the signal generation identical to that used for pitch. Yaw torquing is sequenced to be accomplished after the pitch program has been completed.

A typical Scout trajectory for a circular orbit is illustrated in Figure 1. The length of the coast periods between thrust phases are all variable; however the third stage coast to fourth stage ignition is the longest. Upon completion of the programmed third stage coast the intervalometer closes a relay

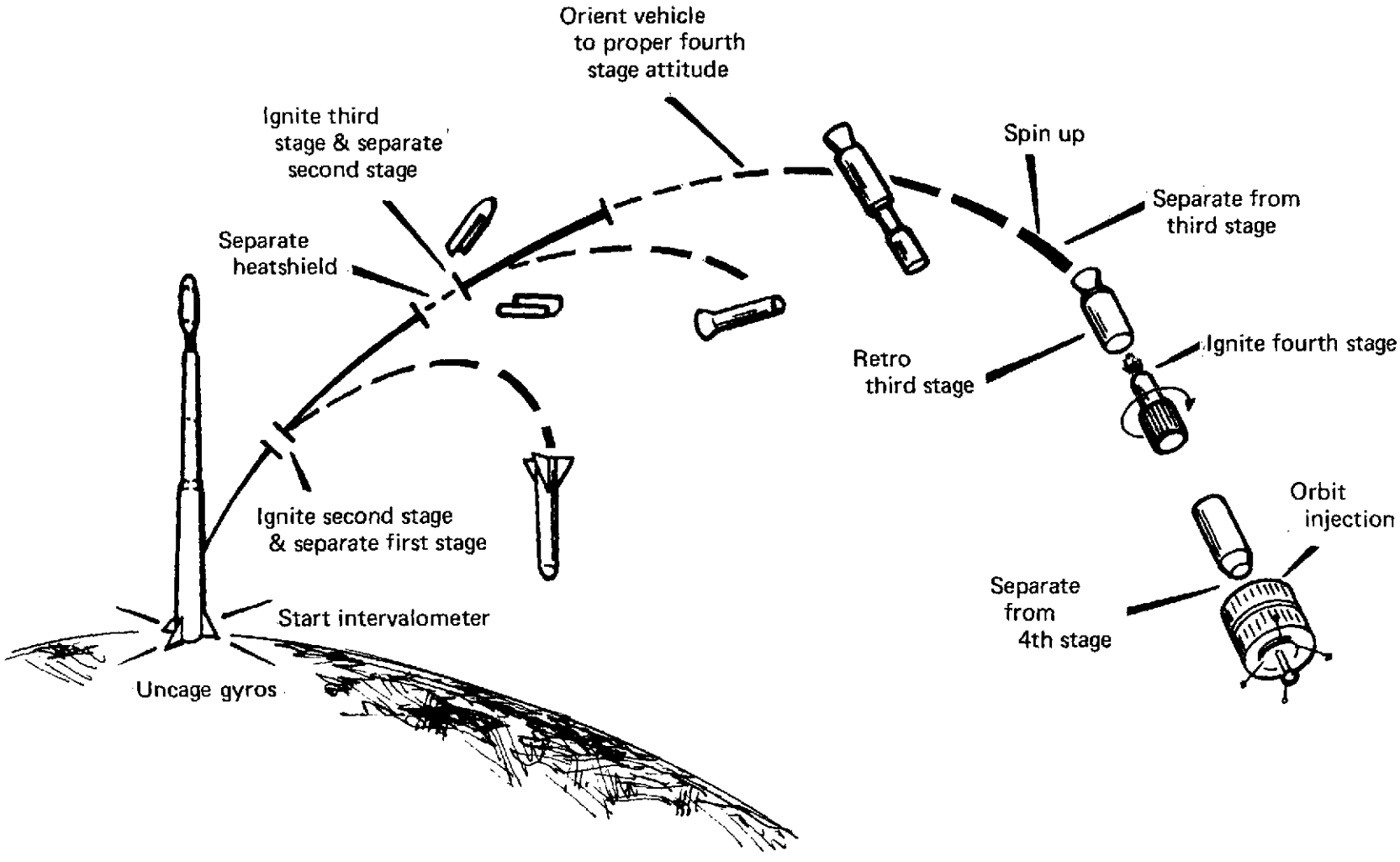


FIGURE 1. – TYPICAL SCOUT MISSION PROFILE

which fires 6-second delay squibs in the fourth stage motor igniter. At the same time the fourth stage spin motor igniters are fired to provide the spin rate for the fourth stage and payload. A spin bearing permits the spin-up while still attached to the third stage. One and one-half seconds after firing the fourth stage motor igniter squibs, the fourth stage separation system is activated. Springs which are compressed between the two stages supply the initial separation forces. After the remaining 4.5 seconds have elapsed, fourth stage motor ignition occurs.

## 3.2 AVC Corrections

The initial method of utilizing the AVC system, as outlined in the SOW, was to accomplish the following functions.

(1) Correct the attitude of fourth stage prior to motor ignition and maintain that attitude throughout the fourth stage boost phase.

(2) Incorporate two aft-facing reaction control motors to accomplish an incremental velocity ($\Delta V$) correction after the termination of fourth stage thrust.

The separation effects and motor ignition disturbances cause significant attitude deviations during fourth stage burn; pitch and yaw error magnitudes are 3.54 deg (0.62 rad), $3\sigma$ as determined from flight experience data. The AVC system then needs to correct this error source. The purpose of the IMU is to provide an attitude reference from which to determine the correction. It must operate in the nominal spinning environment of the fourth stage. Two options are available for operation of the IMU:

(1) First, it can be aligned and operated independent of the existing third stage IRP. In this manner, the IMU would operate throughout the trajectory but no vehicle correction or control signals would be generated until after fourth stage separation. The nominal fourth stage attitude would have to be inserted into the system during vehicle processing so that the measured values can be compared in flight to the nominals.

(2) Second, the AVC IMU can assume the vehicle attitude established by the current third stage system near the end of third stage coast as the reference and then maintain that attitude throughout fourth stage burn. Obviously this choice is affected by the errors of the existing IRP and the control deadband for third stage coast.

The specified initial velocity correction scheme consisted of the use of a body mounted accelerometer to measure the forces applied along the longitudinal axis of the vehicle. This measurement and its integral would be made for all four boost phases. Any correction would then be determined from the integral of the longitudinal load factor, identified as the $\int N_X$ system. The velocity correction accomplished would be restricted in that it would be applied in the same direction (either positive or negative) as the velocity increment added by the fourth stage. The form of the equation to be solved in the AVC CEU to compute the magnitude of the velocity correction would be:

$$V_C = V_N - (K_1 \Delta V_1 + K_2 \Delta V_2 + K_3 \Delta V_3 + K_4 \Delta V_4) \text{ where}$$

$V_C$ = Computed velocity correction

$V_N$ = Nominal velocity measurement value

K's = Mission dependent constants

$\Delta V$'s = Velocity increments of each stage.

The nominal velocity ($V_N$) and stage gains (K's) would be mission dependent, computed in the pre-flight planning phase and inserted in the AVC equipment during the vehicle processing.

Battelle Columbus Laboratories studied this correction approach in Reference 1 and investigated the effects of varying the K's to achieve several different criteria. The Battelle data indicated that for a near circular orbit the use of unity gains resulted in near maximum achievable improvement in the reduction of both apogee and perigee deviations. No attempt was made in this study effort to define the optimum gain combination. Instead, unity gains were used to evaluate the accuracy of the $\int N_X$ approach.

At the conclusion of the $\int N_X$ investigation several other means of using the AVC system to gain additional accuracy improvements were studied. The manner in which these options operate is discussed later in this report.

## 4.0 GUIDANCE EQUIPMENT ERROR BUDGETS

In order to assure maximum realism and correlation to existing hardware in the establishment of guidance hardware budgets, a request for information was sent to several vendors to obtain data on the type systems they would propose for the AVC application. The general operating scheme and requirements to be imposed on the AVC equipments were provided to the vendors. Emphasis was placed on the vendor submitting data on hardware that is in or near a production status and already subjected to an environmental qualification program if possible. They were encouraged to give a higher weighting factor to production status than size and weight. Other desirable features listed were simplicity of checkout and operation and high reliability.

Each vendor was given the option of suggesting that their system be considered for operation from launch or accepting the vehicle attitude established at the end of third coast as the reference. If the option of operating from the end of third stage coast were selected, the IMU would have to be aligned as necessary prior to launch and then caged or locked as required.

The data obtained from the vendors were not intended for any comparative analyses, ranking or selection of a preferred system. Instead the intended use was to determine the types of systems that would be proposed and the span of component error sources.

### 4.1 Vendor Responses

A brief summary of the type guidance systems suggested in response to the request for information is presented. These are provided in this report to show the type selections that are considered by the guidance vendors as most promising.

4.1.1 Honeywell Modified H-478 System. – the system consists of a basic strapdown inertial measurement unit mounted in a single roll gimbal. The measurement unit would be the basic H-478 inertial sensor assembly developed by Honeywell. It can be configured with one of several single degree-of-freedom gyros. Gyro selection is determined by the quality of measurement desired of the unit. The longitudinal or vehicle x-axis accelerometer would be integrated to provide the integral of the longitudinal load factor (frequently denoted as velocity) data. The outputs of the other two accelerometers would be used for telemetry. The attitude reference portion of this system would operate from the end of third stage coast – assuming the vehicle attitude established there as the reference. A digital differential analyzer would then compute the pitch and

yaw error angles from the point of operation. The basic strapdown inertial measurement unit is in production, a prototype of the gimbal has been assembled and tested, and preliminary design of the electronic circuits has been completed. Estimated weight of the unit is 20 lbm (9.07 kg) with a size of 13.9 x 7.8 x 6.0 inches (35.3 x 19.8 x 15.2 cm).

4.1.2 Ball Brothers Research Corporation (BBRC) Digital Attitude Control System (DACS). – the DACS is a single package, self-contained configuration that houses a strapdown reference system in a single roll gimbal. The package incorporates the roll stabilized platform, a programmable digital processor, reaction control valve drivers, plus support elements such as batteries, inverter, converter and signal commutator. It provides all the functions required to accomplish attitude control of a spinning body. An accelerometer would have to be added to measure the vehicle longitudinal acceleration. A complete set, or triad, of accelerometers could be added to determine all three components of acceleration. BBRC recommended that the system be operated from launch; however it could be either caged until the end of third stage coast or updated to the nominal values at that time.

One flight unit has been built and subjected to a qualification program. The unit was tested to both random and sine vibration levels comparable to the Scout levels; however, it did not undergo any shock or linear acceleration testing. The complete unit has been designed to fit within a 15 inch (38.1 cm) diameter with a length of 10.75 inches (27.3 cm). Weight of the total system is about 52 pounds (23.59 kg).

4.1.3 Kearfott Pershing II IMU. – the Pershing II IMU is being developed to missile environmental and accuracy requirements which are comparable to Scout general requirements. This IMU will be designed, developed and qualified during the course of the Pershing II program. The IMU falls within the KT-70 family of inertial platforms. It is a four-gimbal unit containing two two-degree-of-freedom Kearfott gyros. Two accelerometers, one single axis and one dual axis are used to provide the system a measurement of vehicle acceleration. The inertial cluster of the Pershing II is common to all the IMU's of the KT-70 family. The electronics required to support the IMU are housed in the same package. The roll gimbal torquer is designed to operate in the 3 revolutions per second Scout environment.

The Pershing II IMU is designed to interface with a digital computer. In fact the IMU electronics includes serial core memory storage which is utilized to store the coefficients of the gyros and accelerometers within that platform. All IMU control, monitoring and sequencing control would nominally come from the digital computer or processor. A promising approach for the AVC system is to interface the IMU with a control electronics unit which includes the digital processor from the Kearfott SKC-3000 computer unit. This combination would then be able to accomplish the inertial navigation type computations plus the spinning body attitude commands and the velocity correction control. The system would operate from launch independent of the Scout third stage guidance system.

The first of 6 advanced development IMU's will be delivered in March 1975. These will be followed by engineering development systems for operational evaluation.

The Pershing II IMU will weigh 30.8 pounds (13.97 kg), the maximum dimensions are 13 inches x 10.5 inches x 9.0 inches (33.0 x 26.7 x 22.9 cm). A CEU is expected to weigh about 6 pounds (2.72 kg).

4.1.4 Teledyne SOFT System. – the Teledyne system that would best fit the Scout AVC application is a version of the attitude control subsystem developed for the SOFT experiment. The platform consists of two, two-axis Teledyne strapdown gyros mounted on a roll stabilized gimbal system. The roll gimbal is basically the same as the Space Vector Midas platform which was flown successfully on Scout Vehicle S-191. The SOFT system includes on accelerometer that is now used

in the alignment process. The alignment and gyrocompassing for this system, which is accomplished in a self-contained manner, has been programmed and demonstrated in vehicle tests. The total SOFT system has been produced and delivered in a limited quantity. First flight usage is expected in 1975.

The primary change to be incorporated for AVC use is the integration of the TDY-52 digital processor in the platform electronics. The existing SOFT system uses a TDY-43 computer which is a much larger package. The combined weight of the roll stabilized platform and the platform electronics would be 30 pounds (13.6 kg). A thruster electronics unit would have to be added to convert the attitude and velocity command signals into solenoid or relay drive signals to interface the attitude and velocity control motors.

When used in the $\int N_X$ approach, only one accelerometer is required. Two other accelerometers could be added to provide complete velocity data. The system would normally operate from launch because of the highly accurate gyros. However, it could accept the third stage coast attitude as a reference and operate from that point.

4.1.5 Space Vector Platforms. – data on two optional platforms were provided by Space Vector. The first option is an improved version of the Midas platform which was used in the NPE attitude correction system on Scout vehicle S-191. The Midas platform consists basically of two-degree-of-freedom free gyros mounted on a single roll gimbal. The electronics are integral to the platform. Torques to stabilize the gimbal are provided by a servo motor and a ring gear, pitch and yaw attitude come directly from the free gyros. The NPE system controlled the attitude of a Scout fourth stage to orient it for firing a fifth stage motor; however, it did not assume control until after fourth stage burnout. A control electronics package provided the signal processing for the development of steering commands, timing functions, power switching, telemetry processing and system interface. An accelerometer and the required computational capability would have to be added for AVC operation. The attitude portion (platform) of the system would operate from the end of third stage coast because of the high drift rates of the gyros. The Midas platform itself weighs about 9 pounds (4.08 kg).

The second option is one that would operate throughout the entire Scout trajectory. It is a modified version of the SOFT roll-stabilized platform which uses Teledyne strapdown gyros. The modification involves the addition of a second gimbal with limited angular freedom (approximately ±20 deg (0.35 rad)) to isolate the vehicle yaw motion. The pitch gyro would operate in a strapdown manner and pitch attitude data would be derived from integrating the torquing current. Three accelerometers could be mounted on the inner gimbal to provide complete vehicle acceleration data. A preliminary design of the second gimbal has been completed. The control electronics package for this option would utilize much of the circuitry from the unit that interfaces the Midas platform but it would require extensive expansion to accomplish the additional computations required. The estimated weight of the two gimbal platform is 12 pounds (5.44 kg).

4.1.6 General Electric Miniature Attitude Reference (GEMAR). – this system is composed of a three gimbal platform and an electronics package. The designed system was aimed at the high acceleration and vibration environment of a spinning re-entry vehicle. Four systems were flown on the Atlas missile in the upper-stage FAIR experiments. In this application the system provided attitude data only; however, it operated during the Atlas boost phase plus a subsequent twenty to thirty minute flight time. The platform has been qualified for a spin rate of two revolutions per second. The roll torquer can be exchanged, with no other platform changes, for one that has a five revolution per second capability. The platform cluster houses three Honeywell GG49 floated, rate-integrating gyros. The inner gimbal which would measure vehicle yaw is limited to ±65 degrees (1.13 rad). In the Atlas application a two-axis pendulum was used initially to level the cluser; however, the platform data obtained showed the booster to be stable and vertical within a few arc-minutes. In subsequent

flights, alignment and erection relative to the platform case were used. The platform may be offset to any desired angle for each gimbal by the use of resolver matching loops in which the offsets are input to the ground equipment. The self-contained heat sink capability of both the platform and electronics is such that with platform ambient temperature of no more than 90°F (305.4°K) the system will operate for 45 minutes with no additional cooling.

A case mounted accelerometer would be used for the $\int N_X$ case. However, if inertial velocity is required, the platform would have to be modified to incorporate a triad of accelerometers on the cluster. A digital processor would have to be added to accomplish the inertial navigation type computations plus the attitude and velocity control functions. The existing platform and electronics package weigh 24.1 pounds (10.93 kg).

4.1.7 Northrop Quasi-Stabilized Inertial Reference (QSIR). – the QSIR system configured for Scout would be a strapdown reference package mounted in a roll-stabilized gimbal. The reference package contains three rate integrating gyros and three accelerometers. System computations and inertial sensor compensation would utilize both analog and digital techniques to minimize hardware complexity. The QSIR processor would be a scaled down version of the Northrop computer on the B-1 aircraft. The processor and platform electronics could be housed in a common package. The processor could accomplish the attitude control and velocity correction computations in addition to the platform associated functions.

The platform is designed such that it can accomodate either one of two gyros – the G1-G6 ball bearing or the G1-G6G gas bearing design. Both are Northrop gyros that have an existing production base. Selection of the gyro would depend upon the manner in which the system is used. For applications when the third stage coast attitude is used as the reference, the ball bearing gyro would be used. If it were desirable for the attitude reference system to operate from launch, the gas bearing gyro would be used because of the much lower drift rate coefficients. Both the platform and the electronics/processor unit would utilize a cold plate structure to prevent excessive temperatures during the mission.

The gyros and accelerometers to be used in the QSIR system are production items and the electronic circuits have been built. However, the system as such would require integration and development. Estimated weight of the two units, platform and processor (electronics), is 26.5 pounds (12.02 kg).

4.1.8 Hamilton Standard TARGIT III Platform. – the Three Axis Rate Gyro Inertial Tracker (TARGIT) III is a third-generation system based upon two earlier versions which have flow on AEROBEE 150A and Athena flights. The system consists of a three gimbal platform and a separately mounted electronics assembly. The platform instrument cluster contains three Hamilton Standard SUPERGYROS and three linear accelerometers. The gyros would be selected units from a large production base. In flight, the accelerometers are normally used only to compensate the gyros in order to provide a reduced drift rate. The horizontal accelerometers are also used for initial alignment; the outputs are transmitted to the ground support equipment where error signals are derived to drive the gimbal servo loops. When it is desirable to align the inertial element to an off-set pre-determined orientation, the ground support equipment generates error signals by comparing the gimbal resolver angles with the pre-determined command orientation angles. Once the alignment loops have settled, the platform may be switched to the inertial mode.

Development required would be to interface the production platform with a digital processor to compute the required velocity. Also the accuracy of the accelerometers would have to be evaluated to assess their adequacy.

The platform and a separate electronics package will weigh about 17 pounds (7.71 kg).

4.1.9 Sperry System. – Sperry's base-line approach to the implementation of the Scout AVC system consists of a single package containing three ring laser angular rate sensors, three accelerometers and the associated electronics. The sensors are mounted on a roll-stabilized gimbal. The gyro cluster would be contained in a single hermetically sealed container with the accelerometers mounted on the underside of the same casting containing the gyros. A special purpose processor would perform three major functions: gyro data normalization, clock and timing, and attitude computation. Data normalization consists of bias removal and scale factor correction. Attitude computation converts the normalized accelerometer and gyro data into body referenced velocity and attitude correction information. If inertial velocity were desired, additional computations would be necessary. The attitude computer would also supply roll information for the roll gimbal servo. This system could be operated throughout the trajectory or the third stage coast attitude could be assumed as the reference.

The system is based upon the laser gyro which is not yet in wide application or production. Thus there is a significant amount of development associated with the entire system. Estimated weight of the total system (one package) configured for the $\int N_X$ case is 20 pounds (9.07 kg).

## 4.2 Error Budgets

Each vendor supplied performance data (error coefficients) on the gyros and accelerometers employed in their systems. Some inputs were more comprehensive than others. The range of error coefficients is illustrated by Table 1 which lists those values provided by the guidance vendors. In some cases more than one set of instruments could be used or even the same sensor could have different performance under different conditions. Only one Space Vector system is shown since the second system discussed utilizes the Teledyne components. The Space Vector system listed represents the improved Midas platform. Table 1 is not meant to indicate the only performance values available from each vendor, instead it is meant to be representative of the equipments that could be used in the Scout fourth stage AVC system. In fact, each of the indicated budgets could be varied significantly depending upon the environmental characteristics and the degree of compensation employed in the system.

Two error budgets were established from the vendor data provided – one budget represents the maximum error values and the other the minimum. The minimum and maximum gyro and accelerometer error budgets used in the analysis are listed in Table 2. These values represent the region or span of performance values available for the 4th stage AVC system. Neither budget is associated with a specific hardware system. The gyro torquer scale factor error and misalignment of the input axis are not applicable for a completely gimballed inertial platform because the gyro orientation remains at the inertial reference established at launch.

Because of the two options regarding the operation of the attitude reference portion of the AVC system (operating from launch or from the end of 3rd stage coast), a separate gyro error budget was established for those systems which operate only from the end of 3rd stage coast. In this case the time of operation is significantly reduced, thus it would be of little benefit to use highly accurate gyros for this condition. Based upon the data supplied by vendors that suggested their system accept the third stage coast attitude as the reference, the gyro error budgets shown in Table 3 were assembled.

AVC system measurement errors were computed for each error budget shown in Table 2. The only additional error input required for the determination of the AVC system errors is that of vehicle alignment (on the launcher) to the reference coordinate system. Pitch and yaw alignment errors of 0.0572 deg (1.0 mrad) each and a roll or azimuth error of 0.0688 deg (1.2 mrad) were used, based upon data from previous analyses, primarily Reference 2.

## TABLE 1. – SUMMARY – EQUIPMENT ERRORS, 4TH STAGE AVC SYSTEMS

● $3\sigma$ Values

| Error sources | Units | Candidate Systems | | | | | | | | | |
|---|---|---|---|---|---|---|---|---|---|---|---|
| | | Honeywell | Kearfott Pershing II | Ball Bros. | G.E. | Teledyne | Space Vector | Northrop no. 1 | Northrop no. 2 | Ham. Std. | Sperry |
| Gyro: | | | | | | | | | | | |
| Fixed drift | deg/hr | 6.0 | 0.006 | 2.0 | 0.05 | 0.03 | 4.35 | 15.0 | 0.3 | 6.0 | 2.0 |
| Mass unbalance, IA | deg/hr/G | 7.5 | 0.075 | 1.8 | 2.24 | 0.06 | 4.29 | 15.0 | 0.6 | 9.0 | NA |
| Mass unbalance, SA | deg/hr/G | 7.5 | 0.03 | 1.8 | 2.1 | 0.06 | 4.29 | 15.0 | 0.6 | 9.0 | NA |
| Anisoelastic | deg/hr/$G^2$ | 0.9 | 0.03 | 0.05 | 0.06 | 0.05 | 0.3 | 0.04 | 0.04 | 0.72 | NA |
| Torquer scale factor error | percent | 0.15 | NA | 0.06 | NA | 0.0003 | NA | 0.1 | 0.1 | NA | 0.01 |
| Input axis misalignment | arc s | – | NA | – | NA | 62 | NA | 618 | 618 | NA | 20 |
| Accelerometer: | | | | | | | | | | | |
| Bias | $\mu$ G | 1000 | 150 | – | 900 | 150 | 0.07% of $\Delta V$-total error | 600 | 600 | – | 300 |
| Scale factor error | $\mu$ G/G | 600 | 450 | – | 100 | 450 | | 1000 | 1000 | – | 300 |
| Linearity error | $\mu$ G/$G^2$ | – | 30 | – | – | 60 | | 30 | 30 | – | – |
| Input axis misalignment | arc s | – | 60 | – | – | 60 | | 618 | 618 | – | 60 |

## TABLE 2. – AVC EQUIPMENT ERROR BUDGETS

- Systems operate from launch

Gyro Errors • 3σ Values

| Error Source | Min Budget | Max Budget | Existing 3rd Stage IRP |
|---|---|---|---|
| Fixed drift | 0.03 deg/hr | 3.0 deg/hr | 0.5 deg/hr |
| Mass unbalance (Input axis and spin axis) | 0.06 deg/hr/G | 3.0 deg/hr/G | 3.5 deg/hr/G |
| Anisoelastic drift | 0.05 deg/hr/$G^2$ | 0.2 deg/hr/$G^2$ | 0.02 deg/hr/$G^2$ |
| Torquer scale factor error | 0.003% | 0.09% | 0.2% |
| Input axis misalignment | 60 arc s | 120 arc s | 412 arc s |

Accelerometer Errors • 3σ Values

| Error Source | Min Budget | Max Budget |
|---|---|---|
| Bias | 150 μG | 1000 μG |
| Scale factor error | 450 μG/G | 1000 μG/G |
| Linearity error | 30 μG/$G^2$ | 100 μG/$G^2$ |
| Input axis misalignment | 60 arc s | 120 arc s |

## TABLE 3. – GYRO ERROR BUDGETS, FOURTH STAGE OPERATION ONLY

• 3σ Values

| Error Source | Max Budget | Min Budget |
|---|---|---|
| Fixed drift repeatibility | 15 deg/hr | 2.0 deg/hr |
| Mass unbalance | 15 deg/hr/G | 1.8 deg/hr/G |
| $G^2$ sensitive | 0.6 deg/hr/$G^2$ | 0.04 deg/hr/$G^2$ |

## 5.0 REFERENCE TRAJECTORIES

Two reference or nominal missions, as required by the SOW, were selected for the study. These missions were used to evaluate the accuracy improvements achievable and the payload performance capabilities of the AVC systems studied. The baseline missions chosen were 600 n. mi. (1111.2 km) and 200 n. mi. (370.4 km) circular orbits for a due east launch from Wallops Island. The logic used in selecting these particular missions was to use near the minimum and maximum circular orbit altitudes of interest to potential Scout users. Complete trajectories for these two missions were calculated for the Scout F-1 configuration with the 42 in. (1.067 m) diameter –45 in. (1.143 m) nose station heat-shield. The rocket motors which compose the Scout F-1 configuration are:

| Stage | Motor name |
|---|---|
| First | Algol IIIA |
| Second | Castor IIA |
| Third | Antares IIB |
| Fourth | Altair IIIA |

The pitch programs (sequence of commanded vehicle pitch rates) and mission sequence of events are shown in Tables 4 and 5 for the two trajectories. Scout is alunched from the vertical orientation and the negative pitch rates indicate a pitch down motion. Acceleration time histories are shown in Figures 2 and 3. These accelerations are those which occur with the heaviest payload or orbit weight capability for the F-1 configuration.

Fourth stage AVC components will have to be designed to withstand much higher acceleration capability to accomodate lighter payload weights and future vehicle growth. However, the acceleration and attitude data from these two trajectories were used to determine the measurement errors for the AVC equipments evaluated.

The time histories of the integral of $N_X$ for both trajectories are pictured in Figure 4 and 5. Figure 4 depicts stages 1 and 2 while stages 3 and 4 are in Figure 5. These plots represent the precise parameter that the integral of the longitudinal accelerometer would yield.

Another parameter used extensively throughout the study is the payload performance or weight capability. The reference used in the study is the capability of the Scout F-1 configuration. The payload capabilities in terms of weight above the fourth stage motor of the reference trajectories are:

| Orbit | Payload weight |
|---|---|
| 600 n. mi. (1111.2 km) | 267.56 lbm (121.37 km) |
| 200 n. mi. (370.4 km) | 438.51 lbm (198.91 km) |

## 6.0 EVALUATION OF MEASUREMENT AND SYSTEM ERRORS

The integral of $N_X$ approach, with its associated control system, involves essentially the correction of two parameters. These are:

(1) Fourth stage inertial attitude (pitch and yaw body attitudes)

TABLE 4. – PITCH PROGRAM AND SEQUENCE OF EVENTS, 600 N. MI. (1111.2 KM) CIRCULAR ORBIT

| Time, seconds | Event |
|---|---|
| 0.00 | Lift off |
| 1.00 | Pitch rate no. 1 = –1.92790 deg/s (.03365 rad/s) |
| 6.00 | Pitch rate no. 2 = –0.69000 deg/s (.01204 rad/s) |
| 38.00 | Pitch rate no. 3 = –0.51000 deg/s (.00890 rad/s) |
| 47.00 | Pitch rate no. 4 = –0.40000 deg/s (.00698 rad/s) |
| 58.00 | Pitch rate no. 5 = –0.30000 deg/s (.00524 rad/s) |
| 81.69 | Stage 1 burnout |
| 83.14 | Stage 2 ignition |
| 95.00 | Pitch rate no. 5 = –0.22000 deg/s (.00384 rad/s) |
| 110.00 | Pitch rate no. 7 = –0.13000 deg/s (.00227 rad/s) |
| 122.50 | Stage 2 burnout |
| 127.50 | Stage 3 ignition |
| 156.40 | Stage 3 burnout |
| 170.00 | Pitch rate no. 8 = –1.00000 deg/s (.01745 rad/s) |
| 223.70 | Pitch rate no. 9 = –0.00000 deg/s |
| 789.16 | Stage 4 ignition |
| 820.92 | Stage 4 burnout |

TABLE 5. – PITCH PROGRAM AND SEQUENCE OF EVENTS, 200 N. MI. (370.4 KM) CIRCULAR ORBIT

| Time, seconds | Event |
|---|---|
| 0.00 | Lift off |
| 1.00 | Pitch rate no. 1 = –2.41043 deg/s (.04207 rad/s) |
| 6.00 | Pitch rate no. 2 = –0.90000 deg/s (.01571 rad/s) |
| 35.00 | Pitch rate no. 3 = –0.64000 deg/s (.01117 rad/s) |
| 48.00 | Pitch rate no. 4 = –0.46000 deg/s (.00803 rad/s) |
| 60.00 | Pitch rate no. 5 = –0.34000 deg/s (.00593 rad/s) |
| 81.69 | Stage 1 burnout |
| 92.60 | Stage 2 ignition |
| 105.00 | Pitch rate no. 6 = –0.27000 deg/s (.00471 rad/s) |
| 120.00 | Pitch rate no. 7 = –0.15000 deg/s (.00262 rad/s) |
| 131.96 | Stage 2 burnout |
| 139.78 | Stage 3 ignition |
| 168.68 | Stage 3 burnout |
| 180.00 | Pitch rate no. 8 = –0.50000 deg/s (.00873 rad/s) |
| 238.81 | Pitch rate no. 9 = –0.00000 deg/s |
| 505.37 | Stage 4 ignition |
| 537.13 | Stage 4 burnout |

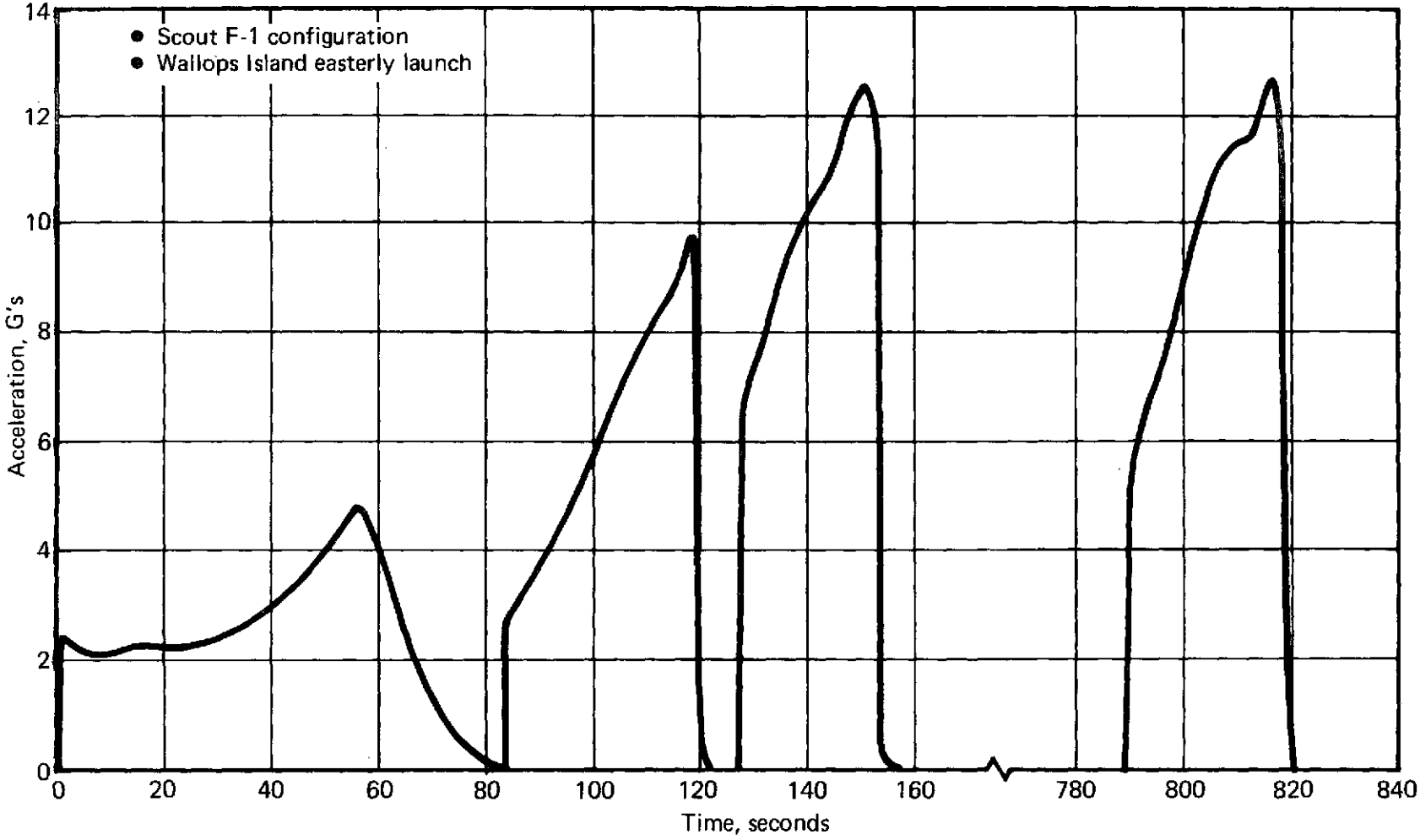


FIGURE 2. – ACCELERATION HISTORY, 600 N. MI. (1111.2 KM) CIRCULAR ORBIT

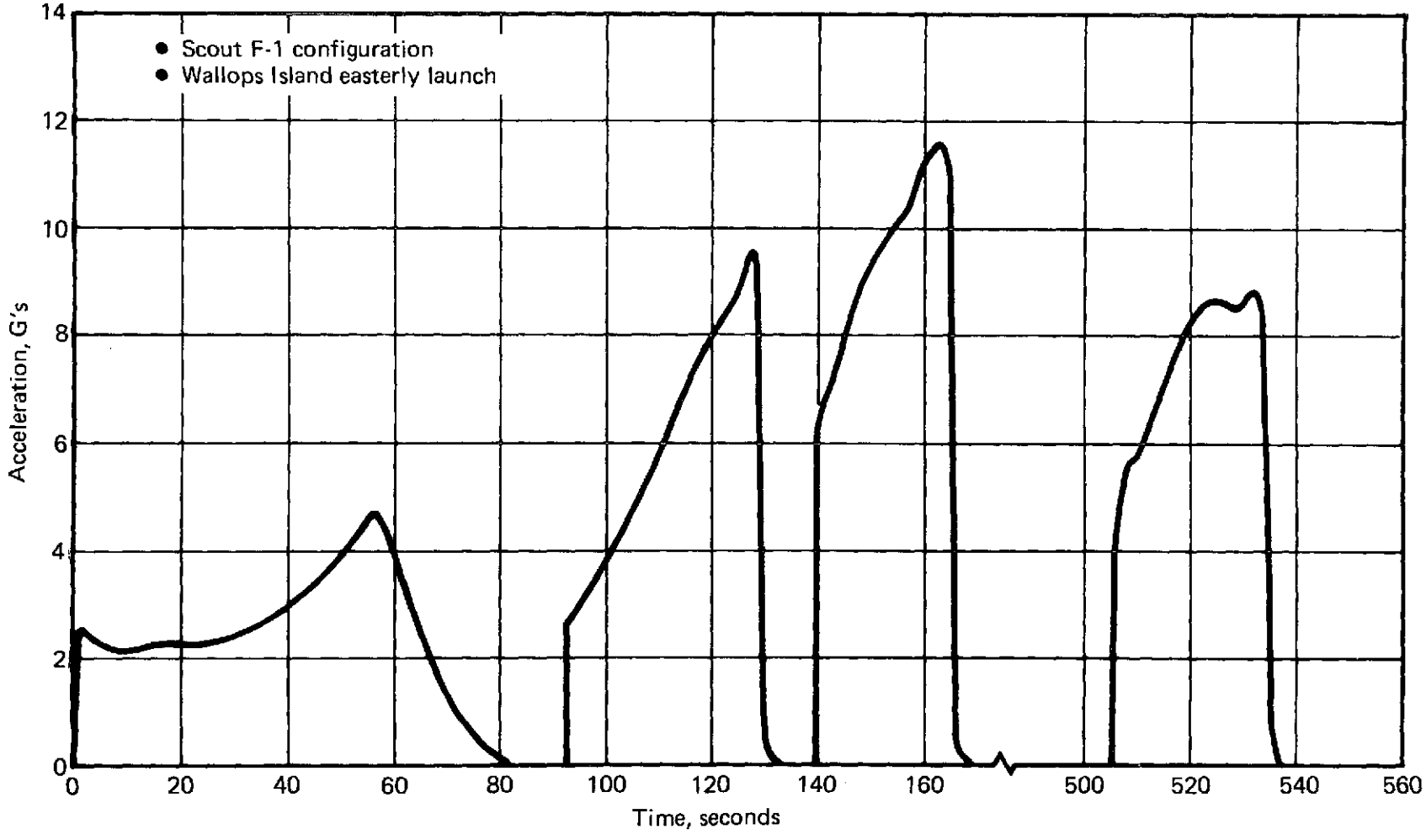


FIGURE 3. – ACCELERATION HISTORY, 200 N. MI. (370.4 KM) CIRCULAR ORBIT

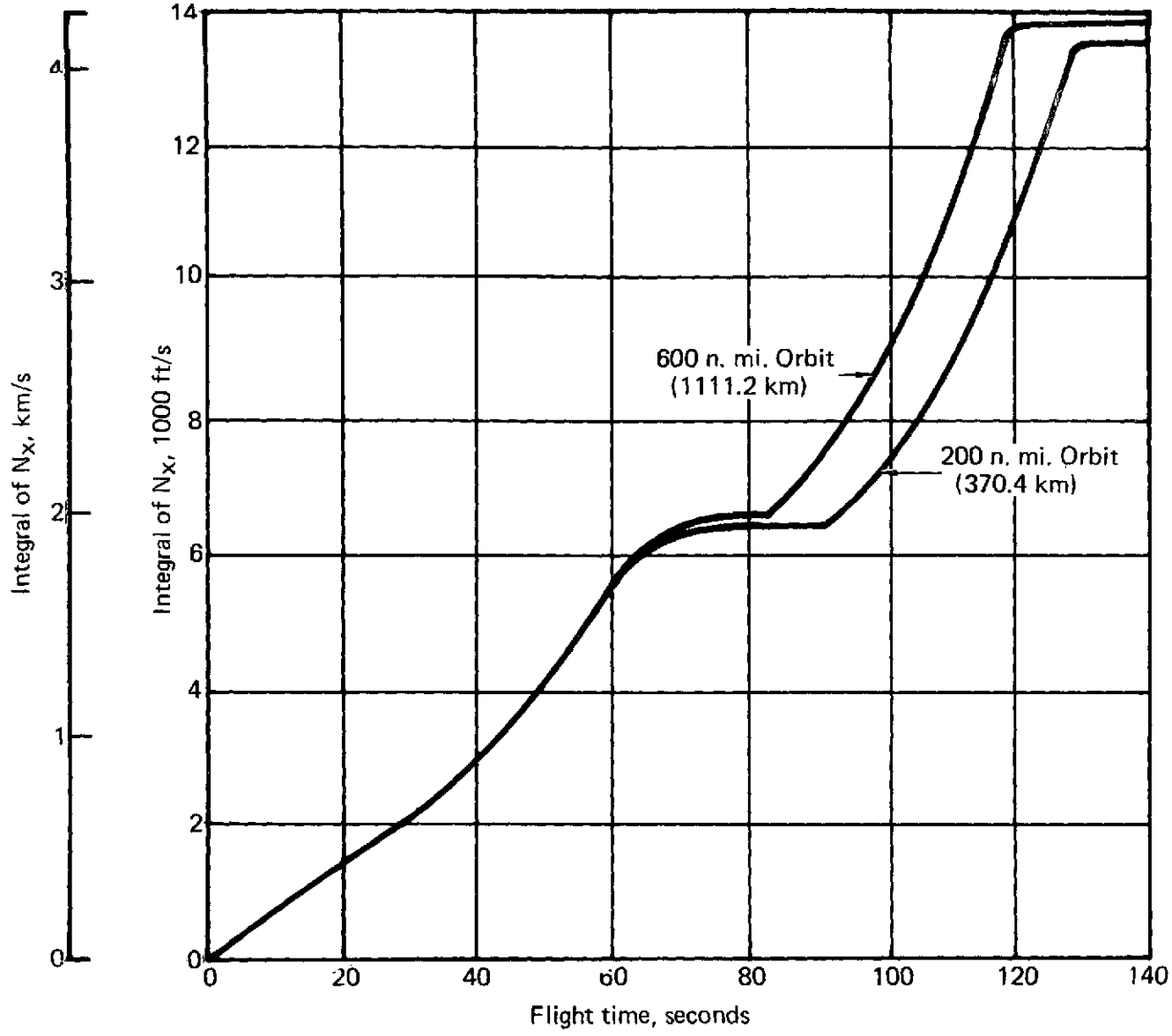


FIGURE 4. – INTEGRAL OF $N_X$ TIME HISTORY, STAGES 1 AND 2

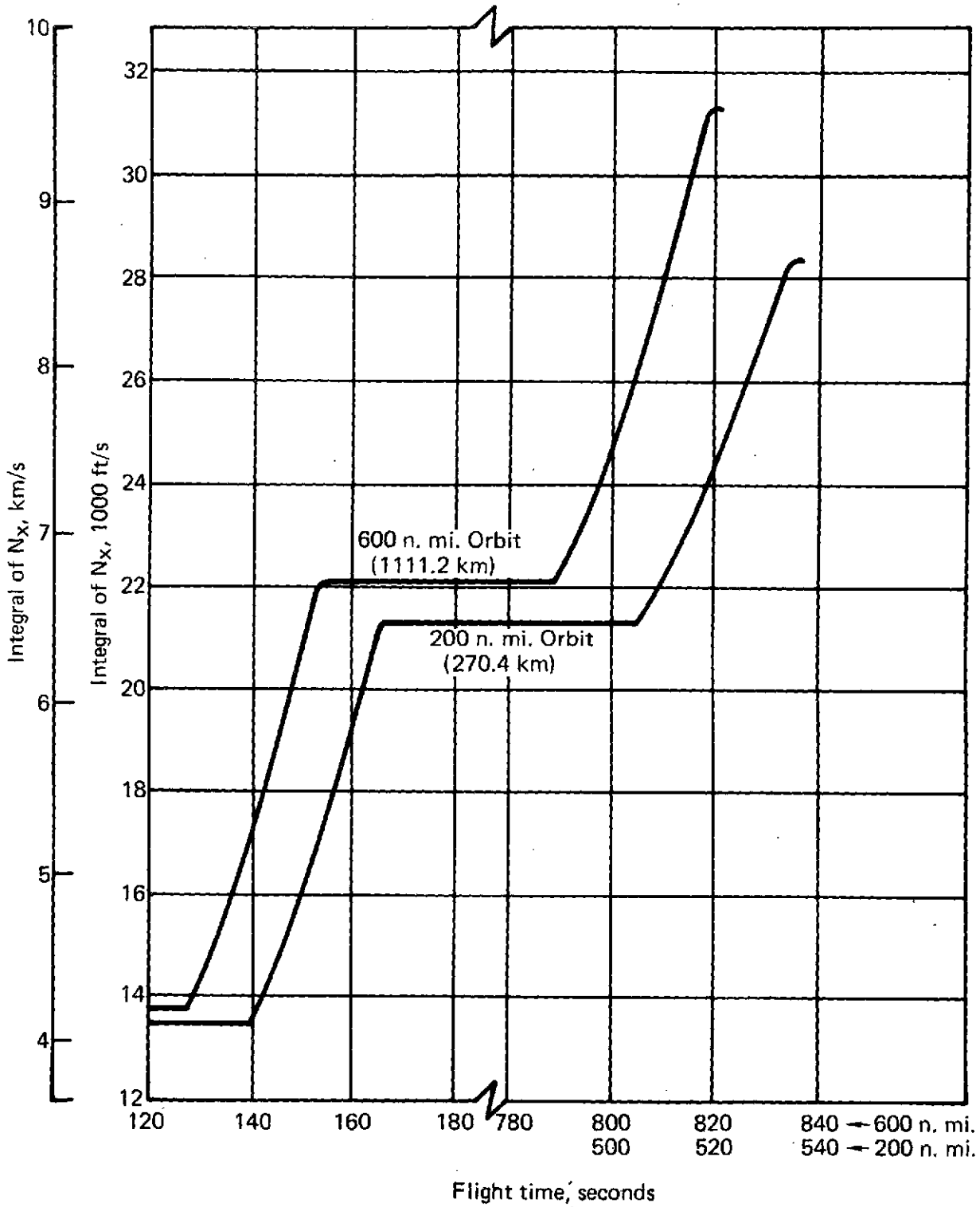


FIGURE 5. – INTEGRAL OF $N_X$ TIME HISTORY, STAGES 3 AND 4

(2) Integral of applied forces as measured by a body mounted accelerometer with its sensitive axis along the vehicle longitudinal axis.

Evaluation of the AVC system equipment measurement errors then can be restricted to these two quantities. Although an inertial measurement unit has inherent capability to measure additional parameters, the $\int N_X$ investigation was restricted to these values for which a correction capability was included.

## 6.1 Attitude Measurement Errors

In considering the operation of the fourth stage AVC system, the basic guideline used throughout the alignment phase as well as the actual flight was that the AVC system will not interfere with the operation of the basic third stage guidance system. The third stage IRP is aligned mechanically to the lower D transition section and an externally mounted poroprism. The vehicle is leveled (pitch and yaw alignment) by adjusting or shimming the launcher. The leveling is accomplished by precisely located transits to sight on alignment targets installed on the upper C and lower D transition sections. Azimuth (roll) alignment is then accomplished by rotating the launcher until the poroprism is properly aligned. The vehicle will continue to be aligned in this manner when the AVC system is utilized. Determination of the AVC attitude errors was predicated on maintaining this alignment procedure.

The gyro error budgets and vehicle alignment errors together with the acceleration and attitude data from the two reference orbit trajectories (given in Section 5.0) were input to the guidance accuracy analysis routine to compute the resulting attitude uncertainties. The guidance accuracy analysis routine is discussed in Appendix A. Attitude errors were determined first for the condition in which the AVC attitude reference operates from launch independent of the existing third stage guidance system. The errors were evaluated both for gimballed and strapdown systems. The resulting attitude errors both at fourth stage ignition and burnout are summarized in Table 6. The launch point coordinate system used is $X_L$-down-range and in the trajectory plane, $Z_L$-vertical and $Y_L$-out of plane completing a right-handed system. There is approximately an order of magnitude difference between the errors corresponding to the maximum and minimum error budgets. Additionally, there is no significant difference between the attitude errors of the strapdown and gimballed systems. In some instances the magnitude of an individual error decreases from 4th stage ignition to 4th stage burnout; this results from the change in direction of 4th stage acceleration causing the mass unbalance and anisoelastic drift terms to decrease slightly.

In the case of operating the 4th stage AVC system attitude reference from the end of third stage coast, the errors were computed at fourth stage ignition and at the 15 second point into the burn time. The 15 second point was selected because 4th stage disturbing moments are maximum at the beginning of burn and tend to decrease thereafter. Once the initial errors are corrected and the 4th stage attitude is maintained within the deadbands, control can be terminated because no further improvement can be achieved. The total time used to evaluate the sensor errors for this option was 35 seconds; 15 seconds – 4th stage burn, 6 seconds – spin-up to ignition, and 14 seconds – 3rd stage coast.

## TABLE 6. – AVC SENSOR ATTITUDE MEASUREMENT ERRORS

- Attitude reference unit operates from launch
- 3$\sigma$ Values

| Condition | Pitch Error | | | | Yaw Error | | | |
|---|---|---|---|---|---|---|---|---|
| | Min Budget | | Max Budget | | Min Budget | | Max Budget | |
| | deg | mrad | deg | mrad | deg | mrad | deg | mrad |
| 600 n. mi. (111.2 km) orbit | | | | | | | | |
| Strapdown – 4th stg ignition | .0684 | 1.194 | .8800 | 15.359 | .0751 | 1.311 | .6815 | 11.894 |
| – 4th stg burnout | .0694 | 1.211 | 1.0661 | 18.607 | .0749 | 1.307 | .6535 | 11.406 |
| Gimballed – 4th stg ignition | .0581 | 1.014 | .7524 | 13.132 | .0762 | 1.330 | .8724 | 15.226 |
| – 4th stg burnout | .0579 | 1.011 | .7310 | 12.758 | .0719 | 1.255 | .9701 | 16.931 |
| 200 n. mi. (370.4 km) orbit | | | | | | | | |
| Strapdown – 4th stg ignition | .0668 | 1.166 | .7304 | 12.748 | .0742 | 1.295 | .4575 | 7.985 |
| – 4th stg burnout | .0675 | 1.178 | .8674 | 15.139 | .0742 | 1.295 | .4521 | 7.891 |
| Gimballed – 4th stg ignition | .0576 | 1.005 | .4891 | 8.536 | .0722 | 1.260 | .6825 | 11.912 |
| – 4th stg burnout | .0575 | 1.004 | .4876 | 8.510 | .0713 | 1.244 | .8081 | 14.104 |

The 14 seconds is for uncage or initiation and stabilization of the attitude reference system. Pitch and yaw errors were computed for the two reference trajectories utilizing the error coefficients previously listed and applying the 4th stage acceleration for the first 15 seconds. The resulting sensor measurement pitch and yaw errors at fourth stage ignition and at the 15 second burn point are given below.

- $3\sigma$ Error quantities

| Condition | Pitch and Yaw Errors | | | |
|---|---|---|---|---|
| | Max Error Budget | | Min Error Budget | |
| | deg | mrad | deg | mrad |
| 600 n. mi. (1111.2 km) orbit | | | | |
| At 4th stage ignition | 0.0833 | 1.454 | 0.0111 | 0.194 |
| At 15 sec burn point | 0.5305 | 9.259 | 0.0620 | 1.082 |
| 200 n. mi. (370.4 km) orbit | | | | |
| At 4th stage ignition | 0.0833 | 1.454 | 0.0111 | 0.194 |
| At 15 sec burn point | 0.5709 | 9.964 | 0.0667 | 1.164 |

Errors in the initial inertial reference (established by the third stage coast control system) are not included in the above values.

## 6.2 System Errors

The ultimate objective of the attitude control portion of the AVC system is to control the inertial orientation at which the fourth stage total incremental velocity is added. This requires then that the thrust axis of the fourth stage be positioned to the desired orientation. All system errors which contribute to the inaccuracy of the inertial orientation of the fourth stage thrust axis must be included in the error analysis.

6.2.1 AVC Attitude Reference Alignment and Readout Errors. – one of the most significant error sources is that of aligning the sensitive axes of the gyros in the attitude reference package or IMU to the vehicle axes. The alignment approach most compatible with the existing Scout procedures is to mechanically align the case of the platform to the vehicle. This approach depends upon a known or fixed alignment of the gyro axes to the case. With a platform, this means that the accuracy of the resolvers or gimbal angle outputs are direct error contributors since they are used to position the inertial cluster relative to the case. With a strapdown type system, the alignment of the gyro sensitive axes to the mounting surfaces of the package can be controlled to a fairly close tolerance. The maximum error permitted for the Scout IRP is ±2 milliradians (0.1146 deg). Gimballed systems vary over a rather wide range if alignment is accomplished by caging the platform and using a mechanical approach. Some specifications require that the angular measurement error from the cluster to the body axes (including readout) not exceed 6 to 8 minutes, (1.75 to 5.33 mrad), for each axis ($1\sigma$). These type accuracies are usually associated with systems that employ a closed loop type control law based upon derived position and velocity data, thus vehicle alignment is not critical. The GEMAR platform alignment accuracy is in the region of 0.15 deg (5.62 mrad) each axis ($3\sigma$) for case type alignment. Space shuttle alignment to the IMU mounting surface will be controlled to one arc minute, (0.29 mrad), each axis.

The errors associated with a gimbal system were used in establishing the alignment and readout error budgets. A maximum budget value of 0.3 deg (5.24 mrad) (3$\sigma$) was used for the error associated with IMU mechanical alignment and resolver readout. The minimum alignment and readout uncertainty values assumed a self-align capability, a laboratory calibration of the platform synchro or resolver outputs at the fourth stage orientation angles and compensation of any known gimbal off-sets. The synchro calibration and determination of any gimbal off-sets would be accomplished in the laboratory. The error values used for the minimum budget case were:

| | | |
|---|---|---|
| Platform alignment | 0.0573 deg | 1.00 mrad (3$\sigma$ values) |
| Synchro repeatability | 0.0167 | 0.29 |
| Gimbal offset compensation | 0.0500 | 0.87 |
| RSS | 0.0779 deg | 1.36 mrad |

The platform self-alignment approach is not applicable to the condition in which the attitude reference operates from the end of third stage coast. For this case, an error of 0.15 deg (2.62 mrad) was used for minimum alignment and readout error budget.

6.2.2 Vehicle Mechanical Alignment Errors. – the pitch and relative yaw errors caused by vehicle build-up uncertainties were the same as those included in the analysis accomplished in Reference 3. Figure 6 shows the locations of the current third stage IRP and the AVC IMU to illustrate the vehicle build-up terms. Those which contribute in the case where the attitude reference operates from launch and mechanical alignment is utilized are:

| | |
|---|---|
| (1) ±0.005 in. (.013 cm) parallelism from aft flange of new transition section to platform mounting plate; 18.0 in. (45.72 cm) diameter | 0.0159 deg (0.277 mrad) |
| (2) ±0.005 in. (.013 cm) perpendicularity tolerance between each end of the fourth stage motor and the motor centerline; 8.98 in. (22.81 cm) radius | 0.0638 deg (1.113 mrad) |
| (3) ±0.005 in. (.013 cm) parallelism between forward surface of lower D section and forward surface of upper D section; 18.04 in. (45.82 cm) diameter | 0.0159 deg (0.277 mrad) |
| (4) ±0.005 in. (.013 cm) parallelism from forward surface of lower D to the IRP shelf | 0.0123 deg (0.215 mrad) |
| Sum = | 0.1079 deg (1.883 mrad) |

All these items are mechanical independent build-up tolerances and were summed to represent the worst case condition. This was the value used for the maximum error budget.

For the minimum error budget case where the platform operates from launch and is self-aligned, the only mechanical build-up tolerances that apply are the first two ( (1) and (2) ) sources. These affect the system because they represent the alignment to the 4th stage axis. This error then is 0.0797 deg (1.391 mrad).

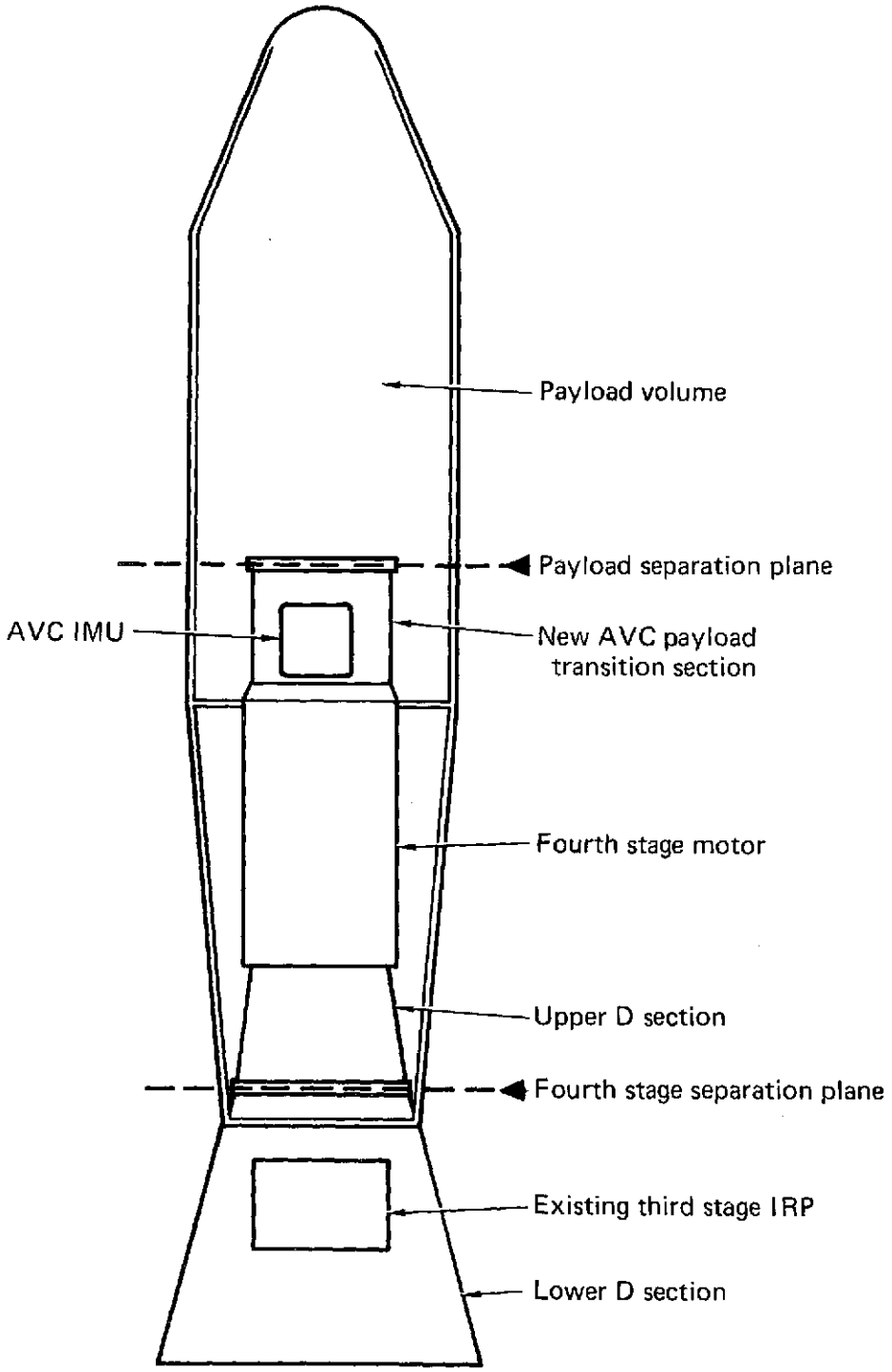


FIGURE 6. – RELATIVE LOCATION OF CURRENT AND AVC GUIDANCE COMPONENTS

6.2.3 AVC System Deadbands. – the deadbands achievable with the AVC system have not been established by system simulations. Maximum and minimum pitch and yaw deadbands of 0.5 and 0.35 deg (8.73 and 6.11 mrad) were used in the analysis.

6.2.4 AVC System Uncage Transient. – this error source was added to account for pitch and yaw errors resulting from any transients caused by uncaging the unit during flight. The maximum and minimum values of 0.15 deg and 0.0167 deg (2.62 to 0.29 mrad) are felt to be conservative in both cases.

## 6.3 Total Errors

6.3.1 Attitude Errors Summary. – the total attitude error summaries are shown in Tables 7 through 14. In each case the AVC system errors shown are those for a gimballed platform. Tables 7 through 10 summarize the errors associated with an AVC system which determines or computes the vehicle attitude from launch. Errors for the 600 n. mi. (111.2 km) trajectory at fourth stage ignition and at fourth stage burnout are given in Tables 7 and 8. The greatest difference in attitude error in going from the minimum error budget values to the maximum is about 0.6 deg (10.47 mrad) in pitch. Equivalent values for the 200 n. mi. (370.4 km) orbit are in Tables 9 and 10.

Tables 11 through 14 show similar data for the case in which the fourth stage AVC attitude reference system operates only during fourth stage, assuming the vehicle attitude near the end of third stage coast as the reference. Some additional errors are considered for this case. First, an uncage transient error is included since the vehicle is in motion at the start of operation. The second, and most significant additional error (which is the largest error source of all), is that of the attitude uncertainties of the current third stage guidance system. The values shown in Tables 11 through 14 were derived from flight data assembled for the 37 flight samples. These errors represent the total vehicle inertial orientation errors which include the third stage deadband errors, as well as the guidance system contributions. The total angular variation from minimum to maximum error budgets for systems which operate from third stage coast is less than that for systems operating from launch; the greatest difference being about 0.3 deg (5.24 mrad) in pitch.

6.3.2 Acceleration Measurement Errors. – errors in measurement of the integral of the longitudinal load factor were evaluated for both trajectories. Parameters to be measured are those shown in Figures 4 and 5. The maximum and minimum accelerometer error budgets as shown in Table 2 were used to compute the measurement errors at each burnout. The results are given in Table 15. The maximum errors are roughly a factor of 3 greater than the minimum values.

## TABLE 7. – FOURTH STAGE IGNITION ATTITUDE ERRORS – SYSTEM OPERATION FROM LAUNCH, 600 N. MI. (1111.2 KM) ORBIT

• 3$\sigma$ Error values

| Source | Pitch Error | | | | Yaw Error | | | |
|---|---|---|---|---|---|---|---|---|
| | Max Budget | | Min Budget | | Max Budget | | Min Budget | |
| | deg | mrad | deg | mrad | deg | mrad | deg | mrad |
| I. AVC measurement errors (drift & vehicle alignment) | 0.7524 | 13.132 | 0.0581 | 1.014 | 0.8724 | 15.226 | 0.0762 | 1.330 |
| II. IMU alignment and readout | | | | | | | | |
| Mechanical align. to new transition sect. - platform caging | 0.3000 | 5.236 | | | 0.3000 | 5.236 | | |
| Platform self-align + synchro error + gimbal offset compensation | | | 0.0779 | 1.360 | | | 0.0779 | 1.360 |
| III. Vehicle mechanical alignment | | | | | | | | |
| From new transition section to lower D | 0.1079 | 1.883 | | | 0.1079 | 1.883 | | |
| From new transition sect. to 4th stg long. axis for platform self-alignment case | | | 0.0797 | 1.391 | | | 0.0797 | 1.391 |
| IV. AVC system deadband | 0.5000 | 8.727 | 0.3500 | 6.109 | 0.5000 | 8.727 | 0.3500 | 6.109 |
| Total (RSS) | 0.9580 | 16.720 | 0.3719 | 6.491 | 1.0549 | 18.411 | 0.3751 | 6.547 |

## TABLE 8. – FOURTH STAGE BURNOUT ATTITUDE ERRORS – SYSTEM OPERATION FROM LAUNCH, 600 N. MI. (1111.2 KM) ORBIT

- $3\sigma$ Error values

| Source | Pitch Error | | | | Yaw Error | | | |
|---|---|---|---|---|---|---|---|---|
| | Max Budget | | Min Budget | | Max Budget | | Min Budget | |
| | deg | mrad | deg | mrad | deg | mrad | deg | mrad |
| I. AVC measurement errors (drift & vehicle alignment) | 0.7310 | 12.758 | 0.0579 | 1.011 | 0.9701 | 16.931 | 0.0791 | 1.255 |
| II. IMU alignment and readout | | | | | | | | |
| Mechanical align. to new transition sect. – platform caging | 0.3000 | 5.236 | | | 0.3000 | 5.236 | | |
| Pltfm self-align + synchro error + gimbal offset compensation | | | 0.0779 | 1.360 | | | 0.0779 | 1.360 |
| III. Vehicle mech. alignment | | | | | | | | |
| From new transition sect. to lower D | 0.1079 | 1.833 | | | 0.1079 | 1.833 | | |
| From new transition sect. to 4th stg long. axis for platform self-alignment case | | | 0.0797 | 1.391 | | | 0.0797 | 1.391 |
| IV. AVC system deadband | 0.5000 | 8.727 | 0.3500 | 6.109 | 0.5000 | 8.727 | 0.3500 | 6.109 |
| Total (RSS) | 0.9413 | 16.429 | 0.3719 | 6.491 | 1.1369 | 19.843 | 0.3743 | 6.533 |

## TABLE 9. – FOURTH STAGE IGNITION ATTITUDE ERRORS – SYSTEM OPERATION FROM LAUNCH, 200 N. MI. (370.4 KM) ORBIT

- $3\sigma$ Error values

| Source | Pitch Error | | | | Yaw Error | | | |
|---|---|---|---|---|---|---|---|---|
| | Max Budget | | Min Budget | | Max Budget | | Min Budget | |
| | deg | mrad | deg | mrad | deg | mrad | deg | mrad |
| I. AVC measure errors (drift & vehicle align.) | 0.4891 | 8.536 | 0.0576 | 1.005 | 0.6825 | 11.912 | 0.0722 | 1.260 |
| II. IMU alignment and readout | | | | | | | | |
| Mech. alignment to new transition sect. – platform caging | 0.3000 | 5.236 | | | 0.3000 | 5.236 | | |
| Pltfm. self-align. + synchro error + gimbal offset compensation | | | 0.0779 | 1.360 | | | 0.0779 | 1.360 |
| III. Vehicle mech. alignment | | | | | | | | |
| From new transition sect. to lower D | 0.1079 | 1.883 | | | 0.1079 | 1.883 | | |
| From new transition sect. to 4th stage long. axis for platform self-alignment case | | | 0.0797 | 1.391 | | | 0.0797 | 1.391 |
| IV. AVC system deadband | 0.5000 | 8.727 | 0.3500 | 6.109 | 0.5000 | 8.727 | 0.3500 | 6.109 |
| Total (RSS) | 0.7687 | 13.416 | 0.3718 | 6.489 | 0.9042 | 15.781 | 0.3754 | 6.552 |

## TABLE 10. – FOURTH STAGE BURNOUT ATTITUDE ERRORS – SYSTEM OPERATION FROM LAUNCH, 200 N. MI. (370.4 KM) ORBIT

- 3$\sigma$ Error values

| Source | Pitch Error | | | | Yaw Error | | | |
|---|---|---|---|---|---|---|---|---|
| | Max Budget | | Min Budget | | Max Budget | | Min Budget | |
| | deg | mrad | deg | mrad | deg | mrad | deg | mrad |
| I. AVC system errors (drift & vehicle alignment) | 0.4876 | 8.510 | 0.0575 | 1.004 | 0.8080 | 14.104 | 0.0713 | 1.244 |
| II. IMU alignment and readout | | | | | | | | |
| Mech. alignment to new transition sect. – platform caging | 0.3000 | 5.236 | | | 0.3000 | 5.236 | | |
| Pltfm. self-alignment + synchro error + gimbal offset compensation | | | 0.0779 | 1.360 | | | 0.0779 | 1.360 |
| III. Vehicle mechanical alignment | | | | | | | | |
| From new transition sect. to lower D | 0.1079 | 1.883 | | | 0.1079 | 1.883 | | |
| From new transition sect. to 4th stg long. axis for platform self-alignment case | | | 0.0797 | 1.391 | | | 0.0797 | 1.391 |
| IV. AVC system deadband | 0.5000 | 8.727 | 0.3500 | 6.109 | 0.5000 | 8.727 | 0.3500 | 6.109 |
| Total (RSS) | 0.7677 | 13.399 | 0.3718 | 6.489 | 1.0023 | 17.493 | 0.3742 | 6.531 |

## TABLE 11. – FOURTH STAGE IGNITION ATTITUDE ERRORS – SYSTEM OPERATION FROM THIRD STAGE COAST, 600 N. MI. (1111.2 KM) ORBIT

- $3\sigma$ Error values

| Source | Pitch Error | | | | Yaw Error | | | |
|---|---|---|---|---|---|---|---|---|
| | Max Budget | | Min Budget | | Max Budget | | Min Budget | |
| | deg | mrad | deg | mrad | deg | mrad | deg | mrad |
| I. AVC measurement errors | 0.0833 | 1.454 | 0.0111 | 0.194 | 0.0833 | 1.454 | 0.0111 | 0.194 |
| II. IMU alignment and readout | | | | | | | | |
| Mech. alignment to new transition sect. – platform caging | 0.3000 | 5.236 | 0.1500 | 2.618 | 0.3000 | 5.236 | 0.1500 | 2.618 |
| Align of third stage IRP to mtg. plate | 0.1146 | 2.000 | 0.1146 | 2.000 | 0.1146 | 2.000 | 0.1146 | 2.000 |
| III. Vehicle mech. alignment | | | | | | | | |
| From new transition sect. to lower D | 0.1079 | 1.883 | 0.1079 | 1.883 | 0.1079 | 1.883 | 0.1079 | 1.883 |
| IV. AVC system deadband | 0.5000 | 8.727 | 0.3500 | 6.109 | 0.5000 | 8.727 | 0.3500 | 6.109 |
| V. AVC system uncage transient | 0.1500 | 2.618 | 0.0167 | 0.291 | 0.1500 | 2.618 | 0.0167 | 0.291 |
| VI. Current third stage guidance errors (including deadband & induced errors) | 0.6245 | 10.900 | 0.6245 | 10.900 | 1.1487 | 20.049 | 1.1487 | 20.049 |
| Total (RSS) | 0.8856 | 15.457 | 0.7485 | 13.064 | 1.3091 | 22.848 | 1.2205 | 21.302 |

## TABLE 12. – FOURTH STAGE ATTITUDE ERRORS, 15 SECOND BURN POINT – SYSTEM OPERATION FROM THIRD STAGE COAST, 600 N. MI. (1111.2 KM) ORBIT

- $3\sigma$ Error values

| Source | Pitch Error | | | | Yaw Error | | | |
|---|---|---|---|---|---|---|---|---|
| | Max Budget | | Min Budget | | Max Budget | | Min Budget | |
| | deg | mrad | deg | mrad | deg | mrad | deg | mrad |
| I. AVC measurement errors | 0.5305 | 9.259 | 0.0620 | 1.082 | 0.5305 | 9.259 | 0.0620 | 1.082 |
| II. IMU alignment and readout | | | | | | | | |
| Mechanical align. to new transition sect. – platform caging | 0.3000 | 5.236 | 0.1500 | 2.618 | 0.3000 | 5.236 | 0.1500 | 2.618 |
| Align. of third stage IRP to mtg. plate | 0.1146 | 2.000 | 0.1146 | 2.000 | 0.1146 | 2.000 | 0.1146 | 2.000 |
| III. Vehicle mechanical align. | | | | | | | | |
| From new transition sect. to lower D | 0.1079 | 1.883 | 0.1079 | 1.883 | 0.1079 | 1.883 | 0.1079 | 1.883 |
| IV. AVC system deadband | 0.5000 | 8.727 | 0.3500 | 6.109 | 0.5000 | 8.727 | 0.3500 | 6.109 |
| V. AVC system uncage transient | 0.1500 | 2.618 | 0.0167 | 0.291 | 0.1500 | 2.618 | 0.0167 | 0.291 |
| VI. Current third stage guidance errors (including deadband and induced errors) | 0.6245 | 10.900 | 0.6245 | 10.900 | 1.1487 | 20.049 | 1.1487 | 20.049 |
| Total (RSS) | 1.0289 | 17.958 | 0.7509 | 13.109 | 1.4100 | 24.609 | 1.2221 | 21.300 |

## TABLE 13. – FOURTH STAGE IGNITION ATTITUDE ERRORS – SYSTEM OPERATION FROM THIRD STAGE COAST, 200 N. MI. (370.4 KM) ORBIT

- 3$\sigma$ Error values

| Source | Pitch Error | | | | Yaw Error | | | |
|---|---|---|---|---|---|---|---|---|
| | Max Budget | | Min Budget | | Max Budget | | Min Budget | |
| | deg | mrad | deg | mrad | deg | mrad | deg | mrad |
| I. AVC measurement errors | 0.0833 | 1.454 | 0.0111 | 0.194 | 0.0833 | 1.454 | 0.0111 | 0.194 |
| II. IMU alignment and readout | | | | | | | | |
| Mech. alignment to new transition sect. – platform caging | 0.3000 | 5.236 | 0.1500 | 2.618 | 0.3000 | 5.236 | 0.1500 | 2.618 |
| Align. of third stage IRP to mtg plate | 0.1146 | 2.000 | 0.1146 | 2.000 | 0.1146 | 2.000 | 0.1146 | 2.000 |
| III. Vehicle mechanical alignment | | | | | | | | |
| From new transition sect. to lower D | 0.1079 | 1.883 | 0.1079 | 1.883 | 0.1079 | 1.883 | 0.1079 | 1.883 |
| IV. AVC system deadband | 0.5000 | 8.727 | 0.3500 | 6.109 | 0.5000 | 8.727 | 0.3500 | 6.109 |
| V. AVC system uncage transient | 0.1500 | 2.618 | 0.0167 | 0.291 | 0.1500 | 2.618 | 0.0167 | 0.291 |
| VI. Current third stage guidance errors (including deadband & induced errors) | 0.6245 | 10.900 | 0.6245 | 10.900 | 1.1487 | 20.049 | 1.1487 | 20.049 |
| Total (RSS) | 0.8856 | 15.457 | 0.7485 | 13.064 | 1.3091 | 22.848 | 1.2205 | 21.302 |

## TABLE 14. – FOURTH STAGE ATTITUDE ERRORS, 15 SECOND BURN POINT – SYSTEM OPERATION FROM THIRD STAGE COAST, 200 N. MI. (370.4 KM) ORBIT

- 3σ Error values

| Source | Pitch Error | | | | Yaw Error | | | |
|---|---|---|---|---|---|---|---|---|
| | Max Budget | | Min Budget | | Max Budget | | Min Budget | |
| | deg | mrad | deg | mrad | deg | mrad | deg | mrad |
| I. AVC measurement errors | 0.5709 | 9.964 | 0.0667 | 1.164 | 0.5709 | 9.964 | 0.0667 | 1.164 |
| II. IMU alignment and readout | | | | | | | | |
| Mechanical align. to new transition sect. – platform caging | 0.3000 | 5.236 | 0.1500 | 2.618 | 0.3000 | 5.236 | 0.1500 | 2.618 |
| Align. of third stage IRP to mtg. plate | 0.1146 | 2.000 | 0.1146 | 2.000 | 0.1146 | 2.000 | 0.1146 | 2.000 |
| III. Vehicle mechanical alignment | | | | | | | | |
| From new transition sect. to lower D | 0.1079 | 1.883 | 0.1079 | 1.883 | 0.1079 | 1.883 | 0.1079 | 1.883 |
| IV. AVC system deadband | 0.5000 | 8.727 | 0.3500 | 6.109 | 0.5000 | 8.727 | 0.3500 | 6.109 |
| V. AVC system uncage transient | 0.1500 | 2.618 | 0.0167 | 0.291 | 0.1500 | 2.618 | 0.0167 | 0.291 |
| VI. Current third stage guidance errors (including deadband & induced errors) | 0.6245 | 10.900 | 0.6245 | 10.900 | 1.1487 | 20.049 | 1.1487 | 20.049 |
| Total (RSS) | 1.0503 | 18.331 | 0.7513 | 13.144 | 1.4257 | 24.883 | 1.2223 | 21.333 |

TABLE 15. – SUMMARY – ACCELEROMETER MEASUREMENT ERRORS

- $3\sigma$ Error values
- Errors in measurement of $\int N_X$

600 n. mi. (1111.2 km) Trajectory

| Trajectory Event | Min Error Budget | | Max Error Budget | |
|---|---|---|---|---|
| | ft/s | m/s | ft/s | m/s |
| Fourth stage burnout | 16.39 | 5.00 | 47.83 | 14.58 |
| Third stage burnout | 11.01 | 3.36 | 27.47 | 8.37 |
| Second stage burnout | 6.54 | 1.99 | 15.85 | 4.83 |
| First stage burnout | 3.03 | 0.92 | 7.32 | 2.23 |

200 n. mi. (370.4 km) Trajectory

| Trajectory Event | Min Error Budget | | Max Error Budget | |
|---|---|---|---|---|
| | ft/s | m/s | ft/s | m/s |
| Fourth stage burnout | 14.28 | 4.35 | 38.52 | 11.74 |
| Third stage burnout | 10.54 | 3.21 | 26.19 | 7.98 |
| Second stage burnout | 6.42 | 1.96 | 15.64 | 4.77 |
| First stage burnout | 2.96 | 0.90 | 7.17 | 2.19 |

## 7.0 SECOND AND THIRD STAGE DEADBAND REDUCTIONS

A investigation of the feasibility of reducing the Scout second and third stage control system deadbands was conducted under a separate contract task. The results are included in this report since they could be applied in conjunction with the AVC system to either gain further accuracy improvements or reduce the correction capability required of the AVC system.

### 7.1 Analysis Approach

Past mission accuracy studies have assumed that the Scout second and third stage pitch and yaw control system deadbands of 0.8 degrees (.014 rad) was a reasonable approximation to the effective pitch or yaw attitude error. These errors propagate to certain errors at fourth stage ignition.

Other Scout studies have shown that during second and third stage boost, filtering was required for the control system. The filter was designed to prevent opposite motor cyling at the bending frequency. When the vehicle had a thrust misalignment disturbance, the cycling of a controlling motor could excite the bending modes to high enough amplitude to cause the error signal to cross the deadband and fire the opposite motor. The body bending filter which attenuates bending frequency signals was introduced to prevent this. The control system response time increased because of the phase lag introduced by the filter. This results in higher duty cycles when there is little or no disturbance

(limit cycle motion). Without disturbances, the duty cycles, and thus control fuel consumption, are functions of the system time delays, control accelerations, and deadband size. High control accelerations and long time delays are accomodated by using a sufficiently large deadband to keep duty cycles within acceptable limits. If a deadband becomes too small, it can be crossed before a control motor turns off. This is known as deadband overshoot. When this occurs, the control system duty cycles approach and, in certain circumstances, exceed 100 percent. Under these circumstances it may be worse to have low disturbances during boost than to have disturbances almost equal to the control motor capability.

The analysis conducted was made to determine if reducing the system deadband to improve accuracy was feasible. This was accomplished by the following tasks:

(1) The minimum allowable deadband was calculated for the deadband overshoot case with no disturbances. This represents the system deadband improvements with an ideal filter and defines the lower limit deadband for second and third stage.

(2) A computer routine was used to estimate the effect of structural coupling on second stage coast duty cycle. Both "filter in" and "filter out" conditions were analyzed.

(3) A Filter Attenuation Requirements Routine was used to calculate the minimum deadband allowable for second and third stage boost to prevent opposite motor cycling at the bending frequency.

(4) Probability distributions of the average pitch and yaw attitude error were calculated for deadband variations.

## 7.2 Analysis

There are at least two important constraints used to determine if the control system deadbands can be reduced; (1) the lower limit deadband for the rigid body deadband overshoot case without disturbances and (2) the opposite motor cycling at the bending frequency due to structural coupling with the control system when disturbing moments exist. Either of these occurrences would result in excessive control fuel consumption. The former was found to be the limiting factor for second stage and the latter for third stage.

7.2.1 Deadband Overshoot Case (Rigid Body). – deadband overshoot occurs when the vehicle passes through the opposite deadband before the firing control motor turns off. This results in a very high duty cycle and thus excessive control fuel usage. The minimum deadband size required to prevent deadband overshoot can be derived from the control system and vehicle parameters. The relationship is given below:

$$d_{MIN} = \frac{F_C\,[(X_C - X_{CG})\cos\beta + Z_C \sin\beta]\,(T_2)\left(\frac{K_R}{K_D} - \frac{T_2}{2}\right)\left(\frac{K_R}{K_D} - \frac{T_1}{2}\right)}{\left[2\frac{K_R}{K_D} - (T_1 + T_2) - HR\left(\frac{K_R}{K_D} - \frac{T_1}{2}\right)\right] 12\, I_{YY}}$$

The minimum allowable deadbands were calculated for the critical cases which are:

| | | 2nd Stage | 3rd Stage |
|---|---|---|---|
| (1) | +3σ Control motor thrust, $F_C$ | 540 lbf<br>($2.402 \times 10^3$ N) | 52 lbf<br>($2.313 \times 10^2$ N) |
| (2) | 100% Booster fuel consumed, $X_{CG}$ | 233.5 in.<br>(5.931 m) | 120 in.<br>(3.048 m) |
| | $I_{YY}$ | 25 200 slug-ft$^2$<br>(34 166 kg-m$^2$) | 1 200 slug-ft$^2$<br>(1 627 kg-m$^2$) |
| (3) | +3σ Control system time delays: | | |
| | Turn on, $T_1$ | .1442 s | .1049 s |
| | Turn off, $T_2$ | .1112 s | .0914 s |
| (4) | Maximum gain ratio, $K_R/K_D$ | 0.55 s | 0.55 s |
| (5) | "Ideal" filter in, time delay (included in (3), $T_1$ and $T_2$) | 0.0459 s | 0.0459 s |

The symbols used in the above expressions, together with compatible units are defined by the following listing:

| Symbol | Units | Definition |
|---|---|---|
| $d_{MIN}$ | radians | Minimum deadband halfwidth |
| $F_C$ | lbf | Control motor force |
| $X_C$ | station (inches) | Control motor location |
| $X_{CG}$ | station (inches) | Center of mass |
| $\beta$ | degrees | Control motor cant angle |
| $Z_C$ | inches | Control motor radial location |
| $K_R/K_D$ | seconds | Gain ratio |
| $T_1$ | seconds | Control system turn on delay |
| $T_2$ | seconds | Control system turn off delay |
| HR | – | Hysteresis ratio |
| $I_{YY}$ | slug-ft$^2$ | Moment of inertia |

Calculations were made for both second and third stages; the results are presented in Figures 7 and 8, respectively. As shown in Figure 7, the minimum allowable second stage deadband is approximately 0.8 degree (.014 rad) which is the current flight value. This rigid body overshoot case with no disturbance was the more critical constraint in determining the second stage deadband size. Previous second and third stage oscillation studies verified that the 0.8 degree (.014 rad) deadband was acceptable when body bending was considered. Based on rigid body response, the second stage coast deadbands with the filter switched out can be smaller. However, since the vehicle is usually in a near symmetric limit cycle during coast, mission accuracy would not be noticeably improved with reduced

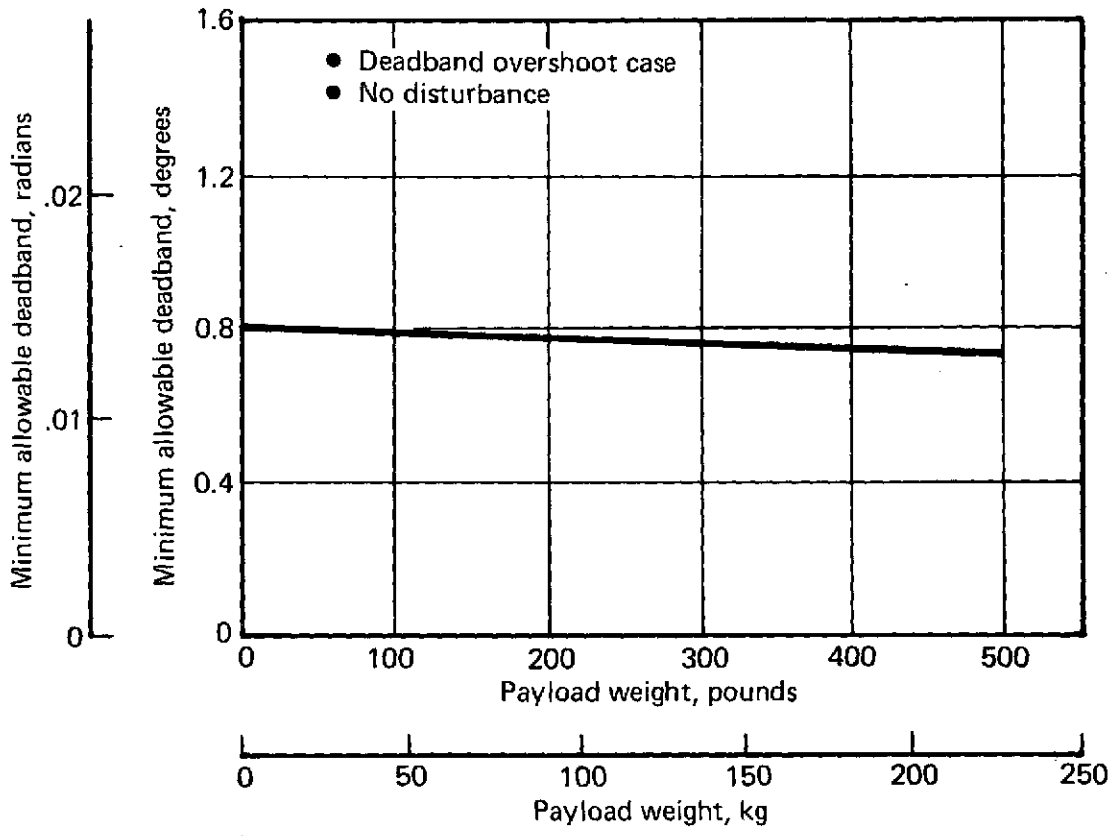


FIGURE 7. – MINIMUM SECOND STAGE DEADBANDS

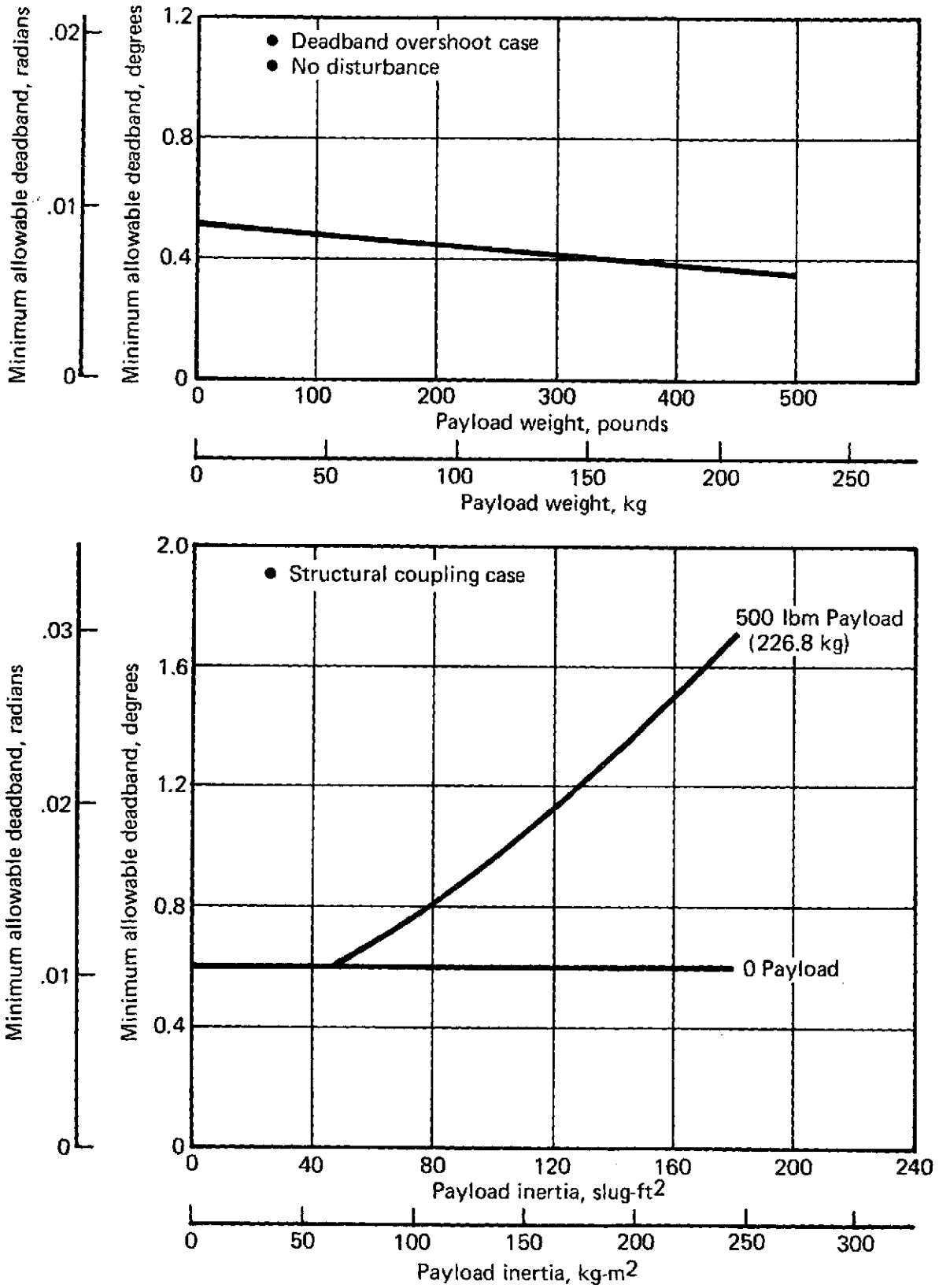


FIGURE 8. – MINIMUM THIRD STAGE DEADBANDS

coast deadbands. This is because the average attitude error is essentially zero. The duty cycle would be greater with narrower deadbands thus reducing coast time due to more control fuel usage. Therefore, the effect of structural coupling on fuel consumption during second stage coast with narrower deadbands was not evaluated.

Figure 8 presents the third stage minimum allowable deadband versus payload weight. This shows that the deadband could be reduced to about 0.4 deg (.007 rad) before deadband overshoot would occur without disturbances. However, as will be discussed in the following paragraph, the structural coupling becomes the critical constraint for third stage.

7.2.2 Structural Coupling. – the deadbands cannot be reduced during second stage boost and coast with the filter in due to the deadband overshoot constraint. An additional investigation was made of the structural coupling using the approach discussed in Reference 4. Both filter in and filter out conditions were analyzed for the current as well as reduced deadbands. The duty cycle increases to an unacceptable level when the deadband is halved: duty cycle = 11 to 17% for 0.8 deg (.014 rad) deadband; duty cycle = 73% for 0.4 deg (.007 rad). The analysis accomplished in Reference 4 for the second stage structural coupling effect showed the current 0.8 deg (.014 rad) deadband (filter out) to be acceptable. The fuel consumption and coast time predictions are also acceptable.

The third stage boost deadband can be reduced to 0.6 degree (.0105 rad) for payloads of up to 500 pounds (226.8 kg) with inertias of less than 46 slug-ft$^2$ (62.4 kg-m$^2$). Figure 8 shows the minimum allowable deadband versus payload inertia for the minimum and maximum payload weight. These data are based on the analyses presented in Reference 5.

The frequency response of the Scout upper stage notch filter is shown in Figure 9. The boundary marked is the attenuation required to prevent opposite motor cycling at the bending frequency with third stage boost disturbances. This is based on the critical case which includes the minimum spin bearing stiffness.

The value of structural damping factor used was 0.005, which is based on flight data and was used for the third stage filter design requirements. It is possible that the structural damping factor has changed since the incorporation of the new spin bearing.

A reduction in the third stage boost deadband to 0.6 degree (.0105 rad) would require some vehicle modification. This would be necessary since a common deadband setting is currently used from second stage ignition through third stage burn-out.

The third stage coast deadbands (a separate gain setting) should not be reduced from the current setting of ±0.229 degree (.004 rad). Many Scout missions have requirements for long third stage coast times (up to 600 seconds) and significant reduction in deadband would reduce the coast time allowable to a value less than that required to achieve high altitude orbits.

7.2.3 Pitch and Yaw Attitude Errors. – the probability distribution functions for the pitch and yaw attitude errors were determined for several conditions. These were predicted based on the motion of the vehicle with the nominal control system characteristics and thrust misalignment probability distributions obtained from flight. Figures 10 and 11 are representative of the probability distribution functions; pitch and yaw errors for third stage with 75% fuel consumed are shown. The character of the contours change somewhat for the other conditions calculated. Data for the 99.87% point are given in Table 16 for all cases considered. The data computed for the 0.8 degree (.014 rad) deadband compare favorably with the flight results obtained.

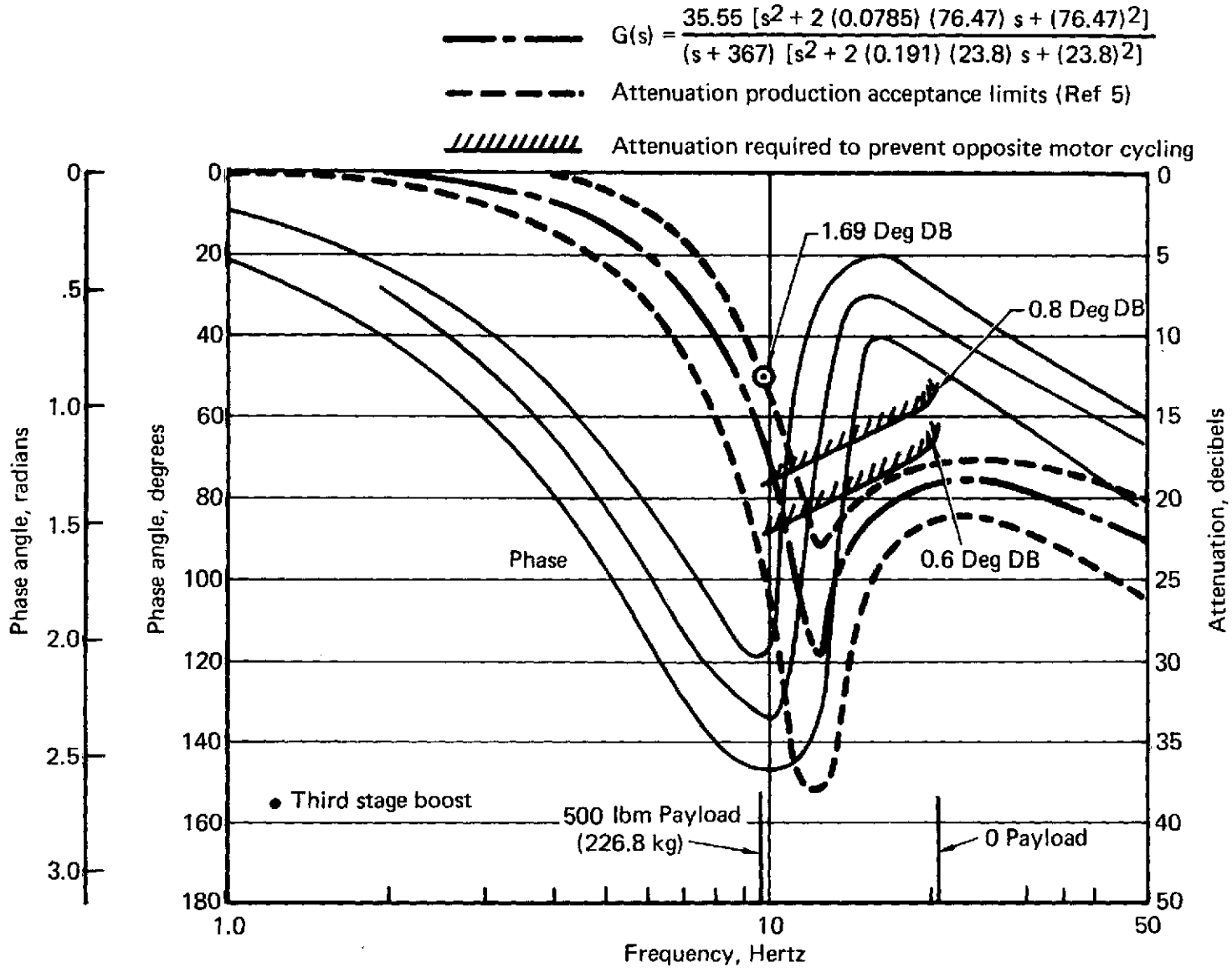


FIGURE 9. – PITCH AND YAW BODY BENDING FILTER FREQUENCY RESPONSE

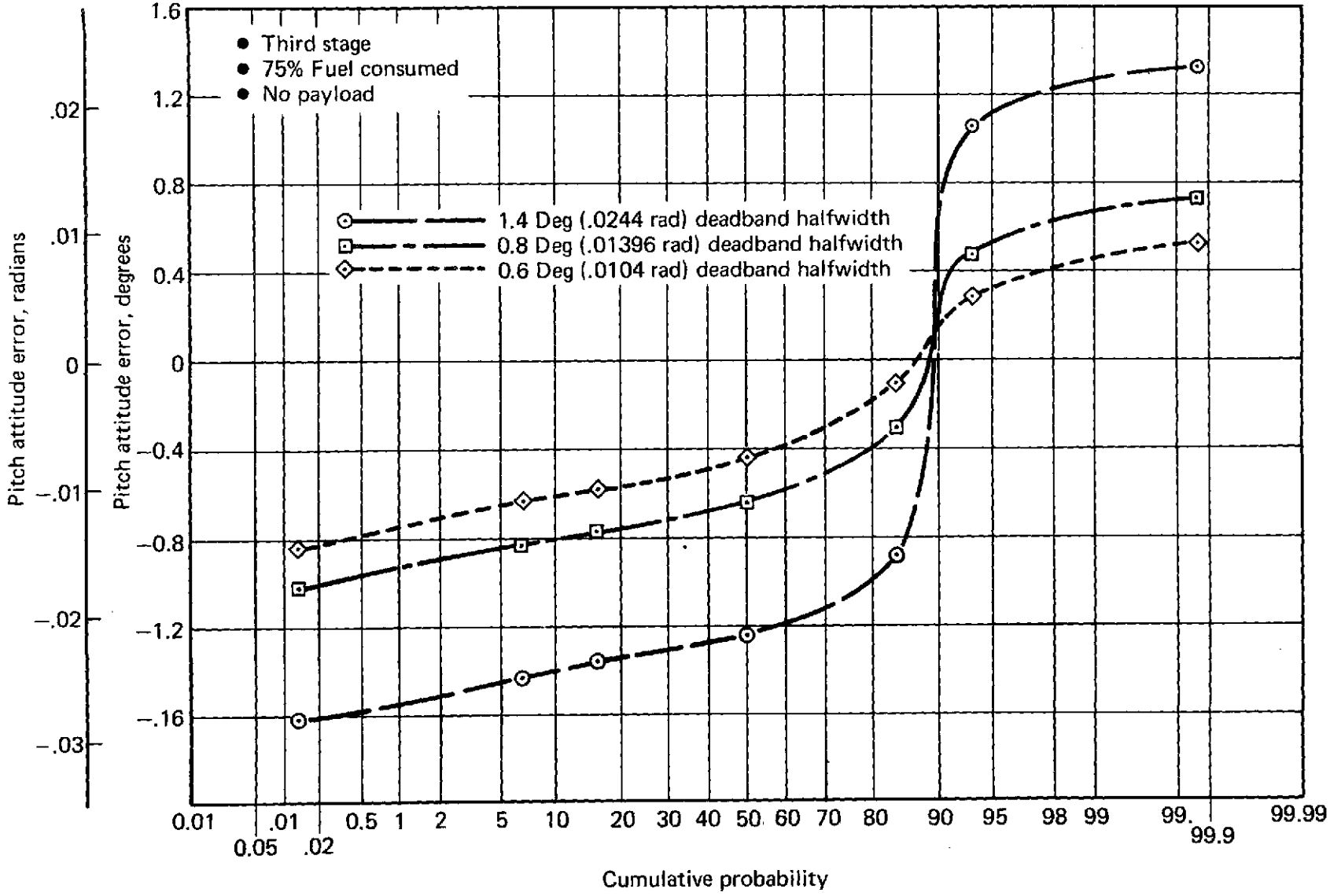


FIGURE 10. – PITCH ATTITUDE ERROR VS CUMULATIVE PROBABILITY

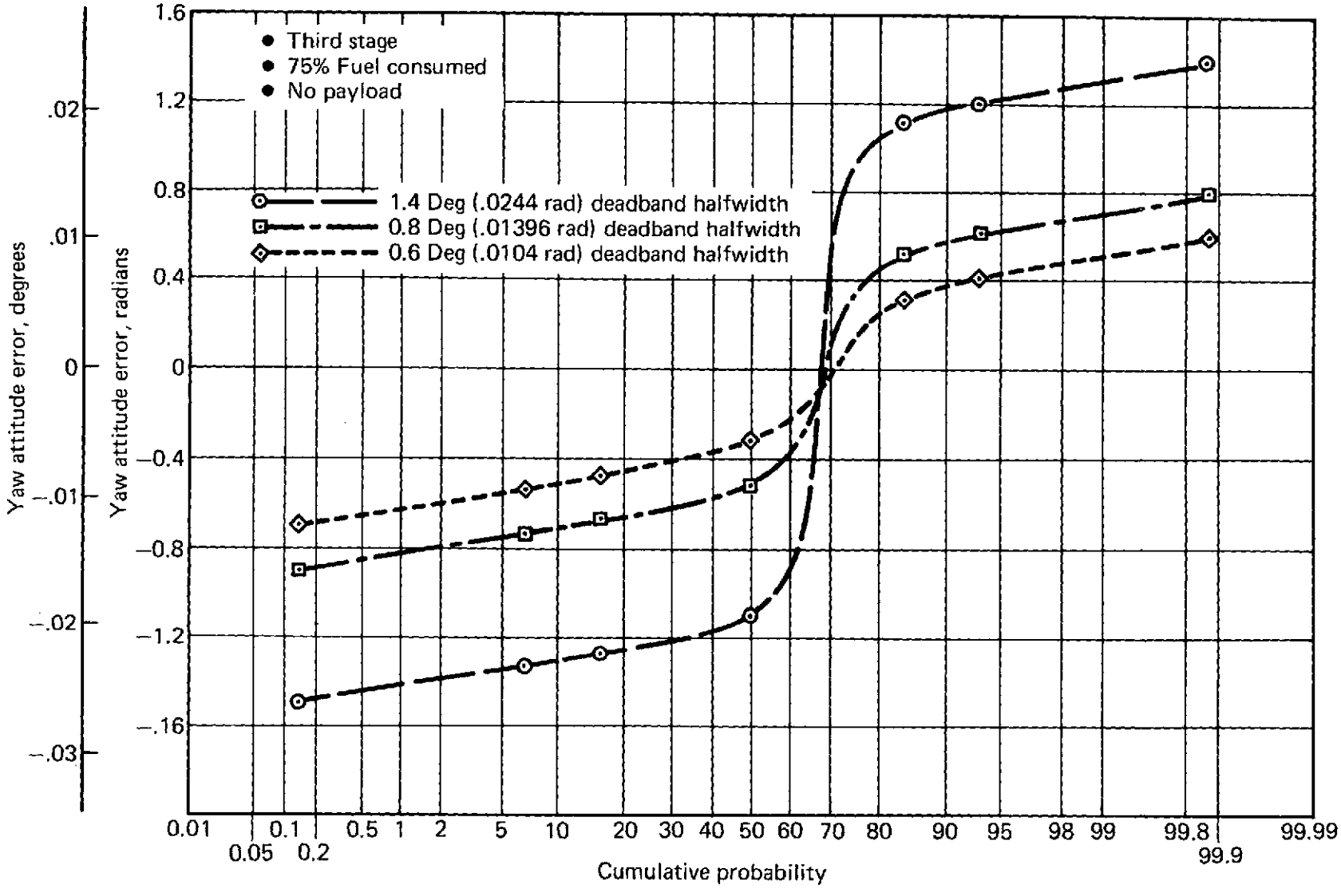


FIGURE 11. – YAW ATTITUDE ERROR VS CUMULATIVE PROBABILITY

TABLE 16. – PITCH AND YAW ATTITUDE ERRORS – CUMULATIVE PROBABILITY

| Condition | 1.4° (.024 rad) Deadband | | | | 0.8° (.014 rad) Deadband | | | | 0.6° (.010 rad) Deadband | | | |
|---|---|---|---|---|---|---|---|---|---|---|---|---|
| | Pitch | | Yaw | | Pitch | | Yaw | | Pitch | | Yaw | |
| | deg | rad | deg | rad | deg | rad | deg | rad | deg | rad | deg | rad |
| Second stage, 0% fuel | +1.32 | .023 | +1.17 | .020 | +0.72 | .013 | +0.60 | .010 | +0.32 | .006 | +0.20 | .003 |
| Consumed | −1.20 | −.021 | −1.13 | −.020 | −0.62 | −.011 | −0.55 | −.010 | −0.23 | −.004 | −0.16 | −.003 |
| Second stage, 75% fuel | +1.40 | .024 | +1.18 | .021 | +0.80 | .014 | +0.68 | .018 | +0.60 | .010 | +0.40 | .007 |
| Consumed | −0.46 | −.008 | −1.06 | −.018 | −0.15 | −.003 | −0.50 | −.009 | −0.13 | −.002 | −0.10 | −.002 |
| Second stage, 94% fuel | +1.43 | .025 | +1.12 | .020 | +0.84 | .015 | +0.54 | .009 | +0.64 | .011 | +0.12 | .002 |
| Consumed | −0.73 | −.013 | −1.02 | −.018 | −0.17 | −.003 | −0.42 | −.007 | −0.11 | −.002 | −0.24 | −.004 |
| Third stage, 0% fuel | +1.32 | .023 | +1.34 | .023 | +0.75 | .013 | +0.77 | .013 | +0.54 | .009 | +0.56 | .010 |
| Consumed | −1.42 | −.025 | −1.40 | −.024 | −0.84 | −.015 | −0.80 | −.014 | −0.64 | −.011 | −0.60 | −.010 |
| Third stage, 75% fuel | +1.32 | .023 | +1.38 | .024 | +0.73 | .013 | +0.78 | .014 | +0.53 | .009 | +0.59 | .010 |
| Consumed | −1.62 | −.028 | −1.50 | −.026 | −1.02 | −.018 | −0.90 | −.016 | −0.84 | −.015 | −0.70 | −.012 |
| Third stage, 92% fuel | +1.44 | .025 | +1.40 | .024 | +0.84 | .015 | +0.80 | .014 | +0.65 | .011 | +0.60 | .010 |
| Consumed | −1.56 | −.027 | −1.80 | −.031 | −0.96 | −.017 | −1.20 | −.021 | −0.76 | −.013 | −1.00 | −.017 |

- Cumulative probability = 99.87%
- No payload

### 7.3 Possible Deadband Reductions

The analyses accomplished lead to the following conclusions regarding the system deadbands.

(1) The current pitch and yaw deadbands used during second stage burn and coast and third stage burn are ±0.8 degree (.014 rad) nominal. No second stage deadband reduction is possible because of deadband overshoot which results in excessive control fuel consumption.

(2) The third stage boost pitch and yaw deadbands can be reduced from ±0.8 degree (.014 rad) to ±0.6 degree (.010 rad) for payloads with pitch inertias less than 46 slug-ft$^2$ (62.4 kg-m$^2$). Reduction below this value is not possible due to control system structural coupling.

(3) The third stage coast pitch and yaw deadbands cannot be reduced from the current value because of control fuel limitations.

## 8.0 ORBITAL DEVIATIONS – $\int N_X$ APPROACH

Orbital accuracy data were calculated for the $\int N_X$ correction system for the two reference trajectories discussed in Section 5.0. Actually the total correction concept involves two independent corrections:

(1) First, the fourth stage burn attitude (pitch and yaw) errors are corrected and control maintained during the burn phase.

(2) The injection velocity (after fourth stage burnout) is adjusted by the measured $\Delta V$ correction determined from the $\int N_X$ data as described in Section 3.0. This $\Delta V$ correction is restricted to the nominal fourth stage burn attitude, in either the positive or negative direction. If the vehicle is configured with only aft-facing thrusters, then an attitude change of 180 degrees (3.14 rad) may be necessary prior to adding the $\Delta V$. Trades involving the $\Delta V$ correction method are discussed in Section 12.0.

The analyses considered attitude reference systems which begin operation at launch and operate continuously from that point and systems which accept the Scout third stage coast attitude as the initial inertial reference. Minimum and maximum equipment error budgets as established in Section 4.0 were considered for both cases.

All orbital accuracies calculated are based upon flight experience data. Flight data were accumulated to determine the statistics of the integral of $N_X$ errors since no information existed on this parameter. Errors derived from the analysis of the AVC systems were combined with the appropriate flight experience values to yield the total injection errors.

### 8.1 Integral Of $N_X$ Statistics

Statistics of integral of $N_X$ errors were calculated using flight data obtained from Scout post-flight analyses. Integral of $N_X$ errors are available only for flights S-150 and subsequent (25 flights). This is because the post-flight analysis technique of adjusting motor performance to match velocity indicated by radar is necessary in order to deduce the integral of $N_X$ error. This technique was not used prior to vehicle S-150. Analyses of some stages of San Marco launched vehicles were precluded by the lack of radar data during operation of these stages. Therefore, a sample of 23 to 25 flights was available for integral of $N_X$ statistics, depending on the stage. The flight errors in the integral of $N_X$ for vehicles S-150 through S-181 are tabulated in Table 17.

## TABLE 17. – INTEGRAL OF $N_X$ FLIGHT ERRORS

| Vehicle | Stage 1 | | Stage 2 | | Stage 3 | | Stage 4 | | Total Vehicle | |
|---|---|---|---|---|---|---|---|---|---|---|
| | ft/s | m/s | ft/s | m/s | ft/s | m/s | ft/s | m/s | ft/s | m/s |
| S-150 | –14.0 | –4.3 | 40.2 | 12.3 | 12.8 | 3.9 | 9.4 | 2.9 | 48.4 | 14.8 |
| S-154 | –1.5 | –0.5 | 27.6 | 8.4 | 20.6 | 6.3 | 0.1 | .03 | 46.4 | 14.1 |
| S-153* | NA | NA | NA | NA | NA | NA | NA | NA | NA | NA |
| S-155 | 9.1 | 2.8 | 23.1 | 7.0 | 31.9 | 9.7 | 0 | 0 | 64.7 | 19.7 |
| S-156 | –6.2 | –1.9 | 5.0 | 1.5 | 28.8 | 8.8 | –70.6 | –21.5 | –43.0 | –13.1 |
| S-157 | –10.5 | –3.2 | –19.2 | –5.9 | 53.6 | 16.3 | –64.8 | –19.8 | –40.9 | –12.5 |
| S-158 | 14.3 | 4.4 | 22.5 | 6.9 | –12.0 | –3.7 | –6.6 | –2.0 | 18.2 | 5.5 |
| S-162 | –9.1 | –2.8 | 22.8 | 6.9 | 22.5 | 6.9 | –150.2 | –45.8 | –114.0 | –34.7 |
| S-161 | –6.7 | –2.0 | 9.2 | 2.8 | 11.3 | 3.4 | –30.3 | –9.2 | –16.5 | –5.0 |
| S-165 | –37.8 | –11.5 | 33.3 | 10.1 | 6.9 | 2.1 | 2.0 | 0.6 | 4.4 | 1.3 |
| S-167 | –12.0 | –3.7 | 24.0 | 7.3 | 17.5 | 5.3 | 15.6 | 4.8 | 45.1 | 13.7 |
| S-172 | –13.3 | –4.1 | 15.4 | 4.7 | –3.2 | –1.0 | –124.9 | –38.1 | –126.0 | –38.4 |
| S-169 | –41.5 | –12.6 | 14.8 | 4.5 | 12.7 | 3.9 | –26.5 | –8.1 | –40.5 | –12.3 |
| S-176 | –19.4 | –5.9 | –22.9 | –7.0 | 9.9 | 3.0 | –24.5 | –7.5 | –56.9 | –17.3 |
| S-174 | –33.1 | –10.1 | –26.0 | –7.9 | 2.7 | 0.8 | –27.8 | –8.5 | –84.2 | –25.7 |

*San Marco launched

TABLE 17. – INTEGRAL OF $N_X$ FLIGHT ERRORS (Continued)

| Vehicle | Stage 1 | | Stage 2 | | Stage 3 | | Stage 4 | | Total Vehicle | |
|---|---|---|---|---|---|---|---|---|---|---|
| | ft/s | m/s | ft/s | m/s | ft/s | m/s | ft/s | m/s | ft/s | m/s |
| S-175* | 16.1 | 4.9 | −12.4 | −3.8 | 0.5 | 0.2 | −1.6 | −0.5 | 2.6 | 0.8 |
| S-173* | 22.2 | 6.8 | −18.0 | −5.5 | NA | NA | NA | NA | NA | NA |
| S-177 | 4.5 | 1.4 | −21.8 | −6.6 | −29.4 | −9.0 | −26.8 | −8.2 | −73.5 | −22.4 |
| S-180 | −5.0 | −1.5 | −29.0 | −8.8 | −38.0 | −11.6 | −55.0 | −16.8 | −127.0 | −38.7 |
| S-163* | 2.9 | 0.9 | −28.2 | −8.6 | NA | NA | −32.5 | −9.9 | NA | NA |
| S-183 | 25.4 | 7.7 | −24.1 | −7.3 | −49.5 | −15.1 | 31.5 | 9.6 | −16.7 | −5.1 |
| S-184 | 31.2 | 9.5 | 7.2 | 2.2 | −20.0 | −6.1 | 23.5 | 7.2 | 41.9 | 12.8 |
| S-182 | −11.4 | −3.5 | −27.4 | −8.4 | −21.2 | −6.5 | −8.5 | −2.6 | −68.5 | −20.9 |
| S-170 | 28.8 | 8.8 | −28.6 | −8.7 | −19.7 | −6.0 | 4.5 | 1.4 | −15.0 | −4.6 |
| S-185 | 37.8 | 11.5 | −1.5 | −0.5 | −11.9 | −3.6 | 16.8 | 5.1 | 41.2 | 12.6 |
| S-181 | 44.4 | 13.5 | −8.2 | −2.5 | −19.6 | −6.0 | 12.9 | 3.9 | 29.5 | 9.0 |
| Standard deviation | ±22.8 | ±6.9 | ±22.9 | ±7.0 | ±24.5 | ±7.5 | ±44.5 | ±13.7 | ±59.1 | ±18.0 |
| Mean value | 0.6 | 0.2 | −0.9 | −0.3 | 0.3 | 0.1 | −22.3 | −6.8 | −20.9 | −6.4 |
| No. of samples | 25 | | 25 | | 23 | | 24 | | 23 | |

*San Marco launched

The integral of $N_X$ error statistics for the fourth stage were restricted to 18 flights which used the Altair IIIA motor and then adjusted for payload weight. These steps were taken to provide a more realistic value to be used in the sizing of the fourth stage velocity correction system. Each of the 18 fourth stage samples was adjusted by the ratio of the natural logarithm of the ignition weight divided by burnout weight for a 435 lbm (197.3 kg) payload to the natural logarithm of the ignition weight divided by the burnout weight of the sample. The 435 lbm (197.3 kg) payload weight corresponds to the injection capability of the Scout F-1 configuration in the reference 200 n.mi. (370.4 km) circular orbit. The adjusted standard deviation of the $\int N_X$ error for the flights which used the Altair IIIA motor was 26.2 ft/s (7.99 m/s). Using the data from Table 17 and the adjusted fourth stage value, the total $\int N_X$ error, based on flight experience, becomes:

| Stage | $\int N_X$ Error, 1$\sigma$ | |
|---|---|---|
| | ft/s | m/s |
| 1 | 23 | 7.01 |
| 2 | 23 | 7.01 |
| 3 | 25 | 7.62 |
| 4 | 26 | 7.92 |
| Root-Sum-Square | 49 | 14.94 |

This was the $\Delta V$ magnitude used in the sizing effort. A 2 $\sigma$ correction limit of 98 ft/s (29.87 m/s) was used in the simulations for the 200 n.mi. (370.4 km) orbit. The $\Delta V$ achievable with the same reaction control system is 134 ft/s (40.84 m/s) for the 600 n.mi. (1111.2 km) orbit with the lighter payload. Corrections were then limited to this larger velocity increment for the 600 n.mi. (1111.2 km) orbit.

## 8.2 AVC Attitude And Velocity Measurement Errors

The attitude errors at fourth stage ignition and at burnout or the 15 second burn point as presented in Section 6.0 (Tables 7 through 14) were averaged and the average value used in the fourth stage simulations. A summary of the attitude and velocity errors used in the analysis is presented in Table 18.

## 8.3 Fourth Stage Attitude Error Simulation

Current analysis of orbital errors which are represented by apogee perigee isoprobability contours and inclination error are generated from flight deviations in injection altitude, velocity, etc. This analysis requires no knowledge of the fourth stage attitude errors or fourth stage performance. However, in order to evaluate the various attitude control systems in this study, fourth stage attitude and performance accuracy had to be considered. This was done by calculating a covariance matrix at fourth stage ignition from flight data and adding this to a random sampling of fourth stage error sources. These error sources are (1) motor performance, (2) pitch attitude and (3) yaw attitude. The sigma magnitude of the motor performance error source was calculated from flight data. Pitch and yaw attitude error sources are dependent upon the guidance choice as shown in Table 18. The covariance matrix at fourth stage ignition was obtained by calculating a covariance matrix due to

## TABLE 18. – AVC ERROR SUMMARY – $\int N_X$ APPROACH

Attitude Errors Fourth Stage Burn

| Orbit | | AVC IMU Reference | Pitch Error | | | | Yaw Error | | | |
|---|---|---|---|---|---|---|---|---|---|---|
| | | | Max Error Budget | | Min Error Budget | | Max Error Budget | | Min Error Budget | |
| n. mi. | km | | deg | mrad | deg | mrad | deg | mrad | deg | mrad |
| 200 | 370.4 | At lift off | 0.77 | 13.4 | 0.37 | 6.5 | 0.95 | 16.6 | 0.37 | 6.5 |
| 200 | 370.4 | At 4th ignition | 0.97 | 16.9 | 0.75 | 13.1 | 1.37 | 23.9 | 1.22 | 21.3 |
| 600 | 1111.2 | At lift off | 0.95 | 16.6 | 0.37 | 6.5 | 1.10 | 19.2 | 0.37 | 6.5 |
| 600 | 1111.2 | At 4th ignition | 0.96 | 16.8 | 0.75 | 13.1 | 1.36 | 23.7 | 1.22 | 21.3 |

Accelerometer Measurement Errors
Integral of $N_X$ Errors, Fourth Stage Burnout

| Orbit | | Max Error Budget | | Min Error Budget | |
|---|---|---|---|---|---|
| n. mi. | km | ft/s | m/s | ft/s | m/s |
| 200 | 370.4 | 38.5 | 11.7 | 14.3 | 4.4 |
| 600 | 1111.2 | 47.8 | 14.6 | 16.4 | 5.0 |

fourth stage boost: based on flight observed error sources and subtracting this from the covariance matrix at fourth stage burnout which is calculated from flight data. This covariance matrix at burnout is the same matrix, for a given altitude, as that for standard Scout accuracy (documented in the Scout User's Manual).

This process results in the necessary information for input to the Statistical Orbital Analysis Routine (SOAR) which generates the statistics from which the isoprobability contours are defined. Thus, the different AVC systems were evaluated by substituting the predicted attitude errors of each system, simulating the vernier and recalculating the orbital accuracy using SOAR.

## 8.4 AVC Simulation In SOAR

The fourth stage burnout covariance and sensitivity matrices together with the nominal orbit characteristics are input to SOAR to determine the apogee-perigee isoprobability contours and inclination diviations. Since the corrections considered consists of two distinct steps, the effect of the attitude correction was evaluated separately and then the attitude correction plus the $\int N_X$ correction was evaluated.

The pitch and yaw attitude errors were treated as independent error sources. The velocity control system using $\int N_X$ was evaluated using a special model. This model consists of (1) defining a regression line (linear best fit) from flight deviations relating inertial velocity and integral of $N_X$, (2) using the regression line to obtain the error in integral of $N_X$ from a random error in inertial velocity, and (3) altering the inertial velocity error by the negative of the measurement error in integral of $N_X$, but not exceeding the velocity capability of the system. The regression line provides a statistical method of calculating the integral of $N_X$ error by knowing the inertial velocity error. Knowledge of the integral of $N_X$ error is mandatory in the evaluation of the system since this is the parameter the velocity control system measures.

## 8.5 Results

Isoprobability contours for the AVC system employing fourth stage attitude control and $\int N_X$ correction are shown in Figures 12 through 14. Figure 12 shows the improvement achieved when fourth stage attitude control alone is employed for the 600 n.mi. (1111.2 km) orbit. The standard Scout accuracy is based upon the flight experience values determined from the 37 flight sample. Similar contours are given in Figure 13 when both the attitude control plus the $\int N_X$ velocity correction are used. Several important factors are evident from these data:

(1) With attitude control only, the difference between the maximum and minimum error budgets is extremely small.

(2) No difference in isoprobability contours is discernable for the case where the AVC IMU is operated from launch versus the case where the Scout vehicle attitude at the end of third stage coast is assumed as the inertial reference.

(3) With attitude control plus $\int N_X$ correction there is still no significant difference in the contours for the two error budgets. Again there is no difference in the results with the IMU operating from launch or the end of third stage coast.

The 200 n.mi. (370.4 km) orbit results are given in Figure 14. In this case there is no difference in the orbital accuracies for the minimum and maximum AVC error budgets. Of course, there is

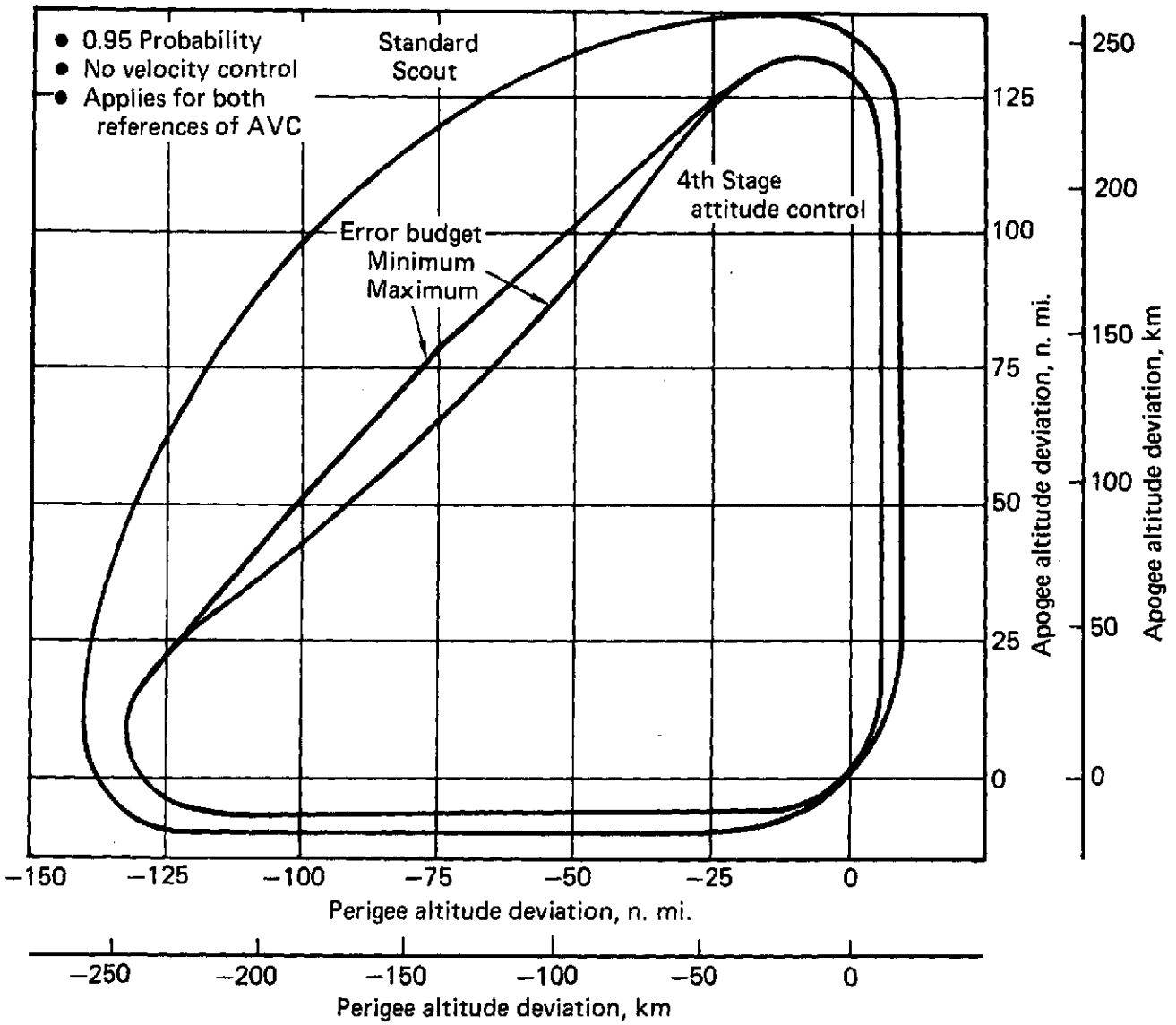


**FIGURE 12. – 600 N. MI. (1111.2 KM) ORBIT – ISOPROBABILITY CONTOURS, ATTITUDE CONTROL**

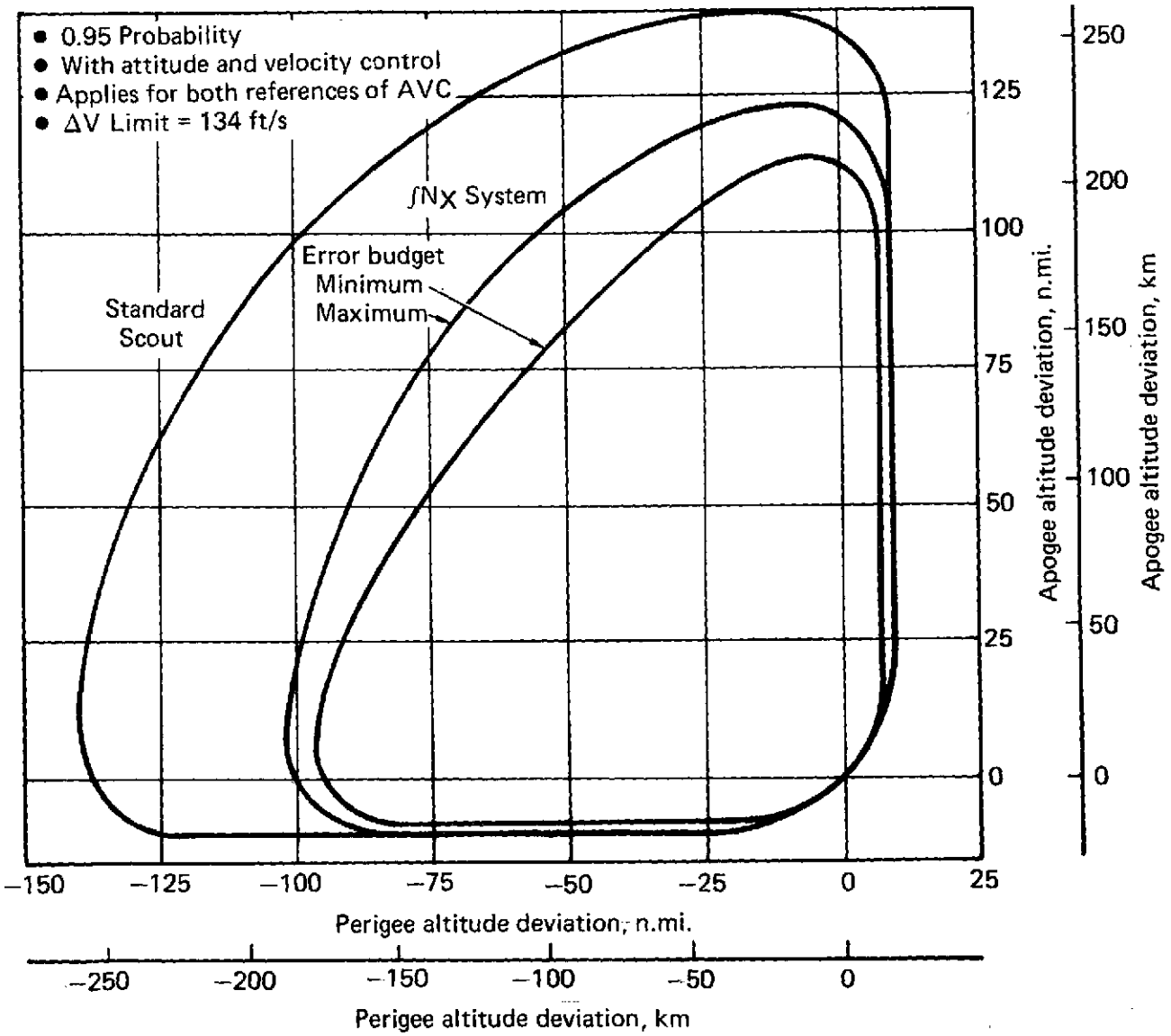


**FIGURE 13. – 600 N. MI. (1111.2 KM) ORBIT – ISOPROBABILITY CONTOURS, ATTITUDE CONTROL + $\int N_X$**

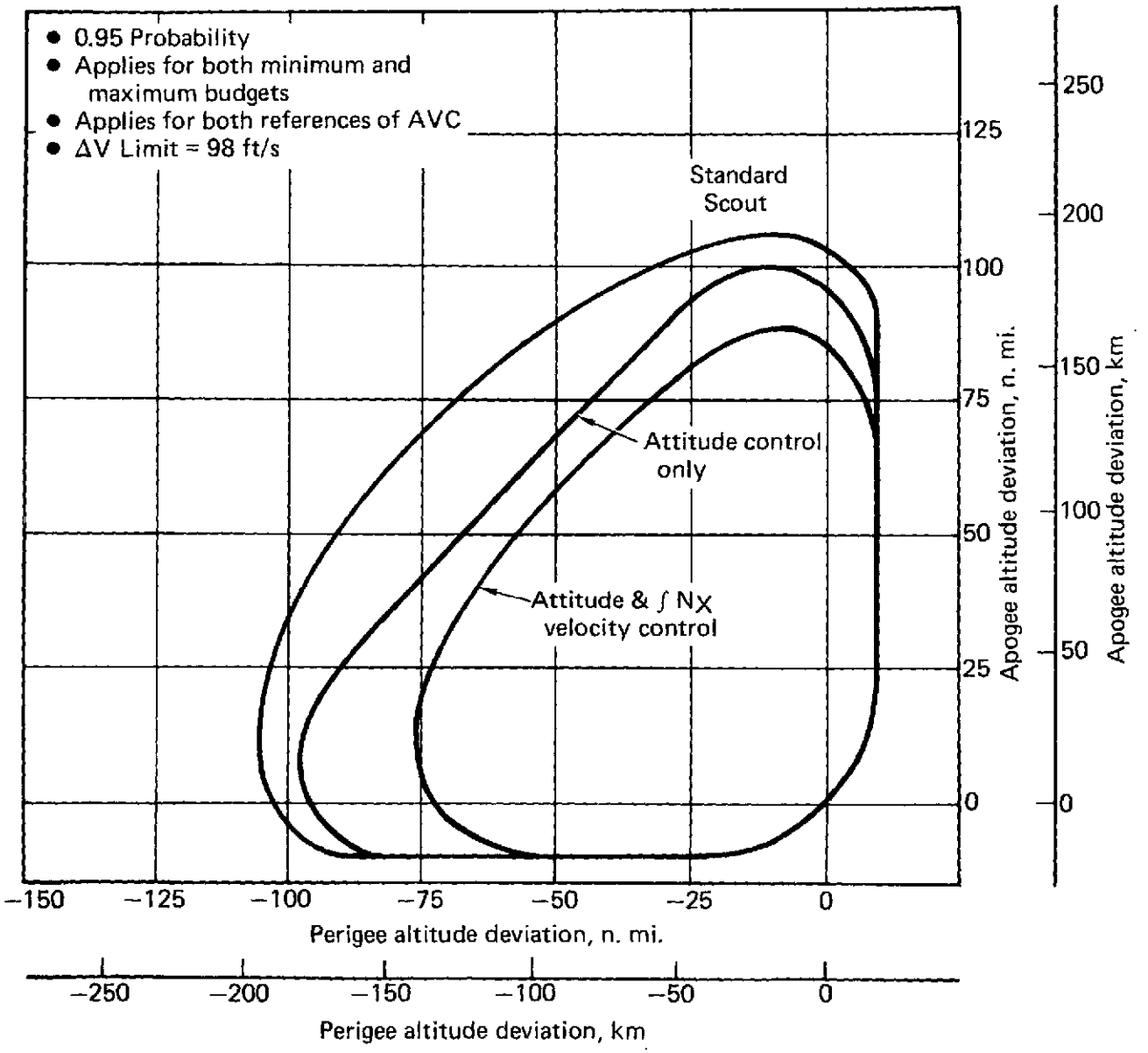


**FIGURE 14. – 200 N. MI. (370.4 KM) ORBIT – ISOPROBABILITY CONTOURS, ATTITUDE CONTROL + ∫ $N_X$**

less time for the equipment errors to propagate for the lower altitude orbit.

The primary effect of the attitude control system, Figures 12 and 14, is basically to produce a convex shape rather than a concave shape. This is due to the reduction in flight path angle deviation caused by the attitude control system.

The primary effect of the velocity control system on the $\int N_X$ contours, is a reduction in the maximum apogee and perigee errors. This is due to the reduction in velocity deviation resulting from the velocity correction capability. Velocity control on the integral of $N_X$ is frequently not advantageous. Often the inertial velocity error will have the opposite sign of the integral of $N_X$ error so that by nulling out the integral of $N_X$ error, the inertial velocity error actually increases. Velocity control does, however, decrease the standard deviation of inertial velocity error, from 70 ft/s (21.3 m/s) to about 48 ft/s (14.6 m/s) on the 200 n.mi. (370.4 km) orbit mission. The significance of this 22 ft/s (6.7 m/s) reduction in standard deviation in inertial velocity is shown by the contour in Figure 14.

The non-symmetry in apogee-perigee errors shown in Figures 13 and 14 with velocity control does not result from the characteristics of the velocity control system components but from the flight samples yielding integral of $N_X$ data used in the AVC simulation. These flight samples are acceptable for calculating integral of $N_X$ statistics but represent a very small sample size. With increasing sample size, the trend is expected to be toward symmetry, i.e., the maximum values of apogee and perigee errors approach equality.

It is possible that the standard deviation in inertial velocity could be further reduced by using non-unity gains on the integral of $N_X$ error of each stage. Unity gains were used in this study to simplify the study and still obtain good comparative data. If this system were implemented, the gains would have to be optimized based on mission requirements.

## 8.6 $\int N_X$ Investigation Conclusions

The analyses and results of the investigation of a fourth stage AVC system employing the $\int N_X$ correction approach lead to several definite conclusions:

(1) The accuracy results show a low sensitivity to equipment error budgets. Thus a highly accurate IMU is not required for this type correction system.

(2) The improvements are independent of the point where the IMU establishes its initial inertial reference. That is, there is no difference in the orbital accuracy for attitude reference systems which utilize ground (pre-launch) alignment or systems which accept the third stage coast hand-off attitude. The velocity measurement ($\int N_X$) portion of the AVC system must however operate throughout the entire trajectory.

(3) The IMU platform can be mechanically aligned to the vehicle rather than resorting to gyrocompassing or other means of independent alignment. Independent alignment is not prohibited but it offers no orbital accuracy improvement.

(4) The degree of improvement achievable with the $\int N_X$ correction is limited. The reduction in apogee-perigee deviations is not as great as expected or desired.

# 9.0 GENERATION OF NEW AVC CONCEPTS

At the conclusion of the $\int N_X$ investigation, the SOW was modified to include the exploration of additional AVC system utilization concepts in an effort to achieve greater accuracy improvements. The general approach followed in the development of the additional concepts was to make better utilization of the IMU velocity measurement capabilities.

## 9.1 Guidelines For Correction Concepts

The basic study guidelines were unchanged for the consideration of the new AVC system concepts. The removal of the restriction which limited the velocity correction to the measurement of vehicle longitudianl acceleration lead to several possibilities. The primary factors which governed the new concepts were:

(1) The IMU would include the capability to measure the three components of vehicle acceleration in an inertial reference frame as is accomplished in conventional inertial navigation systems. The $\int N_X$ investigation lead to the conclusion that knowledge of the inertial velocity is required to make a velocity correction that will result in significant reductions in apogee-perigee deviations. The IMU then would be used to provide 3 axis incremental velocity data throughout the trajectory. Ground alignment and operation from launch is mandatory; hand-off from the current third stage guidance system at the end of third stage coast is not feasible. Additionally the IMU would provide vehicle attitude data for the entire trajectory.

(2) The current third stage guidance system would control the vehicle through third stage coast as in the $\int N_X$ case, and the AVC system would provide no control until after fourth stage spin-up and separation.

(3) The CEU capability would have to be expanded to include the capability of computing the components of inertial velocity. A digital processor or digital computational circuitry would be required to accomplish the necessary integrations and associated computations. Additionally, it may be necessary to transform the attitude data, depending upon the specific IMU selected (gimballed or strapdown) and the initial inertial reference established. The objective in system configuration is to minimize the complexity of the CEU.

(4) The vehicle corrections to be employed would utilize both the inertial velocity and attitude data. All vehicle control would:

(a) use simple correction techniques

(b) minimize in-flight computations

(c) employ closed loop type control laws.

It would be desirable to determine all attitude adjustments and velocity correction by a single computational process. Thus no iterative type control technique like the velocity-to-be-gained concepts used in ballistic missile guidance would be considered for Scout. Instead the corrections would all employ closed loop solutions in the computations and make maximum utilization of data that can be determined in the pre-flight phase.

## 9.2 AVC Trajectory Correction Techniques

The corrections considered for the AVC are illustrated in Figure 15. These consist of first adjusting or biasing the nominal fourth stage burn attitude in pitch and yaw to compensate for a portion of the inertial velocity error accrued through third stage. The corrected or biased attitude would then be maintained throughout the fourth stage burn. The second correction is an actual velocity correction after fourth stage burnout. This velocity correction would not be restricted to the nominal fourth stage burn attitude as was the case with the $\int N_X$ system.

The discussions relating the AVC system correction concepts from this point will utilize the reference coordinate system shown in Figure 15. This coordinate system is defined as:

X – Direction of the nominal injection velocity vector

Z – Vertical at the nominal injection point (fourth stage burnout)

Y – Out-of-plane completing a right handed coordinate system.

9.2.1 Fourth Stage Attitude Adjustment. – the approach for adjusting or biasing the fourth stage burn pitch and yaw attitude is to compensate for errors in two components of inertial velocity at the end of third stage coast. The velocity measurements and attitude computations are made in the injection reference coordinate system. The parameters required for the attitude computations which can be computed during the pre-flight phase and stored in the CEU include:

$\theta_{4N}$, $\psi_{4N}$ – Nominal vehicle pitch and yaw attitudes for fourth stage burn. These could be determined such that they are compatible with the IMU selected.

$V_{Y3CN}$, $V_{Z3CN}$ – Nominal values of Y and Z components of inertial velocity at the end of third stage coast.

$\Delta V_4$ – Nominal velocity increment to be added by the fourth stage.

These parameters are mission dependent and would have to be determined for each flight.

The idea is to bias the fourth stage pitch attitude so that with nominal fourth stage motor performance, the measured vertical velocity error would be cancelled. Yaw would be biased in a like manner to cancel the measured out-of-plane velocity error. The equations for the bias angles are:

$$\Delta\theta_{4B} = \text{Sine}^{-1}\left(-\frac{V_{Z3CM} - V_{Z3CN}}{\Delta V_4}\right)$$

$$\Delta\psi_{4B} = \text{Sine}^{-1}\left(-\frac{V_{Y3CM} - V_{Y3CN}}{\Delta V_4}\right)$$

where $V_{Y3CM}$ and $V_{Z3CM}$ are the measured Y and Z velocity components at the end of third stage coast. In many cases, the nominals for these two velocity components will be zero. The pitch and yaw biases would be added to the nominals and compared with the measured values to determine the errors.

$$\theta_e = \theta_M - (\theta_{4N} + \Delta\theta_{4B})$$

$$\psi_e = \psi_M - (\psi_{4N} + \Delta\psi_{4B})$$

The measured values as determined by the IMU would include any disturbances resulting from fourth stage separation and motor ignition.

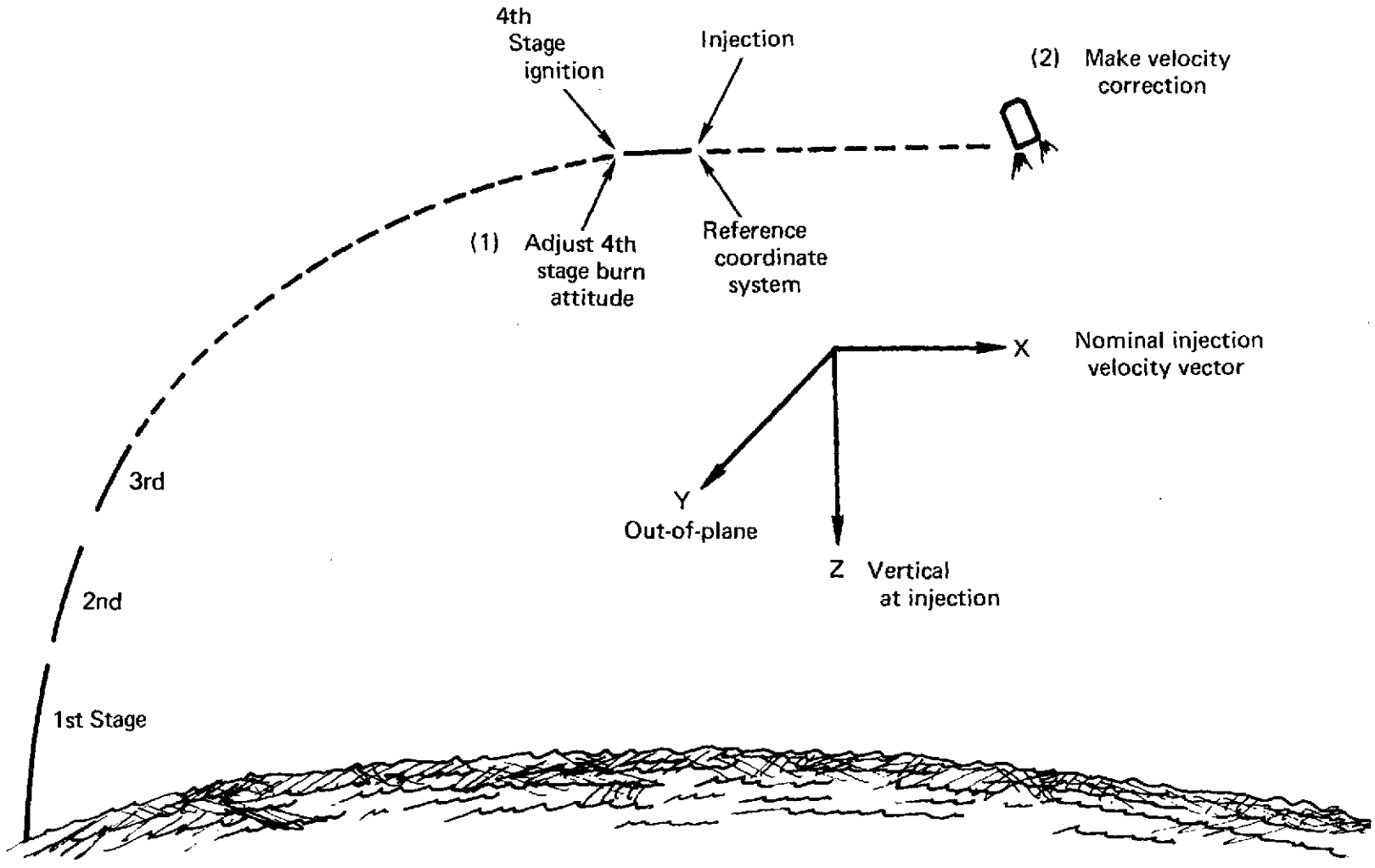


**FIGURE 15. – AVC TRAJECTORY CORRECTIONS**

These computations are all straight forward and offer a means of compensating for two components of velocity error through third stage. No attitude change can compensate for the error in the X velocity component.

9.2.2 Velocity Correction – Fourth Stage Burnout. – the velocity correction is made after the fourth stage motor is burned out. Again the desire was to make the concept as simple as possible. The technique considered makes no attempt to correct for the out-of-plane velocity error component after burnout; instead this error is accepted. Some error will exist because of the fourth stage control system deadband and variations in motor performance.

The technique does correct for the measured X and Z velocity errors. The nominals for these two components at burnout ($V_{XBON}$ and $V_{ZBON}$) would have to be computed in pre-flight and stored in the CEU. The errors can be computed from the following equations:

$$\Delta V_{XBO} = V_{XBOM} - V_{XBON}$$

$$\Delta V_{ZBO} = V_{ZBOM} - V_{ZBON}$$

$$\Delta V_{BO} = [\Delta V_{XBO}^2 + \Delta V_{ZBO}^2]^{1/2}$$

$V_{XBOM}$, $V_{ZBOM}$ are the measured values of velocity components at burnout. The quantity $\Delta V_{BO}$ is the magnitude of the correction velocity vector. Now the pitch angle at which the $\Delta V$ is to be added must be computed. The following sketch helps to illustrate the parameters involved.

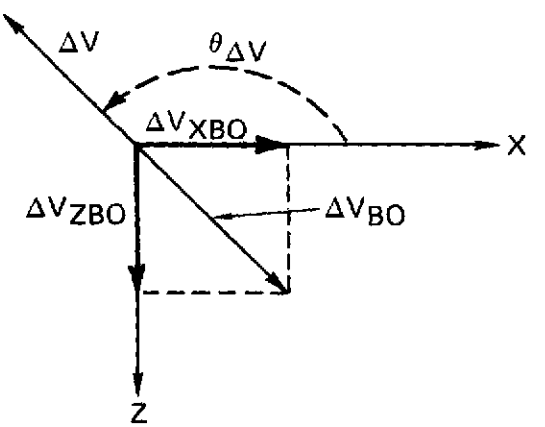


The pitch maneuver angle ($\theta_{\Delta V}$) required for adding the correction $\Delta V$ can be computed from the following expression:

$$\theta_{\Delta V} = \text{Sine}^{-1}\left(-\frac{\Delta V_{ZBO}}{\Delta V_{BO}}\right)$$

Again the computations required to determine the $\Delta V$ to be added and the pitch maneuver angle are direct calculations. As shown in the preceding sketch the pitch maneuver required can vary from 0 to ±180 degrees (3.14 rad). This computation must be made in flight. Additionally, there is no way of predicting the maneuver in the pre-launch phase.

## 9.3 AVC Correction Concepts Investigated

Four different options employing various combinations of the two trajectory correction techniques were investigated. These options are summarized in Table 19. The parameter listed in the table that has not been discussed is the manner or point at which the fourth stage is ignited.

**TABLE 19. – AVC CORRECTION CONCEPTS INVESTIGATED**

| Option | 4th Stage Burn Attitude Adjusted | Velocity Components Corrected by ΔV | ΔV Pitch Maneuver Reqd | 4th Stage Ignition Control |
|---|---|---|---|---|
| 1 | Pitch and yaw | $\Delta V_{XBO}$, $\Delta_{ZBO}$ | Yes | Time from launch |
| 2 | Pitch and yaw | $\Delta V_{XBO}$, $\Delta V_{ZBO}$ | Yes | Nominal altitude (biased high) |
| 3 | Yaw | $\Delta V_{XBO}$, $\Delta V_{ZBO}$ | Yes | $V_Z = 0$ (or a nominal value) |
| 4 | None | $\Delta V_{XBO}$ | No | Time from launch |

9.3.1 Option 1. – Option 1 involves the adjustment or biasing of both pitch and yaw prior to fourth stage burn and then correcting both velocity component errors ($\Delta V_{XBO}$ and $\Delta V_{ZBO}$) subsequent to burnout. The fourth stage is ignited at a nominal time after launch which is the current procedure. The fourth stage squib ignition signal is currently provided by the third stage intervalometer.

9.3.2 Option 2. – Option 2 differs from 1 only in the determination of fourth stage ignition. Since any fourth stage correction system will not be able to correct for altitude errors at injection, the study included the examination of the case where the trajectory is purposely biased to achieve a high altitude and fourth stage is ignited when the nominal altitude is reached. In the analysis of this option the nominal injection altitude was increased to account for a two sigma error in altitude. The fourth stage was ignited when the nominal altitude was first reached. If a deviated trajectory failed to reach the nominal altitude in the simulation, the fourth stage was ignited at apogee.

9.3.3 Option 3. – in Option 3 the fourth stage is ignited when the vertical velocity component ($V_Z$) reaches zero or some other nominal value. This is approximately equivalent to apogee or maximum altitude. The CEU would have to determine the point when $V_Z$ goes to zero.

The other difference in Option 3 is that no pitch attitude adjustment is employed prior to fourth stage ignition. Since the purpose of the pitch adjustment is to compensate for measured vertical velocity error, it is not applicable in this option because ignition occurs when the measured vertical velocity is zero. Thus by definition the pitch adjustment is zero.

9.3.4 Option 4. – Option 4 was included to evaluate a concept similar to the integral of $N_X$ except the velocity correction was based upon the inertial velocity measurement. In this option, no fourth stage attitude adjustments are used. Instead, the fourth stage is oriented to the nominal burn attitude as determined in the pre-launch calculations. The velocity correction made subsequent to

fourth stage burnout corrects only the $V_X$ component of inertial velocity. Thus no computation is required to determine a pitch maneuver angle as used in Option 1, 2, and 3. Instead the velocity correction will be along the axis established by nominal injection velocity vector. The $\Delta V$ may need to be added in either the positive or negative direction. Thus if aft-facing vehicle motors are used, the pitch maneuver would be restricted to either zero or 180 degree (3.14 rad) values. The CEU would need sufficient logic to decide when the maneuver is required.

## 10.0 MEASUREMENT ERRORS – NEW CONCEPTS

The inertial guidance equipment error budgets, maximum and minimum, as discussed in Section 4.0 were used with slight changes to represent the range or bounds of systems that would be used for the new AVC concepts. Again, each budget was evaluated for both the 600 n. mi. (1111.2 km) and 200 n. mi. (370.4 km) orbit trajectories.

### 10.1 Equipment Error Budgets

The inertial guidance error budgets as shown in Table 2 were used to represent the systems that would be used for Option 1 through 4, except for two gyro drift terms in the maximum budget. Table 2 shows 3.0 deg/hr and 3.0 deg/hr/G for the fixed and mass unbalance drift coefficients. Because of the improved gyro performance in full inertial navigation systems and the velocity error sensitivity to these drift terms, the maximum error budget for these two terms only was reduced by a factor of two.

The second change involved the initial alignment uncertainties. The only alignment terms of interest in the operation of an inertial guidance system is the alignment of the inertial platform axes to the reference inertial coordinate system. This differs significantly from the evaluation of the integral of $N_X$ case where the objective was to orient the fourth stage thrust axis to pre-launch computed inertial orientation. When using the inertial system in the conventional manner to measure inertial velocity components, the initial alignment of the vehicle is not as critical since the attitude adjustments are computed from the measured velocity data. The velocity data are, however, contaminated by the initial platform alignment errors. The analyses assume that in all cases the inertial platform is independently aligned rather than mechanically aligned to the vehicle. The error budget values (minimum and maximum) used were 60 arc seconds (0.29 mrad) to 180 arc seconds (0.87 mrad) for the level axes and 120 arc seconds (0.58 mrad) to 360 arc seconds (1.745 mrad) for the azimuth axis.

System errors involved in the trajectory simulations and the determination of systems requirements in terms of correction capability, but which do not affect the velocity and position measurement errors, are the platform attitude readout uncertainties and the deadbands of the fourth stage attitude control system. These variables influence the accuracy of Option 4 and the $\Delta V$ capability required for the other options. Magnitudes ($3\sigma$ values) used in the simulations, which correspond to error sources used in the integral of $N_X$ case, are shown below.

| Source | Pitch | | | | Yaw | | | |
|---|---|---|---|---|---|---|---|---|
| | Min Budget | | Max Budget | | Min Budget | | Max Budget | |
| | deg | mrad | deg | mrad | deg | mrad | deg | mrad |
| Attitude readout | 0.15 | 2.62 | 0.30 | 5.24 | 0.15 | 2.62 | 0.30 | 5.24 |
| ACS deadband | 0.35 | 6.11 | 0.50 | 8.73 | 0.35 | 6.11 | 0.50 | 8.73 |
| RSS | 0.381 | 6.65 | 0.583 | 10.17 | 0.381 | 6.65 | 0.583 | 10.17 |

## 10.2 Velocity and Position Measurement Errors

The guidance accuracy analysis routine as discussed in Appendix A was used to evaluate the two error budgets for both trajectories. In all cases, it was assumed that the IMU was aligned to the injection reference coordinate system at launch. This coordinate system was selected because it is most compatible with the new concepts. However, it is not mandatory that the IMU use this particular system as a reference; any desirable reference could be used and the results (angle and velocity data) transformed. A change in the platform reference orientation would alter the measurement errors; however, the change in the results would not be drastic.

The error coefficient symbols as used in the print-out of the computer program are defined in Table 20. Values for each coefficient for both error budgets are listed in Table 21. The initial alignment terms are referenced to the injection inertial coordinate system; PHZO for example is the initial platform misalignment about the Z injection axis which is vertical at the nominal injection point.

The computer results for the 600 n. mi. (1111.2 km) trajectory are shown in Tables 22 through 27. Velocity and position errors in feet and feet per second respectively are shown at third stage burnout, fourth stage ignition and fourth stage burnout for each error budget. The maximum and minimum error budgets are evaluated as gimballed systems. All values shown in the tables are $3\sigma$ values because the error coefficients were specified in $3\sigma$ magnitudes.

Tables 28 through 33 are similar presentations for the 200 n. mi. (370.4 km) trajectory. The error coefficient magnitudes given in Table 21 can be used together with these velocity and position errors to determine the sensitivity for each.

A comparison of these errors shows an increase approaching an order of magnitude in some parameters in going from the minimum to maximum budget. Increase in other parameters is about a factor of 4.

**TABLE 20. -- ERROR COEFFICIENT SYMBOLS**

| Symbol | Definition |
|---|---|
| RX, RY, RZ | Gyro fixed (non-G sensitive) drift -- deg/hr |
| USX, USY, USZ | Gyro mass unbalance along the spin axis -- deg/hr/G |
| UXX, UYY, UZZ | Gyro mass unbalance along the input axis -- deg/hr/G |
| SX, SY, SZ | Anisoelastic drift error coefficient -- deg/hr/$G^2$ |
| SFX, SFY, SFZ | Gyro torquer scale factor error (strapdown systems only) -- percent |
| THXY, THXZ, THYX, THYZ, THZX, THZY | Gyro input axis misalignment, THij is misalignment of i gyro about j axis -- arc seconds |
| DAX, DAY, DAZ | Accelerometer bias instability -- micro G's ($\mu$G) |
| CX, CY, CZ | Accelerometer scale factor error -- $\mu$G/G |
| DCX, DCY, DCZ | Accelerometer non-linearity -- $\mu G/G^2$ |
| PHXY, PHXZ, PHYX, PHYZ, PHZX, PHZY | Accelerometer input axis misalignment to IMU, PHij is misalignment of i accelerometer about j axis -- arc seconds |
| PHX0, PHY0, PHZ0 | Platform misalignment relative to the inertial reference -- arc seconds |

## TABLE 21. – AVC SYSTEM ERROR BUDGETS – NEW CONCEPTS

- $3\sigma$ Values

| Parameter | Maximum Budget | Minimum Budget |
|---|---|---|
| RX, RY, RZ (deg/hr) | 1.5 | .03 |
| USX, USY, USZ (deg/hr/G) | 1.5 | .06 |
| UXX, UYY, UZZ (deg/hr/G) | 1.5 | .06 |
| SX, SY, SZ (deg/hr/$G^2$) | 0.2 | .05 |
| SFX, SFY, SFZ (%) | .09 | .003 |
| THXY, THXZ, THYX (arc s) THYZ, THZX, THZY | 120. | 60. |
| DAX, DAY, DAZ ($\mu$G) | 1000. | 150. |
| CX, CY, CZ ($\mu$G/G) | 1000. | 450. |
| DCX, DCY, DCZ ($\mu$G/$G^2$) | 100. | 30. |
| PHXY, PHXZ, PHYX (arc s) PHYZ, PHZX, PHZY | 120. | 60. |
| PHX0, PHY 0 (arc s) | 180. | 60. |
| PHZ0 (arc s) | 360. | 120. |

## TABLE 22. – MEASUREMENT ERRORS, MINIMUM BUDGET, 600 N. MI. (1111.2 KM) TRAJECTORY; END OF THRID STAGE BOOST

END OF THIRD STAGE BOOST

• 3σ VALUES

| | DELTA-X-DOT | DELTA-Y-DOT | DELTA-Z-DOT | DELTA-X | DELTA-Y | DELTA-Z |
|---|---|---|---|---|---|---|
| RX | 0. | 2.81314552E-01 | -6.08207786E-04 | 0. | 1.07009141E+01 | -2.01406487E-02 |
| USX | 0. | 4.60908090E-01 | -1.08470586E-03 | 0. | 7.89822105E+00 | -2.05409548E-02 |
| UXX | 0. | -2.73562301E-03 | 6.22587921E-06 | 0. | -7.01616607E-02 | 1.52410278E-04 |
| SX | 0. | -5.92937121E-03 | 1.36862628E-05 | 0. | -1.09666467E-01 | 2.47128337E-04 |
| SFX | 0. | 0. | 0. | 0. | 0. | 0. |
| THXZ | 0. | 0. | 0. | 0. | 0. | 0. |
| THXY | 0. | 0. | 0. | 0. | 0. | 0. |
| RY | -2.81314552E-01 | 0. | -1.44352346E-01 | -1.07009141E+01 | 0. | -4.07510342E+00 |
| USY | 2.73562301E-03 | 0. | 1.56162075E-03 | 7.01616607E-02 | 0. | 3.47379022E-02 |
| UYY | -4.60908090E-01 | 0. | -2.81207052E-01 | -7.89822105E+00 | 0. | -5.24684836E+00 |
| SY | 5.92937121E-03 | 0. | 3.54326222E-03 | 1.09666467E-01 | 0. | 5.98838489E-02 |
| SFY | 0. | 0. | 0. | 0. | 0. | 0. |
| THYZ | 0. | 0. | 0. | 0. | 0. | 0. |
| THYX | 0. | 0. | 0. | 0. | 0. | 0. |
| RZ | 6.08207786E-04 | 1.44352346E-01 | 0. | 2.01406487E-02 | 4.07510342E+00 | 0. |
| USZ | -3.96968567E-03 | -9.64146604E-01 | 0. | -1.17008328E-01 | -2.45155011E+01 | 0. |
| UZZ | -6.22587921E-06 | -1.56162075E-03 | 0. | -1.52410278E-04 | -3.47379022E-02 | 0. |
| SZ | 2.91953217E-05 | 7.44772619E-03 | 0. | 6.15871056E-04 | 1.44157710E-01 | 0. |
| SFZ | 0. | 0. | 0. | 0. | 0. | 0. |
| THZX | 0. | 0. | 0. | 0. | 0. | 0. |
| THZY | 0. | 0. | 0. | 0. | 0. | 0. |
| DAX | 7.48046639E-01 | 0. | 0. | 5.79736145E+01 | 0. | 0. |
| CX | 3.54919953E+00 | 0. | 0. | 1.03503797E+02 | 0. | 0. |
| PHXZ | -1.07952141E-02 | 0. | 0. | -4.56842619E-01 | 0. | 0. |
| PHXY | 5.81325468E+00 | 0. | 0. | 3.38425372E+02 | 0. | 0. |
| DCX | 1.03771280E+00 | 0. | 0. | 2.54535583E+01 | 0. | 0. |
| DAY | 0. | 7.48046639E-01 | 0. | 0. | 5.79736145E+01 | 0. |
| CY | 0. | -1.67000456E-02 | 0. | 0. | -7.06729156E-01 | 0. |
| PHYZ | 0. | -2.29426732E+00 | 0. | 0. | -6.69067424E+01 | 0. |
| PHYX | 0. | 5.81325468E+00 | 0. | 0. | -3.38425372E+02 | 0. |
| DCY | 0. | 1.79287639E-05 | 0. | 0. | 6.00074103E-04 | 0. |
| DAZ | 0. | 0. | 7.48046639E-01 | 0. | 0. | 5.79736145E+01 |
| CZ | 0. | 0. | -6.99302388E+00 | 0. | 0. | -5.23539329E+02 |
| PHZX | 0. | 0. | 1.07952141E-02 | 0. | 0. | 4.56842619E-01 |
| PHZY | 0. | 0. | 2.29426732E+00 | 0. | 0. | 6.69067424E+01 |
| DCZ | 0. | 0. | 3.61933372E+00 | 0. | 0. | 1.44079288E+02 |
| PHX0 | 0. | 5.81325468E+00 | -1.07952141E-02 | 0. | 3.38425372E+02 | -4.56842619E-01 |
| PHY0 | -5.81325468E+00 | 0. | -2.29426732E+00 | -3.38425372E+02 | 0. | -6.69067424E+01 |
| PHZ0 | 2.15904283E-02 | 4.58853464E+00 | 0. | 9.13685237E-01 | -2.55441722E+02 | 0. |

THREE STANDARD DEVIATION OF ALL ERROR SOURCES

| | | | | | |
|---|---|---|---|---|---|
| 9.06163972E+00 | 9.78305250E+00 | 1.02548095E+01 | 4.93926402E+02 | 5.50405702E+02 | 5.54265995E+02 |

TOTAL VELOCITY RSS = 1.68220852E+01 ELAPSED TIME = 1.55000000E+02

TOTAL POSITION RSS = 9.24186410E+02 PITCH = 56.68 ROLL = -.21 HEADING = -.20

# TABLE 23. – MEASUREMENT ERRORS, MINIMUM BUDGET, 600 N. MI. (1111.2 KM) TRAJECTORY; END OF THIRD STAGE COAST

END OF THIRD STAGE COAST

• 3σ VALUES

| | DELTA-X-DOT | DELTA-Y-DOT | DELTA-Z-DOT | DELTA-X | DELTA-Y | DELTA-Z |
|---|---|---|---|---|---|---|
| RX | 0. | 2.81332779E-01 | -6.08250552E-04 | 0. | 1.89065887E+02 | -4.05771477E-01 |
| USX | 0. | 4.60965563E-01 | -1.08484070E-03 | 0. | 3.00150359E+02 | -7.08329892E-01 |
| UXX | 0. | -2.73589343E-03 | 6.22651368E-06 | 0. | -1.80471796E+00 | 4.10001963E-03 |
| SX | 0. | -5.93021259E-03 | 1.36882369E-05 | 0. | -3.86942083E+00 | 8.92546952E-03 |
| SFX | 0. | 0. | 0. | 0. | 0. | 0. |
| THXZ | 0. | 0. | 0. | 0. | 0. | 0. |
| THXY | 0. | 0. | 0. | 0. | 0. | 0. |
| RY | -2.81332779E-01 | 0. | -1.44364358E-01 | -1.89065887E+02 | 0. | -9.56021006E+01 |
| USY | 2.73589343E-03 | 0. | 1.56179896E-03 | 1.80471796E+00 | 0. | 1.02491835E+00 |
| UYY | -4.60965563E-01 | 0. | -2.81244926E-01 | -3.00150359E+02 | 0. | -1.83556112E+02 |
| SY | 5.93021259E-03 | 0. | 3.54381668E-03 | 3.86942083E+00 | 0. | 2.30666335E+00 |
| SFY | 0. | 0. | 0. | 0. | 0. | 0. |
| THYZ | 0. | 0. | 0. | 0. | 0. | 0. |
| THYX | 0. | 0. | 0. | 0. | 0. | 0. |
| RZ | 6.08250552E-04 | 1.44364358E-01 | 0. | 4.05771477E-01 | 9.56021006E+01 | 0. |
| USZ | -3.97002733E-03 | -9.44242569E-01 | 0. | -2.63400548E+00 | -6.35845242E+02 | 0. |
| UZZ | -6.22651368E-06 | -1.56179896E-03 | 0. | -4.10001963E-03 | -1.02491835E+00 | 0. |
| SZ | 2.91489675E-05 | 7.44875021E-03 | 0. | 1.91280146E-02 | 4.86666483E+00 | 0. |
| SFZ | 0. | 0. | 0. | 0. | 0. | 0. |
| THZX | 0. | 0. | 0. | 0. | 0. | 0. |
| THZY | 0. | 0. | 0. | 0. | 0. | 0. |
| DAX | 3.80779870E+00 | 0. | 0. | 1.50217659E+03 | 0. | 0. |
| CX | 3.54943854E+00 | 0. | 0. | 2.35384771E+03 | 0. | 0. |
| PHXZ | -1.07957642E-02 | 0. | 0. | -7.30135683E+00 | 0. | 0. |
| PHXY | 5.81348912E+00 | 0. | 0. | 4.02417736E+03 | 0. | 0. |
| DCX | 1.03771306E+00 | 0. | 0. | 6.83363639E+02 | 0. | 0. |
| DAY | 0. | 3.80779870E+00 | 0. | 0. | 1.50217659E+03 | 0. |
| CY | 0. | -1.67008965E-02 | 0. | 0. | -1.12950971E+01 | 0. |
| PHYZ | 0. | -2.29442182E+00 | 0. | 0. | -1.52157010E+03 | 0. |
| PHYY | 0. | 5.81348912E+00 | 0. | 0. | -4.02417736E+03 | 0. |
| DCY | 0. | 1.79287872E-05 | 0. | 0. | 1.19669252E-02 | 0. |
| DAZ | 0. | 0. | 3.80779870E+00 | 0. | 0. | 1.50217659E+03 |
| CZ | 0. | 0. | -8.99338656E+00 | 0. | 0. | -6.22534622E+03 |
| PHZX | 0. | 0. | 1.07957642E-02 | 0. | 0. | 7.30135683E+00 |
| PHZY | 0. | 0. | 2.29442182E+00 | 0. | 0. | 1.52157010E+03 |
| DCZ | 0. | 0. | 3.61933433E+00 | 0. | 0. | 2.43873725E+03 |
| PHX0 | 0. | 5.81348912E+00 | -1.07957642E-02 | 0. | 4.02417736E+03 | -7.30135683E+00 |
| PHY0 | -5.81348912E+00 | 0. | -2.29442182E+00 | -4.02417736E+03 | 0. | -1.52157010E+03 |
| PHZ0 | 2.15915284E-02 | 4.58884364E+00 | 0. | 1.46027137E+01 | -2.55463708E+02 | 0. |

THREE STANDARD DEVIATION OF ALL ERROR SOURCES

| | | | | | |
|---|---|---|---|---|---|
| 9.80103483E+00 | 1.04717296E+01 | 1.09136999E+01 | 6.38578533E+03 | 6.12898231E+03 | 7.18555543E+03 |

TOTAL VELOCITY RSS = 1.80229368E+01 ELAPSED TIME = 7.89000000E+02

TOTAL POSITION RSS = 1.14006528E+04 PITCH = .86 ROLL = -.12 HEADING = .03

# TABLE 24. – MEASUREMENT ERRORS, MINIMUM BUDGET, 600 N. MI. (1111.2 KM) TRAJECTORY; END OF FOURTH STAGE BOOST

END OF FOURTH STAGE BOOST

•3σ VALUES

| | DELTA-X-DOT | DELTA-Y-DOT | DELTA-Z-DOT | DELTA-X | DELTA-Y | DELTA-Z |
|---|---|---|---|---|---|---|
| RX | 0. | 2.97430832E-01 | -1.17152815E-03 | 0. | 1.98018906E+02 | -4.32734607E-01 |
| USX | 0. | 4.76446738E-01 | -1.62653152E-03 | 0. | 3.14638076E+02 | -7.48880520E-01 |
| UXX | 0. | -2.78498443E-03 | 7.94422822E-06 | 0. | -1.89022737E+00 | 4.31741975E-03 |
| SX | 0. | -6.09636784E-03 | 1.95020786E-05 | 0. | -4.05554211E+00 | 9.42974717E-03 |
| SFX | 0. | 0. | 0. | 0. | 0. | 0. |
| THXZ | 0. | 0. | 0. | 0. | 0. | 0. |
| THXY | 0. | 0. | 0. | 0. | 0. | 0. |
| RY | -2.97430832E-01 | 0. | -1.21620850E+00 | -1.98018906E+02 | 0. | -1.15504654E+02 |
| USY | 2.78498443E-03 | 0. | 4.83038669E-03 | 1.89022737E+00 | 0. | 1.11972265E+00 |
| UYY | -4.76446738E-01 | 0. | -1.31201602E+00 | -3.14638076E+02 | 0. | -2.05443643E+02 |
| SY | 6.09636784E-03 | 0. | 1.46068027E-02 | 4.05554211E+00 | 0. | 2.56864150E+00 |
| SFY | 0. | 0. | 0. | 0. | 0. | 0. |
| THYZ | 0. | 0. | 0. | 0. | 0. | 0. |
| THYX | 0. | 0. | 0. | 0. | 0. | 0. |
| RZ | 1.17152815E-03 | 1.21620850E+00 | 0. | 4.32734607E-01 | 1.15504654E+02 | 0. |
| USZ | -4.84172944E-03 | -2.62297850E+00 | 0. | -2.76967918E+00 | -6.89718345E+02 | 0. |
| UZZ | -7.94422822E-06 | -4.83038669E-03 | 0. | -4.31741975E-03 | -1.11972265E+00 | 0. |
| SZ | 3.84805660E-05 | 2.51104270E-02 | 0. | 2.01674575E-02 | 5.35308381E+00 | 0. |
| SFZ | 0. | 0. | 0. | 0. | 0. | 0. |
| THZX | 0. | 0. | 0. | 0. | 0. | 0. |
| THZY | 0. | 0. | 0. | 0. | 0. | 0. |
| DAX | 3.95740803E+00 | 0. | 0. | 1.62253729E+03 | 0. | 0. |
| CX | 7.66631890E+00 | 0. | 0. | 2.52346635E+03 | 0. | 0. |
| PHXZ | -1.21942971E-02 | 0. | 0. | -7.65626731E+00 | 0. | 0. |
| PHXY | 5.85345815E+00 | 0. | 0. | 4.20497402E+03 | 0. | 0. |
| DCX | 3.80958591E+00 | 0. | 0. | 7.51789621E+02 | 0. | 0. |
| DAY | 0. | 3.95740803E+00 | 0. | 0. | 1.62253729E+03 | 0. |
| CY | 0. | -1.88644075E-02 | 0. | 0. | -1.18441387E+01 | 0. |
| PHYZ | 0. | -4.95564838E+00 | 0. | 0. | -1.63121468E+03 | 0. |
| PHYX | 0. | 5.85345815E+00 | 0. | 0. | -4.20497402E+03 | 0. |
| DCY | 0. | 1.86943045E-05 | 0. | 0. | 1.25327308E-02 | 0. |
| DAZ | 0. | 0. | 3.95740803E+00 | 0. | 0. | 1.62253729E+03 |
| CZ | 0. | 0. | -9.05521808E+00 | 0. | 0. | -6.50503613E+03 |
| PHZX | 0. | 0. | 1.21942971E-02 | 0. | 0. | 7.65626731E+00 |
| PHZY | 0. | 0. | 4.95564838E+00 | 0. | 0. | 1.63121468E+03 |
| DCZ | 0. | 0. | 3.61995958E+00 | 0. | 0. | 2.55094479E+03 |
| PHX0 | 0. | 5.85345815E+00 | -1.21942971E-02 | 0. | 4.20497402E+03 | -7.65626731E+00 |
| PHY0 | -5.85345815E+00 | 0. | -4.95564838E+00 | -4.20497402E+03 | 0. | -1.63121468E+03 |
| PHZ0 | 2.43885942E-02 | 9.91129676E+00 | 0. | 1.53125346E+01 | -3.11556080E+02 | 0. |

THREE STANDARD DEVIATION OF ALL ERROR SOURCES

| | | | | | |
|---|---|---|---|---|---|
| 1.25613969E+01 | 1.46851959E+01 | 1.27702838E+01 | 6.71325851E+03 | 6.43285475E+03 | 7.53875577E+03 |

TOTAL VELOCITY RSS = 2.31629838E+01 ELAPSED TIME = 8.20000000E+02

TOTAL POSITION RSS = 1.19700584E+04 PITCH = .86 ROLL = -.12 HEADING = -.03

# TABLE 25. – MEASUREMENT ERRORS, MAXIMUM BUDGET, 600 N. MI. (1111.2 KM) TRAJECTORY; END OF THIRD STAGE BOOST

END OF THIRD STAGE BOOST

* 3σ VALUES

| | DELTA-X-DOT | DELTA-Y-DOT | DELTA-Z-DOT | DELTA-X | DELTA-Y | DELTA-Z |
|---|---|---|---|---|---|---|
| RX | 0. | 1.40657276E+01 | -3.04103893E-02 | 0. | 5.35045704E+02 | -1.00703243E+00 |
| USX | 0. | 1.15227022E+01 | -2.71176465E-02 | 0. | 1.97455526E+02 | -5.13523869E-01 |
| UXX | 0. | -6.83905752E-02 | 1.55646980E-04 | 0. | -1.75404152E+00 | 3.81025694E-03 |
| SX | 0. | -2.37174849E-02 | 5.47450513E-05 | 0. | -4.38665870E-01 | 9.88513349E-04 |
| SFX | 0. | 0. | 0. | 0. | 0. | 0. |
| THXZ | 0. | 0. | 0. | 0. | 0. | 0. |
| THXY | 0. | 0. | 0. | 0. | 0. | 0. |
| RY | -1.40657276E+01 | 0. | -7.21761731E+00 | -5.35045704E+02 | 0. | -2.03755171E+02 |
| USY | 6.83905752E-02 | 0. | 3.90405189E-02 | 1.75404152E+00 | 0. | 8.68447555E-01 |
| UYY | -1.15227022E+01 | 0. | -7.03017829E+00 | -1.97455526E+02 | 0. | -1.31171209E+02 |
| SY | 2.37174849E-02 | 0. | 1.41730489E-02 | 4.38665870E-01 | 0. | 2.39535396E-01 |
| SFY | 0. | 0. | 0. | 0. | 0. | 0. |
| THYZ | 0. | 0. | 0. | 0. | 0. | 0. |
| THYX | 0. | 0. | 0. | 0. | 0. | 0. |
| RZ | 3.04103893E-02 | 7.21761731E+00 | 0. | 1.00703243E+00 | 2.03755171E+02 | 0. |
| USZ | -9.92421417E-02 | -2.41036651E+01 | 0. | -2.92520820E+00 | -6.12887526E+02 | 0. |
| UZZ | -1.55646980E-04 | -3.90405189E-02 | 0. | -3.81025694E-03 | -8.68447555E-01 | 0. |
| SZ | 1.16781287E-04 | 2.97909048E-02 | 0. | 2.46348422E-03 | 5.76630841E-01 | 0. |
| SFZ | 0. | 0. | 0. | 0. | 0. | 0. |
| THZX | 0. | 0. | 0. | 0. | 0. | 0. |
| THZY | 0. | 0. | 0. | 0. | 0. | 0. |
| DAX | 4.98697759E+00 | 0. | 0. | 3.86490764E+02 | 0. | 0. |
| CX | 7.88711008E+00 | 0. | 0. | 2.30008438E+02 | 0. | 0. |
| PHXZ | -2.15904283E-02 | 0. | 0. | -9.13685237E-01 | 0. | 0. |
| PHXY | 1.16265094E+01 | 0. | 0. | 6.76850744E+02 | 0. | 0. |
| DCX | 3.45904266E+00 | 0. | 0. | 8.48451944E+01 | 0. | 0. |
| DAY | 0. | 4.98697759E+00 | 0. | 0. | 3.86490764E+02 | 0. |
| CY | 0. | -3.71112125E-02 | 0. | 0. | -1.57050924E+00 | 0. |
| PHYZ | 0. | -4.58853464E+00 | 0. | 0. | -1.33813485E+02 | 0. |
| PHYX | 0. | 1.16265094E+01 | 0. | 0. | -6.76850744E+02 | 0. |
| DCY | 0. | 5.97626129E-05 | 0. | 0. | 2.00024701E-03 | 0. |
| DAZ | 0. | 0. | 4.98697759E+00 | 0. | 0. | 3.86490764E+02 |
| CZ | 0. | 0. | -1.99844975E+01 | 0. | 0. | -1.16342073E+03 |
| PHZX | 0. | 0. | 2.15904283E-02 | 0. | 0. | 9.13685237E-01 |
| PHZY | 0. | 0. | 4.58853464E+00 | 0. | 0. | 1.33813485E+02 |
| DCZ | 0. | 0. | 1.20644457E+01 | 0. | 0. | 4.80264292E+02 |
| PHX0 | 0. | 1.74397640E+01 | -3.23856424E-02 | 0. | 1.01527612E+03 | -1.37052786E+00 |
| PHY0 | -1.74397640E+01 | 0. | -6.88280197E+00 | -1.01527612E+03 | 0. | -2.00720227E+02 |
| PHZ0 | 6.47712848E-02 | 1.37656039E+01 | 0. | 2.74105571E+00 | -7.66325167E+02 | 0. |

THREE STANDARD DEVIATION OF ALL ERROR SOURCES

| | | | | | |
|---|---|---|---|---|---|
| 2.94788153E+01 | 4.04777049E+01 | 2.71983608E+01 | 1.42255896E+03 | 1.72796546E+03 | 1.36033019E+03 |

TOTAL VELOCITY RSS = 5.69841736E+01 ELAPSED TIME = 1.55000000E+02

TOTAL POSITION RSS = 2.61916721E+03 PITCH = 56.68 ROLL = -.21 HEADING = -.20

## TABLE 26. – MEASUREMENT ERRORS, MAXIMUM BUDGET, 600 N. MI. (1111.2 KM) TRAJECTORY; END OF THIRD STAGE COAST

END OF THIRD STAGE COAST

• 3σ VALUES

| | DELTA-X-DOT | DELTA-Y-DOT | DELTA-Z-DOT | DELTA-X | DELTA-Y | DELTA-Z |
|---|---|---|---|---|---|---|
| RX | 0. | 1.40666390E+01 | -3.04125276E-02 | 0. | 9.45329436E+03 | -2.02885739E+01 |
| USX | 0. | 1.15241391E+01 | -2.71210175E-02 | 0. | 7.50375898E+03 | -1.77082473E+01 |
| UXX | 0. | -6.83973358E-02 | 1.55662842E-04 | 0. | -4.51179490E+01 | 1.02500491E-01 |
| SX | 0. | -2.37208504E-02 | 5.47529474E-05 | 0. | -1.54776833E+01 | 3.57018781E-02 |
| SFX | 0. | 0. | 0. | 0. | 0. | 0. |
| THXZ | 0. | 0. | 0. | 0. | 0. | 0. |
| THXY | 0. | 0. | 0. | 0. | 0. | 0. |
| RY | -1.40666390E+01 | 0. | -7.21821792E+00 | -9.45329436E+03 | 0. | -4.78010503E+03 |
| USY | 6.83973358E-02 | 0. | 3.90449741E-02 | 4.51179490E+01 | 0. | 2.56229589E+01 |
| UYY | -1.15241391E+01 | 0. | -7.03112314E+00 | -7.50375898E+03 | 0. | -4.58890281E+03 |
| SY | 2.37208504E-02 | 0. | 1.41752667E-02 | 1.54776833E+01 | 0. | 9.22665340E+00 |
| SFY | 0. | 0. | 0. | 0. | 0. | 0. |
| THYZ | 0. | 0. | 0. | 0. | 0. | 0. |
| THYX | 0. | 0. | 0. | 0. | 0. | 0. |
| RZ | 3.04125276E-02 | 7.21821792E+00 | 0. | 2.02885739E+01 | 4.78010503E+03 | 0. |
| USZ | -9.92506832E-02 | -2.41066642E+01 | 0. | -6.58501371E+01 | -1.58961311E+04 | 0. |
| UZZ | -1.55662842E-04 | -3.90449741E-02 | 0. | -1.02500491E-01 | -2.56229589E+01 | 0. |
| SZ | 1.16795870E-04 | 2.97950008E-02 | 0. | 7.65120586E-02 | 1.94666593E+01 | 0. |
| SFZ | 0. | 0. | 0. | 0. | 0. | 0. |
| THZX | 0. | 0. | 0. | 0. | 0. | 0. |
| THZY | 0. | 0. | 0. | 0. | 0. | 0. |
| DAX | 2.53853247E+01 | 0. | 0. | 1.00145106E+04 | 0. | 0. |
| CX | 7.88764119E+00 | 0. | 0. | 5.23077269E+03 | 0. | 0. |
| PHXZ | -2.15915284E-02 | 0. | 0. | -1.46027137E+01 | 0. | 0. |
| PHXY | 1.16269782E+01 | 0. | 0. | 8.04835472E+03 | 0. | 0. |
| DCX | 3.45904353E+00 | 0. | 0. | 2.27787880E+03 | 0. | 0. |
| DAY | 0. | 2.53853247E+01 | 0. | 0. | 1.00145106E+04 | 0. |
| CY | 0. | -3.71131034E-02 | 0. | 0. | -2.51002159E+01 | 0. |
| PHYZ | 0. | -4.58884364E+00 | 0. | 0. | -3.04314019E+03 | 0. |
| PHYX | 0. | 1.16269782E+01 | 0. | 0. | -8.04835472E+03 | 0. |
| DCY | 0. | 5.97626240E-05 | 0. | 0. | 3.98897506E-02 | 0. |
| DAZ | 0. | 0. | 2.53853247E+01 | 0. | 0. | 1.00145106E+04 |
| CZ | 0. | 0. | -1.99853035E+01 | 0. | 0. | -1.38341027E+04 |
| PHZX | 0. | 0. | 2.15915284E-02 | 0. | 0. | 1.46027137E+01 |
| PHZY | 0. | 0. | 4.58884364E+00 | 0. | 0. | 3.04314019E+03 |
| DCZ | 0. | 0. | 1.20644478E+01 | 0. | 0. | 8.12912417E+03 |
| PHX0 | 0. | 1.74404674E+01 | -3.23872925E-02 | 0. | 1.20725321E+04 | -2.19040705E+01 |
| PHY0 | -1.74404674E+01 | 0. | -6.88326545E+00 | -1.20725321E+04 | 0. | -4.56471029E+03 |
| PHZ0 | 6.47745851E-02 | 1.37665309E+01 | 0. | 4.38081410E+01 | -7.66391123E+02 | 0. |

THREE STANDARD DEVIATION OF ALL ERROR SOURCES

| | | | | | |
|---|---|---|---|---|---|
| 3.85830000E+01 | 4.75209032E+01 | 3.68694868E+01 | 2.21143055E+04 | 2.72373278E+04 | 2.07788921E+04 |

TOTAL VELOCITY RSS = 7.14579820E+01 ELAPSED TIME = 7.69000000E+02

TOTAL POSITION RSS = 4.07759352E+04 PITCH = .86 ROLL = -.12 HEADING = -.03

# TABLE 27. – MEASUREMENT ERRORS, MAXIMUM BUDGET, 600 N. MI. (1111.2 KM) TRAJECTORY; END OF FOURTH STAGE BOOST

END OF FOURTH STAGE BOOST

• 3σ VALUES

| | DELTA-X-DOT | DELTA-Y-DOT | DELTA-Z-DOT | DELTA-X | DELTA-Y | DELTA-Z |
|---|---|---|---|---|---|---|
| RX | 0. | 1.48715416E+01 | -5.85764076E-02 | 0. | 9.90094528E+03 | -2.16367303E+01 |
| USX | 0. | 1.19111685E+01 | -4.66633379E-02 | 0. | 7.86595190E+03 | -1.87220130E+01 |
| UXX | 0. | -6.96246107E-02 | 1.98605705E-04 | 0. | -4.72556842E+01 | 1.07935494E-01 |
| SX | 0. | -2.43854714E-02 | 7.80083145E-05 | 0. | -1.62221684E+01 | 3.77189847E-02 |
| SFX | 0. | 0. | 0. | 0. | 0. | 0. |
| THXZ | 0. | 0. | 0. | 0. | 0. | 0. |
| THXY | 0. | 0. | 0. | 0. | 0. | 0. |
| RY | -1.48715416E+01 | 0. | -6.08104248E+01 | -9.90094528E+03 | 0. | -5.77523270E+03 |
| USY | 6.96246107E-02 | 0. | 1.20759667E-01 | 4.72556842E+01 | 0. | 2.79930663E+01 |
| UYY | -1.19111685E+01 | 0. | -3.28004004E+01 | -7.86595190E+03 | 0. | -5.13409107E+03 |
| SY | 2.43854714E-02 | 0. | 5.84272107E-02 | 1.62221684E+01 | 0. | 1.02745660E+01 |
| SFY | 0. | 0. | 0. | 0. | 0. | 0. |
| THYZ | 0. | 0. | 0. | 0. | 0. | 0. |
| THYX | 0. | 0. | 0. | 0. | 0. | 0. |
| RZ | 5.85764076E-02 | 6.08104248E+01 | 0. | 2.16367303E+01 | 5.77523270E+03 | 0. |
| USZ | -1.21043236E-01 | -6.55744625E+01 | 0. | -6.92419794E+01 | -1.72429586E+04 | 0. |
| UZZ | -1.98605705E-04 | -1.20759667E-01 | 0. | -1.07935494E-01 | -2.79930663E+01 | 0. |
| SZ | 1.53922264E-04 | 1.00441708E-01 | 0. | 8.06698302E-02 | 2.14123353E+01 | 0. |
| SFZ | 0. | 0. | 0. | 0. | 0. | 0. |
| THZX | 0. | 0. | 0. | 0. | 0. | 0. |
| THZY | 0. | 0. | 0. | 0. | 0. | 0. |
| DAX | 2.63827202E+01 | 0. | 0. | 1.08169153E+04 | 0. | 0. |
| CX | 1.70362642E+01 | 0. | 0. | 5.60770300E+03 | 0. | 0. |
| PHXZ | -2.43885942E-02 | 0. | 0. | -1.53125346E+01 | 0. | 0. |
| PHXY | 1.17069163E+01 | 0. | 0. | 8.40994803E+03 | 0. | 0. |
| DCX | 1.26986197E+01 | 0. | 0. | 2.50596540E+03 | 0. | 0. |
| DAY | 0. | 2.63827202E+01 | 0. | 0. | 1.08169153E+04 | 0. |
| CY | 0. | -4.19209055E-02 | 0. | 0. | -2.63203826E+01 | 0. |
| PHYZ | 0. | -9.91129676E+00 | 0. | 0. | -3.26242936E+03 | 0. |
| PHYX | 0. | 1.17069163E+01 | 0. | 0. | -8.40994803E+03 | 0. |
| DCY | 0. | 6.23143482E-05 | 0. | 0. | 4.17757692E-02 | 0. |
| DAZ | 0. | 0. | 2.63827202E+01 | 0. | 0. | 1.08169153E+04 |
| CZ | 0. | 0. | -2.01227068E+01 | 0. | 0. | -1.44556358E+04 |
| PHZX | 0. | 0. | 2.43885942E-02 | 0. | 0. | 1.53125346E+01 |
| PHZY | 0. | 0. | 9.91129676E+00 | 0. | 0. | 3.26242936E+03 |
| DCZ | 0. | 0. | 1.20665319E+01 | 0. | 0. | 8.50314931E+03 |
| PHX0 | 0. | 1.75603744E+01 | -3.65828913E-02 | 0. | 1.26149220E+04 | -2.29688019E+01 |
| PHY0 | -1.75603744E+01 | 0. | -1.08669451E+01 | -1.26149220E+04 | 0. | -8.89364404E+03 |
| PHZ0 | 7.31657826E-02 | 2.97338903E+01 | 0. | 4.59376039E+01 | -9.34668241E+02 | 0. |

THREE STANDARD DEVIATION OF ALL ERROR SOURCES

| | | | | | |
|---|---|---|---|---|---|
| 4.42269597E+01 | 1.02395278E+02 | 7.96218020E+01 | 2.33346814E+04 | 2.91370121E+04 | 2.21946170E+04 |

TOTAL VELOCITY RSS = 1.37041776E+02 ELAPSED TIME = 8.20000000E+02

TOTAL POSITION RSS = 4.34289518E+04 PITCH = .86 ROLL = -.12 HEADING = -.03

# TABLE 28. — MEASUREMENT ERRORS, MINIMUM BUDGET, 200 N. MI. (370.4 KM) TRAJECTORY; END OF THIRD STAGE BOOST

END OF THIRD STAGE BOOST

• 3σ VALUES

| | DELTA-X-DOT | DELTA-Y-DOT | DELTA-Z-DOT | DELTA-X | DELTA-Y | DELTA-Z |
|---|---|---|---|---|---|---|
| RX | 0. | 2.1543639JE-01 | -4.58012640E-04 | 0. | 9.62791369E+00 | -1.80990605E-02 |
| USX | 0. | 6.86869101E-01 | -1.45550478E-03 | 0. | 1.82984253E+01 | -3.99128951E-02 |
| UYX | 0. | -1.52108941E-03 | 3.39011872E-06 | 0. | -4.92902844E-02 | 1.05145095E-04 |
| SX | 0. | -4.73335247E-03 | 1.07030310E-05 | 0. | -1.16614581E-01 | 2.53159824E-04 |
| SFX | 0. | 0. | 0. | 0. | 0. | 0. |
| THXZ | 0. | 0. | 0. | 0. | 0. | 0. |
| THXY | 0. | 0. | 0. | 0. | 0. | 0. |
| RY | -2.15436190E-01 | 0. | -2.43202955E-01 | -9.62791369E+00 | 0. | -8.32642149E+00 |
| USY | 1.52108941E-03 | 0. | 1.87332457E-03 | 4.92902848E-02 | 0. | 5.18226140E-02 |
| UYY | -6.86869101E-01 | 0. | -8.17163972E-01 | -1.82984253E+01 | 0. | -2.03484184E+01 |
| SY | 4.73335247E-03 | 0. | 6.09948108E-03 | 1.16614581E-01 | 0. | 1.32600206E-01 |
| SFY | 0. | 0. | 0. | 0. | 0. | 0. |
| THYZ | 0. | 0. | 0. | 0. | 0. | 0. |
| THYX | 0. | 0. | 0. | 0. | 0. | 0. |
| RZ | 4.58012640E-04 | 2.43202955E-01 | 0. | 1.80990605E-02 | 8.32642149E+00 | 0. |
| USZ | -2.27779295E-03 | -1.21823465E+00 | 0. | -8.58303369E-02 | -3.94761256E+01 | 0. |
| UZZ | -3.39011872E-06 | -1.87332457E-03 | 0. | -1.05145095E-04 | -5.18226140E-02 | 0. |
| SZ | 1.12046196E-05 | 6.26537845E-03 | 0. | 3.15282240E-04 | 1.58002020E-01 | 0. |
| SFZ | 0. | 0. | 0. | 0. | 0. | 0. |
| THZY | 0. | 0. | 0. | 0. | 0. | 0. |
| THZY | 0. | 0. | 0. | 0. | 0. | 0. |
| DAX | 8.10786035E-01 | 0. | 0. | 6.81060269E+01 | 0. | 0. |
| CX | 6.05023046E+00 | 0. | 0. | 2.63975561E+02 | 0. | 0. |
| PHXZ | -7.96596455E-03 | 0. | 0. | -4.22256765E-01 | 0. | 0. |
| PHXY | 4.46323045E+00 | 0. | 0. | 3.18949934E+02 | 0. | 0. |
| DCX | 2.34917433E+00 | 0. | 0. | 7.03020262E+01 | 0. | 0. |
| DAY | 0. | 8.10786035E-01 | 0. | 0. | 6.81060269E+01 | 0. |
| CY | 0. | -1.23232360E-02 | 0. | 0. | -6.53225324E-01 | 0. |
| PHYZ | 0. | -3.91097933E+00 | 0. | 0. | -1.70638618E+02 | 0. |
| PHYY | 0. | 4.46323045E+00 | 0. | 0. | -3.18949934E+02 | 0. |
| DCY | 0. | 9.06964182E-06 | 0. | 0. | 4.36017866E-04 | 0. |
| DAZ | 0. | 0. | 8.10786035E-01 | 0. | 0. | 6.81060269E+01 |
| CZ | 0. | 0. | -6.90455522E+00 | 0. | 0. | -4.93411098E+02 |
| PHZX | 0. | 0. | 7.96596455E-03 | 0. | 0. | 4.22256765E-01 |
| PHZY | 0. | 0. | 3.91097933E+00 | 0. | 0. | 1.70638618E+02 |
| DCZ | 0. | 0. | 1.89900677E+00 | 0. | 0. | 1.04491638E+02 |
| PHXO | 0. | 4.46323045E+00 | -7.96596455E-03 | 0. | 3.18949934E+02 | -4.22256765E-01 |
| PHYO | -4.46323045E+00 | 0. | -3.91097933E+00 | -3.18949934E+02 | 0. | -1.70638618E+02 |
| PHZO | 1.59319291E-02 | 7.82195847E+00 | 0. | 8.44513531E-01 | -1.46571644E+02 | 0. |

THREE STANDARD DEVIATION OF ALL ERROR SOURCES

| | | | | | |
|---|---|---|---|---|---|
| 9.11522542E+00 | 1.09080401E+01 | 9.12442200E+00 | 5.32124134E+02 | 5.10639824E+02 | 5.63675693E+02 |

TOTAL VELOCITY RSS = 1.68916473E+01 ELAPSED TIME = 1.68000000E+02

TOTAL POSITION RSS = 9.28245340E+02 PITCH = 34.19 ROLL = -.10 HEADING = -.09

# TABLE 29. – MEASUREMENT ERRORS, MINIMUM BUDGET, 200 N. MI. (370.4 KM) TRAJECTORY; END OF THIRD STAGE COAST

END OF THIRD STAGE COAST

30 VALUES

| | DELTA-X-DOT | DELTA-Y-DOT | DELTA-Z-DOT | DELTA-X | DELTA-Y | DELTA-Z |
|---|---|---|---|---|---|---|
| RX | 0. | 2.15436390E-01 | -4.58012640E-04 | 0. | 8.20145408E+01 | -1.71991307E-01 |
| USX | 0. | 6.46869101E-01 | -1.45550878E-03 | 0. | 2.35646443E+02 | -5.28963846E-01 |
| UXX | 0. | -1.52108941E-03 | 3.39011872E-06 | 0. | -5.60376326E-01 | 1.24422499E-03 |
| SX | 0. | -4.73335247E-03 | 1.07030310E-05 | 0. | -1.70702101E+00 | 3.84937823E-03 |
| SFX | 0. | 0. | 0. | 0. | 0. | 0. |
| THXZ | 0. | 0. | 0. | 0. | 0. | 0. |
| THXY | 0. | 0. | 0. | 0. | 0. | 0. |
| RY | -2.15436390E-01 | 0. | -2.43202955E-01 | -8.20145408E+01 | 0. | -9.00426144E+01 |
| USY | 1.52108941E-03 | 0. | 1.87332457E-03 | 5.60376326E-01 | 0. | 6.81259670E-01 |
| UYY | -6.46869101E-01 | 0. | -8.17163972E-01 | -2.35646443E+02 | 0. | -2.94915513E+02 |
| SY | 4.73335247E-03 | 0. | 6.09948108E-03 | 1.70702101E+00 | 0. | 2.18202585E+00 |
| SFY | 0. | 0. | 0. | 0. | 0. | 0. |
| THYZ | 0. | 0. | 0. | 0. | 0. | 0. |
| THYX | 0. | 0. | 0. | 0. | 0. | 0. |
| RZ | 4.58012640E-04 | 2.43202955E-01 | 0. | 1.71991307E-01 | 9.00426144E+01 | 0. |
| USZ | -2.27779295E-03 | -1.21823465E+00 | 0. | -8.51168767E-01 | -4.48802969E+02 | 0. |
| UZZ | -3.39011872E-06 | -1.87332457E-03 | 0. | -1.24422499E-03 | -6.81259670E-01 | 0. |
| SZ | 1.12046196E-05 | 6.26537845E-03 | 0. | 4.08003442E-03 | 2.26316918E+00 | 0. |
| SFZ | 0. | 0. | 0. | 0. | 0. | 0. |
| THZX | 0. | 0. | 0. | 0. | 0. | 0. |
| THZY | 0. | 0. | 0. | 0. | 0. | 0. |
| DAX | 2.43235810E+00 | 0. | 0. | 6.12954242E+02 | 0. | 0. |
| CX | 6.05023046E+00 | 0. | 0. | 2.29685100E+03 | 0. | 0. |
| PHXZ | -7.96596455E-03 | 0. | 0. | -3.09882086E+00 | 0. | 0. |
| PHXY | 4.46323045E+00 | 0. | 0. | 1.81859536E+03 | 0. | 0. |
| DCX | 2.34917433E+00 | 0. | 0. | 8.59666600E+02 | 0. | 0. |
| DAY | 0. | 2.43235810E+00 | 0. | 0. | 6.12954242E+02 | 0. |
| CY | 0. | -1.23232360E-02 | 0. | 0. | -4.79383262E+00 | 0. |
| PHYZ | 0. | -3.91097933E+00 | 0. | 0. | -1.48472767E+03 | 0. |
| PHYX | 0. | 4.46323045E+00 | 0. | 0. | -1.81859536E+03 | 0. |
| DCY | 0. | 9.06964182E-06 | 0. | 0. | 3.48341752E-03 | 0. |
| DAZ | 0. | 0. | 2.43235810E+00 | 0. | 0. | 6.12954242E+02 |
| CZ | 0. | 0. | -6.90855522E+00 | 0. | 0. | -2.81334165E+03 |
| PHZX | 0. | 0. | 7.96596455E-03 | 0. | 0. | 3.09882086E+00 |
| PHZY | 0. | 0. | 3.91097933E+00 | 0. | 0. | 1.48472767E+03 |
| DCZ | 0. | 0. | 1.89900677E+00 | 0. | 0. | 7.42557912E+02 |
| PHX0 | 0. | 4.46323045E+00 | -7.96596455E-03 | 0. | 1.81859536E+03 | -3.09882086E+00 |
| PHY0 | -4.46323045E+00 | 0. | -3.91097933E+00 | -1.81859536E+03 | 0. | -1.48472767E+03 |
| PHZ0 | 1.59319291E-02 | 7.82195867E+00 | 0. | 6.19748171E+00 | -1.46571644E+02 | 0. |

THREE STANDARD DEVIATION OF ALL ERROR SOURCES

| | | | | | |
|---|---|---|---|---|---|
| 9.39927266E+00 | 1.11844941E+01 | 9.40819158E+00 | 3.61885209E+03 | 3.08026132E+03 | 3.45320907E+03 |

TOTAL VELOCITY RSS = 1.73923694E+01 ELAPSED TIME = 5.04000000E+02

TOTAL POSITION RSS = 5.99179283E+03 PITCH = 3.04 ROLL = -.08 HEADING = -.04

## TABLE 30. – MEASUREMENT ERRORS, MINIMUM BUDGET, 200 N. MI. (370.4 KM) TRAJECTORY; END OF FOURTH STAGE BOOST

END OF FOURTH STAGE BOOST

• 3σ VALUES

| | DELTA-X-DOT | DELTA-Y-DOT | DELTA-Z-DOT | DELTA-X | DELTA-Y | DELTA-Z |
|---|---|---|---|---|---|---|
| RX | 0. | 2.43658959E-01 | -8.35114550E-04 | 0. | 8.93253263E+01 | -1.92217156E-01 |
| USX | 0. | 7.03944431E-01 | -2.21813305E-03 | 0. | 2.57141387E+02 | -5.86164464E-01 |
| UXX | 0. | -1.62165974E-03 | 4.73391076E-06 | 0. | -6.10510144E-01 | 1.37220295E-03 |
| SX | 0. | -5.18737994E-03 | 1.67696164E-05 | 0. | -1.86499393E+00 | 4.27880173E-03 |
| SFX | 0. | 0. | 0. | 0. | 0. | 0. |
| THXZ | 0. | 0. | 0. | 0. | 0. | 0. |
| THXY | 0. | 0. | 0. | 0. | 0. | 0. |
| RY | -2.43658959E-01 | 0. | -7.75004360E-01 | -8.93253263E+01 | 0. | -1.05679320E+02 |
| USY | 1.62165974E-03 | 0. | 3.76838389E-03 | 6.10510144E-01 | 0. | 7.68697370E-01 |
| UYY | -7.03944431E-01 | 0. | -1.89264157E+00 | -2.57141387E+02 | 0. | -3.36047545E+02 |
| SY | 5.18737994E-03 | 0. | 1.46547777E-02 | 1.86499393E+00 | 0. | 2.49979584E+00 |
| SFY | 0. | 0. | 0. | 0. | 0. | 0. |
| THYZ | 0. | 0. | 0. | 0. | 0. | 0. |
| THYX | 0. | 0. | 0. | 0. | 0. | 0. |
| RZ | 8.35114550E-04 | 7.75004360E-01 | 0. | 1.92217156E-01 | 1.05679320E+02 | 0. |
| USZ | -2.97637707E-03 | -2.20340076E+00 | 0. | -9.34424174E-01 | -5.02404995E+02 | 0. |
| UZZ | -4.73391076E-06 | -3.76838389E-03 | 0. | -1.37220295E-03 | -7.68697370E-01 | 0. |
| SZ | 1.59893942E-05 | 1.30130236E-02 | 0. | 4.50966662E-03 | 2.56390679E+00 | 0. |
| SFZ | 0. | 0. | 0. | 0. | 0. | 0. |
| THZX | 0. | 0. | 0. | 0. | 0. | 0. |
| THZY | 0. | 0. | 0. | 0. | 0. | 0. |
| DAX | 2.58679354E+00 | 0. | 0. | 6.93260669E+02 | 0. | 0. |
| CX | 9.20770719E+00 | 0. | 0. | 2.53748919E+03 | 0. | 0. |
| PHXZ | -9.41327939E-03 | 0. | 0. | -3.37528865E+00 | 0. | 0. |
| PHXY | 4.57154849E+00 | 0. | 0. | 1.96303207E+03 | 0. | 0. |
| DCX | 3.94723911E+00 | 0. | 0. | 9.57026516E+02 | 0. | 0. |
| DAY | 0. | 2.58679354E+00 | 0. | 0. | 6.93260669E+02 | 0. |
| CY | 0. | -1.45622119E-02 | 0. | 0. | -5.22152445E+00 | 0. |
| PHYZ | 0. | -5.95202989E+00 | 0. | 0. | -1.64027930E+03 | 0. |
| PHYX | 0. | 4.57154849E+00 | 0. | 0. | -1.96303207E+03 | 0. |
| DCY | 0. | 9.87319178E-06 | 0. | 0. | 3.78480295E-03 | 0. |
| DAZ | 0. | 0. | 2.58679354E+00 | 0. | 0. | 6.93260669E+02 |
| CZ | 0. | 0. | -7.07212173E+00 | 0. | 0. | -3.03678323E+03 |
| PHZX | 0. | 0. | 9.41327939E-03 | 0. | 0. | 3.37528865E+00 |
| PHZY | 0. | 0. | 5.95202989E+00 | 0. | 0. | 1.64027930E+03 |
| DCZ | 0. | 0. | 1.90350755E+00 | 0. | 0. | 8.03388619E+02 |
| PHX0 | 0. | 4.57154849E+00 | -9.41327939E-03 | 0. | 1.96303207E+03 | -3.37528865E+00 |
| PHY0 | -4.57154849E+00 | 0. | -5.95202989E+00 | -1.96303207E+03 | 0. | -1.64027930E+03 |
| PHZ0 | 1.88265588E-02 | 1.19040598E+01 | 0. | 6.75057731E+00 | -1.91524204E+02 | 0. |

THREE STANDARD DEVIATION OF ALL ERROR SOURCES

| | | | | | |
|---|---|---|---|---|---|
| 1.22232389E+01 | 1.52195220E+01 | 1.16346982E+01 | 3.95177350E+03 | 3.35447698E+03 | 3.98161855E+03 |

TOTAL VELOCITY RSS = 2.27246039E+01 ELAPSED TIME = 5.36000000E+02

TOTAL POSITION RSS = 6.53622858E+03 PITCH = 3.04 ROLL = -.08 HEADING = -.04

# TABLE 31. – MEASUREMENT ERRORS, MAXIMUM BUDGET, 200 N. MI. (370.4 KM) TRAJECTORY; END OF THIRD STAGE BOOST

END OF THIRD STAGE BOOST

• 3σ VALUES

| | DELTA-X-DOT | DELTA-Y-DOT | DELTA-Z-DOT | DELTA-X | DELTA-Y | DELTA-Z |
|---|---|---|---|---|---|---|
| RY | 0. | 1.07718196E+01 | -2.29006320E-02 | 0. | 4.81395686E+02 | -9.04953026E-01 |
| USX | 0. | 1.61717275E+01 | -3.43877193E-02 | 0. | 4.57460629E+02 | -9.97822366E-01 |
| UYX | 0. | -3.80272355E-02 | 8.47529681E-05 | 0. | -1.23225713E+00 | 2.62862738E-03 |
| SX | 0. | -1.99334099E-02 | 4.24121236E-05 | 0. | -4.66458322E-01 | 1.01263929E-03 |
| SFX | 0. | 0. | 0. | 0. | 0. | 0. |
| THXZ | 0. | 0. | 0. | 0. | 0. | 0. |
| THXY | 0. | 0. | 0. | 0. | 0. | 0. |
| RY | -1.07718196E+01 | 0. | -1.21601477E+01 | -4.81395686E+02 | 0. | -4.16321071E+02 |
| USY | 3.80272355E-02 | 0. | 4.68331141E-02 | 1.23225713E+00 | 0. | 1.29556534E+00 |
| UYY | -1.61717275E+01 | 0. | -2.04290990E+01 | -4.57460629E+02 | 0. | -5.06710452E+02 |
| SY | 1.99334099E-02 | 0. | 2.43979241E-02 | 4.66458322E-01 | 0. | 5.30400819E-01 |
| SFY | 0. | 0. | 0. | 0. | 0. | 0. |
| THYZ | 0. | 0. | 0. | 0. | 0. | 0. |
| THYY | 0. | 0. | 0. | 0. | 0. | 0. |
| RZ | 2.29006320E-02 | 1.21601477E+01 | 0. | 9.04953026E-01 | 4.16321071E+02 | 0. |
| USZ | -5.49448238E-02 | -3.04558662E+01 | 0. | -2.14575843E+00 | -9.86903133E+02 | 0. |
| UZZ | -8.47529681E-05 | -4.68331141E-02 | 0. | -2.62862738E-03 | -1.29556534E+00 | 0. |
| SZ | 4.48184786E-05 | 2.50615138E-02 | 0. | 1.26112896E-03 | 6.32008080E-01 | 0. |
| SFZ | 0. | 0. | 0. | 0. | 0. | 0. |
| THZX | 0. | 0. | 0. | 0. | 0. | 0. |
| THZY | 0. | 0. | 0. | 0. | 0. | 0. |
| DAX | 5.40524023E+00 | 0. | 0. | 4.54040179E+02 | 0. | 0. |
| CX | 1.34449565E+01 | 0. | 0. | 5.86612352E+02 | 0. | 0. |
| PHXZ | -1.59319291E-02 | 0. | 0. | -8.44513531E-01 | 0. | 0. |
| PHXY | 8.92646093E+00 | 0. | 0. | 6.37899870E+02 | 0. | 0. |
| DCX | 7.83058101E+00 | 0. | 0. | 2.34473417E+02 | 0. | 0. |
| DAY | 0. | 5.40524023E+00 | 0. | 0. | 4.54040179E+02 | 0. |
| CY | 0. | -2.73849089E-02 | 0. | 0. | -1.45161183E+00 | 0. |
| PHYZ | 0. | -7.82195862E+00 | 0. | 0. | -3.41277232E+02 | 0. |
| PHYY | 0. | 8.92646093E+00 | 0. | 0. | -6.37899870E+02 | 0. |
| DCY | 0. | 3.02321394E-05 | 0. | 0. | 1.45339289E-03 | 0. |
| DAZ | 0. | 0. | 5.40524023E+00 | 0. | 0. | 4.54040179E+02 |
| CZ | 0. | 0. | -1.53434561E+01 | 0. | 0. | -1.09646911E+03 |
| PHZX | 0. | 0. | 1.59319291E-02 | 0. | 0. | 8.44513531E-01 |
| PHZY | 0. | 0. | 7.82195862E+00 | 0. | 0. | 3.41277232E+02 |
| DCZ | 0. | 0. | 6.33002263E+00 | 0. | 0. | 3.48305463E+02 |
| PHX0 | 0. | 1.33896914E+01 | -2.38978937E-02 | 0. | 9.56849805E+02 | -1.26677030E+00 |
| PHY0 | -1.33896914E+01 | 0. | -1.17329379E+01 | -9.56849805E+02 | 0. | -5.11915849E+02 |
| PHZ0 | 4.77957873E-02 | 2.34658759E+01 | 0. | 2.53358059E+00 | -4.39714932E+02 | 0. |

THREE STANDARD DEVIATION OF ALL ERROR SOURCES

| | | | | | |
|---|---|---|---|---|---|
| 3.01302595E+01 | 4.85077700E+01 | 3.26921254E+01 | 1.53907389E+03 | 1.85115332E+03 | 1.52982264E+03 |

TOTAL VELOCITY RSS = 5.57997782E+01 ELAPSED TIME = 1.68000000E+02

TOTAL POSITION RSS = 2.85234542E+03 PITCH = 34.19 ROLL = -.10 HEADING = -.09

## TABLE 32. – MEASUREMENT ERRORS, MAXIMUM BUDGET, 200 N. MI. (370.4 KM) TRAJECTORY; END OF THIRD STAGE COAST

END OF THIRD STAGE COAST

• 3σ VALUES

| | DELTA-X-DOT | DELTA-Y-DOT | DELTA-Z-DOT | DELTA-X | DELTA-Y | DELTA-Z |
|---|---|---|---|---|---|---|
| RX | 0. | 1.07718196E+01 | -2.29006320E-02 | 0. | 4.10072706E+03 | -8.59956538E+00 |
| USX | 0. | 1.61717275E+01 | -3.63877193E-02 | 0. | 5.89116107E+03 | -1.32240961E+01 |
| UXX | 0. | -3.80272355E-02 | 8.47529681E-05 | 0. | -1.40094082E+01 | 3.11056246E-02 |
| SX | 0. | -1.89334099E-02 | 4.28121236E-05 | 0. | -6.82808405E+00 | 1.53975128E-02 |
| SFX | 0. | 0. | 0. | 0. | 0. | 0. |
| THXZ | 0. | 0. | 0. | 0. | 0. | 0. |
| THXY | 0. | 0. | 0. | 0. | 0. | 0. |
| RY | -1.07718196E+01 | 0. | -1.21601477E+01 | -4.10072706E+03 | 0. | -4.50213070E+03 |
| USY | 3.80272355E-02 | 0. | 4.68331141E-02 | 1.40094082E+01 | 0. | 1.70314917E+01 |
| UYY | -1.61717275E+01 | 0. | -2.04290990E+01 | -5.89116107E+03 | 0. | -7.37288773E+03 |
| SY | 1.89334099E-02 | 0. | 2.43979241E-02 | 6.82808405E+00 | 0. | 8.72810330E+00 |
| SFY | 0. | 0. | 0. | 0. | 0. | 0. |
| THYZ | 0. | 0. | 0. | 0. | 0. | 0. |
| THYX | 0. | 0. | 0. | 0. | 0. | 0. |
| RZ | 2.29006320E-02 | 1.21601477E+01 | 0. | 8.59956538E+00 | 4.50213070E+03 | 0. |
| USZ | -5.69448238E-02 | -3.04558662E+01 | 0. | -2.12792192E+01 | -1.12200742E+04 | 0. |
| UZZ | -8.47529681E-05 | -4.68331141E-02 | 0. | -3.11056246E-02 | -1.70314917E+01 | 0. |
| SZ | 4.48184786E-05 | 2.50615138E-02 | 0. | 1.63201378E-02 | 9.05267672E+00 | 0. |
| SFZ | 0. | 0. | 0. | 0. | 0. | 0. |
| THZX | 0. | 0. | 0. | 0. | 0. | 0. |
| THZY | 0. | 0. | 0. | 0. | 0. | 0. |
| DAX | 1.62157207E+01 | 0. | 0. | 4.08636162E+03 | 0. | 0. |
| CX | 1.34449565E+01 | 0. | 0. | 5.10411773E+03 | 0. | 0. |
| PHXZ | -1.59319291E-02 | 0. | 0. | -6.19764171E+00 | 0. | 0. |
| PHXY | 8.92646093E+00 | 0. | 0. | 3.63719074E+03 | 0. | 0. |
| DCX | 7.83058101E+00 | 0. | 0. | 2.86554864E+03 | 0. | 0. |
| DAY | 0. | 1.62157207E+01 | 0. | 0. | 4.08636162E+03 | 0. |
| CY | 0. | -2.73849689E-02 | 0. | 0. | -1.06529614E+01 | 0. |
| PHYZ | 0. | -7.82195862E+00 | 0. | 0. | -2.96945533E+03 | 0. |
| PHYX | 0. | 8.92644093E+00 | 0. | 0. | -3.63719074E+03 | 0. |
| DCY | 0. | 3.02321394E-05 | 0. | 0. | 1.16113917E-02 | 0. |
| DAZ | 0. | 0. | 1.62157207E+01 | 0. | 0. | 4.08636162E+03 |
| CZ | 0. | 0. | -1.53434561E+01 | 0. | 0. | -6.25187036E+03 |
| PHZX | 0. | 0. | 1.59319291E-02 | 0. | 0. | 6.19764171E+00 |
| PHZY | 0. | 0. | 7.82195862E+00 | 0. | 0. | 2.96945533E+03 |
| DCZ | 0. | 0. | 6.33002263E+00 | 0. | 0. | 2.47519307E+03 |
| PHX0 | 0. | 1.33896914E+01 | -2.38978937E-02 | 0. | 5.45578611E+03 | -9.29646257E+00 |
| PHY0 | -1.33896914E+01 | 0. | -1.17329379E+01 | -5.45578611E+03 | 0. | -4.45418299E+03 |
| PHZ0 | 4.77957873E-02 | 2.34658759E+01 | 0. | 1.85929251E+01 | -4.39714932E+02 | 0. |

THREE STANDARD DEVIATION OF ALL ERROR SOURCES

| | | | | | |
|---|---|---|---|---|---|
| 3.37870533E+01 | 5.08599717E+01 | 3.60902763E+01 | 1.20614838E+04 | 1.63213308E+04 | 1.28529226E+04 |

TOTAL VELOCITY RSS = 7.09282013E+01 ELAPSED TIME = 5.04000000E+02

TOTAL POSITION RSS = 2.40221325E+04 PITCH = 3.04 ROLL = -.08 HEADING = -.04

# TABLE 33. – MEASUREMENT ERRORS, MAXIMUM BUDGET, 200 N. MI. (370.4 KM) TRAJECTORY; END OF FOURTH STAGE BOOST

END OF FOURTH STAGE BOOST

• 3σ VALUES

| | DELTA-X-DOT | DELTA-Y-DOT | DELTA-Z-DOT | DELTA-X | DELTA-Y | DELTA-Z |
|---|---|---|---|---|---|---|
| RX | 0. | 1.21829482E+01 | -4.17557275E-02 | 0. | 4.46626634E+03 | -9.61085778E+00 |
| USX | 0. | 1.75986109E+01 | -5.54533260E-02 | 0. | 6.42853467E+03 | -1.44541115E+01 |
| UXX | 0. | -4.05414940E-02 | 1.18347769E-04 | 0. | -1.52627537E+01 | 3.43050739E-02 |
| SX | 0. | -2.07495200E-02 | 6.70784655E-05 | 0. | -7.45997573E+00 | 1.71152066E-02 |
| SFX | 0. | 0. | 0. | 0. | 0. | 0. |
| THXZ | 0. | 0. | 0. | 0. | 0. | 0. |
| THXY | 0. | 0. | 0. | 0. | 0. | 0. |
| RY | -1.21829482E+01 | 0. | -3.87502179E+01 | -4.46626634E+03 | 0. | -5.28396597E+03 |
| USY | 4.05414940E-02 | 0. | 9.42095971E-02 | 1.52627537E+01 | 0. | 1.92174342E+01 |
| UYY | -1.75986109E+01 | 0. | -4.73160389E+01 | -6.42853467E+03 | 0. | -8.40118853E+03 |
| SY | 2.07495200E-02 | 0. | 5.86191102E-02 | 7.45997573E+00 | 0. | 9.99918626E+00 |
| SFY | 0. | 0. | 0. | 0. | 0. | 0. |
| THYZ | 0. | 0. | 0. | 0. | 0. | 0. |
| THYX | 0. | 0. | 0. | 0. | 0. | 0. |
| RZ | 4.17557275E-02 | 3.87502179E+01 | 0. | 9.61085778E+00 | 5.28396597E+03 | 0. |
| USZ | -7.44094271E-02 | -5.50850159E+01 | 0. | -2.33606044E+01 | -1.25601248E+04 | 0. |
| UZZ | -1.18347769E-04 | -9.42095971E-02 | 0. | -3.43050739E-02 | -1.92174342E+01 | 0. |
| SZ | 6.39575773E-05 | 5.20520946E-02 | 0. | 1.80386666E-02 | 1.02556272E+01 | 0. |
| SFZ | 0. | 0. | 0. | 0. | 0. | 0. |
| THZX | 0. | 0. | 0. | 0. | 0. | 0. |
| THZY | 0. | 0. | 0. | 0. | 0. | 0. |
| DAX | 1.72452903E+01 | 0. | 0. | 4.62173779E+03 | 0. | 0. |
| CX | 2.04615714E+01 | 0. | 0. | 5.63886483E+03 | 0. | 0. |
| PHXZ | -1.88265588E-02 | 0. | 0. | -6.75057731E+00 | 0. | 0. |
| PHXY | 9.14309705E+00 | 0. | 0. | 3.92606416E+03 | 0. | 0. |
| DCX | 1.31574636E+01 | 0. | 0. | 3.19008835E+03 | 0. | 0. |
| DAY | 0. | 1.72452903E+01 | 0. | 0. | 4.62173779E+03 | 0. |
| CY | 0. | -3.23604708E-02 | 0. | 0. | -1.16063877E+01 | 0. |
| PHYZ | 0. | -1.19040597E+01 | 0. | 0. | -3.28055858E+03 | 0. |
| PHYX | 0. | 9.14309705E+00 | 0. | 0. | -3.92606416E+03 | 0. |
| DCY | 0. | 3.29106693E-05 | 0. | 0. | 1.26160098E-02 | 0. |
| DAZ | 0. | 0. | 1.72452903E+01 | 0. | 0. | 4.62173779E+03 |
| CZ | 0. | 0. | -1.57158262E+01 | 0. | 0. | -6.74840720E+03 |
| PHZX | 0. | 0. | 1.88265588E-02 | 0. | 0. | 6.75057731E+00 |
| PHZY | 0. | 0. | 1.19040597E+01 | 0. | 0. | 3.28055858E+03 |
| DCZ | 0. | 0. | 6.34502525E+00 | 0. | 0. | 2.67796209E+03 |
| PHX0 | 0. | 1.37146456E+01 | -2.82398382E+02 | 0. | 5.88909624E+03 | -1.01258660E+01 |
| PHY0 | -1.37146456E+01 | 0. | -1.78560896E+01 | -5.88909624E+03 | 0. | -4.92083787E+03 |
| PHZ0 | 5.64798764E-02 | 3.57121792E+01 | 0. | 2.02517519E+01 | -5.74572615E+02 | 0. |

THREE STANDARD DEVIATION OF ALL ERROR SOURCES

| | | | | | | |
|---|---|---|---|---|---|---|
| | 4.02371812E+01 | 8.35478478E+01 | 6.91760194E+01 | 1.32175766E+04 | 1.81521243E+04 | 1.44066249E+04 |

TOTAL VELOCITY RSS = 1.15693007E+02 ELAPSED TIME = 5.36000000E+02

TOTAL POSITION RSS = 2.44787329E+04 PITCH = 3.04 ROLL = -.08 HEADING = -.04

The computer simulations assume that the accelerometers are used throughout the entire third stage coast phase. This means that the accelerometer bias uncertainties affect the velocity measurement for the whole time period. This is a somewhat conservative approach in that it uses no pre-flight knowledge of coast time when the vehicle drag becomes negligible. It would be possible to lock out the accelerometer output during that time provided the integration technique implemented was compatible.

NOTE: Data in Tables 22 through 33 are given in customary U.S. units. The conversion factors needed to convert these to the Internationale System are:

| From | To | Mulitply by |
|---|---|---|
| Feet/second | Meters/second | 0.3048 |
| Feet | Kilometers | $0.3048 \times 10^{-3}$ |

## 11.0 ORBITAL DEVIATIONS – NEW CONCEPTS

Scout orbital accuracies were calculated for all combinations of the four guidance options, the two reference orbits and the two equipment error budgets. The general procedure followed in the analysis was very similar to that used in the analysis of the integral of $N\chi$ approach as discussed in Section 8.0.

### 11.1 Fourth Stage Error Simulation

As in the integral of $N\chi$ case, the flight deviations at fourth stage ignition are needed. The flight data available are in terms of deviations at fourth stage burnout; these were used as the starting point in the fourth stage error simulations.

A computer program was coded to simulate the new AVC guidance options discussed. A flow chart of this program which illustrates the analysis sequence is shown in Figure 16. As indicated in the figure, the statistics on the flight deviations at fourth stage burnout are measured in terms of:

$\Delta h$ – Altitude
$\Delta V$ – Velocity magnitude
$\Delta\gamma$ – Flight path angle
$\Delta\zeta$ – Heading angle
$\Delta\lambda$ – Latitude
$\Delta\mu$ – Longitude

The data were normalized to the nominal altitude and heading of the two reference trajectories. Fourth stage boost errors were sampled using standard deviations as determined from the 37 flight data. This permits the calculation of the covariance matrix due to fourth stage boost errors which is then subtracted from the covariance matrix at fourth stage burnout to yield the ignition covariance matrix.

Each guidance option was simulated in terms of the fourth stage attitude adjustments made and the measurement errors at fourth stage ignition were added. The appropriate manner of fourth stage ignition was included. The fourth stage boost errors were then included to compute the resulting fourth stage burnout errors in the reference inertial coordinate system. AVC measurement errors for

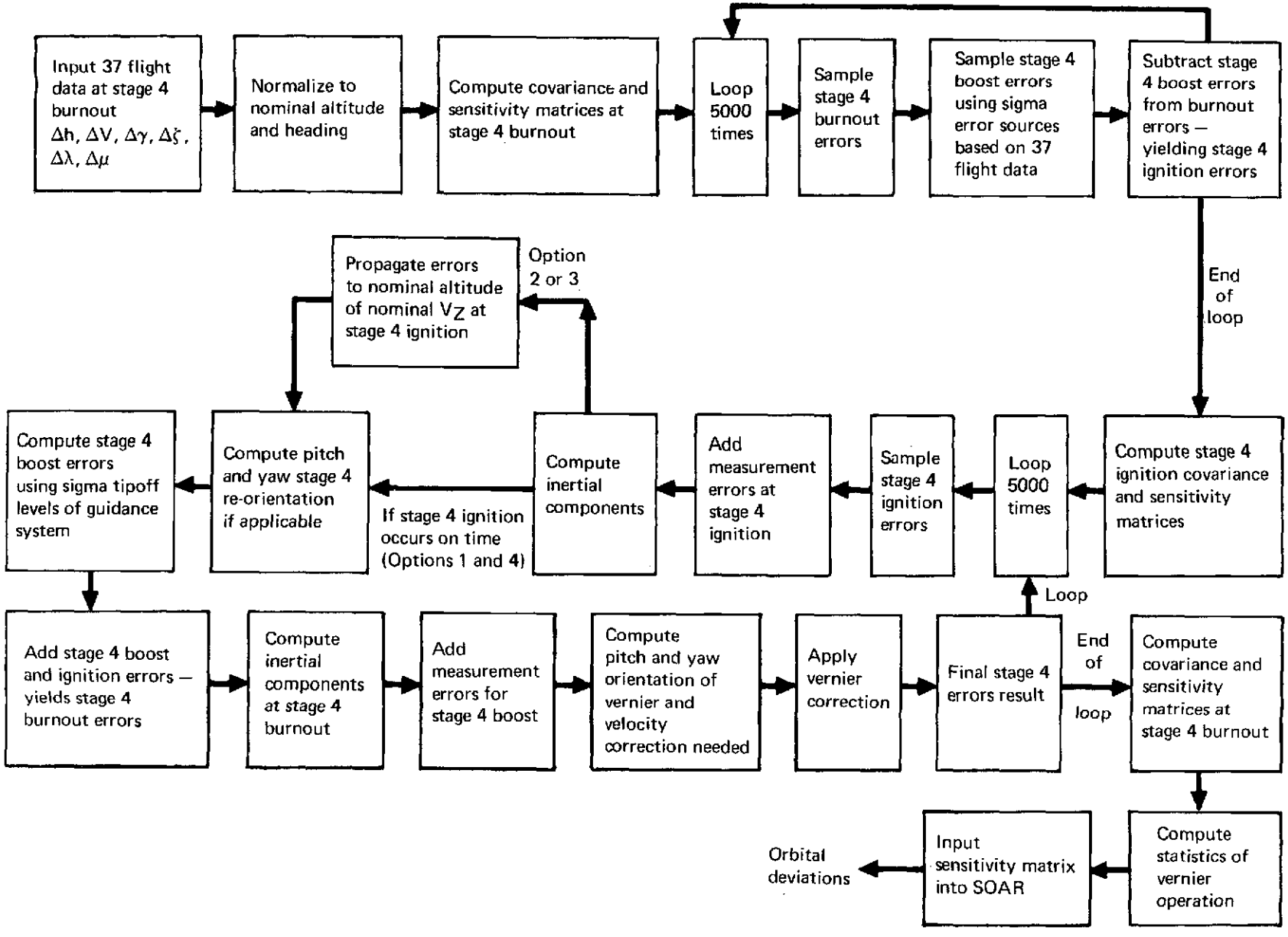


FIGURE 16. – AVC GUIDANCE OPTIONS ORBITAL ACCURACY FLOWCHART

the fourth stage boost phase were added and the appropriate velocity correction computed and applied. This computation included the pitch maneuver angle as required. The loop from the determination of fourth stage ignition errors to the final errors after the velocity correction was performed 5000 times. This 5000 sample was used to determine the covariance and sensitivity matrices which were input to SOAR to determine the actual oribtal deviations.

The AVC inertial guidance system errors used in the simulations discussed are shown in Table 34. This table summarizes the results of the previous section. Inertial system attitude errors used were those presented in Section 10.1.

## 11.2 Results

11.2.1 Isoprobability Contours. – Isoprobability contours for the four guidance options and the two trajectories are presented in Figure 17 through 24. In each case the standard Scout contour is shown together with those for the minimum and maximum AVC guidance equipment error budgets. All are for a 0.95 probability level. In addition, there was no limitation placed upon the magnitude of the $\Delta V$ correction applied. The guidance options involve the two corrections using measured inertial velocity data, however there is no means of deriving the $\Delta V$ required from available flight data. The simulations were accomplished with no limit on the $\Delta V$ applied and then the statistics computed from the 5000 sample as indicated in Figure 16.

Option 1 (Figure 17 and 18) shows vast improvement over the standard Scout accuracy. The reduction in maximum apogee-perigee deviation approaches a factor of 3. There is little difference in the two error budgets especially for the lower orbit altitude case.

Accuracy results for Option 2 as shown in Figure 19 and 20 are very unusual. The shape of the contours reflects essentially errros only in flight path anlge. This is caused by commanding fourth stage ignition at nominal altitude and nulling the velocity error with the vernier. The flight path angle error results from aligning the velocity vector along the nominal direction instead of the local horizontal. Since the range angle will almost always be less than nominal due to early ignition, the path angle after correction will almost always be negative. This effect produces a large path angle error and the resulting isoprobability contour as shown. This characteristic makes Option 2 undesirable.

Option 3 results are shown in Figure 21 and 22. The accuracy improvement achieved is comparable to that of Option 1. The results indicate even a lower sensitivity to the guidance equipment error budgets than did Option 1.

Option 4 accuracies are presented in Figure 23 and 24. These results should be compared with the integral of $N_X$ accuracies in terms of the type of corrections employed. The only correction made in this option, other than controlling fourth stage burn attitude to the nominal value, is to apply a $\Delta V$ correcting only the error measured along the X axis. The shape of the contours for this option shows a slight reduction in flight path angle error resulting from the attitude control of the fourth stage. A vertical velocity correction would reduce the center extrusion of the curve. There is very little sensitivity to the equipment error budget even for this option.

Summary or comparative plots of all options plus the integral of $N_X$ are shown in Figures 25 and 26 for the two orbits. These plots show that the accuracy improvements achievable with Option 1 or 3 are comparable, especially at the higher orbit. Either option would no doubt provide the accuracy required for the vast majority of payloads.

## TABLE 34. – AVC IMU MEASUREMENT ERRORS – SUMMARY

- $3\sigma$ Values, reference coordinate system

600 n. mi. (1111.2 km) Trajectory

| Trajectory Event | Error Budget | $\Delta\dot{X}$ | | $\Delta\dot{Y}$ | | $\Delta\dot{Z}$ | | $\Delta X$ | | $\Delta Y$ | | $\Delta Z$ | |
|---|---|---|---|---|---|---|---|---|---|---|---|---|---|
| | | ft/s | m/s | ft/s | m/s | ft/s | m/s | ft | m | ft | m | ft | m |
| 4th Stage ignition | Min | 9.80 | 2.98 | 10.47 | 3.19 | 10.91 | 3.33 | 6,386 | 1,946 | 6,129 | 1,868 | 7,186 | 2,190 |
| | Max | 38.58 | 11.76 | 47.52 | 14.48 | 36.87 | 11.24 | 22,114 | 6,740 | 27,237 | 8,302 | 28,778 | 8,772 |
| 4th Stage burnout | Min | 12.56 | 3.83 | 14.69 | 4.48 | 12.77 | 3.89 | 6,713 | 2,046 | 6,433 | 1,961 | 7,539 | 2,298 |
| | Max | 44.23 | 13.48 | 102.40 | 31.21 | 79.62 | 24.27 | 23,335 | 7,113 | 29,167 | 8,890 | 22,195 | 6,765 |

200 n. mi. (370.4 km) Trajectory

| Trajectory Event | Error Budget | $\Delta\dot{X}$ | | $\Delta\dot{Y}$ | | $\Delta\dot{Z}$ | | $\Delta X$ | | $\Delta Y$ | | $\Delta Z$ | |
|---|---|---|---|---|---|---|---|---|---|---|---|---|---|
| | | ft/s | m/s | ft/s | m/s | ft/s | m/s | ft | m | ft | m | ft | m |
| 4th Stage ignition | Min | 9.40 | 2.87 | 11.15 | 3.40 | 9.41 | 2.87 | 3,615 | 1,102 | 3,080 | 939 | 3,653 | 1,113 |
| | Max | 33.79 | 10.30 | 50.86 | 15.50 | 36.09 | 11.00 | 12,061 | 3,676 | 16,321 | 4,975 | 12,853 | 3,918 |
| 4th Stage burnout | Min | 12.22 | 3.72 | 15.22 | 4.64 | 11.63 | 3.54 | 3,952 | 1,205 | 3,354 | 1,022 | 3,982 | 1,214 |
| | Max | 40.24 | 12.27 | 83.55 | 25.47 | 69.18 | 21.09 | 13,218 | 4,029 | 18,152 | 5,532 | 14,407 | 4,391 |

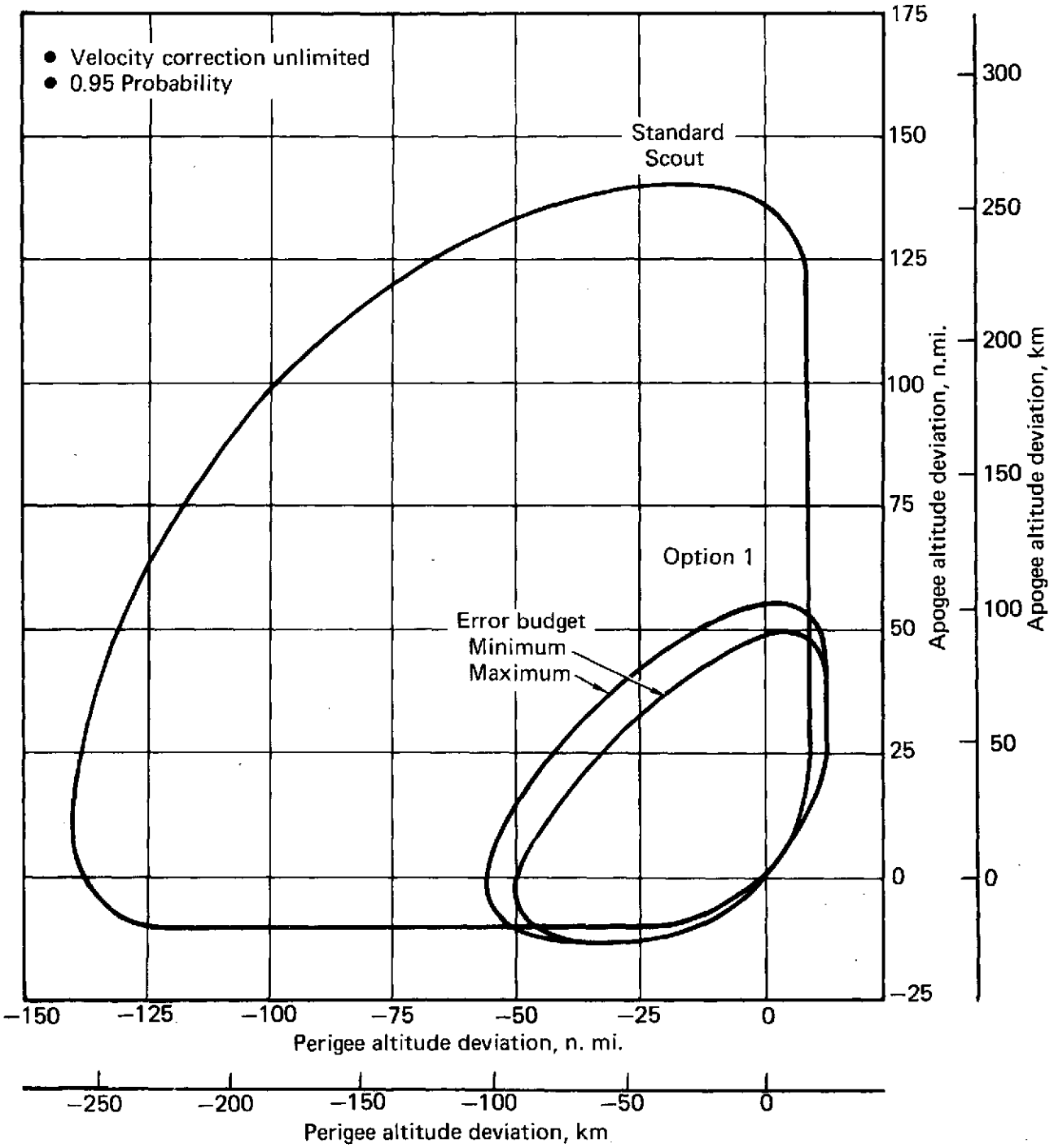


FIGURE 17. – ISOPROBABILITY CONTOURS – OPTION 1 – 600 N. MI. (1111.2 KM) ORBIT

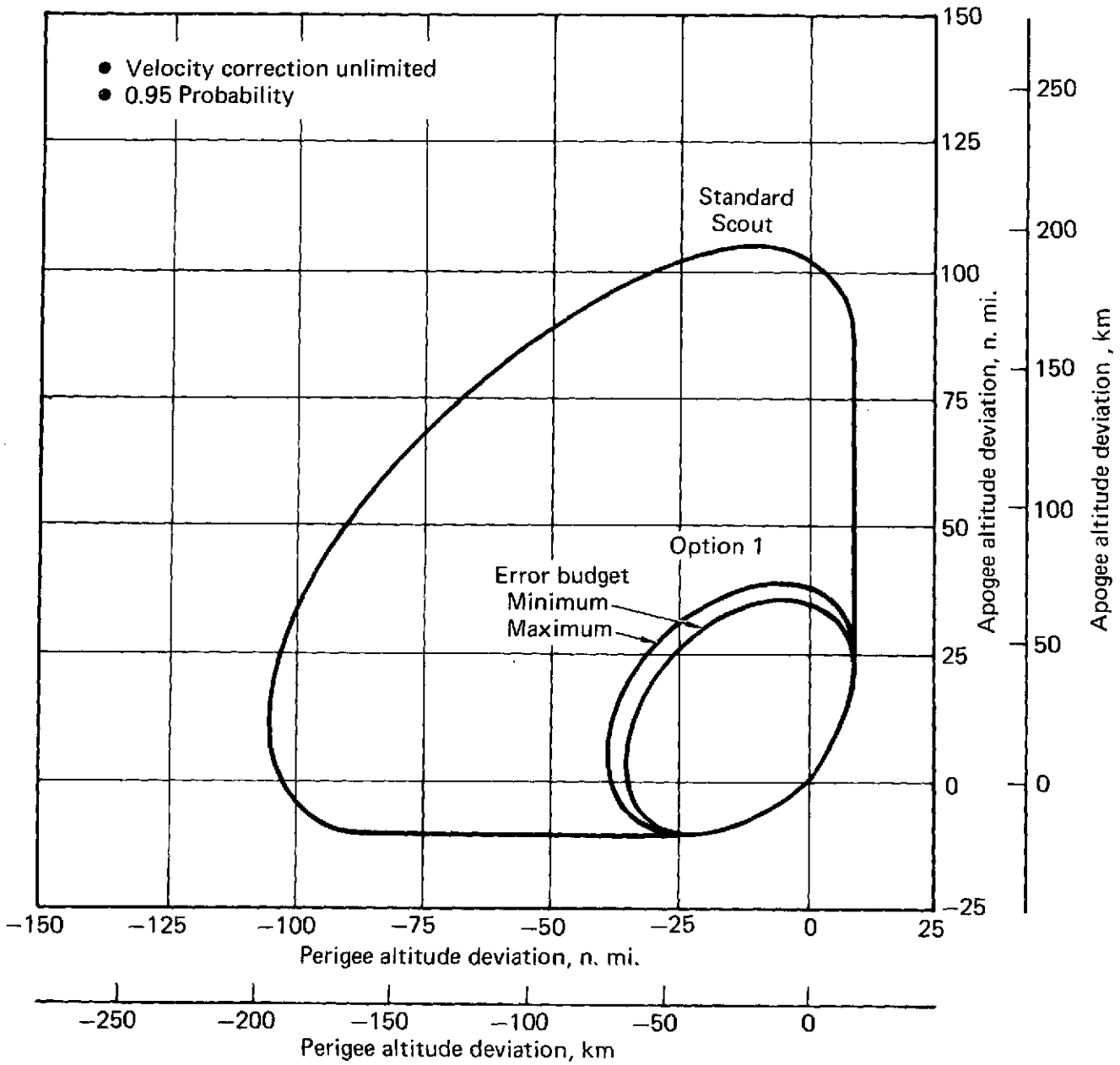


FIGURE 18. – ISOPROBABILITY CONTOURS – OPTION 1 -- 200 N. MI. (370.4 KM) ORBIT

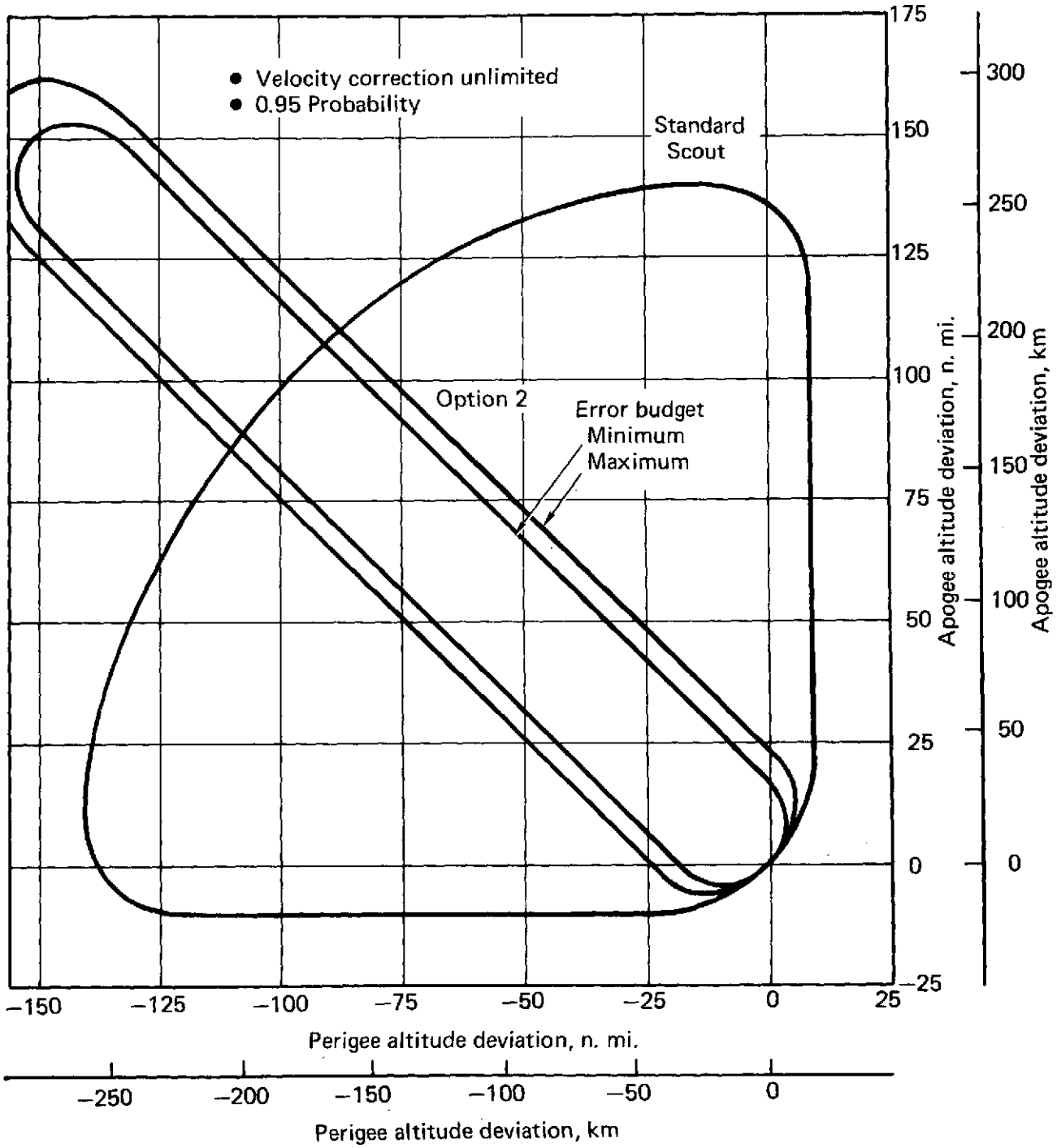


FIGURE 19. – ISOPROBABILITY CONTOURS – OPTION 2 – 600 N. MI. (1111.2 KM) ORBIT

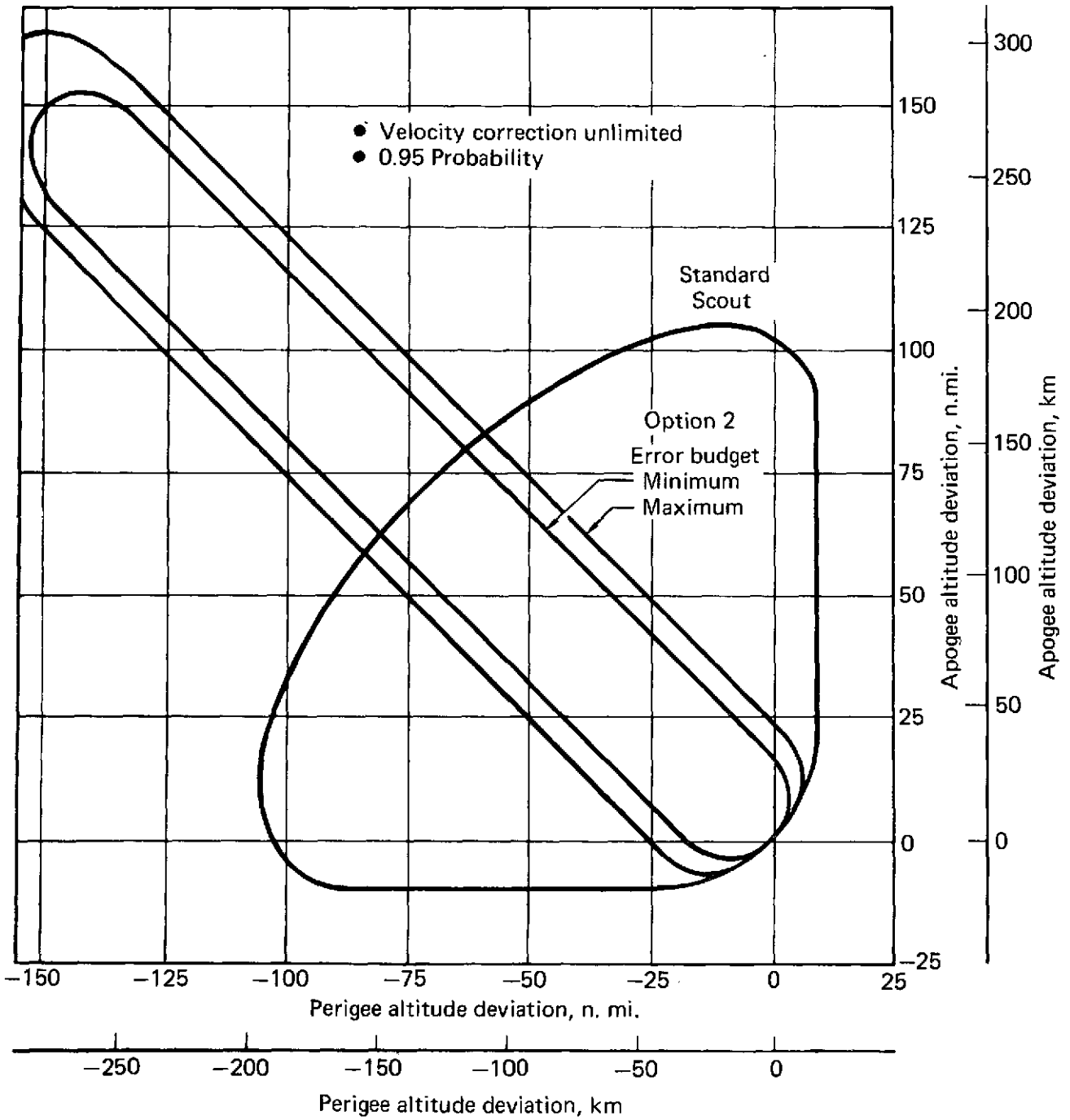


FIGURE 20. – ISOPROBABILITY CONTOURS – OPTION 2 – 200 N. MI. (370.4 KM) ORBIT

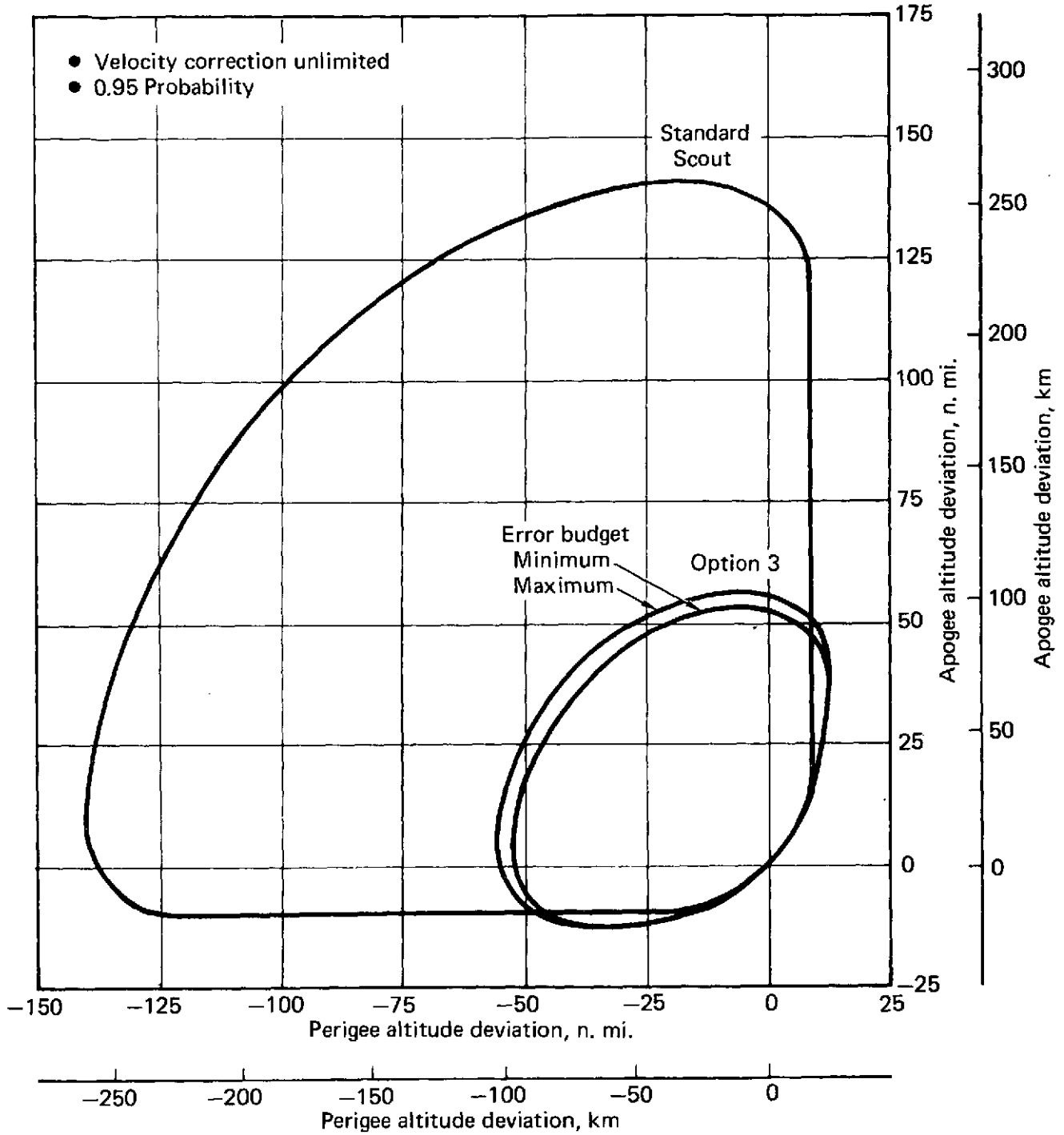


FIGURE 21. – ISOPROBABILITY CONTOURS – OPTION 3 – 600 N. MI. (1111.2 KM) ORBIT

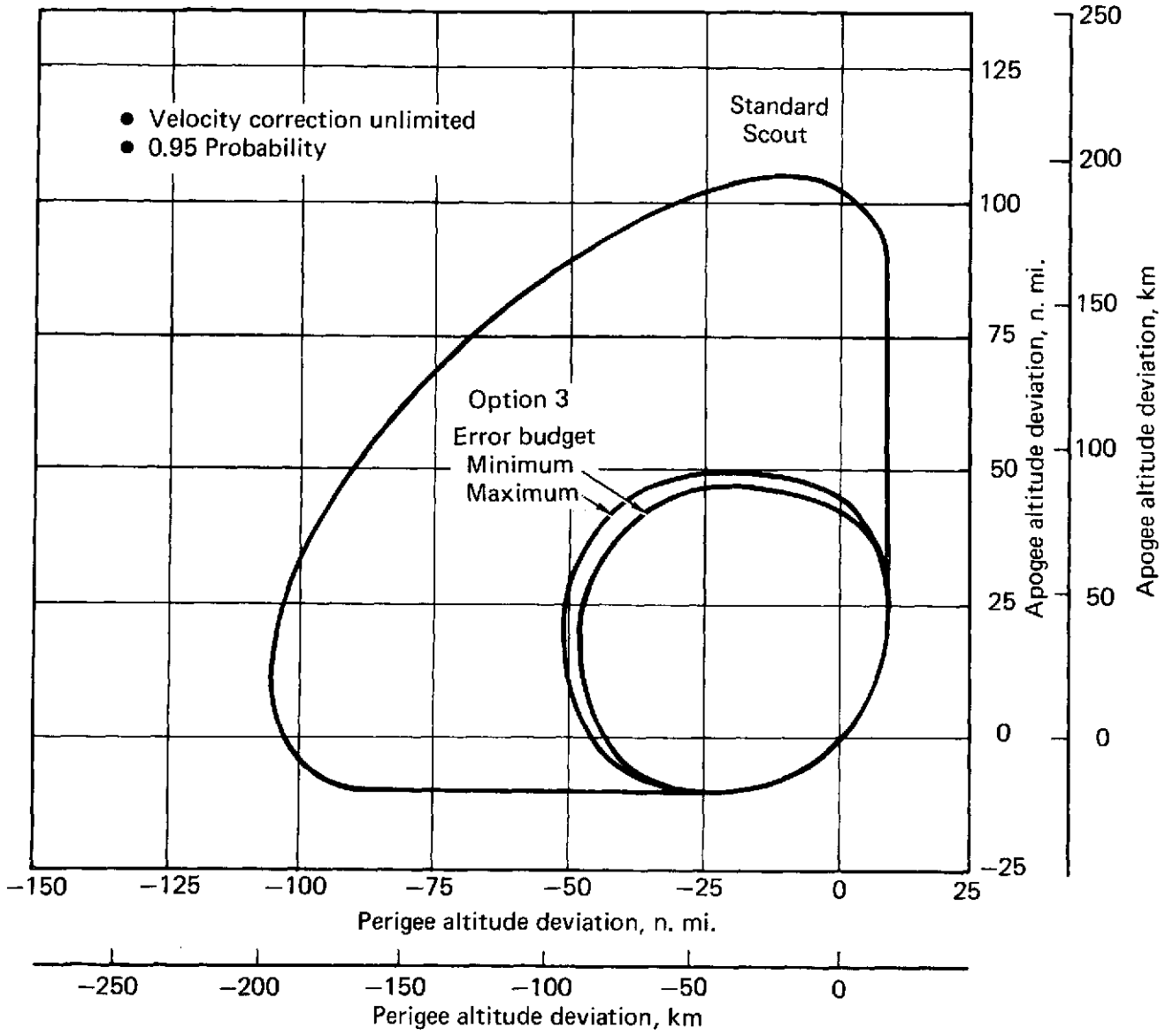


**FIGURE 22. – ISOPROBABILITY CONTOURS – OPTION 3 – 200 N. MI. (370.4 KM) ORBIT**

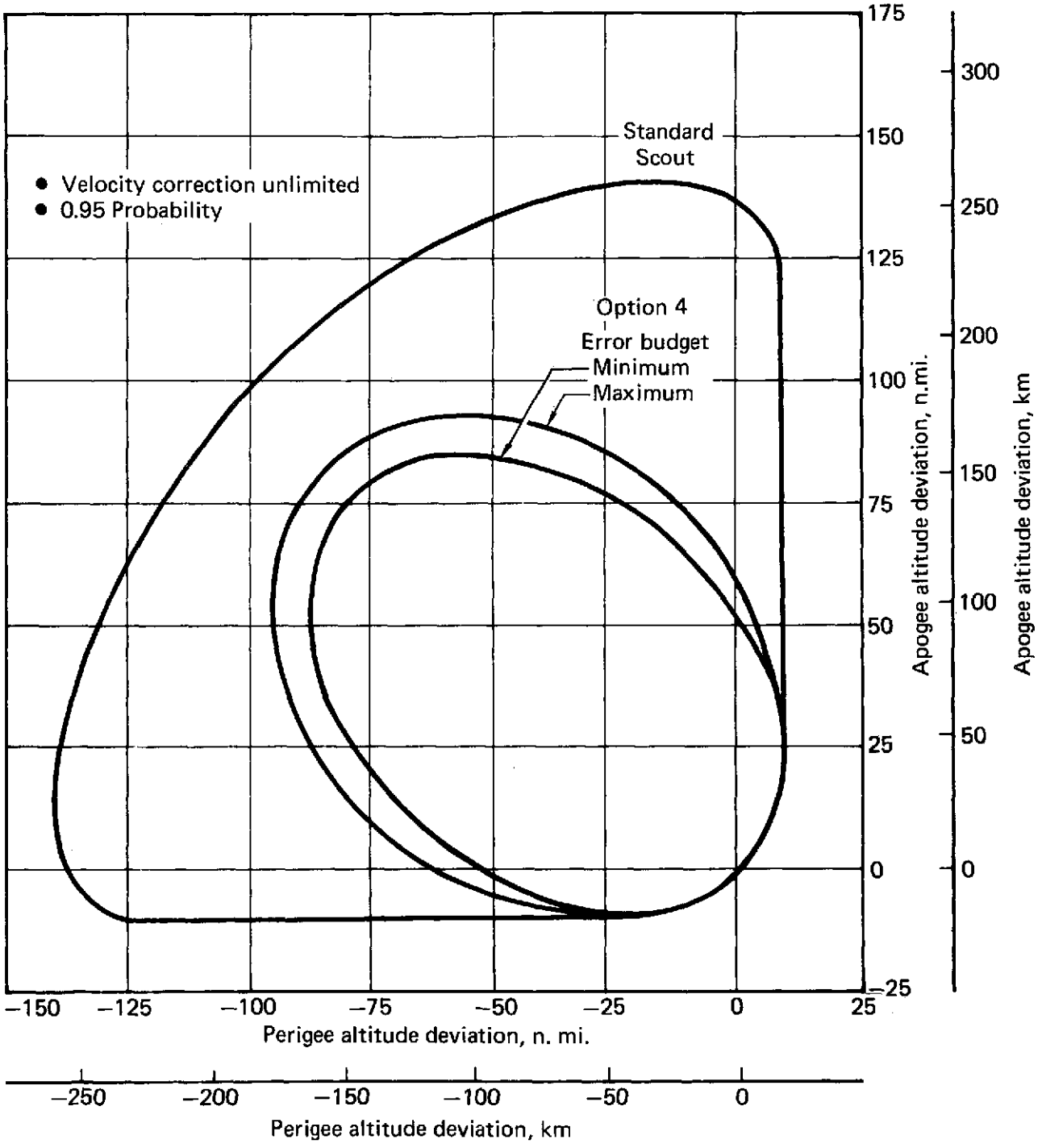


FIGURE 23. – ISOPROBABILITY CONTOURS – OPTION 4 – 600 N. MI. (1111.2 KM) ORBIT

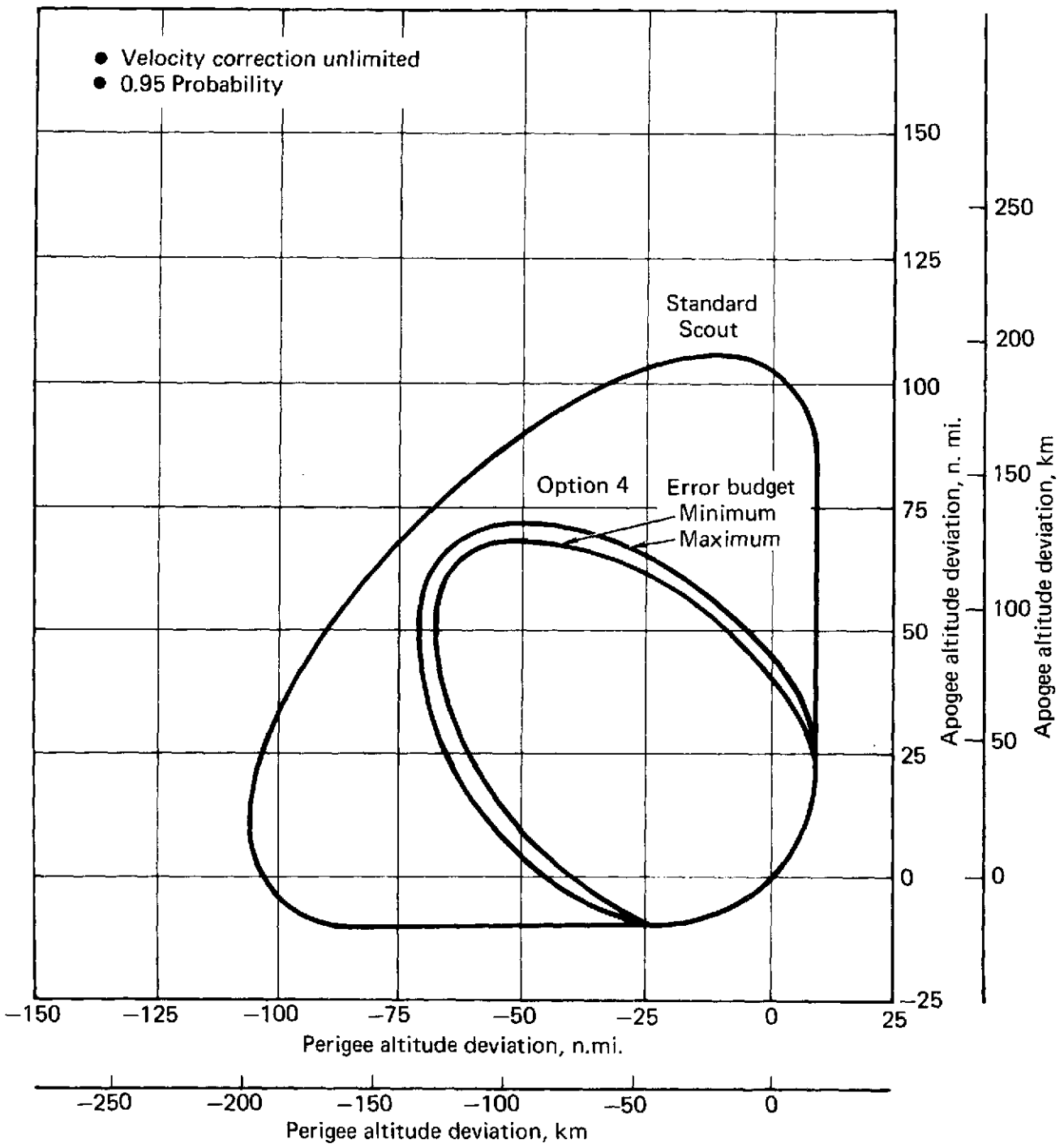


FIGURE 24. – ISOPROBABILITY CONTOURS – OPTION 4 – 200 N. MI. (370.4 KM) ORBIT

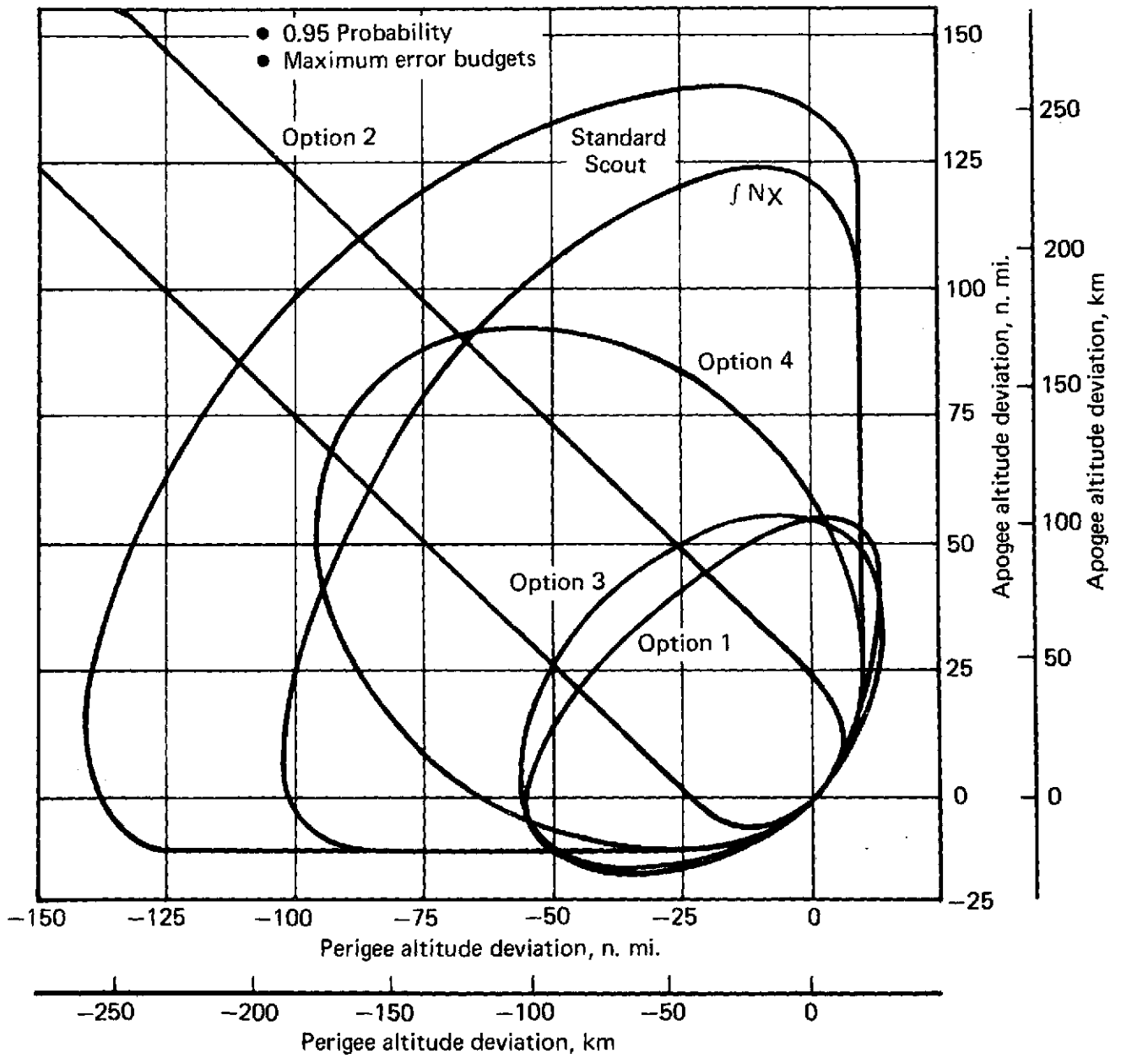


FIGURE 25. – COMPARISON OF ISOPROBABILITY CONTOURS, 600 N . MI. (1111.2 KM) ORBIT

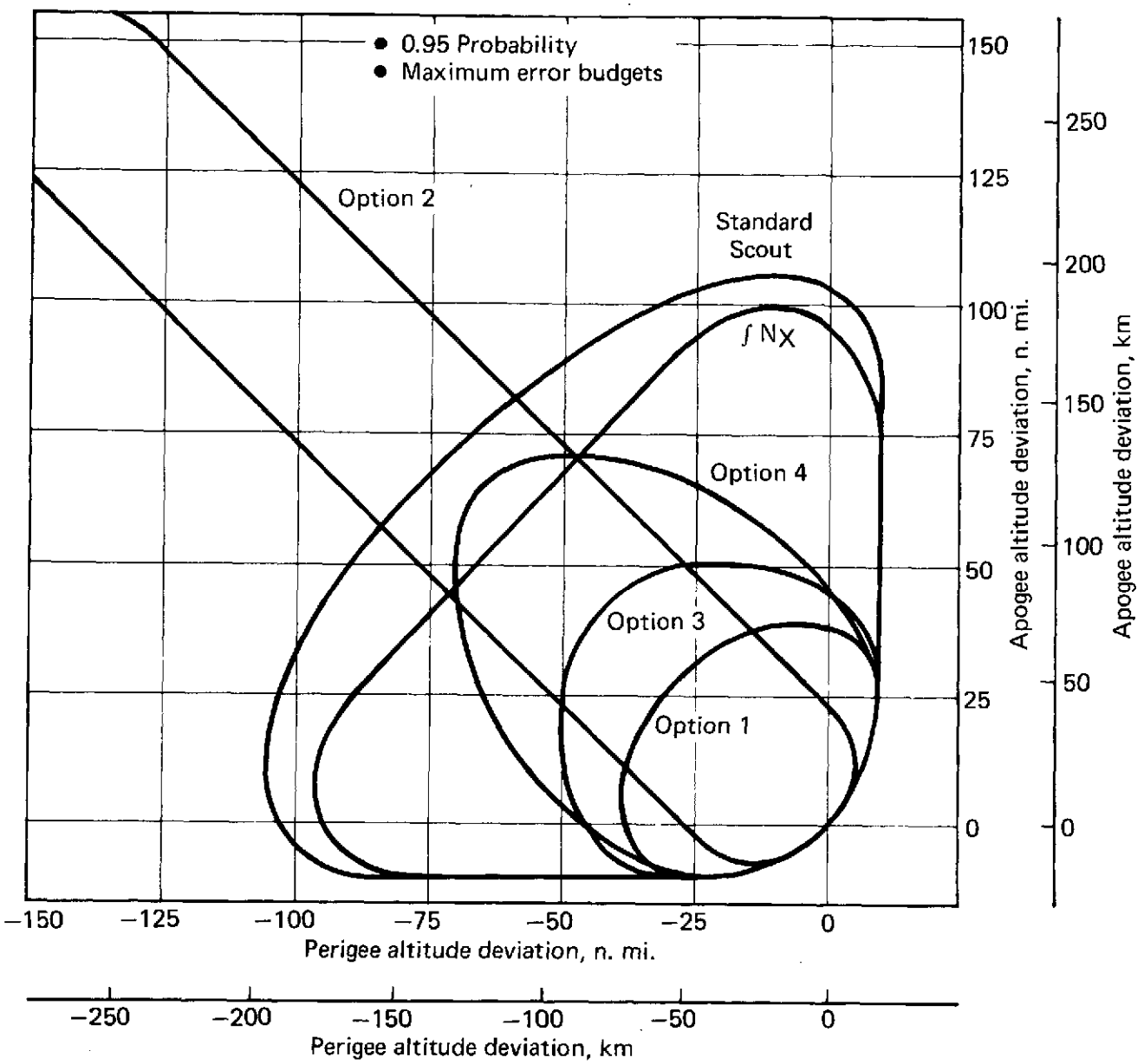


FIGURE 26. – COMPARISON OF ISOPROBABILITY CONTOURS, 200 N. MI. (370.4 KM) ORBIT

11.2.2 Inclination Errors. – the standard deviation in inclination error for all guidance options are listed in Table 35. These data show no difference in Options 1, 2 and 3, as expected, because all three options employ the same yaw attitude adjustment for fourth stage burn and no out-of-plane velocity correction. Option 4 includes no yaw attitude adjustment, thus the degradation in inclination.

One important consideration regarding these results is to recall that both orbits are due East launches from Wallops Island with an orbit inclination of about 37.7 degrees (0.658 rad). The indicated standard Scout inclination accuracies apply only to the two reference orbits; flight experience deviations are greater for higher inclination orbits from Wallops Island.

## TABLE 35. – ORBITAL INCLINATION ERRORS

- Standard deviation ($1\sigma$) values

600 n. mi. (1111.2 km) Orbit Mission

Standard scout accuracy – 0.25 deg. (.0044 rad)

| AVC system | Max budget | | Min budget | |
|---|---|---|---|---|
| | deg | rad | deg | rad |
| Option 1 | 0.13 | .0023 | 0.13 | .0023 |
| Option 2 | 0.13 | .0023 | 0.13 | .0023 |
| Option 3 | 0.13 | .0023 | 0.12 | .0021 |
| Option 4 | 0.19 | .0033 | 0.19 | .0033 |

200 n. mi. (370.4 km) Orbit Mission

Standard scout accuracy – 0.20 deg. (.0035 rad)

| AVC system | Max budget | | Min budget | |
|---|---|---|---|---|
| | deg | rad | deg | rad |
| Option 1 | 0.14 | .0024 | 0.14 | .0024 |
| Option 2 | 0.14 | .0024 | 0.14 | .0024 |
| Option 3 | 0.14 | .0024 | 0.14 | .0024 |
| Option 4 | 0.18 | .0031 | 0.18 | .0031 |

11.2.3 Attitude Maneuvers and $\Delta V$ Correction Statistics. – statistics on the magnitude of the pitch and yaw adjustments for fourth stage burn, pitch maneuver for the $\Delta V$ correction and the $\Delta V$ correction itself are listed in Tables 36 through 39. The indicated standard deviation of the yaw adjustment for the 600 n. mi. (1111.2 km) orbit is 1.4 deg (.0244 rad). This magnitude is well above the expected fourth stage control system deadband. However, the three sigma value is small enough to permit the use of small angle approximations in the computations. In Option 1 the pitch adjustment is slightly smaller than yaw.

TABLE 36. – ATTITUDE MANEUVERS AND ΔV STATISTICS – OPTION 1

600 n. mi. (1111.2 km) Orbit

| Parameter | Maximum Budget | | Minimum Budget | |
|---|---|---|---|---|
| | Mean | Sigma | Mean | Sigma |
| Stage 4 pitch adjustment deg (rad) | 0 | ±0.7 (±.0122) | 0 | ±0.7 (±.0122) |
| Stage 4 yaw adjustment deg (rad) | 0 | ±0.8 (±.0140) | 0 | ±0.8 (±.0140) |
| Vernier pitch maneuver deg (rad) | - 4.3 ( - .0750) | ±102.1 (±1.7812) | - 5.9 ( - .1030) | ±102.0 (±1.7802) |
| Vernier velocity increment ft/s (m/s) | +115.7 (+35.26) | ±62.0 (±18.90) | +111.2 (+33.89) | ±59.6 (±18.17) |

200 n.mi. (370.4 km) Orbit

| Parameter | Maximum Budget | | Minimum Budget | |
|---|---|---|---|---|
| | Mean | Sigma | Mean | Sigma |
| Stage 4 pitch adjustment deg (rad) | 0 | ±1.1 (±.0192) | 0 | ±1.1 (±.0192) |
| Stage 4 yaw adjustment deg (rad) | 0 | ±1.4 (±.0244) | 0 | ±1.4 (±.0244) |
| Vernier pitch maneuver deg (rad) | - 7.4 ( - .1291) | ±101.2 (±1.7663) | - 9.1 ( - .1588) | ±100.7 (±1.7575) |
| Vernier velocity increment ft/s (m/s) | +102.5 (+31.24) | ±56.4 (±17.19) | +99.5 (+30.33) | ±54.8 (±16.70) |

## TABLE 37. – ATTITUDE MANEUVERS AND ΔV STATISTICS – OPTION 2

600 n.mi. (1111.2 km) Orbit

| Parameter | Maximum Budget | | Minimum Budget | |
|---|---|---|---|---|
| | Mean | Sigma | Mean | Sigma |
| Stage 4 pitch adjustment deg (rad) | -11.6 (-.2025) | ±4.2 (±.0733) | -11.6 (-.2025) | ±4.1 (±.0716) |
| Stage 4 yaw adjustment deg (rad) | +0.3 (+.0052) | ±0.8 (±.0140) | +0.3 (+.0052) | ±0.8 (±.0140) |
| Vernier pitch maneuver deg (rad) | -91.8 (-1.6022) | ±35.2 (±.6144) | -91.9 (-1.6040) | ±35.0 (±.6109) |
| Vernier velocity increment ft/s (m/s) | +1145.4 (+349.12) | ±381.4 (±116.25) | +1147.9 (+349.88) | ±376.6 (±114.79) |

200 n.mi. (370.4 km) Orbit

| Parameter | Maximum Budget | | Minimum Budget | |
|---|---|---|---|---|
| | Mean | Sigma | Mean | Sigma |
| Stage 4 pitch adjustment deg (rad) | -15.0 (-.2618) | ±5.6 (±.977) | -15.1 (-.2635) | ±5.5 (±.0960) |
| Stage 4 yaw adjustment deg (rad) | +0.4 (+.0070) | ±1.5 (±.0262) | +0.4 (+.0070) | ±1.5 (±.0262) |
| Vernier pitch maneuver deg (rad) | -95.7 (-1.6703) | ±36.0 (±.6283) | -95.8 (-1.6720) | ±35.9 (±.6266) |
| Vernier velocity increment ft/s (m/s) | +709.9 (+216.38) | ±241.1 (±73.49) | +709.1 (+216.13) | ±237.5 (±72.39) |

## TABLE 38. – ATTITUDE MANEUVERS AND ΔV STATISTICS – OPTION 3

600 n.mi. (1111.2 km) Orbit

| Parameter | Maximum Budget | | Minimum Budget | |
|---|---|---|---|---|
| | Mean | Sigma | Mean | Sigma |
| Stage 4 pitch adjustment deg (rad) | NA | NA | NA | NA |
| Stage 4 yaw adjustment deg (rad) | 0 | ±0.8 (±.0140) | 0 | ±0.8 (±.0140) |
| Vernier pitch maneuver deg (rad) | -26.6 (-.4643) | ±99.6 (±1.7383) | -32.4 (-.5655) | ±98.4 (±1.7174) |
| Vernier velocity increment ft/s (m/s) | +96.2 (+29.32) | ±53.3 (±16.25) | +90.3 (+27.52) | ±52.0 (±15.85) |

200 n.mi. (370.4 km) Orbit

| Parameter | Maximum Budget | | Minimum Budget | |
|---|---|---|---|---|
| | Mean | Sigma | Mean | Sigma |
| Stage 4 pitch adjustment deg (rad) | NA | NA | NA | NA |
| Stage 4 yaw adjustment deg (rad) | +0.1 (+.0018) | ±1.4 (±.0244) | +0.1 (+.0018) | ±1.4 (±.0244) |
| Vernier pitch maneuver deg (rad) | -11.1 (-.1937) | ±102.0 (±1.7802) | -14.3 (-.2496) | ±101.7 (±1.7750) |
| Vernier velocity increment ft/s (m/s) | +92.3 (+28.13) | ±51.4 (±15.67) | +88.8 (+27.07) | ±50.4 (±15.36) |

## TABLE 39. – ATTITUDE MANEUVERS AND ΔV STATISTICS – OPTION 4

600 n.mi. (111.2 km) Orbit

| Parameter | Maximum Budget | | Minimum Budget | |
|---|---|---|---|---|
| | Mean | Sigma | Mean | Sigma |
| Stage 4 pitch adjustment | NA | NA | NA | NA |
| Stage 4 yaw adjustment | NA | NA | NA | NA |
| Vernier pitch maneuver | NA | NA | NA | NA |
| Vernier velocity increment ft/s (m/s) | −1.5 ( −.46) | ±85.5 (±26.06) | −1.8 ( −.55) | ±84.3 (±25.69) |

200 n.mi. (370.4 km) Orbit

| Parameter | Maximum Budget | | Minimum Budget | |
|---|---|---|---|---|
| | Mean | Sigma | Mean | Sigma |
| Stage 4 pitch adjustment | NA | NA | NA | NA |
| Stage 4 yaw adjustment | NA | NA | NA | NA |
| Vernier pitch maneuver | NA | NA | NA | NA |
| Vernier velocity increment ft/s (m/s) | −1.5 ( −.46) | ±73.9 (±22.52) | −1.6 ( −.49) | ±72.6 (±22.13) |

The pitch maneuver angle required for the ΔV correction is defined as −180 deg to +180 deg (−3.14 rad to +3.14 rad). It is interesting to note that the mean value of the pitch maneuver is slightly less for Option 1 than for Option 3. In each case the mean is negative, indicating a pitch down maneuver. The mean for Option 2 is in the vicinity of 90 deg (1.57 rad) corresponding to the predominance of a large vertical velocity error resulting from the biased trajectory.

The vernier velocity increment for Options 1, 2 and 3 is defined as a positive value regardless of the direction in which it is added. Data on this ΔV correction are shown in the tables. In addition, a direct comparison is shown in Table 40. This shows the extreme ΔV requirement for Option 2. The high ΔV plus the undesirable features of the isoprobability contours are enough to eliminate this option from serious consideration. Another significant result is the magnitude of the ΔV required for Option 4. The values shown in Tables 39 and 40 assume that the correction is applied in either a positive or negative direction. The mean value of the ΔV correction is near zero, indicating that the number of positive and negative corrections are essentially equal. The mean plus 2 sigma value of 149.3 ft/s (45.51 m/s) is about 75% of the Option 3 requirement. If Option 4 were selected, then the ΔV capability could be increased to permit a biased trajectory such that the ΔV could always be added in the positive direction, thus no pitch maneuver would ever be needed. This choice would mean, however, that the ΔV would have to be doubled to retain the same probability of correcting the velocity error. For a mean plus 2 sigma correction capability, a ΔV of 298.6 ft/s (91.01 m/s) would be needed with the maximum error budget which is significantly greater than the comparable ΔV requirement for either Option 1 or 3. The mean plus 2 sigma ΔV of Option 3 is about 20 ft/s (6.1 m/s) less than that for Option 1.

**TABLE 40. – COMPARISON OF ΔV REQUIREMENTS**

| Option | Error Budget | 600 n.mi. (1111.2 km) Traj. | | | | 200 n. mi. (370.4 km) Traj. | | | |
|---|---|---|---|---|---|---|---|---|---|
| | | Mean | | Mean + 2 σ | | Mean | | Mean + 2 σ | |
| | | ft/s | m/s | ft/s | m/s | ft/s | m/s | ft/s | m/s |
| 1 | min | 111.2 | 33.89 | 230.4 | 70.23 | 99.5 | 30.33 | 209.1 | 63.73 |
| | max | 115.7 | 35.26 | 239.7 | 73.06 | 102.5 | 31.24 | 215.3 | 65.62 |
| 2 | min | 1147.9 | 349.88 | 1900.9 | 579.39 | 709.1 | 216.13 | 1184.1 | 360.91 |
| | max | 1145.4 | 349.12 | 1908.2 | 581.62 | 709.9 | 216.38 | 1190.1 | 362.74 |
| 3 | min | 90.3 | 27.52 | 194.3 | 59.22 | 88.8 | 27.07 | 189.6 | 57.79 |
| | max | 96.2 | 29.32 | 202.8 | 61.81 | 92.3 | 28.13 | 195.1 | 59.47 |
| 4 | min | − 1.8 | − 0.55 | 170.4 | 51.94 | − 1.6 | − 0.49 | 146.8 | 44.74 |
| | max | − 1.5 | − 0.46 | 172.5 | 52.58 | − 1.5 | − 0.46 | 149.3 | 45.51 |

## 12.0 AVC SYSTEM INTERFACE

All four AVC options discussed in the previous two sections require the determination of the inertial velocity components. The general arrangement of the AVC system needed to implement any of the options is shown in Figure 27 in a block diagram fashion. The same number of system elements (black boxes) are needed for any of the options although they may vary somewhat for different options. In Figure 27 it is assumed that the computational functions are accomplished in the CEU. This implies the use of a digital processor to compute the inertial velocity values. In some inertial guidance systems, the IMU and CEU are combined in one unit.

The basic functions required by the CEU to accomplish the four options are summarized in Table 41. Many other functions related to the normal operation of an inertial guidance system will be accomplished in the CEU, however, these are common to all options. Table 41 shows that the complexity of the CEU functions are essentially equivalent for Options 1, 2 and 3. Fewer functions are needed by Option 4, however the degree of simplification in the CEU which could be achieved by the selection of Option 4 is not expected to be significant when compared to the normal inertial guidance computations.

Recalling the isoprobability contours, the $\Delta V$ requirements and the comparison of CEU functions, the most desirable options can be narrowed to 1 and 3. The only negative factor for Option 4 is the increase in apogee-perigee deviations as depicted by the isoprobability contours.

**TABLE 41. – CONTROL ELECTRONICS UNIT FUNCTIONS**

| Function | Options | | | |
|---|---|---|---|---|
| | 1 | 2 | 3 | 4 |
| Determination of inertial velocity | √ | √ | √ | √ |
| Determination of body attitude | √ | √ | √ | √ |
| Attitude control loop; pitch and yaw commands and logic | √ | √ | √ | √ |
| Compute yaw bias for 4th stage burn | √ | √ | √ | No |
| Compute pitch bias for 4th stage burn | √ | √ | No | No |
| 4th stage ignition determined from parameter other than time | No | √ | √ | No |
| Compute $V_X$ error at burnout | √ | √ | √ | √ |
| Compute $V_Z$ error at burnout | √ | √ | √ | No |
| Compute total $\Delta V$ correction | √ | √ | √ | No |
| Compute variable pitch angle for $\Delta V$ | √ | √ | √ | $0^o$ or $180^o$ |
| Determine $\Delta V$ termination | √ | √ | √ | √ |

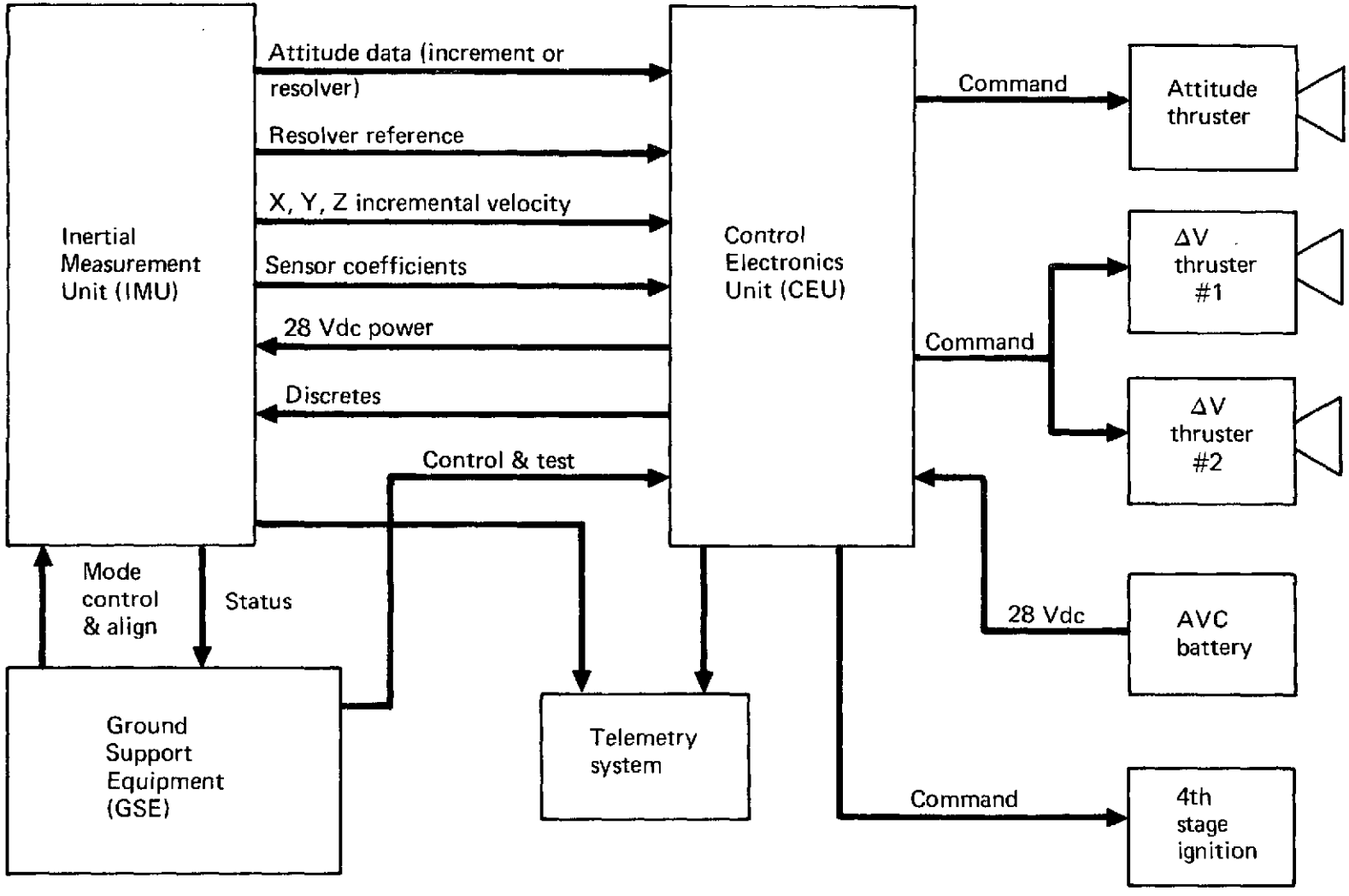


FIGURE 27. – AVC SYSTEM BLOCK DIAGRAM

## 12.1 AVC Interconnections

The IMU now being developed for the Pershing II missile was used as a typical unit in illustrating the signal and functional interconnections in the AVC system. Figure 28 presents a more detailed interface for this particular system. Several pertinent points regarding the configuration and operation of this system are:

(1) In-flight power distribution is through the CEU.

(2) The only in-flight power required is 28 Vdc. The 115 Vac 400 Hz power from the GSE is used for heater power during warm-up.

(3) Alignment is by gyrocompassing with the equations programmed in a computer in the GSE.

(4) Signal conditioning for the thruster commands is accomplished in the CEU; thruster commands are 28 Vdc, one ampere outputs.

(5) Fourth stage ignition command may be direct from the third stage guidance or from the CEU. Generating the command within the CEU would permit variable capture times for the ACS following fourth stage separation.

(6) Signal flow construction is intended to permit ground monitoring of system operation.

## 12.2 Telemetry (T/M)

The present FM/FM telemetry package has a capacity of twelve analog channels but is not compatible with the monitoring of digital information, especially parallel data. A version of the PCM T/M system used in the fourth stage of vehicle S-189 was selected for the AVC system in order to be compatible with the guidance components and provide the needed capacity. The PCM system can be interfaced for digital information and offers the advantage of reduced weight and volume relative to the existing system.

The existing FM/FM T/M signal conditioning package will be replaced with the following individual components which may be individually mounted.

(1) 1 PCM encoder with special modules

(2) 1 Control relay

(3) 2 Signal conditioners

The two signal conditioning assemblies are included to provide an interface with the AVC guidance equipment. In case this equipment can interface directly with the PCM system, the signal conditioners will be deleted. The encoder considered is the Vector model MMP-600 PCM encoder which is the unit flown on Scout vehicle S-189. The encoder contains the power supply for some sensors and a multiplexing capability. A serial to parallel converter module will be added if a guidance system like the Pershing II is selected. In this system the output digital data is in a serial format. Any other special module required can also be added to the basic encoder.

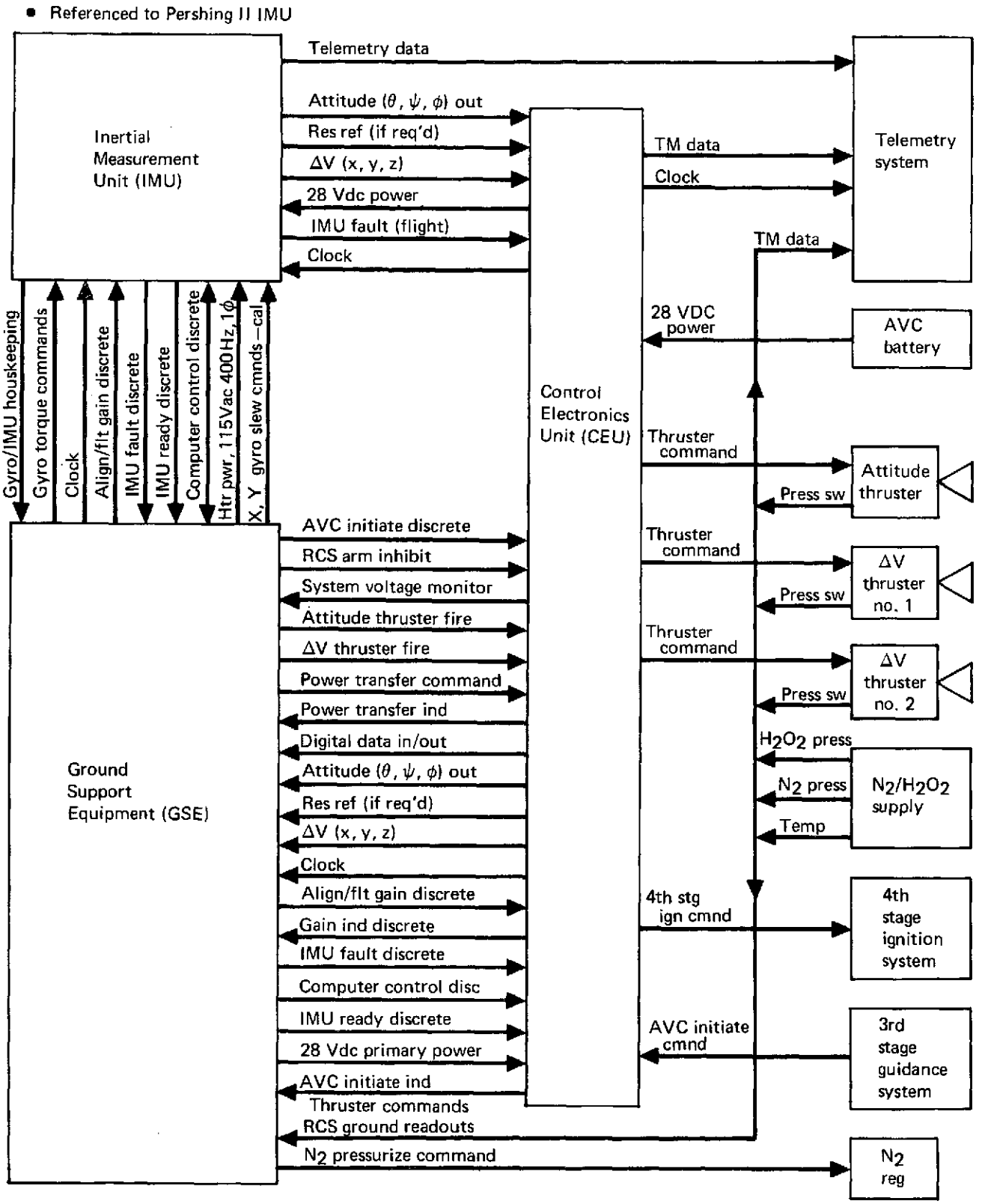


FIGURE 28. – AVC SYSTEM INTERCONNECTIONS – OPTIONS 1 AND 3

The T/M components previously listed will have a combined weight of about 0.9 lbm (0.41 kg) which represents a weight savings of about 0.43 lbm (0.2 kg) over the current FM/FM signal conditioning package. Total volume of the combined components is about one-half of the current signal conditioning unit. The PCM units will require approximately 100 milliamperes more current at 28 Vdc.

The T/M antenna will have to be redesigned, because of the elimination of the ring module, such that it can be installed around the circumferance of the fourth stage motor. The transmitter and the battery will remain identical to the existing FM/FM system. The IMU and CEU functions to be monitored will also increase the interconnecting wiring in the fourth stage.

### 12.3 Equipment Locations

In considering the equipment location and arrangements for the AVC components, the following general guidelines were followed.

(1) The fourth stage T/M ring module will be eliminated and the necessary components relocated in a new payload transition section.

(2) The reaction control system with all tankage and motors will be located in the upper D transition section.

(3) The AVC guidance components will be located in the new payload transition section.

(4) The fourth stage T/M antenna will be installed around the circumferance of the fourth stage motor.

Figure 6 illustrates the relative location of these major AVC system components.

## 13.0 RCS AND ΔV TRADES

Trade studies were conducted on the type of Reaction Control System (RCS) to use for the attitude control during the fourth stage burn and the vernier velocity correction. Analyses and requirements were established based upon a total weight of 585.84 pounds (265.74 kg) at Altair IIIA burnout, which includes all expendables in the RCS. Compared to the nominal Scout F-1 fourth stage burnout weight, this design weight represents about a 55 pound (24.95 kg) payload increase over the injection capability at the reference 200 n. mi. (370.4 km) trajectory. The weight increase was included to account for future increases in payload capabilities from improved propellants or similar vehicle improvements.

## 13.1 Vernier Velocity – Impulse and Fuel Requirements

The impulse and control fuel required to correct the velocity errors is a function of the total weight at fourth stage motor burnout. The weight distribution initially assumed for the weight at Altair IIIA burnout was:

| | | |
|---|---|---|
| Altair IIIA inert + upper D section | 69.8 lbm | 31.68 kg |
| 4th Stage equipments – includes AVC | 81.0 | 36.74 |
| Payload with adapter | 435.0 | 197.32 |
| Total | 585.84 lbm | 265.74 kg |

The weight breakdown assumed is not the significant item, instead it is the total burnout weight.

The first $\Delta V$ requirements were determined for the integral of $N_X$ approach. In establishing the $\Delta V$ needed, the flight data on the integral of $N_X$ errors as presented in Section 8.0 were used for the first three stages. The errors for the 18 flights using the Altair IIIA motor were normalized by fourth stage weight and then adjusted for different payload weights. The total error in the integral of $N_X$ was determined as the root-sum-square value of all four stages. The standard deviation of this error is given in Figure 29. At the indicated design weight, the standard deviation is 49 ft/s (14.94 m/s).

The impulse required for two and four sigma integral of $N_X$ errors are presented in Figure 30. The hydrogen peroxide weight required is also shown in Figure 30; this is based on a steady state specific impulse of 160 lbf-s/lbm (1569 N-s/kg). Assuming a normal distribution with zero mean the two sigma correction capability implies that on 95 percent of the missions all of the sensed integral of $N_X$ error would be corrected.

Two concepts of velocity correction were considered. Concept A is based on velocity addition only. To accomplish plus and minus two sigma velocity correction, the predicted trajectory would be planned such that the velocity at fourth stage burnout would be lower than required by the expected two sigma value. For this concept, in order to correct 95 percent of the integral of $N_X$ error, enough fuel for a 4 sigma velocity correction is required. As shown in Figure 30 approximately 21.7 pounds (9.84 kg) of hydrogen peroxide would be required.

Concept B utilizes aft facing thrusters only but adds or subtracts sensed velocity errors by using the attitude control system to provide a 180 degree (3.14 rad) pitch maneuver when velocity errors are greater than predicted. This scheme requires approximately one-half the hydrogen peroxide weight for velocity correction (11 pounds or 4.99 kg). However, additional fuel is required to rotate the fourth stage 180 degrees (3.14 rad) prior to correction and rotate back to the desired orientation after velocity subtraction.

In considering the new inertial velocity correction concepts (Options 1 through 4), the item of primary interest is the variation of the impulse required with the magnitude of $\Delta V$. The only $\Delta V$ correction approach that is compatible with Options 1, 2 and 3 is to utilize the pitch maneuver. It is impractical to attempt to bias the trajectory to restrict the pitch maneuver. Required impulse as a function of $\Delta V$ is shown in Figure 31 for the design fourth stage weight at Altair IIIA burnout, similar data are shown for the F-1 burnout maximum payload weight at the reference 200 n. mi. (370.4 km) orbit.

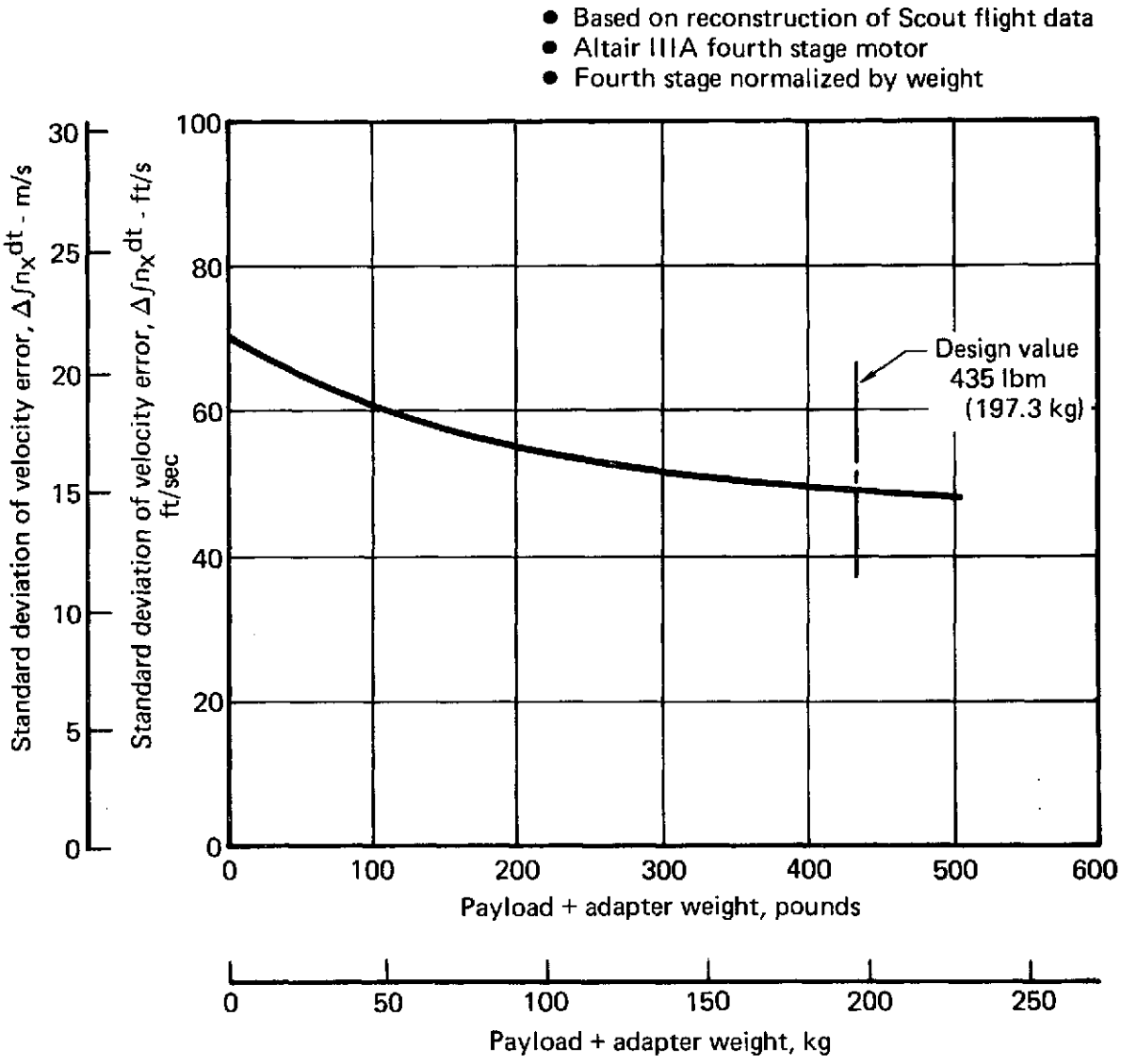


**FIGURE 29. – TOTAL INTEGRAL OF $N_X$ ERROR – FLIGHT EXPERIENCE**

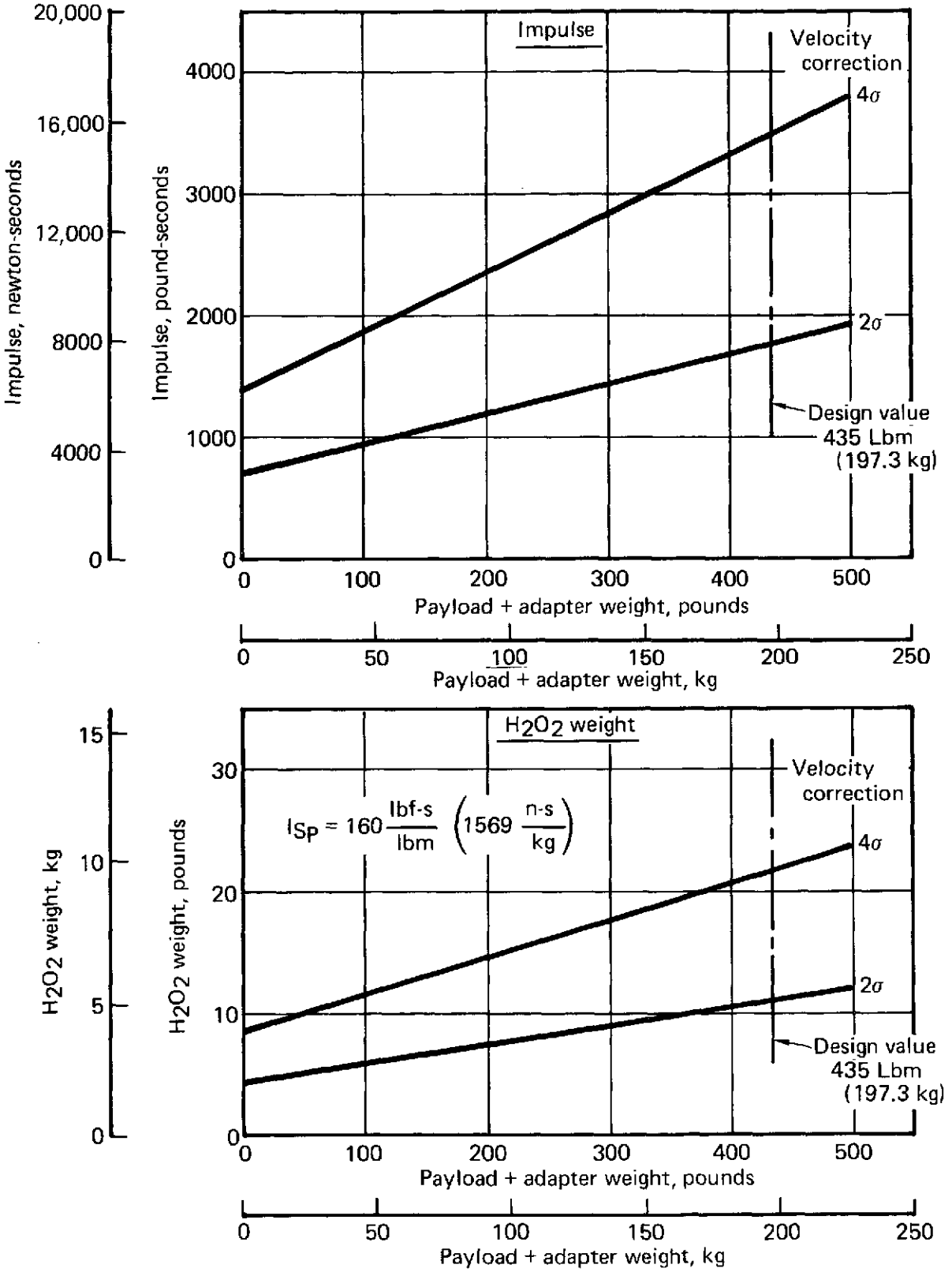


FIGURE 30. — IMPULSE AND HYDROGEN PEROXIDE REQUIRED FOR INTEGRAL OF $N_X$ CORRECTION

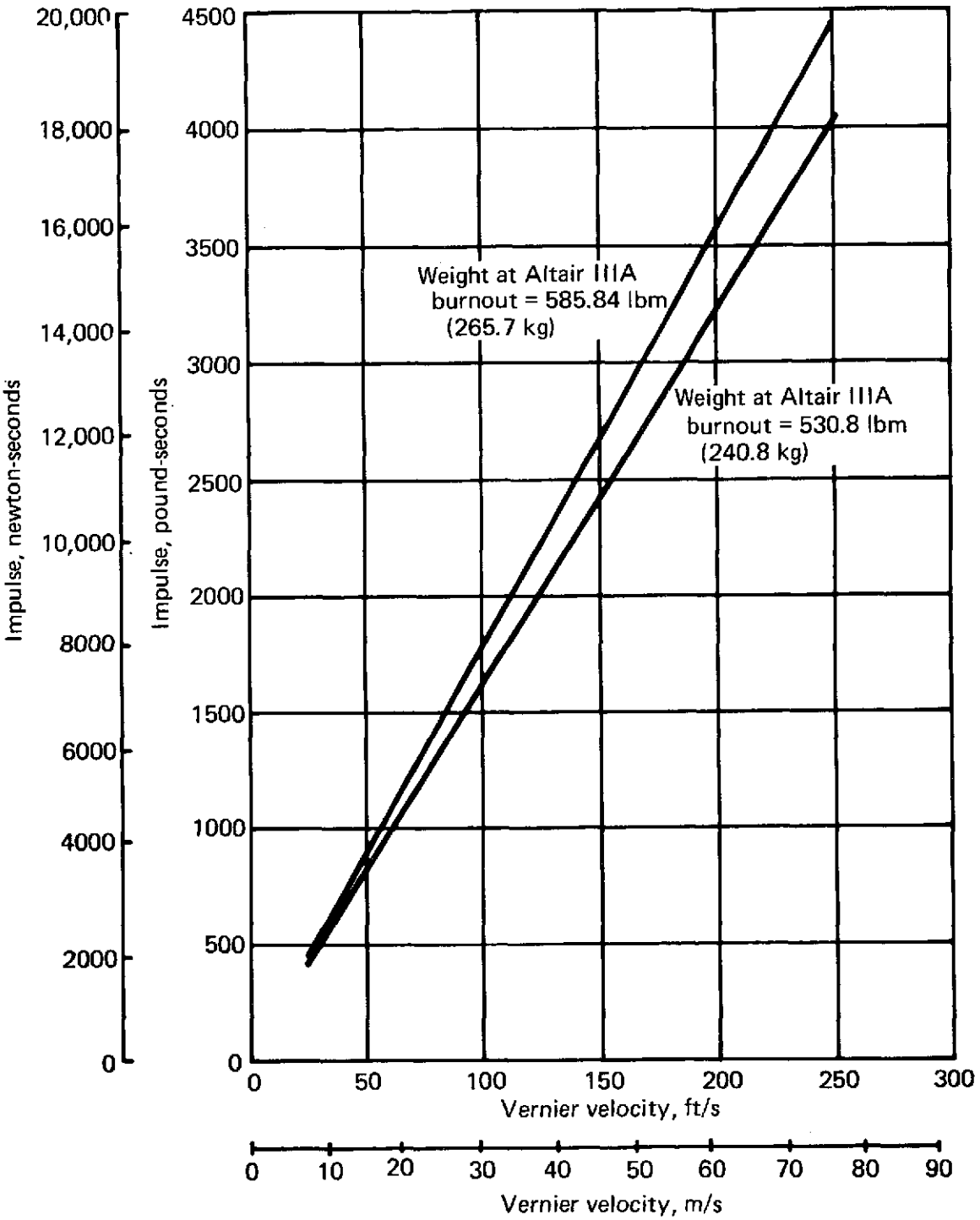


FIGURE 31. – ΔV IMPULSE REQUIREMENTS

## 13.2 RCS Requirements for Pitch Maneuver

An estimate of attitude control system impulse required for a 180 degree (3.14 rad) maneuver was made. The impulse required is primarily a function of the angular momentum of the fourth stage at burnout. Assuming a maximum payload roll moment of inertia of 18 slug $ft^2$ (24.4 kg-$m^2$) and a control system similar to the Scout fourth stage ACS system described in Reference 3, the attitude maneuver was simulated. Spin rates of one and three revolutions per second were used. The impulse and time requirements for the maneuver are presented in Figure 32. The control fuel required is also shown based on both nitrogen gas and hydrogen peroxide. The attitude control jet fuel specific impulse was assumed to be 130 lbf-s/lbm (1275 N-s/kg) for hydrogen peroxide and 60 lbf-s/lbm (588 N-s/kg) for nitrogen gas based on cyclic operation. The actual specific impulse of the attitude control jets will have to be determined more accurately for the very short pulse widths required for the spinning system.

The amount of nitrogen required for two 180 degree (3.14 rad) attitude maneuvers is about 12 pounds (5.44 kg) at 3 rps spin rate. This is considered to be unacceptable in vehicle modifications because of weight and volume required. If a hydrogen peroxide jet is utilized the fuel required is 5.5 pounds (2.49 kg).

## 13.3 Attitude Control During Boost

An estimation of the attitude control requirements during fourth stage boost was made. The estimates of performance are based on a system mechanization similar to the system flown on the Scout NPE mission which used a roll stabilized platform, a control electronics package and a single nitrogen gas jet having about 6.5 pounds (28.9 N) of thrust. The control logic was based on the cross rate mode which is discussed in detail in Reference 3.

The response of the vehicle at fourth stage ignition was simulated using the NEMAR digital computer simulation routine which accurately simulates the spinning vehicle with this type of control system. Two payloads (light and heavy) were simulated with initial attitude errors of 1 and 3 degrees (.017 and .052 rad). The moments of inertia and center of mass of the fourth stage used for both payloads are presented in Table 42. The impulse required to 'capture' the heavy payload with a 3 degree (.052 rad) initial attitude error is about 8 pound-seconds (35.6 N-s) without disturbing moments. With a light payload the impulse to 'capture' with the same initial attitude error is about 5 pound-seconds (22.2 N-s). The time to 'capture' and the impulse required is significantly increased with constant 0.2 degrees (3.5 milli rad) of booster thrust misalignment. In the first ten seconds, approximately 25 pound-seconds (111.2 N-s) of impulse is required. With thrust misalignment, the control motors continued to fire throughout boost because of the high rates during nutation. Therefore a total impulse of about 80 lbf-s (355.9 N-s) was used for the preliminary sizing effort. This represents about 1.3 pounds (.59 kg) of nitrogen or 0.6 pounds (0.27 kg) of hydrogen peroxide.

The time required to completely null a 3 deg (.052 rad) attitude error at fourth stage ignition with the 6.5 pound (28.9 N) thrust jet and the heavy payload is about 8 seconds. This is a somewhat sluggish response. Based upon previous studies, it is felt that a control force of 15 pounds (66.7 N) should be more than adequate. In many cases with lighter payloads the higher thrust level would present other stability problems which must be explored further. Therefore the attitude control force should be adjustable in the range of approximately 6 to 15 pounds (26.7 to 66.7 N). The control force adjustment could be made early in the vehicle processing, as soon as the payload and trajectory are defined. Additionally it is estimated that the control system gains and filtering should be adjustable to provide satisfactory performance over the wide range of payload characteristics flown on Scout. All of these adjustments could be made during vehicle processing. No in flight adjustments are expected to be needed.

- 6.5 $lb_f$ (28.9 N) Control jet force
- 0.8 deg (14 m rad) deadband, cross rate mode
- $I_{XX}$ = 20.4 slug-ft$^2$ (27.7 kg-m$^2$)
- $I_{YY}$ = 94.3 slug-ft$^2$ (127.9 kg-m$^2$)
- $X_{CG}$ = 35.6 station, in. (90.4 cm)

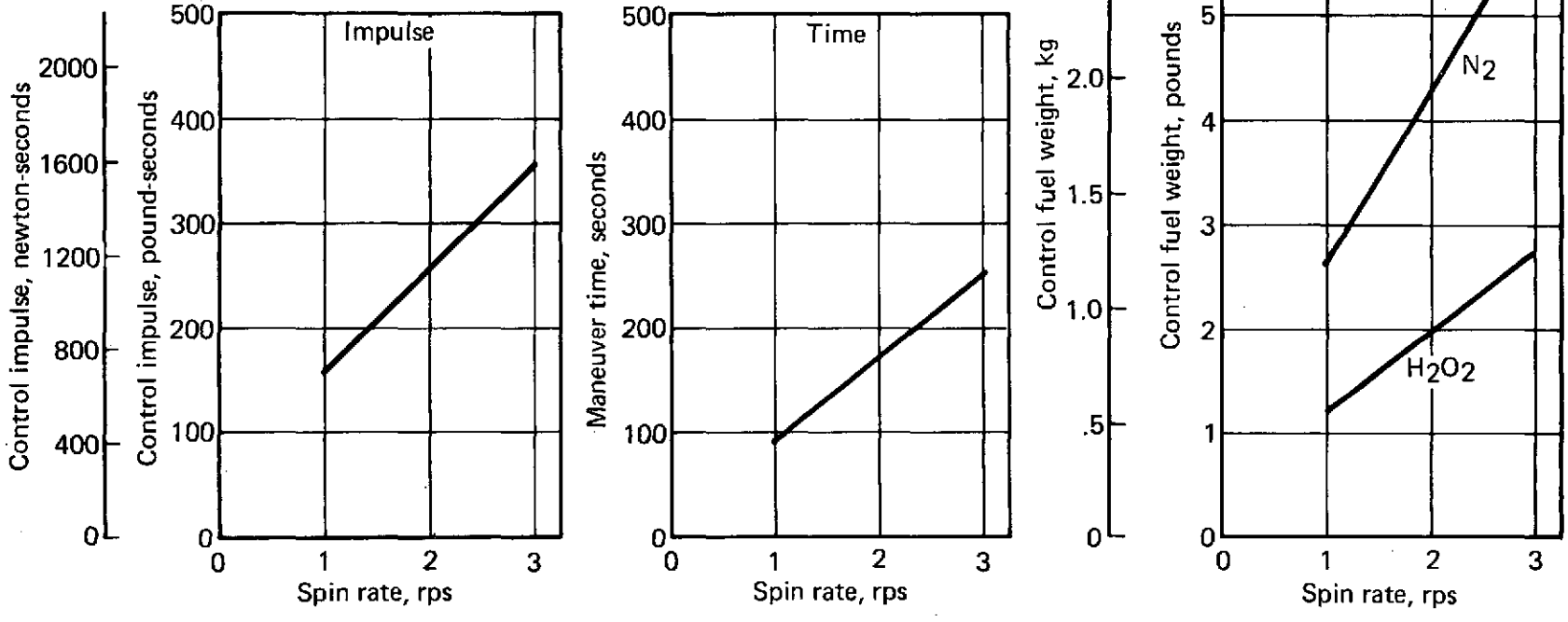


**FIGURE 32. – IMPULSE, TIME AND FUEL REQUIRED FOR 180 DEGREE (3.14 RAD) MANEUVER**

## TABLE 42. — MASS PROPERTIES — BOOST ATTITUDE CONTROL SYSTEM SIMULATION

| Heavy Payload — 435 lbm (197.3 kg) | % Weight Consumed | Ixx | | Iyy | | Xcg sta. | |
|---|---|---|---|---|---|---|---|
| | | slug–ft$^2$ | kg–m$^2$ | slug–ft$^2$ | kg–m$^2$ | inches | cm |
| 4th Stage ignition | 0 | 26.3 | 35.7 | 171 | 231.8 | 50.7 | 128.8 |
| | 25 | 25.6 | 34.7 | 159 | 215.6 | 48.5 | 123.2 |
| | 50 | 24.5 | 33.2 | 143 | 193.9 | 45.7 | 116.1 |
| | 75 | 22.7 | 30.8 | 123 | 166.8 | 41.6 | 105.7 |
| 4th Stage burnout | 100 | 20.4 | 27.7 | 94 | 127.4 | 35.6 | 90.4 |
| Light Payload - 268 lbm (121.6 kg) | | | | | | | |
| 4th Stage ignition | 0 | 7.1 | 9.6 | 61.4 | 83.2 | 60.2 | 152.9 |
| | 25 | 6.8 | 9.2 | 57.2 | 77.6 | 59.1 | 150.1 |
| | 50 | 6.0 | 8.1 | 52.4 | 71.0 | 57.5 | 146.1 |
| | 75 | 4.6 | 6.2 | 46.4 | 62.9 | 54.8 | 139.2 |
| 4th Stage burnout | 100 | 2.7 | 3.7 | 37.7 | 51.1 | 48.7 | 123.7 |

Control jet location sta. — 84 in. (213.4 cm)

## 14.0 RCS SIZING

Present Scout third stage RCS component information and other vendor data were used to perform conceptual design of the RCS for the fourth stage AVC system. An all hydrogen peroxide ($H_2O_2$) monopropellant system and a combination $H_2O_2$ and gaseous nitrogen ($N_2$) system were considered.

### 14.1 Systems for Integral of $N_X$ Approach

Two velocity correction concepts were considered in sizing a system for the integral of $N_X$ RCS requirements as discussed in Section 13.0. Concept A involves velocity addition only. It requires aft thrust forces to add the velocity and a radial thrust force for the attitude correction and control. Concept B contains the capability for two attitude maneuvers of 180 deg (3.14 rad) each such that the $\Delta V$ can either be added or subtracted.

The use of a $N_2$ radial thruster for the attitude maneuvers in Concept B was not considered feasible because it would require 12 lbm (5.4 kg) of $N_2$ and the fourth stage available volume is not sufficient to accommodate such large tankage. The 12 lbm (5.4 kg) represents about 1400 cubic inches (22.9 $m^3$) which is equivalent to 21 of the current C section spherical tanks.

Table 43 presents a component summary with weights for the conceptual RCS designs. Two systems are presented for Concept A – one utilizes an $H_2O_2$ thruster for attitude control and the second a $N_2$ thruster. Only one configuration is shown for Concept B. In each case the system is sized such that the $\Delta V$ fuel included will correct all the measured error in the integral of $N_X$ 95 percent of the time. This quantity of RCS fuel will provide the desired $\Delta V$ at the design Altair IIIA burnout weight of 585.84 lbm (265.74 kg).

14.1.1 Design Considerations. – the normal configuration of the $H_2O_2$ tanks in the Scout B and C sections is the expulsion tube-bladder arrangement. However, since the fourth stage will be spinning at approximately 3 rps, the gravity forces due to spinning can be used as the method to hold the $H_2O_2$ against the outside tank wall and the tank outlet port; therefore, the tank bladder and expulsion tube were removed. This presented a design problem since the $H_2O_2$ will be free to transfer from tank to tank through either the $H_2O_2$ or $N_2$ manifolds. Tank unbalance would permit tip-off unbalance at spin-up which is unacceptable. To prevent this unbalance problem from occurring, the $H_2O_2$ tanks are provided with check valves at the nitrogen inlet port. This will prevent $H_2O_2$ from transferring through the $N_2$ lines but will provide pressure and fuel level balance through the $H_2O_2$ manifold line during spinning and firing of the motors. To help eliminate fuel transfer, the $H_2O_2$ manifold line will be located on the top side of the section so that the highest point of the line is at a higher level than either tank with the vehicle in the horizontal fueling position. When the fuel tanks have been serviced and pressurized, the maximum amount of fuel transfer will be that for filling the $H_2O_2$ manifold line and the amount the ullage gas will be compressed in the lower tank to equalize the pressure head between the tanks (approximately 0.5 psi, $3.45 \times 10^3$ $N/m^2$). The maximum weight of this fuel unbalance is less than 0.05 pounds (0.023 kg).

14.1.2 Component Design. – the regulator and $H_2O_2$ thrusters used in the conceptual design require some changes or modification from the regular Scout components.

(1) Regulator – the current Marotta regulator, RV89-1, is rather bulky for use in the fourth stage AVC system. A new regulator should be selected which is less bulky and complex. For the conceptual design effort a STERER regulator was used as the model.

## TABLE 43. – RCS COMPONENT SUMMARY – INTEGRAL OF $N_x$ APPROACH

| Components – Description | Concept A-1 | | | Concept A-2 | | | Concept B | | |
|---|---|---|---|---|---|---|---|---|---|
| | Number Required & Type | Weight | | Number Required & Type | Weight | | Number Required & Type | Weight | |
| | | lbm | kg | | lbm | kg | | lbm | kg |
| $H_2O_2$ tanks | 2–247.5 $in^3$ (4.06 $m^3$) ea | 8.0 | 3.63 | 2–238.5 $in^3$ (3.91 $m^3$) ea | 7.7 | 3.49 | 2–188 $in^3$ (3.08 $m^3$) ea | 6.1 | 2.77 |
| $N_2$ tanks | 2–68 $in^3$ (1.11$m^3$) ea | 3.8 | 1.72 | 2–136 $in^3$ (2.23 $m^3$) ea | 7.6 | 3.45 | 2–48.5 $in^3$ (0.79 $m^3$) ea | 2.7 | 1.22 |
| ΔV 48 lbf (213.5N) thrusters | 2–$H_2O_2$ | 4.8 | 2.18 | 2–$H_2O_2$ | 4.8 | 2.18 | 2–$H_2O_2$ | 4.8 | 2.18 |
| Att. cntl. 6–15 lbf (26.7–66.7N) thrusters | 1–$H_2O_2$ | 2.0 | 0.91 | 1–$N_2$ | 1.4 | 0.64 | 1–$H_2O_2$ | 2.0 | 0.91 |
| Regulator | 1–$N_2$ | 2.0 | 0.91 | 2–$N_2$ | 4.0 | 1.81 | 1–$N_2$ | 2.0 | 0.91 |
| Check valve | 2–$N_2$ | 0.4 | 0.18 | 2–$N_2$ | 0.4 | 0.18 | 2–$N_2$ | 0.4 | 0.18 |
| Relief valve | 1–$H_2O_2$ | 0.3 | 0.14 | 1–$H_2O_2$ | 0.3 | 0.14 | 1–$H_2O_2$ | 0.3 | 0.14 |
| Decomposition chamber | 1–$H_2O_2$ | 0.3 | 0.14 | 1–$H_2O_2$ | 0.3 | 0.14 | 1–$H_2O_2$ | 0.3 | 0.14 |
| Fill valves | 4–$H_2O_2$ | 0.3 | 0.14 | 4–$H_2O_2$ | 0.3 | 0.14 | 4–$H_2O_2$ | 0.3 | 0.14 |
| Fill valves | 1–$N_2$ | 0.06 | 0.03 | 1–$N_2$ | 0.06 | 0.03 | 1–$N_2$ | 0.06 | 0.03 |
| ΔV fuel | $H_2O_2$ | 21.7 | 9.84 | $H_2O_2$ | 21.7 | 9.84 | $H_2O_2$ | 11.0 | 4.99 |
| Attitude control fuel | $H_2O_2$ | 0.6 | 0.27 | $N_2$ | 1.3 | 0.59 | $H_2O_2$ | 0.6 | 0.27 |
| 2–180 Deg (3.14 rad) maneuvers | None | – | – | None | – | – | $H_2O_2$ | 5.5 | 2.49 |
| Tank pressurant | $N_2$ | 1.09 | 0.49 | $N_2$ | 1.06 | 0.48 | $N_2$ | 0.83 | 0.38 |
| Total weight | | 45.35 | 20.57 | | 50.92 | 23.10 | | 36.89 | 16.73 |

(2) Attitude Control $H_2O_2$ Thruster – the required 6-15 lbf (26.7 to 66.7N) attitude correction thrust can be obtained from the Walter Kidde 14-3 lbf (62.3 to 13.3N) thrust motor presently used on the Scout. This was the motor used in the conceptual design; however some disadvantages do exist. First, the thrust for each particular mission must be predetermined and the motor orifice modified by drilling to the required size to control the fuel flow rate prior to system operational tests at Dallas. Second, there are problems associated in performing air bearing tests using a $H_2O_2$ thruster; such a test presents a potential safety hazard as well as operational problems. Third, $H_2O_2$ thrusters tend to be less predictable in response time than cold gas thrusters. These problems will have to be evaluated and resolved during the final system design.

(3) $\Delta V$ $H_2O_2$ Thruster – the required velocity correction thrust can be obtained from the Walter Kidde 48 lbf (213.5N) thrust motor presently used on Scout. However, the motor has the nozzle mounted at an angle to the side of the thrust chamber. There is insufficient space in the upper D section to mount this motor so that the nozzle will face aft. It will be necessary to modify the motor to place the nozzle in line with the main chamber.

## 14.2 New AVC Guidance Options

Subsequent to the investigation of the new guidance options, the sizing of the reaction control systems was reviewed to define a system compatible with Options 1 or 3. The 21.7 lbm (9.84 kg) of $H_2O_2$ in the two reaction control systems sized for Concept A in the integral of $N_X$ approach provided a $\Delta V$ capability of 196 ft/s (59.74 m/s) in order to be able to correct 95% of the error. Now considering the statistics from the accuracy investigation of Options 1 and 3, some of the results are interestingly comparable to the same $\Delta V$ capability.

(1) The Option 3 mean plus two sigma $\Delta V$ for the maximum error budget with the 200 n. mi. (370.4 km) trajectory is 195.1 ft/s (59.47 m/s) as indicated in Table 40. The mean plus two sigma implies that 97.7% of the total velocity error would be corrected.

(2) The $\Delta V$ statistics for Option 1 with the same trajectory and equipment error budget show a mean of 102.5 ft/s (31.24 m/s) with a standard deviation of ±56.5 ft/s (17.22 m/s). To correct 95% of the total velocity error requires a capability of the mean plus 1.645 times sigma; this value turns out to be 195.3 ft/s (59.5 m/s).

(3) The 196 ft/s (59.74 m/s) $\Delta V$ capability can then be used effectively as that required to correct 97.7% of the velocity error for Option 3 or 95% for Option 1.

Both Options 1 and 3 required the capability to make two pitch attitude maneuvers of up to 180 deg (3.14 rad) each. A reaction control system was sized to include the attitude maneuvers so that it would be compatible with these two options. The results are shown in Table 44, the total RCS weight is 53.59 lbm (24.22 kg). This RCS weight will be used later to determine the total increase in fourth stage weight resulting from the incorporation of the AVC system.

# 15.0 AVC GUIDANCE OPERATING TIME AND EQUIPMENT WEIGHTS

Weight estimates were assembled for a typical IMU and CEU with a battery based upon the maximum AVC operating time. These data were then used in the weight estimates of the total payload transition section.

TABLE 44. – RCS COMPONENT SUMMARY – OPTION 1 AND 3

| Components – Description | Number Required & Type | Weight lbm | Weight kg |
|---|---|---|---|
| $H_2O_2$ tanks | 2–305.8 $in^3$ (5.01 $m^3$) ea. | 9.88 | 4.48 |
| $N_2$ tanks | 2–78.77 $in^3$ (1.29 $m^3$) ea. | 4.4 | 2.00 |
| $\Delta V$ 48 lbf (213.5N) thrusters | 2–$H_2O_2$ | 4.8 | 2.18 |
| Att. cntl. 6–15 lbf (26.7–66.7N) thrusters | 1–$H_2O_2$ | 2.0 | 0.91 |
| Regulator | 1–$N_2$ | 2.0 | 0.91 |
| Check valve | 2–$N_2$ | 0.4 | 0.18 |
| Relief valve | 1–$H_2O_2$ | 0.3 | 0.14 |
| Decomposition chamber | 1–$H_2O_2$ | 0.3 | 0.14 |
| Fill valves | 4–$H_2O_2$ | 0.3 | 0.14 |
| Fill valves | 1–$N_2$ | 0.06 | 0.03 |
| $\Delta V$ Fuel | $H_2O_2$ | 21.7 | 9.84 |
| Attitude control fuel | $H_2O_2$ | 0.6 | 0.27 |
| 2–180 Deg (3.14 rad) maneuvers | $H_2O_2$ | 5.5 | 2.49 |
| Tank pressurant | $N_2$ | 1.35 | 0.61 |
| Total weight | | 53.59 | 24.31 |

15.1 IMU and CEU Characteristics

The Pershing II IMU was used as a typical or reference unit in the establishment of AVC system weights and accomplishment of preliminary layouts. This particular IMU was used because it is being developed for a missile application and will be qualified to environmental levels that closely parallel the Scout environments. The most recent estimates of the characteristics of this IMU are:

| | | |
|---|---|---|
| Weight | 30.8 lbm | (13.97 kg) |
| Length (along vehicle yaw axis) | 13.0 in. | (33.02 cm) |
| Width (along vehicle pitch axis) | 10.5 in. | (26.67 cm) |
| Height (along vehicle roll axis) | 9.0 in. | (22.86 cm) |

These dimensions do not include connectors or mounting feet.

Estimated characteristics of the CEU to operate with the Pershing II IMU were based upon the use of the Kearfott SKC-3000 digital processor. This is basically the same processor used in the SKN-2400 inertial navigation unit; one card for the central processing unit, two input/output cards and one power supply card. The power supply card would also generate the 28 Vdc – 1 ampere commands to the RCS thrusters. Estimated characteristics of the package housing this processor are:

| | | |
|---|---|---|
| Weight | 6.0 lbm | (2.72 kg) |
| Length | 7.1 in. | (18.03 cm) |
| Width | 6.75 in. | (17.15 cm) |
| Height | 4.63 in. | (11.76 cm) |

Since this is not an existing package, it could be configured in a manner to best fit the section layout. The total weight and volume however are representative of the package needed.

## 15.2 Guidance Operating Time

In order to define the battery capacity needed to support the IMU and CEU, the maximum AVC operating time was established. The maximum Scout mission times as defined in Reference 6 were used to determine the boost and coast times for each stage. Times for the other AVC functions were then added.

The total AVC operating time is shown in Table 45. The boost and coast times for the first three stages are taken directly from Reference 6. The 300 seconds for fourth stage burn and outgassing is included to allow for complete Altair IIIA thrust decay prior to beginning the pitch maneuver required for the $\Delta V$ correction. The 250 seconds for the 180 deg. (3.14 rad) pitch maneuver is the maximum time as shown in Figure 32. The maximum total AVC flight operating time as indicated in Table 45 is 2012 seconds or 0.559 hours.

One other time increment is added in establishing the battery requirements; this is the time the system would be on internal power for pre-launch checks. No statistical data existed on the current third stage guidance 28 Vdc battery operating time during pre-launch checks. Logbooks of several vehicles were reviewed and the average operating time for the battery was found to be 5.6 minutes. A period of 6.0 minutes was then allocated for AVC operation on internal power during pre-launch checks.

TABLE 45. – MAXIMUM AVC OPERATING TIME

| Event | Time – seconds | |
|---|---|---|
| First stage burn | 83 | |
| First stage coast | 20 | |
| Second stage burn | 39 | |
| Second stage coast | 400 | 1172 |
| Third stage burn | 30 | |
| Third stage coast | 600 | |
| Fourth stage burn and outgassing | 300 | |
| Accomplish 180 deg (3.14 rad) maneuver | 250 | |
| Make ΔV correction | 40 | 840 |
| Accomplish 180 deg (3.14 rad) maneuver | 250 | |
| Total AVC flight time | 2012 | (0.559 hours) |
| Pre–launch checks | 360 | |
| Total battery operating time | 2372 | (0.659 hours) |

15.3 AVC Power Requirements and Battery Sizing

The estimated IMU and CEU power requirements, using the equipments just discussed are:

| | | |
|---|---|---|
| IMU | Steady State Operation | 125 watts, 28 Vdc |
| | Operation During 3 rps | 150 watts, 28 Vdc |
| CEU | Normal Operation | 45 watts, 28 Vdc |

These power requirements together with the maximum operating times were used to establish the battery capacity needed. The results are given in Table 46. A change in the reference IMU and CEU would necessarily result in some changes in the power and battery capacity requirements.

TABLE 46. – AVC BATTERY CAPACITY REQUIREMENTS

| Unit | Function | Ampere – seconds |
|---|---|---|
| IMU | Pre–launch (4.464 A for 360 s) | 1607.0 |
| | Launch to 3rd stg coast (4.464 A for 1172 s) | 5231.8 |
| | 4th stg ignition to end (5.357 A for 840 s) | 4499.9 |
| CEU | Pre–launch (1.607 A for 360 s) | 578.5 |
| | Launch to end of mission (1.607 A for 2012 s) | 3233.3 |
| | ΔV thruster commands (2 A for 40 s) | 80.0 |
| | Attitude control thruster command, 25% duty cycle (1 A for 280 sec) | 70.0 |
| | Total | 15 297.5 |

IMU requirement = 11 388.7 A–s = 3.15 A–hr

CEU requirement = 3 958.8 A–s = 1.10 A–hr

Total battery capacity needed = 4.25 A–hr

A 28 Vdc battery was sized to provide the capacity given in Table 46. PM 4 type cells were used with a resulting battery rating of approximately 5.4 ampere hours. Characteristics of this battery are:

| | | |
|---|---|---|
| Weight | 7.5 lbm | (3.40 kg) |
| Length | 1.72 in. | (4.37 cm) |
| Width | 0.59 in. | (1.50 cm) |
| Height | 3.36 in. | (8.53 cm) |

## 16.0 AVC FOURTH STAGE WEIGHTS AND PERFORMANCE

The reference AVC guidance equipment and an RCS sized to provide a ΔV of 196 ft/s (59.74 m/s) at maximum payload weight were used to establish the total weight increase resulting from the addition of the AVC system. Some additional accuracy investigations were made to determine the effect of reducing the ΔV capability. The RCS was re-sized for a reduced ΔV and alternate guidance equipment selected. The total fourth stage weight increases for these AVC equipment configurations were determined.

## 16.1 Reference Guidance Equipment With 21.7 lbm (9.84 kg) ΔV Fuel

Layouts were made of a new payload transition section to accommodate the reference Pershing II IMU, associated guidance equipment and the components needed from the T/M ring module. The RCS, as sized with the 21.7 lbm (9.84 kg) $H_2O_2$ ΔV fuel, was included in the upper D section. Total fourth stage weight increase and performance in terms of net payload loss were determined for the configuration.

The RCS configuration that includes 21.7 lbm (9.84 kg) of ΔV fuel was selected because it represents the capability of correcting 95% or more of the velocity error with the maximum guidance error budget for Options 1 and 3. As discussed in Sections 13.0 and 14.0, the 21.7 lbm (9.84 kg) of ΔV $H_2O_2$ provides a ΔV capability of 196 ft/s (59.74 m/s) at the design Altair III burnout weight. For the 600 n. mi. (1111.2 km) case, this same quantity of ΔV fuel will result in a ΔV capability of approximately 277 ft/s (84.43 m/s) because of the weight reduction. The correction capability of this RCS referenced to the maximum error budget is summarized as follows:

| Orbit | Guidance Option | Velocity Error Corrected |
|---|---|---|
| 200 n. mi. (370.4 km) | 1 | mean + 1.645$\sigma$ (95%) |
| | 3 | mean + 2$\sigma$ (97.7%) |
| 600 n. mi. (1111.2 km) | 1 | mean + 2.60$\sigma$ (99.5%) |
| | 3 | mean + 3.39$\sigma$ (99.97%) |

The accuracy achievable with this velocity correction capability approaches the maximum error budget isoprobability contours for Options 1 and 3 as shown in Figures 17, 18, 21 and 22. The noted isoprobability contours were computed with no restriction on the velocity correction.

The total weight of the RCS components with the 21.7 lbm (9.84 kg) of ΔV fuel is 53.59 lbm (24.31 kg) as shown in Table 44. Estimated weight of the plumbing and associated structure in upper D to install this RCS is 6.5 lbm (2.95 kg) as determined from the equipment layout.

The transition section weights are listed in Table 47 with the reference Pershing II IMU. No instrumentation accelerometers are shown in the list of components. The IMU contains three highly accurate accelerometers, the outputs of which are a pulse train with each pulse representing a fixed incremental velocity. These velocity pulses are accumulated in the CEU for use in the computation of inertial velocity. The accumulators are sampled at rates varying from 50 to 200 times per second; these data can be monitored by T/M and differentiated in the post flight analysis process to determine vehicle acceleration.

As indicated in Table 47, the total transition section weight is 74.98 lbm (34.01 kg). This includes the 22.3 lbm (10.12 kg) structure. Note that the structure weight includes the separation system.

## TABLE 47. – ESTIMATED WEIGHTS – PAYLOAD TRANSITION SECTION WITH REFERENCE GUIDANCE COMPONENTS

| Item | Weight | |
|---|---|---|
| | lbm | kg |
| Pershing II IMU | 30.8 | 13.97 |
| Control electronics (with SKN–3000 digital processor) | 6.0 | 2.72 |
| AVC battery | 7.5 | 3.40 |
| Capacitive discharge ignition (CDI) | 3.38 | 1.53 |
| PCM Encoder | 0.9 | 0.41 |
| T/M Transmitter | 1.6 | 0.73 |
| T/M Battery | 2.5 | 1.13 |
| Total weight of components | 52.68 | 23.90 |
| Structure | 22.30 | 10.12 |
| Total transition section weight | 74.98 | 34.01 |
| **Structure Breakdown*** | | |
| Forward ring | 2.75 | 1.25 |
| Aft ring | 2.64 | 1.20 |
| Skin | 5.70 | 2.59 |
| Two metalite shelves | 5.69 | 2.58 |
| Separation clamp | 1.70 | 0.77 |
| Stringers | 1.90 | 0.86 |
| Umbilical fitting | 0.22 | 0.10 |
| Spring installation | 0.40 | 0.18 |
| Screws, nuts, etc. | 0.70 | 0.32 |
| Component attach hardware | 0.60 | 0.27 |
| Total transection sect. structure | 22.30 | 10.12 |

*Based upon a transition section with a 20.5 in. (52.07 cm) inside diameter and a 19.32 in (49.07 cm) length.

The total fourth stage weight increase due to the AVC system can now be calculated. As indicated in Table 48, the total transition section weight plus the increase in upper D is 114.68 lbm (52.02 kg). However, to determine the net payload loss resulting from the incorporation of the AVC system, an E section weight of 9.6 lbm (4.35 kg) must be subtracted since the new transition section functionally replaces the E section. The net payload loss then is 105.08 lbm (47.66 kg) for the AVC system defined.

The accuracies achievable with this AVC configuration, employing either Options 1 or 3, are very acceptable. However the loss in payload weight is significant. In fact, this loss represents about 24% of the total SCout F-1 payload capability for the 200 n. mi. (370.4 km) orbit and 41% at 600

TABLE 48. – AVC FOURTH STAGE WEIGHT INCREASE – REFERENCE GUIDANCE COMPONENTS

| | lbm | kg |
|---|---|---|
| Upper D section: | | |
| AVC Reaction control system (ref Table 44) | 53.59 | 24.31 |
| Plumbing & additional structure | 6.50 | 2.95 |
| Deletion of T/M ring module | −20.30 | −9.25 |
| Net upper D increase | 39.70 | 18.01 |
| Transition section: | | |
| Total component weight (ref Table 47) | 52.68 | 23.90 |
| Structure (ref Table 47) | 22.30 | 10.12 |
| Total transition section | 74.98 | 34.01 |
| Transition section + upper D increase | 114.68 | 52.02 |
| Payload loss | | |
| Transition section + upper D increase | 114.68 | 52.02 |
| Less E section (replaced with new trans. sect.) | −9.60 | −4.35 |
| Net AVC system payload weight penalty | 105.08 | 47.66 |

n. mi. (1111.2 km). This loss in performance is greater than desired, thus an effort was initiated to investigate methods of reducing the AVC system weights. The most direct avenues available for weight reduction are:

(1) Reduce the ΔV capability of the RCS.

(2) Select lighter guidance components (IMU and CEU).

## 16.2 Effect Of Reduced ΔV Capability – Options 1 And 3

The initial task in AVC system weight reduction effort then was to determine the effect of reducing the ΔV capability. The orbital deviations with limited or fixed values of ΔV correction capability were computed for Options 1 and 3 with the maximum equipment error budget and the 600 n.mi. (1111.2 km) orbit. Simulations were made first using a ΔV equal to the mean values as established in the analysis discussed in Section 11.0. The ΔV limits were then reduced to 75 ft/s (22.86 m/s) and 50 ft/s (15.24 m/s). The results of the simulations with ΔV limits are shown in Figures 33 and 34. The surprising result of this investigation is the small increase in the isoprobability contours with the ΔV limited to the mean value when compared to the unlimited ΔV case. In fact, the ΔV capability can be reduced to 75 ft/s (22.86 m/s), which is less than the mean value for both options, without incurring an accuracy degradation that would appear to be unacceptable. The significant outcome is that the AVC RCS weight can be reduced and still realize impressive improvements in orbital accuracy.

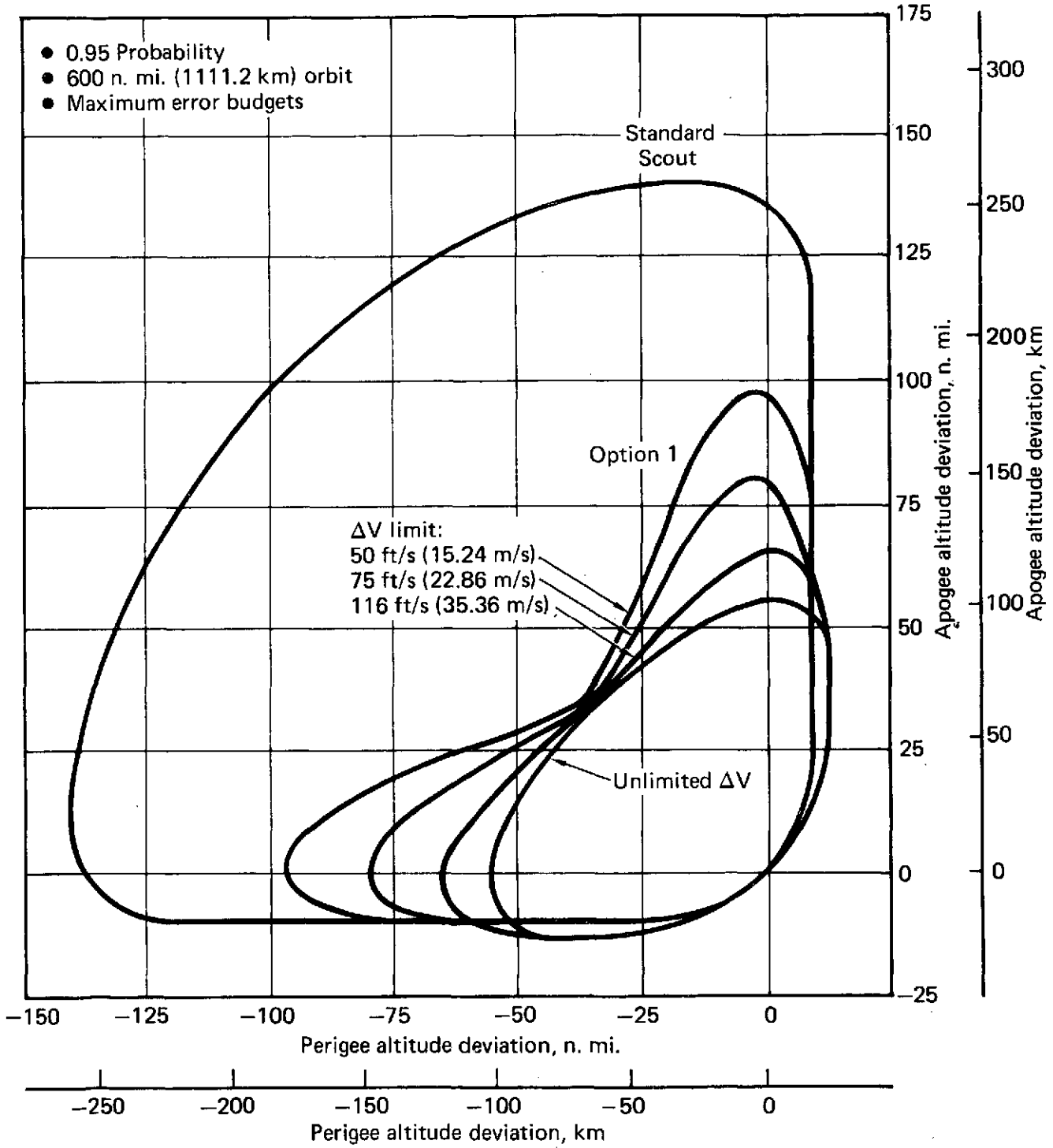


**FIGURE 33. – ISOPROBABILITY CONTOURS – OPTION 1 WITH ΔV LIMITS**

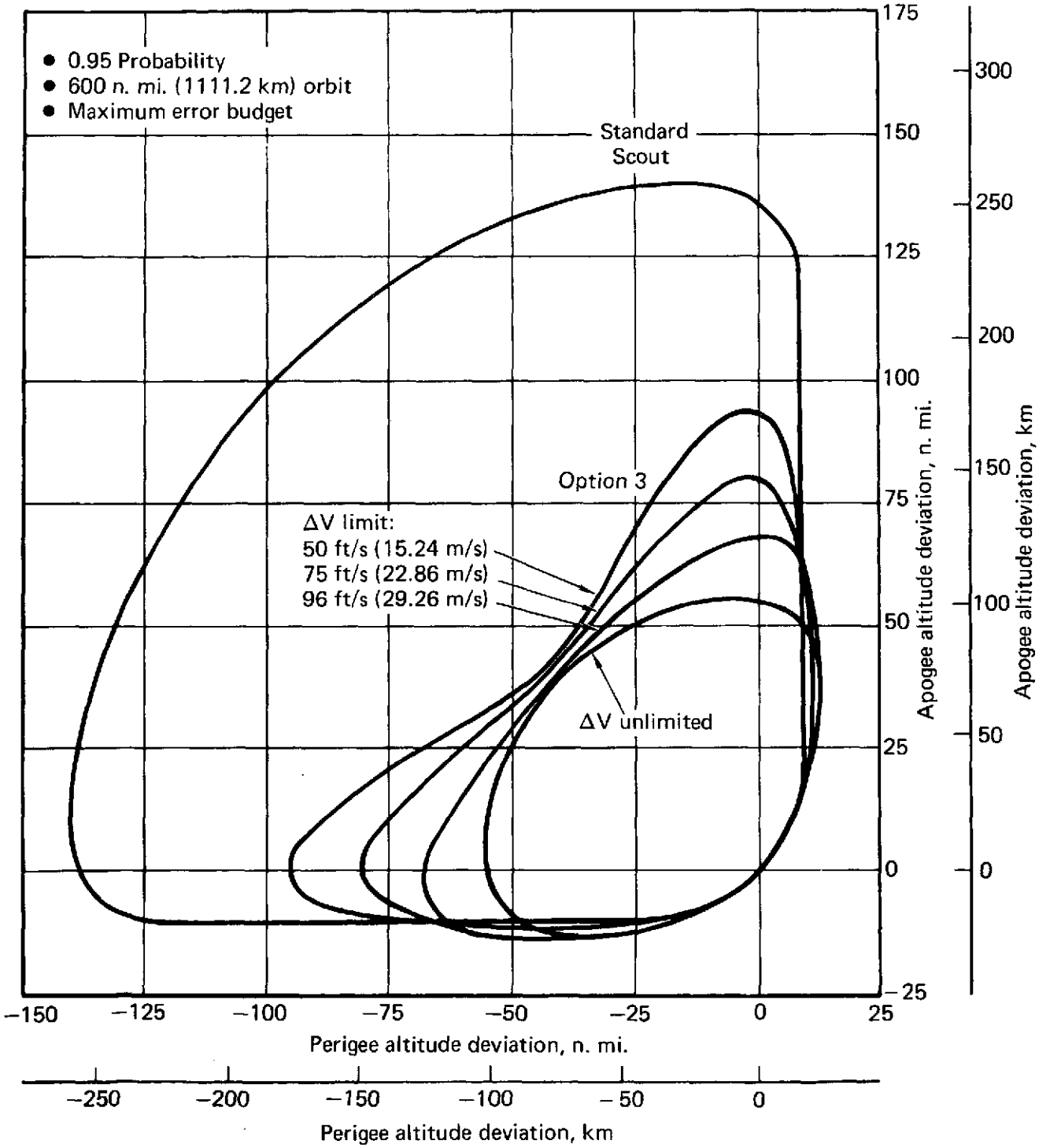


FIGURE 34. – ISOPROBABILITY CONTOURS – OPTION 3 WITH ΔV LIMITS

The $\Delta V$ statistics for Options 1 and 3 (given in Tables 36 and 38) were reviewed to select a reduced $\Delta V$ limit to be used in sizing a new RCS. The $\Delta V$ capability has to be selected for the lower orbit case which corresponds to the maximum or design fourth stage weight at Altair IIIA burnout. A $\Delta V$ capability of 90 ft/s (27.43 m/s) was selected because it corresponds to the average of the mean values for the two error budgets at 200 n.mi. (370.4 km), for Option 3.

## 16.3 RCS With 90 ft/s (27.43 m/s) $\Delta V$ At Maximum Payload Weight

An RCS was sized to provide the $\Delta V$ at the design Altair IIIA burnout weight of 585.84 lbm (265.74 kg). The component summary for this system is presented in Table 49. The $H_2O_2$ required to provide the desired $\Delta V$ is 10.15 lbm (4.60 kg); the total RCS weight is 35.60 lbm (16.15 kg). The reduction in $\Delta V$ from 196 ft/s (59.74 m/s) to 90 ft/s (27.43 m/s) results in an RCS weight savings of 17.99 lbm (8.16 kg), which is a 34% reduction.

The 10.15 lbm (4.60 kg) of $H_2O_2$ $\Delta V$ fuel provides a $\Delta V$ of approximately 127.5 ft/s (38.86 m/s) at an orbit altitude of 600 n.mi. (1111.2 km). The correction capability of this RCS referenced to the maximum error budget is summarized as follows:

| Orbit | Guidance Option | Velocity Error Corrected |
|---|---|---|
| 200 n.mi. (370.4 km) | 1 | 12.5 ft/s (3.81 m/s) less than mean (<50%) |
| | 3 | 2.3 ft/s (0.70 m/s) less than mean (<50%) |
| 600 n.mi. (1111.2 km) | 1 | mean + 0.19$\sigma$ (57.5%) |
| | 3 | mean + 0.59$\sigma$ (72.2%) |

The complete picture of the variation of orbital errors at 600 n.mi. (1111.2 km) as a function of the system $\Delta V$ capability however is given in Figures 33 and 34.

TABLE 49. – RCS COMPONENT SUMMARY – REDUCED ΔV

| Components – Description | Number Required & Type | Weight lbm | Weight kg |
|---|---|---|---|
| $H_2O_2$ Tanks | 2–178.8 $in^3$ (2.93 $m^3$) ea | 5.8 | 2.63 |
| $N_2$ Tanks | 2–46.2 $in^3$ (0.76 $m^3$) ea | 2.6 | 1.18 |
| ΔV 48 lbf (213.5N) thrusters | 2–$H_2O_2$ | 4.8 | 2.18 |
| Att. cntl. 6–15 lbf (26.7–66.7N) thrusters | 1–$H_2O_2$ | 2.0 | 0.91 |
| Regulator | 1–$N_2$ | 2.0 | 0.91 |
| Check valve | 2–$N_2$ | 0.4 | 0.18 |
| Relief valve | 1–$H_2O_2$ | 0.3 | 0.14 |
| Decomposition chamber | 1–$H_2O_2$ | 0.3 | 0.14 |
| Fill valves | 4–$H_2O_2$ | 0.3 | 0.14 |
| Fill valves | 1–$N_2$ | 0.06 | 0.03 |
| ΔV Fuel | $H_2O_2$ | 10.15 | 4.60 |
| Attitude control fuel | $H_2O_2$ | 0.6 | 0.27 |
| 2–180 Deg. (3.14 rad) maneuvers | $H_2O_2$ | 5.5 | 2.49 |
| Tank pressurant | $N_2$ | 0.79 | 0.36 |
| Total weight | | 35.60 | 16.15 |

## 16.4 Fourth Stage Weight With Reduced ΔV And Alternate Guidance Components

The single change of reducing the RCS ΔV capability results in a considerable weight savings. If there is no change to the transition section and the reference guidance components are maintained, the net payload penalty resulting from the AVC system is reduced to 87.09 lbm (39.50 kg).

The second most direct avenue for reducing the total AVC system weight is to select alternate lighter guidance components. Several guidance vendors are currently producing or designing inertial navigators that offer some weight advantage over the Pershing II IMU with an attendant CEU. One example of such a system is the Kearfott SKN–2400 Inertial Navigation Unit (INU). This particular system is currently in production and is now being adapted for use in a missile application. The total system is packaged in a single unit which includes an inertial platform using the same gyros as in Pershing II, electronics, power regulation and a digital processor. The basic elements of the digital processor are the same as those used in the separate CEU that interfaced with the Pershing II IMU. The physical characteristics of the SKN–2400 system are:

| | | |
|---|---|---|
| Weight | 25.0 lbm | (11.34 kg) |
| Length | 13.8 in. | (35.05 cm) |
| Width | 7.66 in. | (19.46 cm) |
| Height | 7.25 in. | (18.42 cm) |

This single unit would replace both the Pershing II IMU and the CEU. The indicated 25.0 lbm (11.34 kg) weight is 2.0 lbm (0.91 kg) more than the current system weight to permit some changes to assure Scout compatibility.

The estimated payload transition weights were revised to reflect the use of the SKN–2400 INU. The new structure weights assume a 2.0 in. (5.08 cm) reduction in the inside diameter of the section. The revised weights are listed in Table 50. Power requirements of the SKN–2400 do not vary significantly from the combined Pershing II IMU–CEU requirements used in Section 15.0, thus the same AVC battery was used. Other inertial navigators do offer lower power consumption thus some battery savings may be possible in the final system design.

TABLE 50. – ESTIMATED WEIGHTS – PAYLOAD TRANSITION SECTION WITH ALTERNATE GUIDANCE UNIT

| Item | Weight | |
|---|---|---|
| | lbm | kg |
| SKN–2400 Inertial navigation unit | 25.0 | 11.34 |
| AVC battery | 7.5 | 3.40 |
| Capacitive discharge ignition (CDI) | 3.38 | 1.53 |
| PCM Encoder | 0.9 | 0.41 |
| T/M Transmitter | 1.6 | 0.73 |
| T/M Battery | 2.5 | 1.13 |
| Total weight of components | 40.88 | 18.54 |
| Structure | 20.24 | 9.18 |
| Total transition section weight | 61.12 | 27.72 |
| Structure Breakdown | | |
| Forward ring | 2.48 | 1.12 |
| Aft ring | 2.38 | 1.08 |
| Skin | 5.36 | 2.43 |
| Two metalite shelves | 4.50 | 2.04 |
| Separation clamp | 1.70 | 0.77 |
| Stringers | 1.90 | 0.86 |
| Umbilical fitting | 0.22 | 0.10 |
| Spring installation | 0.40 | 0.18 |
| Screws, nuts, etc. | 0.70 | 0.32 |
| Component attach hardware | 0.60 | 0.27 |
| Total transition sect. structure | 20.24 | 9.18 |

The total fourth stage weight increase with an AVC system employing both the reduced ΔV and the SKN-2400 INU as given in Table 51 is 82.83 lbm (37.57 kg), with a net payload penalty of 73.23 lbm (33.22 kg). A payload reduction of this magnitude is much more acceptable than is the penalty of 105.08 lbm (47.66 km) for the AVC system with the high ΔV capability and the reference guidance components.

**TABLE 51. – AVC FOURTH STAGE WEIGHT INCREASE – REDUCED ΔV AND ALTERNATE GUIDANCE UNIT**

| | lbm | kg |
|---|---|---|
| Upper D section: | | |
| AVC Reaction Control System (ref Table 49) | 35.60 | 16.15 |
| Plumbing & additional structure | 6.50 | 2.95 |
| Deletion of T/M ring module | – 20.39 | – 9.25 |
| Net upper D increase | 21.71 | 9.85 |
| Transition section: | | |
| Total component weight (ref Table 50) | 40.88 | 18.54 |
| Structure (ref Table 50) | 20.24 | 9.18 |
| Total transition section | 61.12 | 27.72 |
| Transition section + upper D increase | 82.83 | 37.57 |
| Payload loss | | |
| Transition section + upper D increase | 82.83 | 37.57 |
| Less E section (replaced with new trans. sect.) | – 9.60 | – 4.35 |
| Net AVC system payload weight penalty | 73.23 | 33.22 |

### 16.5 Comparison of Payload Penalties for AVC Configuration

A comparison of the total payload penalties for the three AVC configurations developed is tabulated as follows:

| Guidance Components | RCS ΔV Capability at Max Payload Weight | | Net Payload Penalty | |
|---|---|---|---|---|
| | ft/s | m/s | lbm | kg |
| Persing II IMU & CEU | 196 | 59.74 | 105.08 | 47.66 |
| Pershing II IMU & CEU | 90 | 27.43 | 87.09 | 39.50 |
| SKN-2400 INU | 90 | 27.43 | 73.23 | 33.22 |

A Scout fourth stage AVC system utilizing a guidance system of the SKN-2400 INU type and a ΔV capability of 90 ft/s (27.43 m/s) at the maximum payload weight offers highly attractive accuracy improvements with either Option 1 or 3. Additionally the loss in payload capability incurred is reduced to an acceptable value of 73.23 lbm (33.22 kg).

Other possibilities of weight reduction can be investigated. These could include the use of hydrazine in the RCS and further trades in the design of the transition section to consider the use of honeycomb type construction to yield minimum weight.

### 16.6 Restricted ΔV Pitch Maneuvers

A further possibility exists of implementing the AVC system, utilizing Option 1 or 3, in a manner that would restrict or limit the magnitude of the ΔV pitch maneuver. Shaping or biasing the trajectory to always require the addition of velocity along the X-axis would mean that the pitch maneuver is bounded at ± 90 deg (1.57 rad). The ΔV capability would have to be increased to maintain the accuracies presented for Options 1 and 3. Additional study is required to evaluate the trades involved in an approach of this type: (1) magnitude to which the pitch maneuver can be limited (2) ΔV capability required, (3) accuracy changes and (4) increase in RCS weight required.

## 17.0 ENVIRONMENTAL CONSIDERATIONS

Scout environmental flight data were analyzed by individual transition section to establish random vibration and shock environments. Environmental qualification and acceptance test levels were then determined for the AVC equipment.

## 17.1 Vibration And Shock Criteria

Standard Scout random vibration levels and shock environment were determined for upper D and payload transition section components. The baseline for these determinations was the measured flight data from Reference 7, which presents data from thirteen Scout launches. Conclusions reached, based on these data, were:

(1) The levels of sustained vibration are lower than estimated.

(2) Transient vibration due to motor ignition is higher than estimated.

(3) The maximum level of sustained vibration occurs at the time of maximum dynamic pressure and is random in nature.

(4) Vibration due to motor burning is very low.

(5) No sinusoidal vibration was observed.

Since the initial release of this report, five additional Scout vehicles equipped with vibrometers have been launched. The vibration and shock data from these vehicles did not change any of the above conclusions.

A summary of the 95% confidence level Scout flight vibration environment for equipments in the D and E transition sections is shown in Figure 35. Expected vibration levels were estimated for possible growth configurations such as that discussed in Reference 8. The results did not vary significantly from the levels in Figure 35.

Shock spectra for Scout D and E section equipments are presented in Figure 36 for both lateral and longitudinal axes. These curves are actually the envelope of measured and calculated data. Acceleration shock spectrum calculated for possible growth configurations fall within the envelopes shown in Figure 36.

To date no sustained sinusoidal vibration has been measured on Scout flights. There is no indication this type vibration will exist on future growth configurations. Therefore no component sinusoidal testing is included. Vehicle system level sinusoidal vibration testing is included to represent environments to which the equipments may be exposed during handling and shipping.

## 17.2 Equipment Test Levels

Environmental criteria for both the Design Qualification and Scout Standard Environmental Acceptance Tests of the AVC system were established for component and subsystem equipment level testing and for the entire vehicle section. The environmental levels were derived from the vibration and shock criteria just discussed and Scout flight experience presented in Reference 9. The levels presented apply to equipment operation and stand-by conditions. Operation time during the application of an environment will be specified in the individual test procedure. Individual test catagories (component and vehicle systems levels) will consist of one or more of the tests defined; applicable tests for each category are given in Sections 17.3 and 17.4.

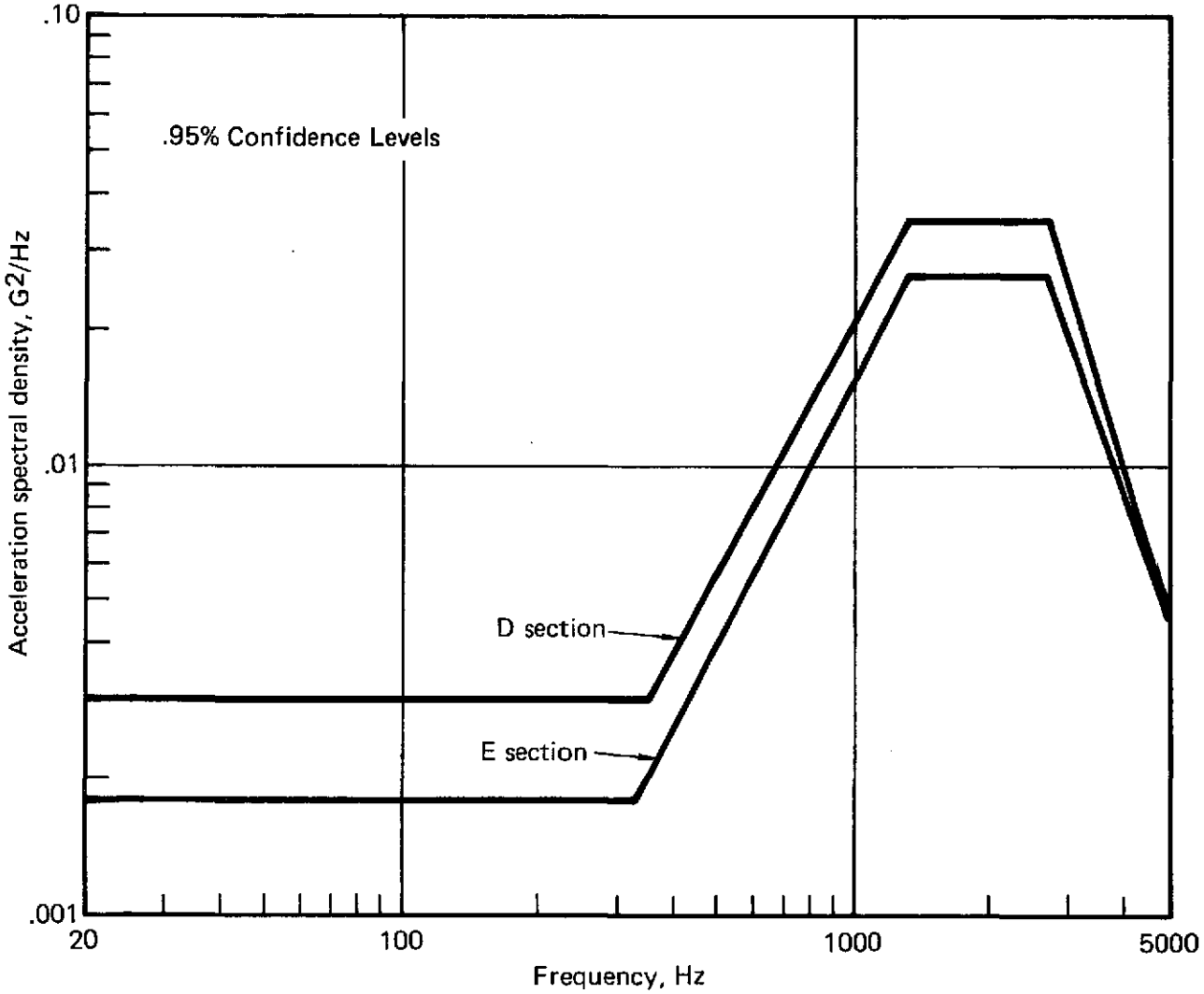


FIGURE 35. – SCOUT COMPONENT RANDOM VIBRATION LEVELS, ALL AXES

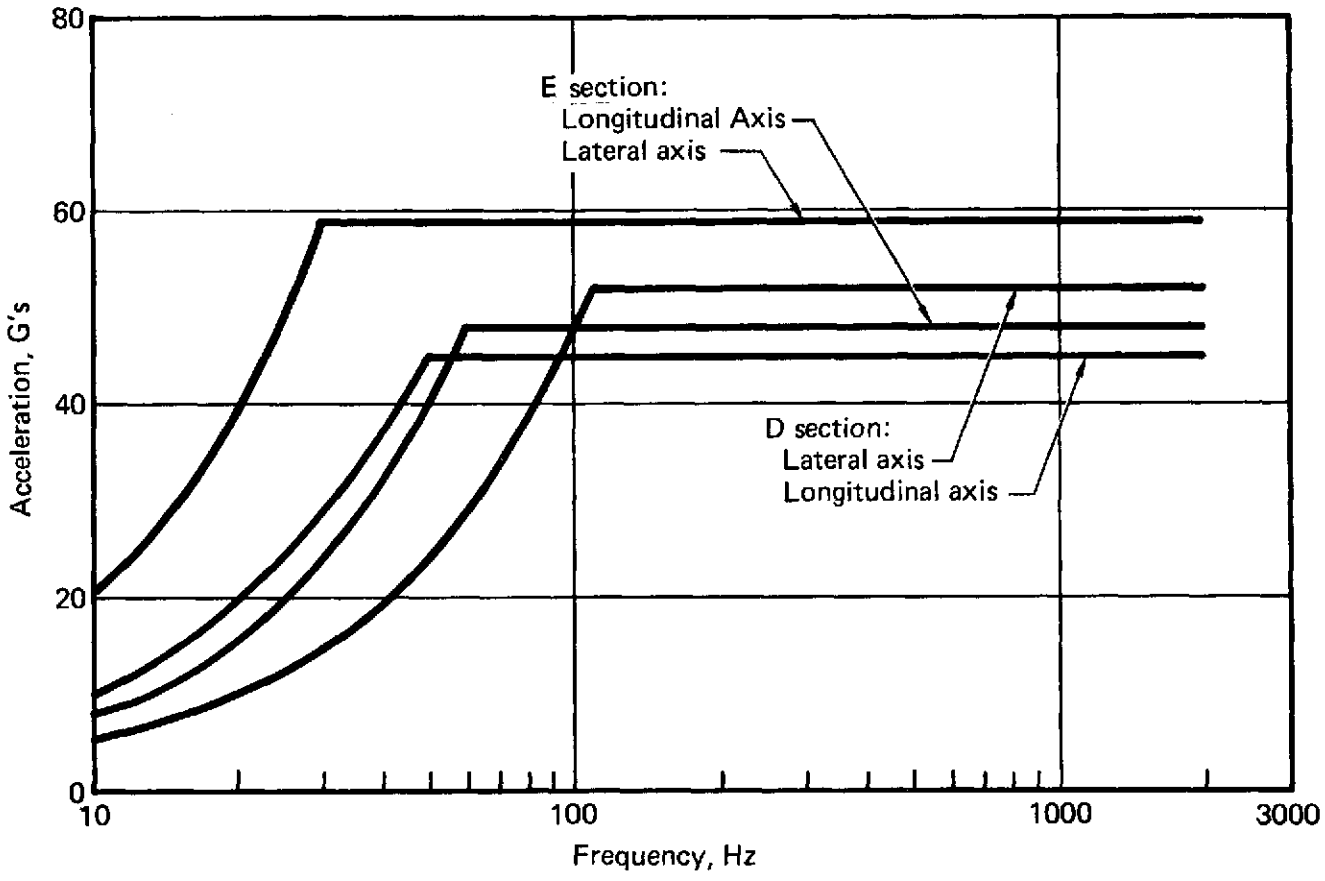


**FIGURE 36. – SCOUT COMPONENT SHOCK SPECTRA**

17.2.1 Design Qualification Test Level Requirements. – the environmental test level requirements for Design Qualification Tests are outlined. The test requirements for vibration and mechanical shock for components and subsystems are such that if either one is applied, the other must also be applied.

17.2.1.1 Component and Subsystem Tests:

17.2.1.1.1 Random Vibration

(1) D Section Components. – the random vibration requirements for each component or subsystem in each of the three major axes are:

| Time Per Axis, Seconds | Frequency, Hz | | Overall Acceleration, Grms |
|---|---|---|---|
| | Lower | Upper | |
| 80 | 20 | 2000 | 9.75 |

The test spectra are shown in Figure 37.

(2) Fourth Stage (Payload Transition Section) Components. – the random vibration requirements for each component or subsystem in each of the three major axes are:

| Time Per Axis, Seconds | Frequency, Hz | | Overall Acceleration, Grms |
|---|---|---|---|
| | Lower | Upper | |
| 80 | 20 | 2000 | 9.1 |

The test spectra are shown in Figure 38.

17.2.1.1.2 Mechanical Shock

(1) D Section Components. – the mechanical shock level requirement is for three shocks of 60 G's for 6 milliseconds duration terminal sawtooth in each direction of each axis for a total of 18 shocks.

(2) Fourth Stage (Payload Transition Section) Components. – the mechanical shock level requirement is for three shocks of 75 G's for 6 milliseconds duration terminal sawtooth in each direction of each axis for a total of 18 shocks.

17.2.1.1.3 Temperature

(1) Low Temperature. – the low temperature requirement is for the equipment to be maintained at zero $^{O}$F (255.37$^{O}$K) for four hours or until the equipment temperature is stabilized, whichever occurs first. Stabilization is defined as three readings taken five minutes apart that are within five $^{O}$F (2.78$^{O}$K) of each other.

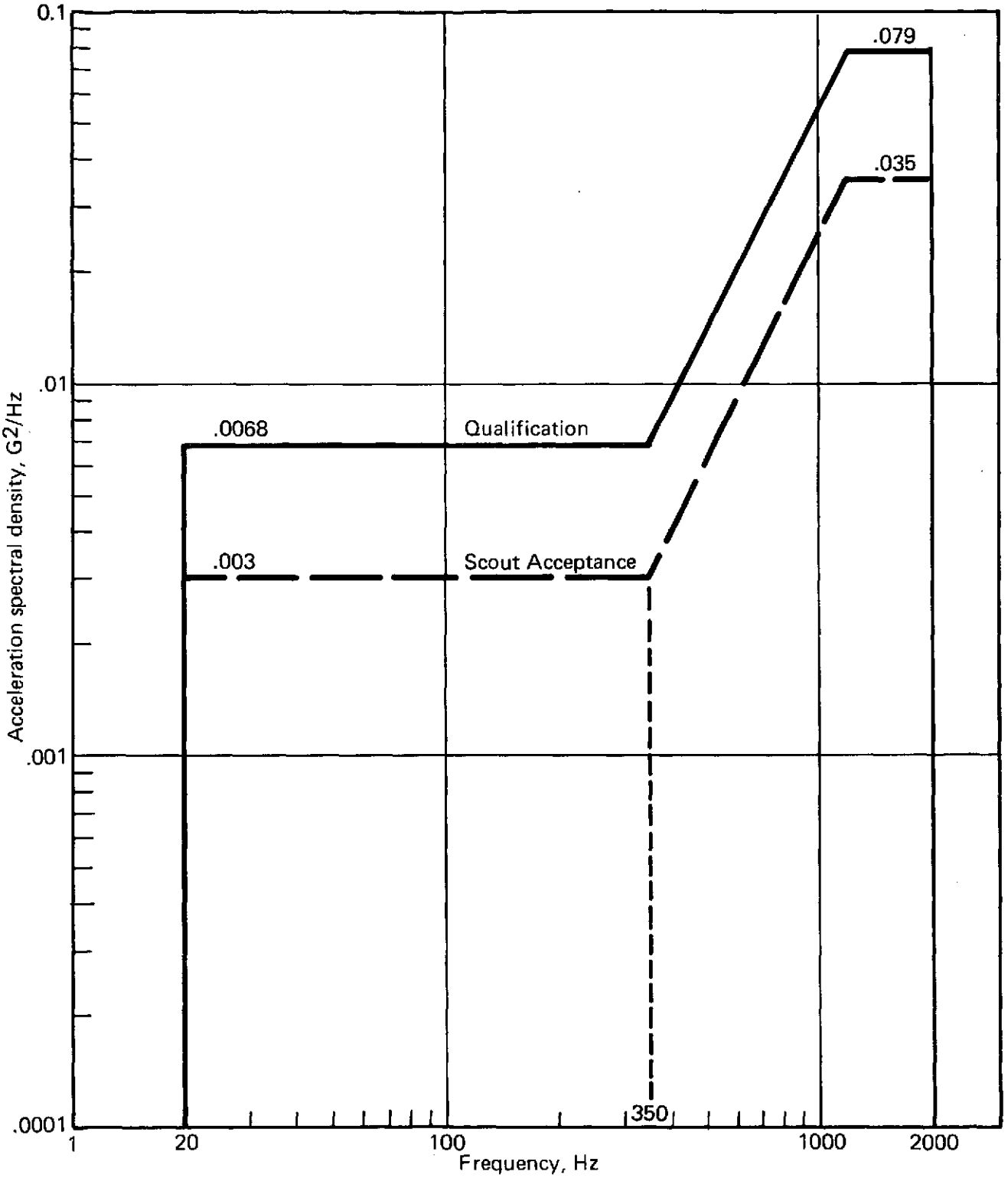


FIGURE 37. – SCOUT VIBRATION SPECTRA FOR D SECTION COMPONENTS

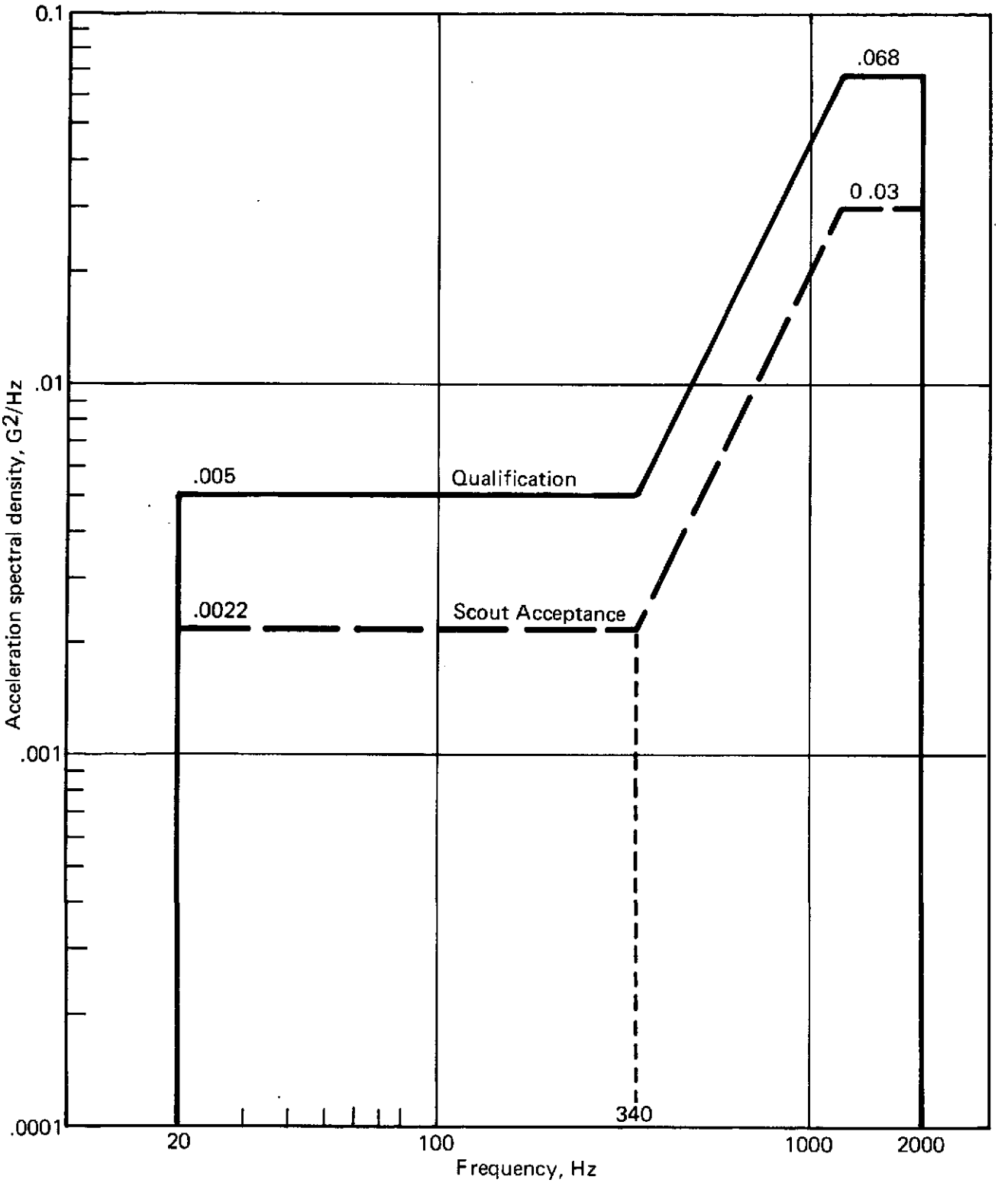


FIGURE 38. – SCOUT VIBRATION SPECTRA FOR FOURTH STAGE COMPONENTS

(2) High Temperature. – the high temperature requirement is for the equipment to be maintained at 176°F (353.15°K) for four hours or until the equipment is stabilized, whichever occurs first.

(3) Temperature Shock. – the equipment shall be exposed to the temperature of 176°F (353.15°K) for a period of one hour or until the temperature of the equipment becomes stabilized, whichever is longer, at the conclusion of which, the equipment shall be operated and evaluated. Within one minute the equipment shall be transferred to a chamber wherein the internal temperature is maintained at zero °F (255.37°K). The equipment shall be subjected to this temperature for one hour or until the temperature of the equipment becomes stabilized, whichever is longer, at the conclusion of which, the equipment shall be operated and evaluated. This constitutes the first temperature shock. Within one minute, the equipment shall be transferred back into the high temperature chamber and shall again be exposed to the high temperature for a period of one hour or until the temperature of the equipment becomes stabilized, whichever is longer, and then operated and evaluated. This step shall be construed as the second temperature shock and the first environmental cycle. Two subsequent environmental cycles shall then be implemented, they being identical to the first environmental cycle. At the completion of three environmental cycles, the equipment shall be removed from the test chamber, returned to ambient temperature, and within a period of one hour shall be operated.

17.2.1.1.4 High Temperature-Altitude – the equipment shall be placed in a test chamber. The internal temperature of the chamber shall be increased and stabilized at 176°F (353.15°K). The internal pressure of the chamber shall be decreased to a simulated 200 000 feet (50 960m) altitude (i.e., 0.148mm of Hg) within five minutes. This simulated altitude shall be maintained for a period of five minutes, at the conclusion of which the equipment shall be operated. The internal pressure shall then be increased to room ambient pressure. This constitutes one complete environmental test cycle. Each equipment shall be subjected to six environmental test cycles, at the conclusion of which, the equipment shall be removed from the chamber and operated.

17.2.1.1.5 Acceleration – the steady state acceleration requirement is 33 G's along each direction of the three major axes for one minute duration per axis.

17.2.1.1.6 EMI – shielding and interference protection and tests accomplished will be in accordance with the applicable requirements of MIL-STD-461.

17.2.1.2 Vehicle Systems Tests:

17.2.1.2.1 Vibration – sinusoidal vibration requirements for the longitudinal (thrust) axis are presented in Figure 39. Lateral axis requirements are presented separately on the same figure. The sweep rate for all axes is two octaves/minute. Random vibration requirements for all axes are presented in Figure 40. The time duration for each axis is two minutes.

17.2.1.2.2 Mechanical Shock – the mechanical shock test requirements apply only to the thrust (longitudinal) axis. The level is 30 G peak for three half-sine pulses of 7 to 13 milliseconds total duration.

17.2.1.2.3 Temperature – the requirements of Section 17.2.1.1.3 apply.

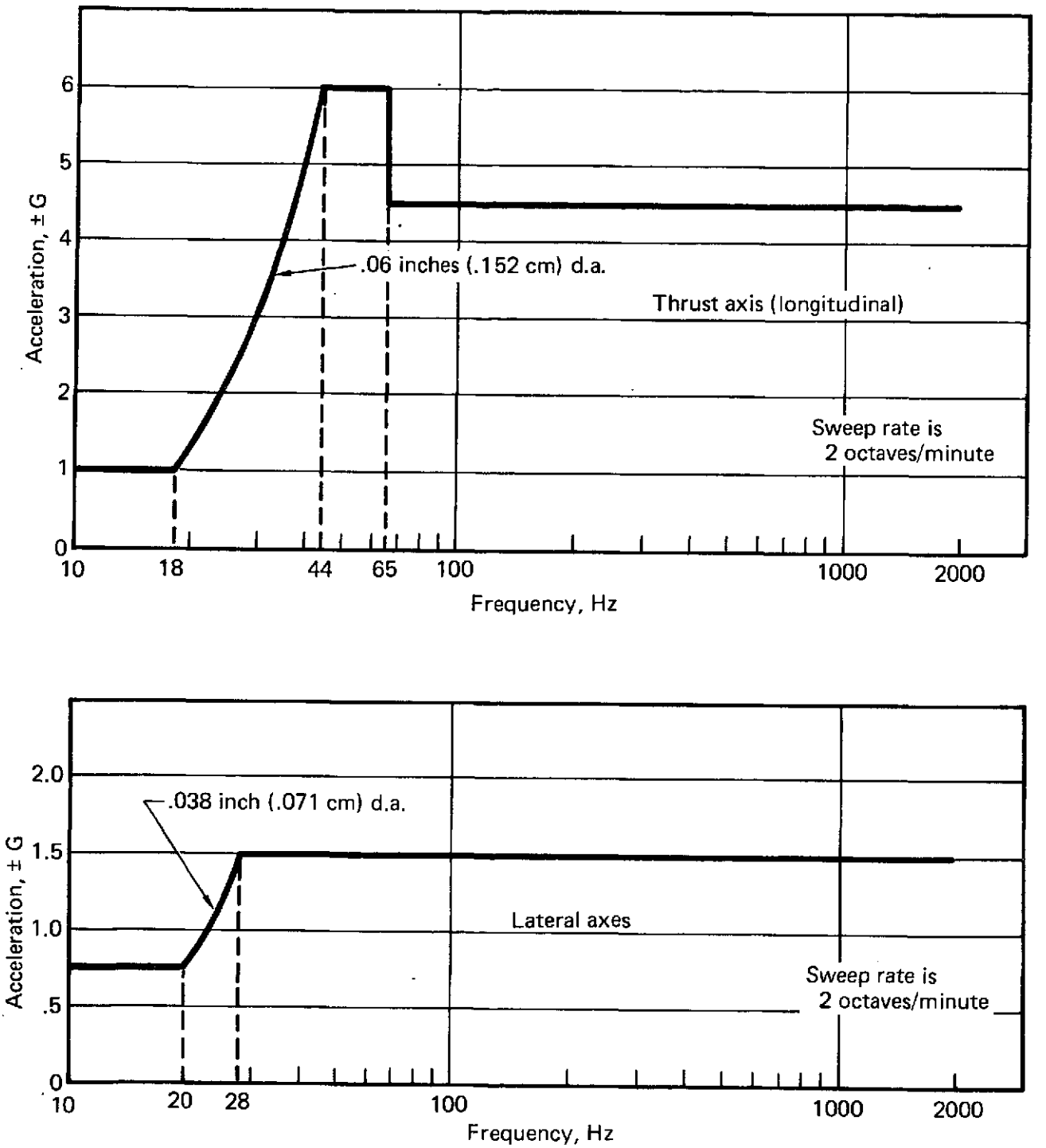


**FIGURE 39. – VEHICLE QUALIFICATION SINUSOIDAL VIBRATION TEST LEVELS**

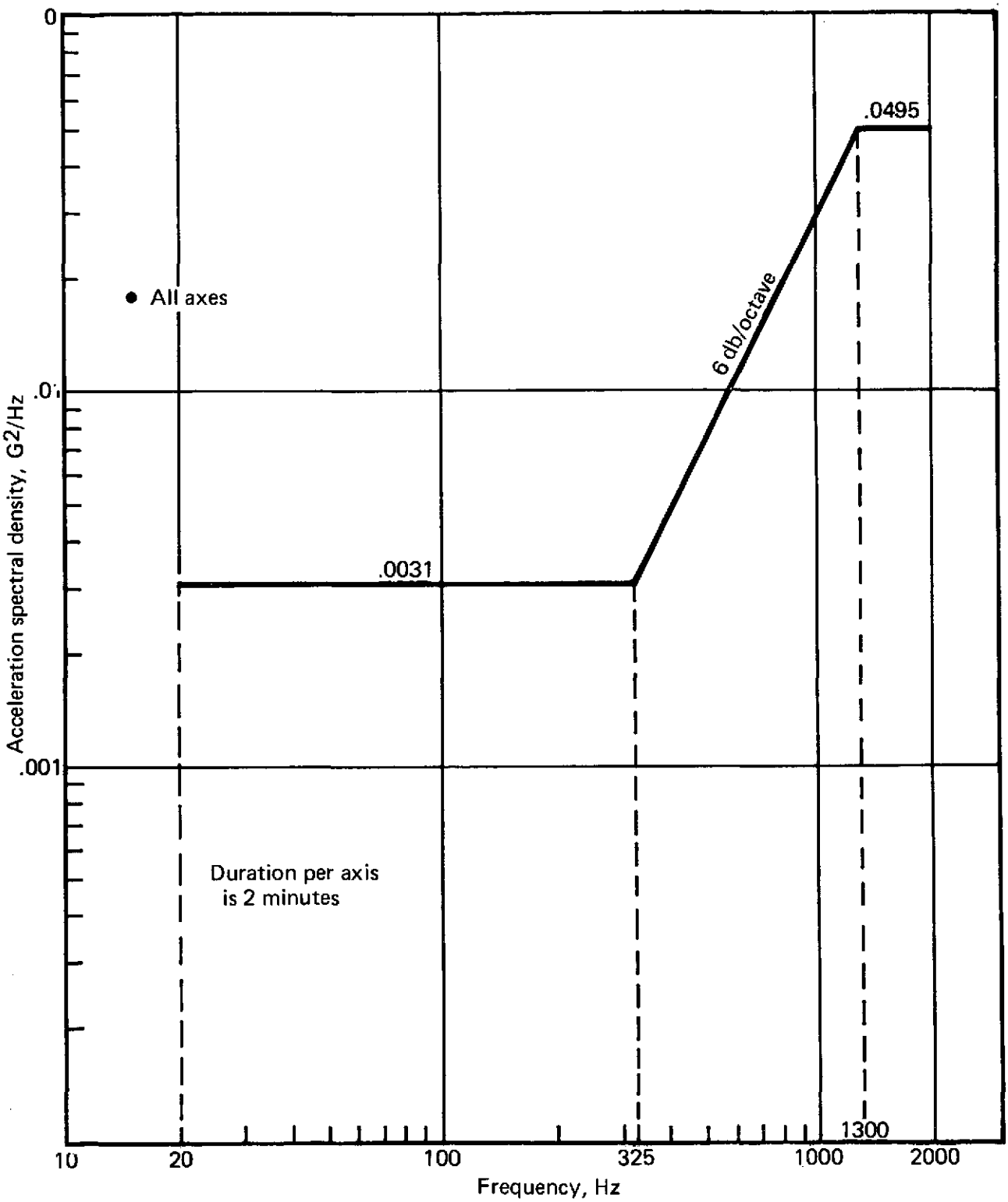


FIGURE 40. – VEHICLE QUALIFICATION RANDOM VIBRATION TEST LEVELS

17.2.1.2.4 Altitude – the requirements of Section 17.2.1.1.4 apply.

17.2.1.2.5 Acceleration – the requirements of Section 17.2.1.1.5 apply.

17.2.1.2.6 EMI – no test required.

17.2.2 Scout Standard Environmental Acceptance Test Level Requirements

17.2.2.1 Component and Subsystem Tests:

17.2.2.1.1 Random Vibration

(1) D Section Components. – the random vibration requirements for each component or subsystem in each of the three major axes are:

| Time Per Axis, Seconds | Frequency, Hz | | Overall Acceleration Grms |
|---|---|---|---|
| | Lower | Upper | |
| 40 | 20 | 2000 | 6.5 |

The test spectra are shown in Figure 37.

(2) Fourth Stage (Payload Transition Section) Components. – the random vibration requirements for each component or subsystem in each of the three major axes are:

| Time Per Axis, Seconds | Frequency, Hz | | Overall Acceleration, Grms |
|---|---|---|---|
| | Lower | Upper | |
| 40 | 20 | 2000 | 6.1 |

The test spectra are shown in Figure 38.

7.2.2.1.2 Mechanical Shock

(1) D Section Components. – the mechanical shock level requirement is for one shock of 40 G's for 6 milliseconds duration terminal sawtooth in each direction of each axis for a total of 6 shocks.

(2) Fourth Stage (Payload Transition Section) Components. – the mechanical shock level requirement is for one shock of 50 G's for 6 milliseconds duration terminal sawtooth in each direction of each axis for a total of 6 shocks.

17.2.2.1.3 Temperature

(1) Low Temperature. – the low temperature requirement is for the equipment to be maintained at zero $^{O}$F (253.37 $^{O}$K) for one hour. The equipment shall be operated for the last five minutes or longer if required to complete a cycle of operation.

(2) High Temperature. – the high temperature requirement is for the equipment to be maintained at 176°F (353.15°K) for one hour. The equipment shall be operated for the last five minutes or longer if required to complete a cycle of operation.

(3) Temperature Shock. – the equipment shall be exposed to the temperature of 176°F (353.15°K) for a period of one-half hour or until the temperature of the equipment becomes stabilized, whichever is longer, at the conclusion of which, the equipment shall be operated and evaluated. Within one minute the equipment shall be transferred to a chamber wherein the internal temperature is maintained at zero °F (253.37°K). The equipment shall be subjected to this temperature for one-half hour or until the temperature of the equipment becomes stabilized, whichever is longer, at the conclusion of which, the equipment shall be operated and evaluated. This constitutes the first temperature shock. Within one minute, the equipment shall be transferred back into the high temperature chamber and shall again be exposed to the high temperature for a period of one-half hour or until the temperature of the equipment becomes stabilized, whichever is longer, and then operated and evaluated. This step shall be construed as the second temperature shock. One more subsequent shock is required. At the completion of the three temperature shocks, the equipment shall be removed from the test chamber, returned to ambient temperature, and within a period of one hour shall be operated.

17.2.2.1.4 High Temperature – Altitude – the equipment shall be placed in a test chamber. The internal temperature of the chamber shall be increased and stabilized at 176°F (353.15°K). The internal pressure of the chamber shall be decreased to a simulated 200 000 feet (60 960 m) altitude (i.e., 0.148 mm of Hg) within five minutes. This simulated altitude shall be maintained for a period of five minutes, at the conclusion of which the equipment shall be operated. The internal pressure shall then be increased to room ambient pressure. This constitutes one complete environmental test cycle. Each equipment shall be subjected to three environmental test cycles, at the conclusion of which, the equipment shall be removed from the chamber and operated.

17.2.2.1.5 Acceleration – the steady state acceleration requirement is 22 G's along each direction of each axis for a minimum duration of one minute per direction per axis.

17.2.2.1.6 EMI – no test required on production units.

17.2.2.2 Vehicle Systems Tests:

17.2.2.2.1 Vibration – sinusoidal vibration requirements are presented in Figure 41. The sweep rate for all axes is four octaves/minute. Random vibration requirements for all axes are presented in Figure 42. The duration for each axis is one minute.

17.2.2.2.2 Mechanical Shock – not required at vehicle level.

17.2.2.2.3 Temperature – the requirements of Section 17.2.2.1.3 apply.

17.2.2.2.4 Altitude – the requirements of Section 17.2.2.1.4 apply.

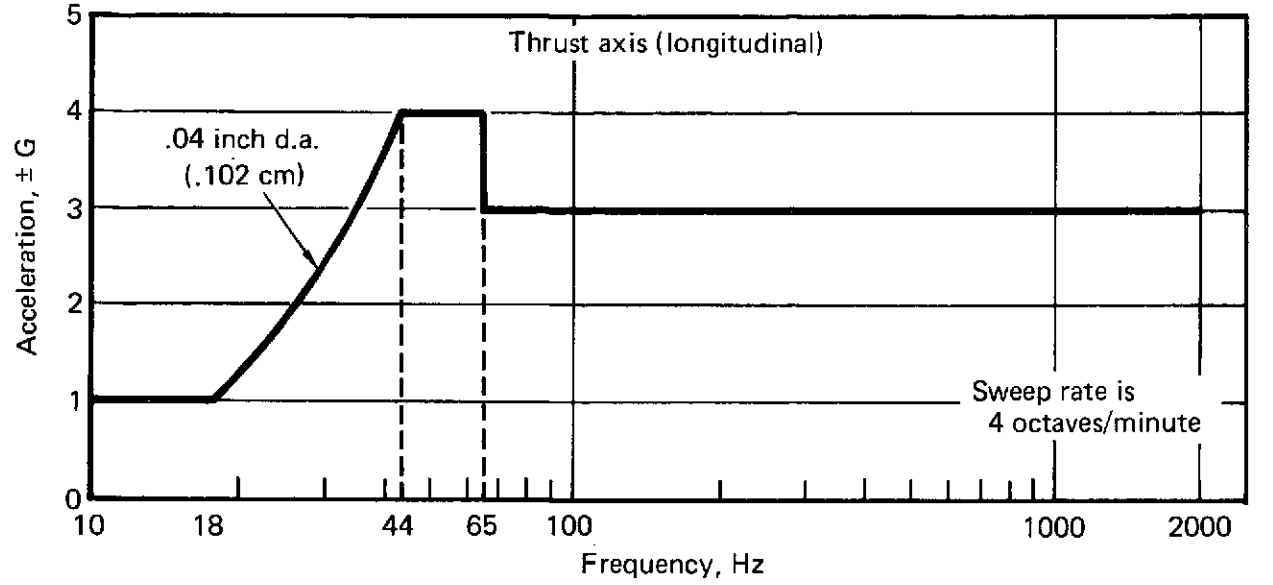


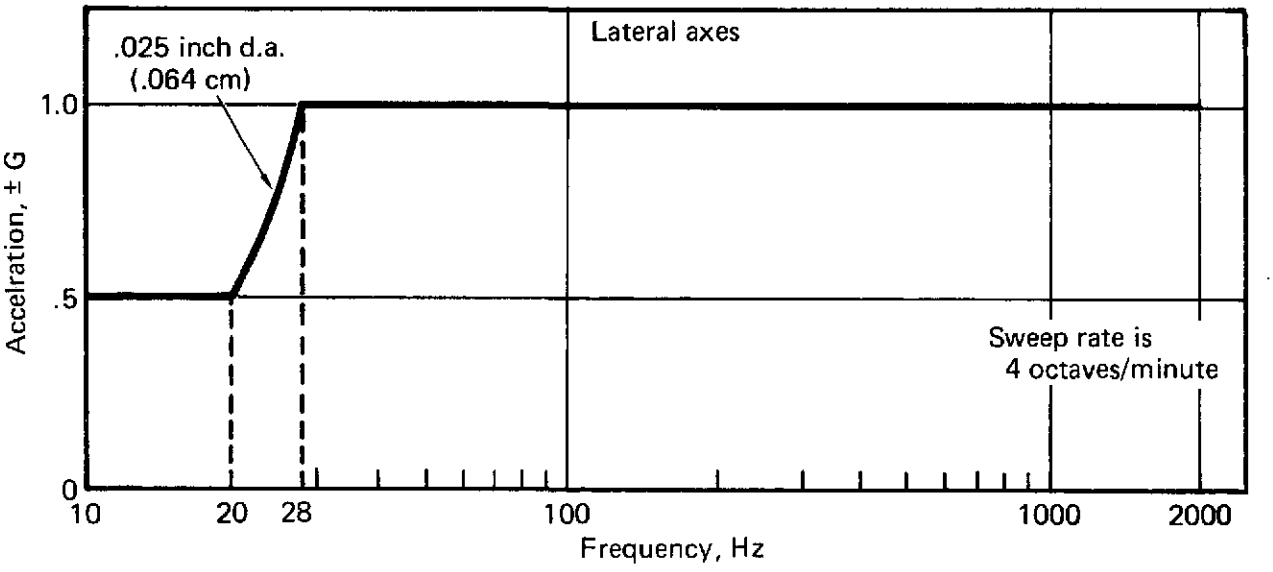


**FIGURE 41. – VEHICLE SYSTEMS ACCEPTANCE SINUSOIDAL VIBRATION TEST LEVELS**

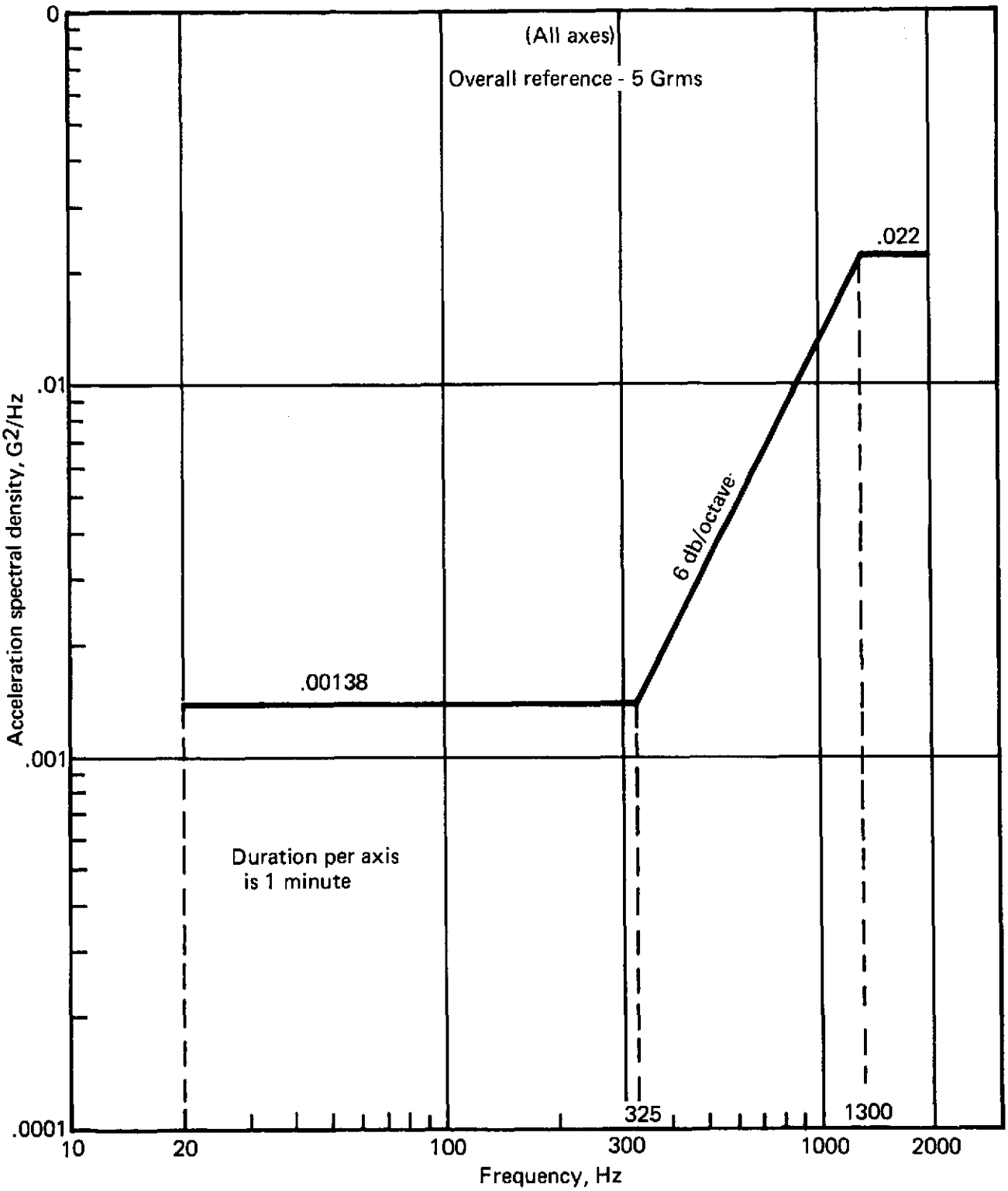


**FIGURE 42. – VEHICLE SYSTEMS ACCEPTANCE RANDOM VIBRATION TEST LEVELS**

17.2.2.2.5 Acceleration – the requirements of Section 17.2.2.1.5 apply.

17.2.2.2.6 EMI – no test required.

## 17.3 Qualification Testing Required

17.3.1 Component and Subsystems. – qualification tests will be performed on components and subsystems fully representative of flight hardware. The qualification test program shall consist of the test described in Section 17.2.1.1: random vibration; mechanical shock; temperature – low, high and shock; high temperature – altitude; acceleration; and EMI. These tests will be conducted by the supplier to demonstrate adequacy of design, unless qualification by similarity and/or usage can be justified. Two justifications exist for the waiving of an environmental qualification test.

17.3.1.1 Qualification by Usage: where the component or subsystem has been effectively qualified by previous operational experience, although not subjected to formal qualification testing, at environmental levels equal to or more than those predicted for the operational mission, the component or subsystem may be qualified for usage. When qualification by prior usage is warranted, justification data of the following type will be required for approval:

(a) Part number and description

(b) Name of program and application of the component or subsystem in that program

(c) Actual operational environment levels and how determined

(d) Number of successful usages and/or other appropriate operational reliability data

(e) Detailed description of any failure and correction action taken

(f) Detailed statement of the difference between the part tested and proposed part to be used and the difference between the part's previous application and the requirements of this program. Also, to be supplied is the supplier's substantiation of why each difference, addition, substitution, or deletion would not make the equipment more susceptible to environmental exposure.

17.3.1.2 Qualification by Similarity: where tests have already been conducted on identical or similar parts and where the test results prove conformance to the program requirements, these parts may be qualified by similarity. When qualification by similarity is warranted, justification data of the following type will be required for approval.

(a) Part number and description of part actually tested

(b) Copy of the test procedure

(c) Copy of the test report

(d) Name of the testing agency

(e) Name of program and application of the part in that program

(f) Detailed statement of the difference between the part tested and proposed part to be used and the difference between the part's previous application and the requirements of this program. Also, to be supplied is the supplier's substantiation of why each difference, addition, substitution, or deletion would not make equipment more susceptible to environmental exposure.

17.3.2 Vehicle Systems Tests. – a non-flight fourth stage vehicle section with the components and/or subassemblies previously subjected to the subsystem tests outlined will be subjected to qualification test by VSD. The qualification test program shall consist of vibration (sinusoidal and random) and mechanical shock as described in Section 17.2.1.2. (No EMI tests are included, however RFI vehicle compatability tests will be accomplished as a part of the demonstration of vehicle integration and processing. EMI will already have been completed at the component level.)

### 17.4 Scout Standard Environmental Accpetance Testing Required

17.4.1 Component and/or Subsystem Tests. – the supplier will subject all components and/or subsystems to Scout Standard Environmental Acceptance Tests prior to delivery to VSD. The acceptance test program shall consist of the following tests as discussed in Section 17.2.2.1: random vibration, mechanical shock, temperature shock, high temperature – altitude and acceleration.

17.4.2 Vehicle Systems Tests. – the first flight section fabricated with flight components installed shall be subjected to acceptance tests; these tests will not be accomplished subsequent to the first flight article. The acceptance test program shall consist of the following tests as described in Section 17.2.2.2: vibration (sinusoidal and random), temperature shock and high temperature – altitude. (RFI vehicle compatability tests will be accomplished as a part of normal vehicle processing.)

## 18.0 AVC SYSTEM TEST CONCEPT AND GSE REQUIREMENTS

A checkout concept that can be implemented for the AVC system was generated. Additionally the overall ground support equipment requirement was defined.

The IMU and CEU may be configured as two separate units (black boxes). However, depending upon the particular vendors selected, the functions allocated to each unit will no doubt vary. For the purposes of testing concepts, it is assumed that the outputs of the IMU will basically be incremental velocity pulses from the accelerometers and either gimbal angles or incremental angular displacements depending upon the type IMU chosen. The integration and all associated computations will be accomplished in the CEU. Since these two units may be procured to separate specifications, they must be tested separately and processed separately through acceptance testing at VSD-T.

### 18.1 Test Concept–Integration and Demonstration

Several non-recurring tests will be conducted during the AVC subsystem development, vehicle modification and integration and demonstration phases of the fourth stage AVC system. The basic test outline and a typical sequence of the component and vehicle testing associated with this development phase are shown in Figure 43. Some of these activities may be pursued simultaneously, thus Figure 43 does not present a time line as such.

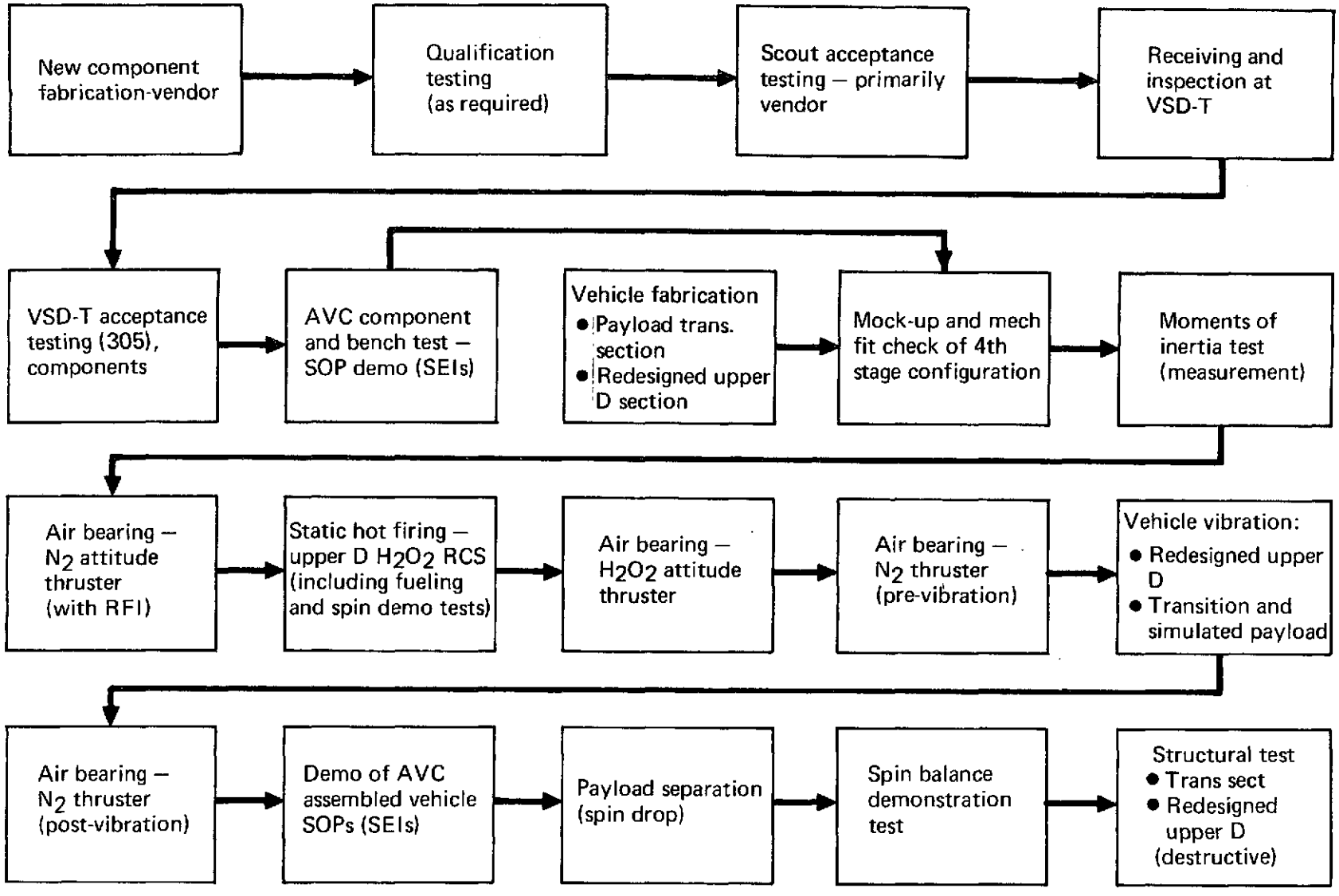


**FIGURE 43. – FOURTH STAGE AVC VEHICLE FABRICATION AND TEST SEQUENCE (INTEGRATION AND DEMONSTRATION)**

(1) Component Development and Fabrication. – the new components required to implement the AVC system will be vendor procured. The single unit requiring the greatest degree of development will be the Control Electronics Unit. Desirably the IMU and the upper D RCS components will be production units. Some development testing of the variable thrust attitude control motor will be required as well as testing to verify performance of the modified $H_2O_2$ $\Delta V$ thrusters.

(2) Component Qualification. – all component qualification testing will be accomplished at the vendor facility unless the capabilities are not available. Hopefully, most components will have been qualified to the Scout environmental levels and thus can be qualified through similarity.

(3) Scout Standard Environmental Acceptance Test. – environmental acceptance testing will be performed by the vendor on the AVC components; both pre- and post- performance tests will be conducted.

(4) Acceptance Testing. – component receiving and inspection and acceptance testing will be conducted on all AVC components.

(5) AVC Component and Bench Test. – the transition section components (primarily IMU and CEU) will be bench tested during which the Standard Procedures (SOP's) for these tests will be demonstrated. Basically, these will be new SOP's for the IMU and CEU since the components are new.

(6) Vehicle Mock-Up. – after new payload transition and upper D sections have been fabricated, a mock-up of the AVC fourth stage configuration will be made. A mechanical fit check of all components will be made. Wire routing, wire lengths, plumbing and similar functions will be established.

(7) Determination of Moments of Inertia. – pendulum type tests will be conducted on the two sections separately to determine the magnitude of the roll, pitch, and yaw moments of inertia.

(8) Air Bearing Test. – the planned approach is to conduct an initial air bearing test using an $N_2$ attitude control jet. Upper D will be replaced with a simulation section housing the $N_2$ system. This test will be for the purpose of verifying system performance prior to static hot firing. After static hot firing, air bearing test using an $H_2O_2$ motor valve will be conducted in the $H_2O_2$ test facility. This series of tests will be performed one time only to determine the correlation between the $N_2$ (for test system) and the $H_2O_2$ flight system. Flight hardware will be used to the maximum extent possible. Simulation of spin momentum/control moment relationships at both fourth stage ignition and 4th stage burnout as defined by spin rates, vehicle inertias and other pertinent parameters will be accounted for in the test. Demonstration of the AVC operation through the entire flight regime will be the intent of the test. A repeat of the test will then be made with the $N_2$ attitude thruster. The correlation of the tests will be established with the intent of using the $N_2$ test for all subsequent testing. This $N_2$ test will be utilized as a pre-environmental system test and will be repeated after environmental testing.

Each production IMU and CEU will be subjected to air bearing tests with the $N_2$ attitude system. The $N_2$ test configuration will be a standard (fixed) arrangement for all tests; it will possess the capability of quickly changing the pertinent control parameters such as moment of inertia ratio. The $N_2$ air bearing simulation will be used for functional verification and as part of the IMU and CEU acceptance testing. The developed 4th stage PCM T/M system will be used to monitor system performance.

(9) Static Hot Firing, Upper D RCS. – upper D section $H_2O_2$ RCS will be hot fired to assure proper operation of the components. These tests will include the demonstration of fueling the $H_2O_2$ and $N_2$ system with the vehicle section in the horizontal position and raising the section to the vertical position. A test will be conducted to demonstrate the operation of the $\Delta V$ thrusters in a spinning environment.

(10) Vehicle Vibration Test. – the fourth stage AVC configuration will be qualified (vibrated) in two sections. The two sections will be the upper D by itself and the transition section with a simulated payload. Each section will have all components installed and operating. Vibration input levels will be controlled to produce the environments specified on the various equipments. After the vehicle level vibration is complete, each component will again be subjected to the same performance test as those accomplished prior to vibration.

(11) Assembled Vehicle SOP Demonstration. – the Standard Procedures as modified to incorporate the testing of the AVC system components at the assembled vehicle level will be performed. These tests are required to verify the test procedures prior to the actual revision of the SOP's.

(12) Spin Balance Demonstration Test. – a test will be conducted at a dynamic balance facility to demonstrate the capability of dynamically balancing the AVC fourth stage with a dummy payload. Testing will be accomplished to determine correlation of spin balancing with empty tankage, tankage containing water in place of $H_2O_2$ ($N_2$ system pressurized) and with actual $H_2O_2$ on board ($N_2$ system pressurized).

(13) Static Tests. – payload separation system tests and then the destructive structural testing of the two sections will be accomplished. The separation tests (a total of three) will be made in the spinning environment.

## 18.2 Test Concept – Production Hardware

18.2.1 VSD-T Testing. – the test flow (typical) for the production AVC system hardware is shown in Figure 44. The VSD-T acceptance and component tests will at least partially parallel the acceptance tests accomplished at the vendor excluding the environmental portions. The AVC system bench tests will be accomplished by a new Standard Procedure. The air bearing tests (as presently conceived) will be used to exercise the IMU and CEU. Simulation sections will be used in a standard air bearing configuration with an $N_2$ attitude control thruster. Upon completion of the air bearing test, the system will be tested in an assembled vehicle configuration, an RFI test conducted and the system operated during simulated flight per standard procedures. After RFI and simulated flight test, the RCS will be subjected to a static hot firing test at the $H_2O_2$ test facility.

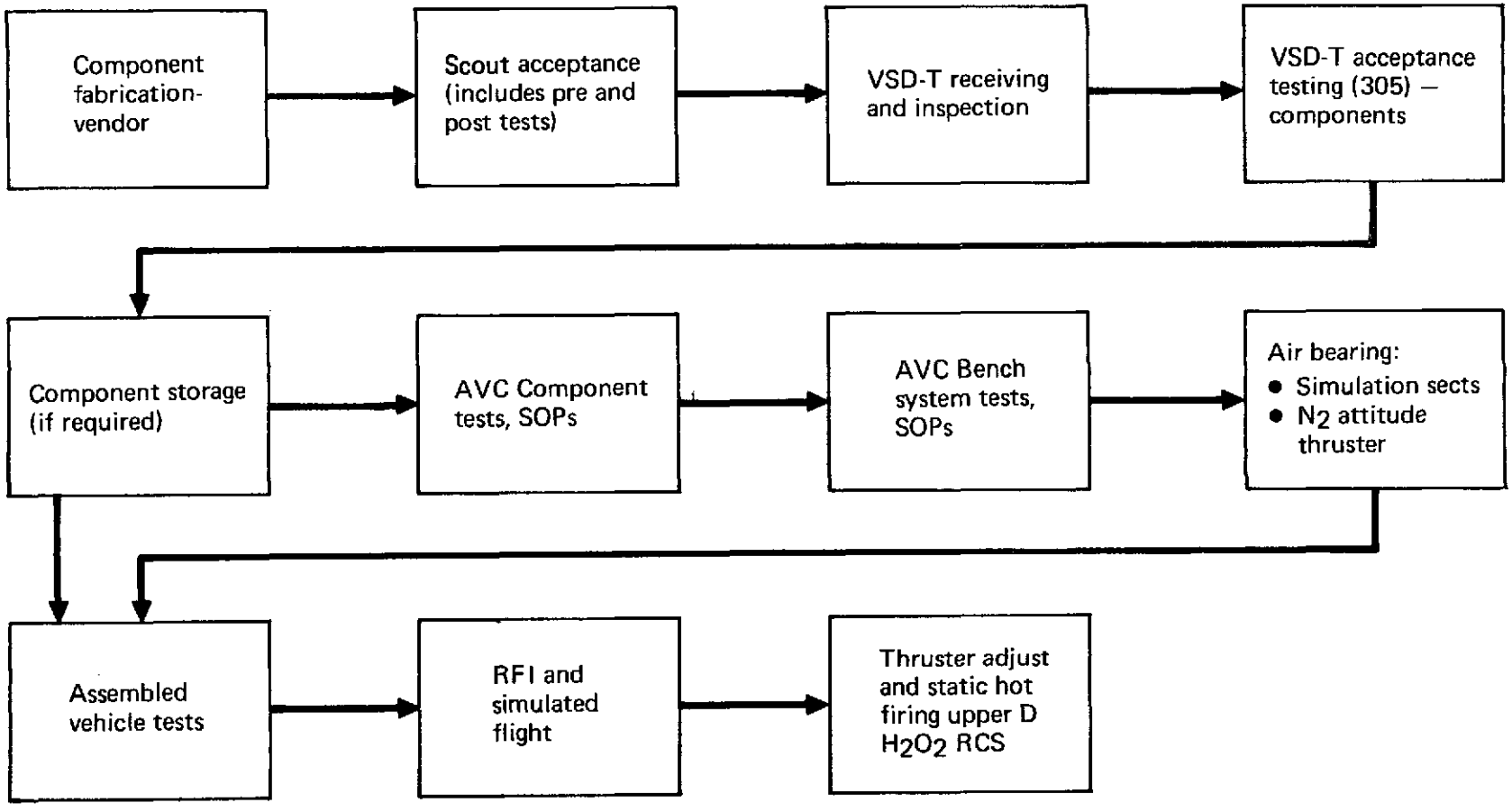


**FIGURE 44. — FOURTH STAGE AVC SYSTEM TEST CONCEPT AND FLOW (PRODUCTION HARDWARE)**

The major functions to be checked or verified during these various tests are summarized in Table 52.

18.2.2 Field Testing. — AVC system field testing will consist of:

- Component and calibration
- Assembled vehicle
- AVC RCS Surveillance leak check
- AVC Checks on launcher

The All Systems Test, Electronic Functional, Dress Rehearsal and Countdown will be changed to add the additional AVC parameters or functions to be checked during these procedures. One significant variation from the nominal Scout checks involves the fourth stage $H_2O_2$ RCS thrusters, which are located under the heatshield. These particular thrusters cannot be warmed by firing during the countdown. Instead they will be fired during third stage coast or heaters employed to heat the catalyst beds. Another change involves the alignment of the IMU. The specific alignment technique employed will depend upon the IMU alignment method and may require the use of a ground based computer to perform the real time computations needed to support the IMU. Air bearing tests are not shown as a normal part of field processing, however the capability will exist and the test may be added later.

## 18.3 GSE Requirements

18.3.1 Standard Scout System Test ($S^3T$) Equipment. — test equipment necessary to accomplish the testing for the Integration and Demonstration phase of AVC will be essentially the same as that required for production testing. The GSE for these tests is noted on Table 52 and described in Table 53. The exact configuration for component, bench and system testing will depend upon the type IMU and CEU selected. Most IMU vendors utilize a standard test console for all hardware produced. This test console will consist of control panels, bench test panel, power supplies and possibly a digital control processing unit. A two-bay full-standing standard sized relay rack configuration should adequately contain this hardware. In addition, a teletype console will be required. This equipment should be portable in nature and be utilized for both the 305 type testing, bench and component testing as well as the air bearing testing of Figures 43 and 44. It is possible that some of this GSE may be supplied by the IMU/CEU vendor with VSD supplying the required interface and GSE integration as well as bench, component, and system interconnection cabling.

Since the AVC system is to be an add-on concept for an otherwise standard Scout vehicle, maximum use should be made of adapter cables as opposed to modifications to existing GSE. The eventual procurement of identical $S^3T$ test equipment for both Dallas and each field site is recommended.

## TABLE 52. – AVC TEST FUNCTIONS AND EQUIPMENT

Dallas & Field

| Test | Test Description | GSE Items Required (See Table 53) |
|---|---|---|
| I. Dallas component acceptance (305) and calibration tests | Power & temperature tests | (1), (2), (3), (6), (7), (9), (14), (16) |
| A. IMU Tests | Mode function test | |
| | Spin rate capability verification | |
| | Gyro & accelerometer performance parameter measurements | |
| | Gyro & accelerometer calibration (biases, drift rates, scale factors) | |
| B. CEU | 4th Stage burn attitude presets and adjustments | (1), (2), (3), (8), (9), (14) |
| | Velocity presets & correction | |
| | Velocity correction maneuver | |
| C. RCS | Electrical & leak checks<br>• Pull in/drop out voltage<br>• Operating current<br>• Response time | None |
| II. Dallas transition checks | Section leak checks | (24) |
| | Section motor alignment | (28), (29) |
| | Section hot firing | (24), (25), (26), (27), (29) |
| III. Dallas system bench test (IMU & CEU) | Gains | (1), (2), (3), (9), (10), (11), (12), (14), (16) |
| | Deadbands | |
| | Scale factors | |
| | Velocity computation | |
| | Verification of derived vehicle rates | |
| | IMU alignment | |

TABLE 52. – AVC TEST FUNCTIONS AND EQUIPMENT (Continued)

**Dallas & Field**

| Test | Test Description | GSE Items Required (See Table 53) |
|---|---|---|
| IV. Dallas – air bearing test | Programmed air bearing maneuver<br>4th Stage burn attitude corrections<br>Attitude maneuver for velocity correction | (1), (2), (3), (9), (10), (12), (14), (15), (16) |
| V. Dallas & field – AVC assembled vehicle tests | Program events, timing and sequencing<br>Deadband verification (IMU on dividing head)<br>Velocity correction maneuver verification (IMU on dividing head) | (1), (2), (3), (9), (12), (13), (14), (16) |
| VI. Dallas and field – RFI & simulated flight/all systems test | Verification of program events timing & sequencing<br>RFI/EMI check | (12), (2), (3), (9), (12), (13), (14), (16) |
| VII. Field – electronic functional | Alignment verification<br>Program events and timing<br>Power switching/vehicle systems compatibility – RFI | (17), (18), (19), (20), (21), (22), (23) |
| VIII. Field – dress rehearsal and countdown | Alignment verification<br>Program events and timing<br>Power switching/vehicle systems compatibility – RFI<br>RCS functional check (H/S off) | (17), (18), (19), (20), (21), (22), (23) |

## TABLE 53. – AVC GSE REQUIRED

$S^3T$ GSE

Bay no. 1

(1) Digital computer, 4K word memory CPU (minicomputer)
(2) Computer power supply
(3) Tape punch/reader
(4) Digital voltmeter*
(5) Digital timer/counter*
(6) Drift test panel
(7) IMU test point panel
(8) CEU test point panel

Bay no. 2

(9) Power supplies (28 Vdc & 115 Vac 400 Hz 1$\phi$)
(10) Bench/system test panel
(11) System/bench test load simulator
(12) System power switching
(13) Assembled vehicle test panel

Other

(14) Minicomputer teletype/printer
(15) Air bearing support hardware
(16) IMU Cooling air supply

*For use in all tests.

Note: Items (6), (7), and (8) configuration may vary depending upon AVC configuration selected.

TABLE 53. – AVC GSE REQUIRED (Continued)

SLC GSE

(17) Digital computer (same type as item (1))
(18) Same type as (2)
(19) Same type as (3)
(20) Same type as (14)
(21) AVC Blockhouse test/operating panel
(22) AVC RCS Test/operating panel
(23) AVC Monitor hardware (internal power timer, RCS $H_2O_2$ pressure recorder, $N_2$ pressure recorder)

Note: Cooling is provided as a part of normal vehicle support when the vehicle is on the launcher.

Other GSE required – Dallas

(24) Section RCS leak test apparatus
(25) Hot firing test stand
(26) Electrical cabling for hot firing
(27) Plumbing for hot firing
(28) Motor alignment tooling
(29) Section handling dolly

18.3.2 Standard Launch Complex (SLC) Test Hardware. – the blockhouse equipment necessary to monitor and check the AVC will consist of a test panel of about the same complexity as the existing third stage guidance console. Included as a part of this test hardware may be a digital processor to accomplish the IMU alignment on the launcher and other AVC test functions. Parameters to be monitored shall include the following as a minimum:

- Attitude outputs (gimbal angles or attitude pulses)
- Accelerometer outputs
- AVC voltages
- AVC power status
- IMU Ready/fault indications
- AVC-RCS thruster heater on-off

AVC control functions available to the console operator should include the following:

- AVC Power control/transfer
- AVC Mode control (align/operate)
- AVC-RCS Nozzle fire command
- AVC-RCS Regulator – pressurize/vent command
- AVC-$H_2O_2$ Dump capability (emergency only)
- AVC RCS Thruster heater (catalyst bed – if required)

In addition, the AVC monitor (supervisory) console in the blockhouse should have the following monitor functions:

- AVC Unregulated pressure
- AVC $H_2O_2$ Pressure
- AVC Internal power clock timer

Modifications to the launcher to service the fourth stage $N_2$ and $H_2O_2$ systems are as follows:

- Launcher $H_2O_2$ and $N_2$ plumbing to make these fluids available for servicing the fourth stage.
- Adaptation of the Vinson unit to include the AVC system.

18.3.3 Other GSE. – to implement the testing of Figures 43 and 44 which is not performed on the $S^3T$ or SLC, the following is required:

- Wiring changes in the form of adapter cabling to accomodate the fourth stage AVC at the $H_2O_2$ facility for hot firing..

- Necessary additional timing circuitry required to test the AVC attitude thruster in the short thrust environment required by the spinning vehicle control law.

- Interconnect cabling to operate both the AVC and support systems (such as telemetry) on the air bearing. It is assumed that the same test panel used for $S^3T$ will be utilized to support AVC in air bearing testing.

- Cooling air will be required by the IMU and CEU when the vehicle is on the launcher. However no mods to the launcher cooling system will be needed other than access hosing.

18.3.4 Other Subsystems. – the GSE changes required for the PCM T/M and Capacitive Discharge Ignition Systems will be accomplished under a separate effort and are not addressed in this report.

Other GSE items or changes needed for checkout of a fourth stage AVC system include:

- RCS thruster alignment tools (Dallas only)

- Thrust stand for upper D $H_2O_2$ hot firing

- Electrical cabling for upper D $H_2O_2$ hot firing

- Support and handling equipment for the new transition section

- Vehicle simulator

- AVC battery simulator

- Cable and switch modifications to the battery console.

## 19.0 CONCLUSIONS AND RECOMMENDATIONS

This study has established the feasibility of incorporating an AVC system in the Scout fourth stage to achieve significant improvements in payload orbital accuracies. The initial study phase determined that attitude control of the fourth stage and a velocity correction subsequent to fourth stage burnout based upon a measurement of the integral of $N_X$ resulted in insufficient reduction of apogee–perigee deviations. In order to achieve the desired improvements in payload delivery accuracy, fourth stage corrections need to be determined from measured inertial velocity data.

New correction concepts, utilizing inertial velocity and attitude as determined by the IMU and CEU, were identified and evaluated. Two of these concepts (Options 1 and 3) resulted in radical reductions in apogee-perigee deviations. Both options employ fourth stage attitude adjustments as determined from inertial velocity variation through the first three stages and a final velocity correction based upon the measured in-plane component errors at injection. The two options differ only in the control of fourth stage ignition. Either can be implemented by the addition of an RCS in upper D and the guidance equipment in a payload transition section.

Using an RCS sized to correct a mean plus two sigma magnitude of velocity error together with the reference IMU and CEU in the Scout F–1 vehicle configuration results in a net payload weight penalty of 105.08 pounds (47.66 kg); which is highly undesirable. Additional system studies identified means by which this payload weight penalty can be significantly reduced. First, the $\Delta V$ correction capability can be reduced to the mean value of the in-plane injection velocity error with a very small degradation in orbital accuracy. The apogee-perigee deviations corresponding to the reduced $\Delta V$ capability are well below expected payload requirements. A second means of reducing AVC system weight is to use an alternate inertial navigator which combines the IMU and CEU in a single package.

Employing an RCS, sized to provide a $\Delta V$ correction capability essentially equivalent to the mean inertial velocity error, together with the inertial navigator reduces the net payload weight penalty to about 73.23 pounds (33.22 kg). A payload weight penalty of this magnitude is much less severe. The payload delivery accuracy achievable with such a system offers a highly attractive alternative to payload users desiring improved orbital accuracy.

Based on the results of this study effort, VSD recommends that the design and development of the AVC system be pursued. AVC development should be accompanied, in a timely manner, by a continuation of the current efforts to achieve a substantial improvement in Scout payload performance. The ideal relationship would be such that the current Scout payload carrying capability is maintained when the AVC system is added. Development of the guidance system (IMU and CEU) should be initiated. Once a system is selected, the design of the payload transition section can be started. Weight will be a highly emphasized criteria in the selection of a guidance system. Design studies directed toward the investigation of possible weight reduction methods in the selection and design of subsystems and the vehicle transition sections should be initiated. Areas to be considered and evaluated in the weight reduction include:

- Use of hydrazine in the RCS rather than $H_2O_2$
- Design trades of the RCS components – especially the attitude control motor
- Material trades of the basic structure and component mounting substructure in the payload transition section, consider lighter weight cores in sandwich construction and the usage of graphite/boron composites.
- Possibility of combining the guidance and T/M batteries
- Review of the design requirements of the separation system

Several system trades and studies should be accomplished prior to design phase; these include:

- Restriction of the magnitude of the $\Delta V$ pitch maneuver – trajectory shaping or biasing to always require the addition of velocity in the nominal injection velocity direction will limit the pitch maneuver magnitude. Related trades which need to be considered involve the pitch maneuver magnitude, increase in the correction $\Delta V$ required, changes in achievable accuracy and the resulting increase in RCS weight.
- Accuracy improvements achievable for other missions – payload delivery accuracies attainable with an AVC system for non-circular orbital, re-entry and probe missions should be established.

## REFERENCES


1. Battelle Columbus Laboratories Report BCL—VSPRE—IM—73-5

   Analysis of a Number of Potential Scout Missions, F. G. Rea and J. D. Allen, 5 June 1973

2. LTV Astronautic Division Report 23.1

   Description and Error Analysis of Scout Guidance, J. R. Powell, 12 March 1962, Revised 18 October 1966

3. Vought Systems Division Report 23.569

   Final Report — Fourth Stage Attitude Correction System (ACS), P. B. Patterson, 18 December 1973

4. Vought Systems Division Report 23.256

   Scout Upper Stage Fuel Consumption Analysis, R. N. Knauber, M. N. Glazier, 11 January 1966, Revised 26 October 1971

5. Vought Systems Division Report 23.480

   Scout Stability and Control Report, C. C. Browning and R. N. Knauber, 31 March 1971, Revised 26 February 1974

6. Vought Systems Division Report 23.434 — Revision B

   Scout Preflight Planning and Launch Constraints, R. N. Knauber, 31 July 1972

7. Vought Systems Division Report 00.766

   Scout Flight Vibration and Shock Environment, R. B. Bost, 2 March 1966, Revised 30 October 1973

8. NASA Langley Research Center Report NASA CR—112054

   Final Report Advanced Small Launch Vehicle (ASLV) Study, G. E. Reins and J. F. Alvis, 8 March 1972

9. Vought Systems Division Report 3—34100/9R—12

   Scout Flight Data Historical Summary Volume I, H. D. Teague and C. E. Black, 17 March 1969, Revised 18 July 1973

# APPENDIX A

## GUIDANCE ACCURACY ANALYSIS ROUTINE

### I. Routine Construction

The Guidance Accuracy Analysis Routine (GAAR) was written to compute errors in vehicle attitude, position and velocity as a function of the hardware error budget of a specific guidance system and a particular launch vehicle trajectory. The parameters needed to evaluate a system are the magnitude of the error sources associated with the platform including the gyros and accelerometers plus the boost attitude and acceleration profile. The computer program is constructed to evaluate both gimballed and strapdown type inertial platforms. No trajectory computation capability is included, instead the trajectory inputs needed are taken from vehicle trajectories generated by the Near-Earth Mission Analysis Routine (NEMAR) or similar computer programs.

The basic equations used to evaluate the error contributions are those expressed in Reference (A1).

$$\ddot{\overline{R}} = \overline{A}_t + \overline{G} \qquad (1)$$

where $\overline{R}$ = position in inertial space
$\overline{A_t}$ = thrust acceleration as sensed by an accelerometer
$\overline{G}$ = gravitational acceleration

The vehicle velocity and position as computed by the inertial system during flight is governed by the following integrations:

$$\overline{V}_c = \int_o^t (\overline{A}_\iota + \overline{G}c)\, dt \qquad (2)$$

$$\overline{R}_c = \int_o^t \overline{V}c\, dt \qquad (3)$$

where $\overline{V}c$, $\overline{R}c$ = computed velocity and position
$\overline{A}_\iota$ = indicated or measured acceleration
$\overline{G}c$ = computed gravitational acceleration.

The indicated acceleration may be written as:

$$\overline{A}_\iota = \overline{A}_t + \Delta\overline{A} \qquad (4)$$

where $\Delta\overline{A}$ = acceleration measurement error.

Using equations (4) and (3) and differentiating

$$\ddot{\overline{R}}c = \overline{A}_t + \Delta\overline{A} + \overline{G}c \qquad (5)$$

The difference between (5) and (1) which represents the total error, now is:

$$\Delta\ddot{\overline{R}} = \Delta\overline{A} + \Delta\overline{G} \qquad (6)$$

where $\Delta\overline{R}$ = error in computed position
$\Delta\overline{G}$ = error in computed gravitational acceleration.

The operating time for an inertial guidance system in a vehicle of the Scout type is short relative to the Schuler period (84 minutes) thus the gravity loop appears to be open and introduces no position and velocity sinusoidal oscillations as is the case with aircraft systems. Additionally, Scout flies a trajectory that is known well in advance of launch thus the gravity computations can be fitted if desired. Since the differences in gravitational acceleration resulting from trajectory perturbations are very small and a standard trajectory is used, no gravity errors are included in the guidance accuracy analysis routine.

The error in sensed acceleration is the forcing function in equation (4). It is composed of two general contributions and may be expressed as:

$$\Delta\bar{A} = \delta\bar{A} - \Delta\bar{\Phi} \times \ddot{\bar{R}} \qquad (7)$$

where $\delta A$ is the error associated with the accelerometer itself in measuring acceleration and $\Delta\Phi$ angular rotation of the inertial reference package axis away from the reference orientation. The components of equation (7) may be expressed as:

$$\Delta Ax = \delta Ax - \Delta\Phi y\,\ddot{R}z + \Delta\Phi z\ddot{R}y \qquad (8)$$

$$\Delta Ay = \delta Ay + \Delta\Phi x\,\ddot{R}z - \Delta\Phi z\ddot{R}x$$

$$\Delta Az = \delta Az - \Delta\Phi x\,\ddot{R}y + \Delta\Phi y\ddot{R}x$$

where the $\Delta\Phi$'s are in radians.

These equations are doubly integrated to obtain the errors in velocity and position as a function of time.

The reference inertial coordinate system used in the routine is defined by:

$X_I$ – in the plane of the trajectory and positively directed down range

$Z_I$ – launch point vertical and positive down

$Y_I$ – completes a right handed coordinate system and normal to trajectory plane.

The inertial reference system is related to the body axes by the following transformation:

$$\begin{bmatrix} X_I \\ Y_I \\ Z_I \end{bmatrix} = \left[B\,(\phi, \theta, \psi)\right] \begin{bmatrix} X_B \\ Y_B \\ Z_B \end{bmatrix}$$

$$\begin{bmatrix} X_I \\ Y_I \\ Z_I \end{bmatrix} = \begin{bmatrix} \cos\psi\cos\theta & -\sin\psi\cos\phi + \cos\psi\sin\theta\sin\phi & \sin\psi\sin\phi + \cos\psi\sin\theta\cos\phi \\ \sin\psi\cos\theta & \cos\psi\cos\phi + \sin\psi\sin\theta\sin\phi & -\cos\psi\sin\phi + \sin\psi\sin\theta\cos\phi \\ -\sin\psi & \cos\theta\sin\phi & \cos\theta\cos\phi \end{bmatrix} \begin{bmatrix} X_B \\ Y_B \\ Z_B \end{bmatrix} \qquad (10)$$

The elements of the matrix [B] are direction cosines relating the inertial or reference axes to the body axes. These direction cosines are used in the routine to define the body attitude in the reference system. $\phi$, $\psi$ and $\theta$ are the vehicle roll, yaw and pitch angles.

The body attitude is determined from body rates which are used to update matrix [B]. [B] may be written as:

$$\left[B\,(\phi, \theta, \psi)\right] = \begin{bmatrix} \ell_1 & m_1 & n_1 \\ \ell_2 & m_2 & n_2 \\ \ell_3 & m_3 & n_3 \end{bmatrix} \tag{11}$$

The inertial angular velocities about the body axes are given by

$$\overline{\omega}_B = P\overline{X}_B + Q\overline{Y}_B + R\overline{Z}_B \quad \text{(P, Q, and R are taken from NEMAR)}$$

The following expression can be derived defining the rate of change of the direction cosine elements in terms of vehicle rates.

$$\begin{bmatrix} \dot{\ell}_1 & \dot{m}_1 & \dot{n}_1 \\ \dot{\ell}_2 & \dot{m}_2 & \dot{n}_2 \\ \dot{\ell}_3 & \dot{m}_3 & \dot{n}_3 \end{bmatrix} = \begin{bmatrix} \ell_1 & m_1 & n_1 \\ \ell_2 & m_2 & n_2 \\ \ell_3 & m_3 & n_3 \end{bmatrix} \begin{bmatrix} 0 & -R & Q \\ R & 0 & -P \\ -Q & P & 0 \end{bmatrix} \tag{12}$$

The $\ell_i$ and $m_i$ ($i = 1, 2, 3$) terms are derived by integration; the $n_i$ terms are computed from:

$$\begin{aligned} n_1 &= \ell_2 m_3 - \ell_3 m_2 \\ n_2 &= \ell_3 m_1 - \ell_1 m_3 \\ n_3 &= \ell_1 m_2 - \ell_2 m_1 \end{aligned} \tag{13}$$

Another relationship used in the routine is that of relating one coordinate system to another by a small angle matrix. Determination of the misalignment angles ($\Delta\Phi$'s) in equation (8) uses this relation. The small angle matrix is:

$$\Delta\Phi_1 = \begin{bmatrix} 1 & -\Delta\Phi z & \Delta\Phi y \\ \Delta\Phi z & 1 & -\Delta\Phi x \\ -\Delta\Phi y & \Delta\Phi x & 1 \end{bmatrix} \tag{14}$$

where $\Delta\Phi i$ = rotation about the i axis.

Evaluation of the small angle matrix is computed from:

$$\begin{bmatrix} \Delta\Phi_{x1} \\ \Delta\Phi_{y1} \\ \Delta\Phi_{z1} \end{bmatrix} = \begin{bmatrix} \ell_1 & m_1 & n_1 \\ \ell_2 & m_2 & n_2 \\ \ell_3 & m_3 & n_3 \end{bmatrix} \begin{bmatrix} \Delta P \\ \Delta Q \\ \Delta R \end{bmatrix} \text{ or } \dot{\overline{\Delta\Phi}}_1 = [B]\ \overline{\Delta\omega} \tag{15}$$

where $\Delta P$, $\Delta Q$, and $\Delta R$ are errors in measurement of vehicle rates ($\Delta\omega$).

The remaining requirement is to transform the accelerometer errors of equations (7) and (8) to the inertial launch reference coordinate systems. For the strapdown type system this transformation is of the form

$$\delta\overline{A} = [B] \begin{bmatrix} \delta Ax \\ \delta Ay \\ \delta Az \end{bmatrix} \qquad (16)$$

The difference in evaluating gimballed systems is that the body accelerations must be resolved into the inertial reference system first and then the accelerometer error sources evaluated.

II. Component Error Models

The component error models must be developed to evaluate $\delta\overline{A}$ and $\Delta\overline{\Phi}$ throughout the trajectory.

Gyros

The error model used to represent the gyro performance is of the form:

$$\Delta\omega = R + Usi\,(A_{ii}) + U_{ii}\,(Asi) + Si\,(A_{ii})\,(Asi) \qquad (17)$$

where:

$\Delta\omega$ = drift rate of the gyro about its input axis
R = fixed or uncompensated drift rate in degrees per hour (deg/hr)
Usi, $U_{ii}$ = mass unbalance along the spin axis of the i gyro and mass unbalance along the input axis of the i gyro in degrees per hour per G (deg/hr/G)
Si = anisoelastic (compliance) coefficient of the i gyro expressed in degrees per hour per $G^2$ (deg/hr/$G^2$)
$A_{ii}$, Asi = components of applied acceleration along the input and spin axes of the i gyro.

These error sources represent the performance disturbances that are applicable whether the gyro is utilized in a gimballed platform configuration or in a strapdown mode.

When used in a strapdown fashion, additional gyro error parameters become significant because the gyros themselves are subjected to large angular rotations. These are the uncertainty or instability of the gyro torquer scale factor and misalignment of the input axes. The misalignment angles represent non-orthogonality which results from the inability to achieve alignment with an ideal reference coordinate frame. Contamination of the knowledge of the guidance package orientation resulting from the gyro torquer scale factor error is directly proportioned to the angular rotation of the package. With P, Q, and R representing the angular velocity components of a vehicle about the body axes system, the measurement rate errors are the product of the appropriate gyro torquer scale factor errors (SFX, SFY, SFZ) and the P, Q, R rates. The error in measured vehicle rate resulting from the misalignment of the gyros can be expressed as

$$\Delta\overline{\omega_1} = \begin{bmatrix} 0 & \Theta xz & -\Theta xy \\ -\Theta yz & 0 & \Theta yx \\ \Theta zy & -\Theta zx & 0 \end{bmatrix} \begin{bmatrix} P \\ Q \\ R \end{bmatrix} \qquad (18)$$

where $\Delta\overline{\omega_1}$ is the rate measurement error from this source and $\Theta_{ij}$ is the misalignment of the i gyro input axis about j .

The total gyro hardware and alignment error contributions to the uncertainty in the determination of the change of the orientation of the guidance package as determined by the gyros relative to the gyro coordinate system can be described as:

$$\Delta\overline{\omega} = \begin{bmatrix} Rx \\ Ry \\ Rz \end{bmatrix} + \begin{bmatrix} Usx & 0 & 0 \\ 0 & Usy & 0 \\ 0 & 0 & Usz \end{bmatrix}\begin{bmatrix} Ax \\ Ay \\ Az \end{bmatrix} + \begin{bmatrix} Uxx & 0 & 0 \\ 0 & Uyy & 0 \\ 0 & 0 & Uzz \end{bmatrix}\begin{bmatrix} Asx \\ Asy \\ Asz \end{bmatrix} + \begin{bmatrix} Sx & 0 & 0 \\ 0 & Sy & 0 \\ 0 & 0 & Sz \end{bmatrix}\begin{bmatrix} Ax & Asx \\ Ay & Asy \\ Az & Asz \end{bmatrix} +$$

$$\begin{bmatrix} SFX & 0 & 0 \\ 0 & SFY & 0 \\ 0 & 0 & SFZ \end{bmatrix}\begin{bmatrix} P \\ Q \\ R \end{bmatrix} + \begin{bmatrix} 0 & \Theta xz & -\Theta xy \\ -\Theta yz & 0 & \Theta yx \\ \Theta zy & -\Theta zx & 0 \end{bmatrix}\begin{bmatrix} P \\ Q \\ R \end{bmatrix} \qquad (19)$$

The drift, unbalance and anisoleastic terms are applicable to both gimbal and strapdown systems, however, the specific gyro orientation arrangement must be defined.

As previously discussed, the scale factor and alignment terms apply only for strapdown systems. In the case of a gimbal system, the cluster orientation remains fixed in inertial space. The gyros then do not rotate with the vehicle and these two error sources are negligible.

Now $\Delta\Phi$ in equation (7) can be evaluated.

$$\Delta\overline{\Phi} = \begin{bmatrix} \phi_{xo} \\ \phi_{yo} \\ \phi_{zo} \end{bmatrix} + \int_o^t [B]\,\Delta\overline{\omega} \qquad (20)$$

$\phi_{io}$ is the initial misalignment of the inertial reference package to the inertial reference frame. [B] is required for strapdown systems.

Accelerometer

The accelerometers were described by the following mathematical error model:

$$\delta A = D_A + C(A_i) + D_C\,(A_i)^2 \qquad (21)$$

where $\delta A$ = error in sensed or measured acceleration
$D_A$ = accelerometer bias instability in micro G's ($\mu$G)
C = accelerometer scale factor error in micro G's per G($\mu$G/G)
$D_C$ = accelerometer non-linearity in micro G's per $G^2$ ($\mu G/G^2$)
$A_i$ = component of applied acceleration along the input axis of the accelerometer

In addition to these error sources the measured acceleration is also corrupted by any misalignment of the accelerometer input axes. The resulting errors cay be expressed in the same manner as the rate measurement errors caused by gyro misalignments. Misalignment of the accelerometer input axis is denoted by:

$\phi_{ij}$ = misalignment of the i accelerometer input axis about the j axis.

Acceleration measurement error models are identical for both gimballed and strapdown systems.

The accelerometer measurement errors can be expressed as:

$$\delta A = \begin{bmatrix} D_{AX} \\ D_{AY} \\ D_{AZ} \end{bmatrix} + \begin{bmatrix} C_X & 0 & 0 \\ 0 & C_Y & 0 \\ 0 & 0 & C_Z \end{bmatrix} \begin{bmatrix} A_X \\ A_Y \\ A_Z \end{bmatrix} + \begin{bmatrix} D_{CX} & 0 & 0 \\ 0 & D_{CY} & 0 \\ 0 & 0 & D_{CZ} \end{bmatrix} \begin{bmatrix} A_X{}^2 \\ A_Y{}^2 \\ A_Z{}^2 \end{bmatrix}$$

$$+ \begin{bmatrix} 0 & \phi_{XY} & -\phi_{XY} \\ -\phi_{YZ} & 0 & \phi_{YX} \\ \phi_{ZY} & -\phi_{ZX} & 0 \end{bmatrix} \begin{bmatrix} A_X \\ A_Y \\ A_Z \end{bmatrix} \qquad (22)$$

## III. Computer Program Output

The output of the program is the individual error contributions on a probability basis at the end of each boost and coast phase. Additionally the attitude errors are determined from the contributions to $\Delta\Phi$, equation (20). The individual error sources are combined according to the Central Limit Theorem to yield the total or final error. This theorem states that the standard deviations of the sum, $\sigma_s$, is the root-sum-square of the standard deviations of the individual components.

$$\sigma_s^2 = \sum_{i=1}^{n} \sigma_i^2 \qquad (23)$$

The format of the routine output is illustrated below:

| | $\Delta\dot{X}$ | $\Delta\dot{Y}$ | $\Delta\dot{Z}$ | $\Delta X$ | $\Delta Y$ | $\Delta Z$ |
|---|---|---|---|---|---|---|
| RX | – | – | – | – | – | – |
| USX | – | – | – | – | – | – |
| UXX | – | – | – | – | – | – |
| ↓ | | | | | | |
| PHZ0 | – | – | – | – | – | – |

A total of 39 error sources are evaluated for strapdown systems, 30 for gimballed.

Reference (A1), "Inertial Guidance" Edited by George R. Pitman, Jr., John Wiley and Sons Inc., Copyright 1962